

UCSF

UC San Francisco Electronic Theses and Dissertations

Title

Connecting beta2-adrenergic receptor to the actin cytoskeleton and inhibiting microtubule polymerization: EBP50/NHERF, ilimaquinone, and Op18/stathmin

Permalink

<https://escholarship.org/uc/item/2f41t8n2>

Author

Deacon, Heather Winsome

Publication Date

2005

Peer reviewed|Thesis/dissertation

**Connecting beta2-adrenergic receptor to the actin cytoskeleton
and inhibiting microtubule polymerization:
EBP50/NHERF, ilimaquinone, and Op18/stathmin**

by

Heather Winsome Deacon

DISSERTATION

Submitted in partial satisfaction of the requirements for the degree of

DOCTOR OF PHILOSOPHY

in

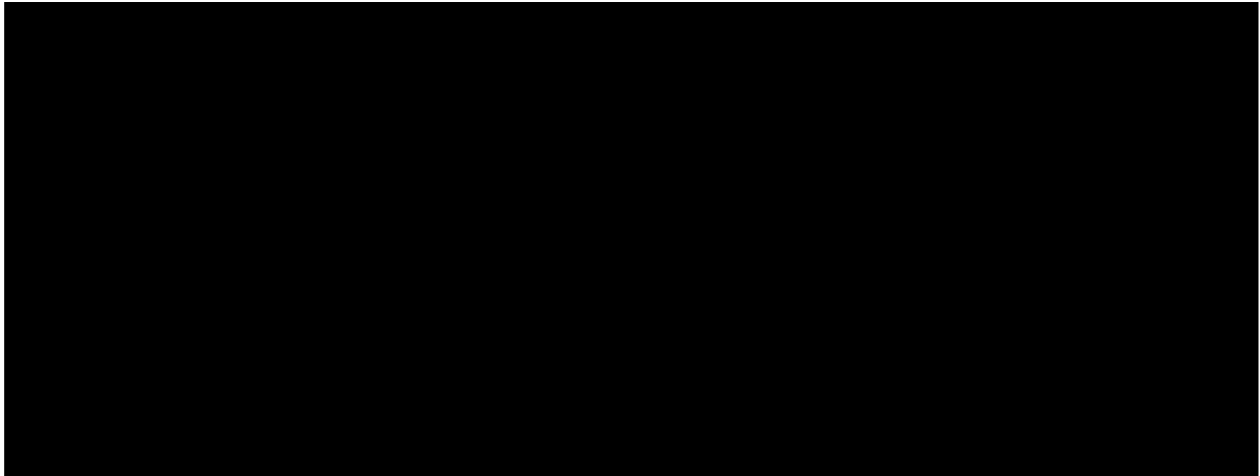
Biochemistry and Biophysics

in the

GRADUATE DIVISION

of the

UNIVERSITY OF CALIFORNIA, SAN FRANCISCO



Date

University Librarian

Degree Conferred:.....

Copyright 2005

by

Heather Winsome Deacon

ilimaquinone sensitive factor, and protocols for protease digestions. Fluorescence polarization of tubulin was a collaborative project with Paul Peluso.

My second debt of gratitude must go to Tim Mitchison, who assembled the “second wave” of his laboratory (and affiliates) that, for a time, included me. Claire Walczak, Sarita Jain, Matt Welch, Michelle “Yenta” Shirasu, Jennifer Frazier, Jason Swedlow, Tatsuye “Walt” Hirano, Louise “Another Great One” Cramer, Arshad, Chris, Karen “Yet Another Great One” Oegema, Jody “I Don’t Take No Guff” Rosenblatt, Yixian Zheng, Ann Yonetani, Aneil “Pure Ghee” Mallavarapu, Lisa Belmont. Lisa Belmont provided much advice on Op18, and we co-wrote Appendix I, a review article (Belmont et al., 1996). In particular, it was Arshad Desai’s idea to purify *Xenopus* tubulin, and this purification of *Xenopus* tubulin was a collaborative project. I was also trained on many techniques involving *Xenopus* extract-ology during a rotation project with Arshad (Desai et al., 1997). Both Arshad Desai and Karen Oegema provided much of the advice and training needed for the sucrose gradient sedimentation and gel filtration chromatography. Karen Oegema also developed the protocols for and provided training on analytical ultracentrifugation. The entire Mitchison lab were involved in purifying bovine brain tubulin for dynamic instability experiments. Claire Walczak provided the protocol for purification of MAPs, amino acid analysis, and generation and testing of anti-peptide antibodies.

My third debt of gratitude must go to the scientists who accomplished the Herculean task of divert my “stream of consciousness” scientific style into coherent, publishable units: Arshad Desai, Lynne Cassimeris, Mimi Shirasu, Martin Gullberg, Bonnie Howell, Jennifer “Shoes n’ Booze” Whistler, Mark “Z” von Zastrow, Alan “The

Derminator” Derman, Karen Oegema and my committee members David Morgan and Dyche Mullins. Bonnie Howell and Lynne Cassimeris used the anti-Op18 antibody I generated to demonstrate that Op18 was a catastrophe factor *in vivo* (Howell et al., 1999a). Lynne Cassimeris and Mimi Shirasu provided critical advice on the thesis. Martin Gullberg gave much advice and shared Op18 reagents, and we co-wrote Appendix II, a book chapter (Deacon et al., 1999). Dyche Mullins provided the key insight that went into the model of how an EBP50/NHERF family member might segregate B2AR in the early endosome and promote tubulation, and suggested the method to quantify endosome tubule size. Special thanks must go to David Morgan persuaded me to remain at the UCSF campus after Tim Mitchison left the university, and members of his lab gave me my early training in basic protein methods. Also special thanks must be given to Ron Vale, in whose laboratory the ilimaquinone project was conceived and the early purification work was initiated during a rotation project. The Vale laboratory provided much helpful advice; Josh Nicklas in particular provided lots of support, sage advice, buffers, tubulin, and *Xenopus* extracts. Members from my lab also helped me extensively revise my thesis introduction: Rani Dhavan, Michael Tanowitz, Ben Lauffer, Mike “I Don’t Have Time To Bleed” Gage and Aylin Hanyaloglu. Rani Dhavan also persuaded me to do confocal microscopy of EEA1 staining with appropriate controls, and Aylin Hanyaloglu shared much unpublished data on B2AR trafficking. Yang “Kevin” Xiang critically read the section on the signaling of B2AR in the heart, and Kathleen Liu did the same for the function of B2AR in the kidney. Maya Ponte contributed by providing a stable B2A1a cell line and by assisting with the biochemistry of B2AR and EBP50/NHERF on M2 beads. Finally, Jeff “Art Snob” Levin and Mike Gage have

provided critical help on innumerable occasions with computer assistance and advice. Jeff Levin in particular helped to create macros and databases that enabled me to tabulate co-localization data and to calculate MSD. Also Mats Gustafsson, in the laboratories of John Sedat and David Agard, invented the structured illumination microscope, and collaborated with me to capture and process the images. Lin Shao also helped me acquire images with this hauntingly powerful microscope.

A fourth debt of gratitude goes out to my confidantes and kindred spirits, who've been a great source of comfort and helped kept me sane over these many, many years: Suzanne Derrick, Rani Dhavan, Manu Hegde, Sarita Jain, Jennifer Jungkuntz, Kathleen "Kathleencubus" Liu, Francis Lee, Aaron Marley, Alan Derman, Cory Ondrejka, Jim Wilhelm, Paul Peluso, Kayvan Roayaie, Ted Mau, Jessica Roulette, Andy Shiau, Mimi Shirasu, Michael Tanowitz, Tom Wang, Lisa Cameron and Jennifer Whistler. Jennifer Whistler in particular has listened to my project ideas and provided feedback innumerable times. Cory Ondrejka has written two programs that enabled me to analyze much of the vesicle motility data. Kathleen Liu has been very helpful obtaining reagents and protocols for confocal microscopy. Alan Derman has provided sage and practical advice on the proper use of the English language. Without friends and colleagues like you, my head would have exploded "scanners"-style long ago.

Thanks also to my family; there are a lot of you out there, and you all have been exceptionally supportive. There is of course no way I could have done this without your love and, in many cases, logistical support.

Finally, I'd like to thank the administrative staff who has, really, put up with a lot from me of over the years: Sue Adams, Rachel Mozesson, Danny Dam and many, many others.

While I have striven to thank everybody who has helped me over the years, I hope you will permit this old brain some inaccuracies and omissions. They were not intended.

For those not as fortunate to know these exceptionally caring individuals, but whom are suffering through a "long hard slog," I would like to also point you towards some inanimate objects which also deserve thanks: "Are You Being Served," "Mike and Mike in the Morning," Chopin's "Double Thirds," Russian Caravan with milk and sugar and "The Brickhouse," all of which have mystical curative properties.



23 February 2005

Our ref: HG/HDN/FEB05/J178

Ms Heather Deacon
UCSF
Genentech Hall, 600 16th Street
2nd Floor
San Francisco, 94143-2140
USA

Dear Ms. Deacon

**TRENDS IN BIOCHEMICAL SCIENCES, Vol 21, No 6, 1996, pp 197 – 198, L
Belmont et al, “Catastrophic Revelations about Op18/Stathmin”**

As per your letter dated 15th February 2005, we hereby grant you permission to reprint the aforementioned material at no charge **in your thesis** subject to the following conditions:

1. If any part of the material to be used (for example, figures) has appeared in our publication with credit or acknowledgement to another source, permission must also be sought from that source. If such permission is not obtained then that material may not be included in your publication/copies.
2. Suitable acknowledgment to the source must be made, either as a footnote or in a reference list at the end of your publication, as follows:

“Reprinted from Publication title, Vol number, Author(s), Title of article, Pages No., Copyright (Year), with permission from Elsevier”.
3. Reproduction of this material is confined to the purpose for which permission is hereby given.
4. This permission is granted for non-exclusive world **English** rights only. For other languages please reapply separately for each one required. Permission excludes use in an electronic form. Should you have a specific electronic project in mind please reapply for permission.
5. This includes permission for UMI to supply single copies, on demand, of the complete thesis. Should your thesis be published commercially, please reapply for permission.

Yours sincerely

Helen Gainford
Rights Manager



23 February 2005

Our ref: HG/HDN/FEB05/B028

Ms Heather Deacon
UCSF
Genentech Hall, 600 16th Street
2nd Floor
San Francisco, 94143-2140
USA

Dear Ms. Deacon

PRIMER ON KIDNEY DISEASES, 3RD EDITION, (ISBN – 0122991001), 2001, J P Briggs et al, 1 figure only

As per your letter dated 15th February 2005, we hereby grant you permission to reprint the aforementioned material at no charge **in your thesis** subject to the following conditions:

1. If any part of the material to be used (for example, figures) has appeared in our publication with credit or acknowledgement to another source, permission must also be sought from that source. If such permission is not obtained then that material may not be included in your publication/copies.
2. Suitable acknowledgment to the source must be made, either as a footnote or in a reference list at the end of your publication, as follows:

"Reprinted from Publication title, Vol number, Author(s), Title of article, Pages No., Copyright (Year), with permission from Elsevier".
3. Reproduction of this material is confined to the purpose for which permission is hereby given.
4. This permission is granted for non-exclusive world **English** rights only. For other languages please reapply separately for each one required. Permission excludes use in an electronic form. Should you have a specific electronic project in mind please reapply for permission.
5. This includes permission for UMI to supply single copies, on demand, of the complete thesis. Should your thesis be published commercially, please reapply for permission.

Yours sincerely

Helen Gainford
Rights Manager



16 March 2005

Our ref: HG/smc/March 2005.jl363

Ms Heather Deacon

Dear Ms Deacon

CELL, Vol 85, No 7, 1996, Pages 1067-1076, Doyle et al, 'Crystal structure of a ...', 1 Figure only

As per your letter dated 28 February 2005, we hereby grant you permission to reprint the aforementioned material at no charge **in your thesis** subject to the following conditions:

1. If any part of the material to be used (for example, figures) has appeared in our publication with credit or acknowledgement to another source, permission must also be sought from that source. If such permission is not obtained then that material may not be included in your publication/copies.
2. Suitable acknowledgment to the source must be made, either as a footnote or in a reference list at the end of your publication, as follows:

"Reprinted from Publication title, Vol number, Author(s), Title of article, Pages No., Copyright (Year), with permission from Elsevier".
3. Reproduction of this material is confined to the purpose for which permission is hereby given.
4. This permission is granted for non-exclusive world **English** rights only. For other languages please reapply separately for each one required. Permission excludes use in an electronic form. Should you have a specific electronic project in mind please reapply for permission.
5. This includes permission for UMI to supply single copies, on demand, of the complete thesis. Should your thesis be published commercially, please reapply for permission.

Yours sincerely

Helen Gainford
Rights Manager

Connecting beta2-adrenergic receptor to the actin cytoskeleton and inhibiting microtubule polymerization: EBP50/NHERF, ilimaquinone, and Op18/stathmin

Heather Winsome Deacon

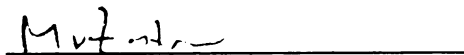
Department of Biochemistry and Biophysics, Program in Cell Biology, UCSF, California 94143

Abstract. Both the actin and the microtubule cytoskeleton are involved in transporting transmembrane proteins through cells. Using fluorescent imaging of living cells, we have found that endocytosed beta2-adrenergic receptor enters membrane tubules that rapidly move along microtubules. Using epi-fluorescent and confocal microscopy, we have demonstrated that beta2-adrenergic receptor clustering, endocytosis, recycling, and entry into membrane tubules are sensitive to latrunculin. Using co-immunoprecipitation, we have discovered that EBP50/NHERF (50 kDa ERM-binding phosphoprotein/ Na^+ - H^+ exchanger regulatory factor), a component of the apical actin cytoskeleton that binds to the beta2-adrenergic receptor *in vitro*, also binds to the beta2-adrenergic receptor in cells. This bound EBP50/NHERF is phosphorylated, and possibly exists as a homo-dimer in cells. Binding to EBP50/NHERF or a related protein -- possibly in a larger complex that contains actin -- may regulate beta2-adrenergic receptor trafficking in tissue culture cells.

Microtubule arrays are established in cells by a number of stabilizing and destabilizing proteins. Microtubule associated proteins, or MAPs, are a class of *microtubule* stabilizing proteins. We identify a ~100 kDa factor that destabilizes *microtubules* by causing catastrophes in the presence of the drug, ilimaquinone. We also demonstrate that this factor is not a MAP. Op18 family members, which are also not

MAPs, destabilize microtubules both by causing catastrophes and by sequestering tubulin subunits. Using video-enhanced DIC microscopy, we provide evidence that Op18 causes catastrophes at both ends of microtubules *in vitro*, indicating that Op18 disrupts protofilament packing. Furthermore, hydrodynamic analysis of Op18 *in vitro* and *in vivo* demonstrates that Op18 does not act as a microtubule sequestering protein in *Xenopus* egg extracts, but is found in a large complex of unknown composition in interphase extracts.

Signed:

A handwritten signature in black ink, appearing to read "M. von Zastrow", is written above a solid horizontal line.

Mark von Zastrow
Associate Professor, UCSF
Dept. Psychiatry/Dept. Cellular and Molecular Pharmacology
Chairperson and Thesis Advisor

TABLE OF CONTENTS

1	INTRODUCTION: THE BETA2-ADRENERGIC RECEPTOR	1
1.1	FUNCTION	1
1.1.1	Heart.....	2
1.1.2	Kidney Epithelia.....	5
1.2	STRUCTURE.....	5
1.3	SIGNALING	8
1.4	REGULATION OF SIGNALING.....	13
1.4.1	Desensitization	13
1.4.2	Control of Receptor Number	22
1.5	TRAFFICKING.....	24
1.5.1	Endocytosis.....	24
1.5.2	Endocytosis sequences.....	26
1.5.3	Recycling	28
1.5.4	Endosomes.....	29
1.5.5	Recycling Sequences.....	31
1.6	EBP50/NHERF.....	37
1.6.1	Functions of EBP50/NHERF.....	37
1.6.1.1	<i>Binding B2AR in vivo</i>	38
1.6.1.2	<i>Other functions of EBP50/NHERF and ERM proteins</i>	38
1.6.2	Proposed Mechanism of Action on B2AR.....	39
1.6.2.1	<i>Titration</i>	40

1.6.2.2	<i>Phosphorylation</i>	41
1.6.2.3	<i>Enabling G_i signaling</i>	41
1.6.2.4	<i>Oligomerization</i>	42
1.6.3	Testing these Models.....	43
1.7	TETHERING.....	45
2	SUMMARY OF RESULTS.....	47
3	BETA2-ADRENERGIC RECEPTOR BINDS EBP50/NHERF IN CELLS.....	51
3.1	<i>Materials and Methods</i>	56
3.2	<i>Results and Discussion</i>	60
4	SORTING BETA2-ADRENERGIC RECEPTOR INTO DYNAMIC ENDOSOMAL TUBULES IS DEPENDENT ON ITS RECYCLING SEQUENCE AND ON ACTIN	82
4.1	<i>Materials and Methods:</i>	85
4.2	<i>Results</i>	90
4.3	<i>Discussion</i>	111
5	ACTIN-DEPENDENT CLUSTERING OF BETA2-ADRENERGIC RECEPTOR	122
5.1	<i>Materials and Methods</i>	123
5.2	<i>Results and Discussion</i>	126
6	ACTIVITY OF ILIMAQUINONE ON MICROTUBULES.....	141
6.1	<i>Materials and Methods</i>	141
6.2	<i>Results and Discussion</i>	144
7	CHARACTERIZATION OF ONCOPROTEIN 18.....	150
7.1	<i>Materials and Methods</i>	155

7.2	<i>Results and Discussion</i>	158
8	APPENDIX I: DISCOVERY OF OP18 FUNCTION	172
9	APPENDIX 2: SUMMARY OF OP18 PROPERTIES	175
10	APPENDIX 3: ENDOSOMAL MOTOR PROTEINS	179
11	BIBLIOGRAPHY	182

LIST OF TABLES

Table 1 <i>Proteins that co-immunoprecipitate with B2AR</i>	53
Table 2 <i>Vesicle movements</i>	94

LIST OF FIGURES

Figure 1 <i>B2AR function in heart muscle and epithelial cells of the kidney proximal tubule</i>	3
Figure 2 <i>Sequence alignment of B2AR, B1AR and B3AR with rhodopsin</i>	7
Figure 3 <i>Activation of GPCRs</i>	10
Figure 4 <i>G_s signaling cascade</i>	12
Figure 5 <i>Sequence alignment of the carboxy terminal tail of B2AR</i>	16
Figure 6 <i>The signaling triggered by GPCR agonists can block signaling from further agonist treatments by a number of mechanisms</i>	21
Figure 7 <i>Trafficking of B2AR</i>	23
Figure 8 <i>EBP50/NHERF and ERM proteins</i>	35
Figure 9 <i>B2AR stimulation of Na⁺/H⁺ exchange in the kidney does not occur via G_s and is dependent on the intact carboxy terminus, which can bind to EBP50/NHERF</i>	44
Figure 10 <i>Biochemistry of B2AR in extracts</i>	62
Figure 11 <i>Detection of EBP50/NHERF</i>	65
Figure 12 <i>Sucrose gradient of EBP50/NHERF in HEK293 cell extracts</i>	68
Figure 13 <i>Co-immunoprecipitation of EBP50/NHERF with B2AR in the presence of crosslinker</i>	72
Figure 14 <i>EBP50/NHERF specifically co-immunoprecipitates with B2AR</i>	76
Figure 15 <i>Effects of B2AR agonist on EBP50/NHERF co-immunoprecipitation</i>	79

Figure 16 <i>Live cell imaging of B2AR, B2AlaR and DOR</i>	92
Figure 17 <i>Epi-fluorescence microscopy of transferrin receptor with GPCRs</i>	97
Figure 18 <i>Histogram of tubule length for GPCRs</i>	100
Figure 19 <i>Quantification of co-localization of transferrin and EEA1 with GPCRs</i>	104
Figure 20 <i>Actin is necessary for B2AR to be found in elongated tubules</i>	107
Figure 21 <i>Confocal microscopy of transferrin and EEA1 with GPCRs</i>	108
Figure 22 <i>Structured illumination pictures of enlarged structure and tubule</i>	110
Figure 23 <i>Model for the role of EBP50/NHERF in B2AR recycling</i>	119
Figure 24 <i>The EBP50/NHERF binding site is required to inhibit constitutive endocytosis</i>	128
Figure 25 <i>Latrunculin inhibits clustering of B2AR</i>	130
Figure 26 <i>Dependence of GPCR clustering on actin is not due to EBP50/NHERF binding</i>	134
Figure 27 <i>Latrunculin inhibits endocytosis of B2AR but not ligand binding</i>	137
Figure 28 <i>Effect of ilimaquinone on microtubule polymerization in extracts and in vivo</i>	146
Figure 29 <i>Sizing column of interphase high speed supernatant</i>	148
Figure 30 <i>Op18 sequence and structure</i>	153
Figure 31 <i>Characterization of Xenopus Op18</i>	160
Figure 32 <i>Microtubule polymerization dynamics influenced by Xenopus Op18</i>	165
Figure 33 <i>Op18 in Xenopus egg extracts</i>	170

1 INTRODUCTION: THE BETA2-ADRENERGIC RECEPTOR

1.1 FUNCTION (Vander et al., 1990)).

The beta2-adrenergic receptor (B2AR) and the related protein, the beta1-adrenergic receptor (B1AR), bind the catecholamines epinephrine and norepinephrine.

Catecholamines are small molecules that are released by neurons of the autonomic nervous system to control many functions in the body. These neurons control effector cells in muscles and glands; they can also control other neurons. Two major tissues release catecholamines: sympathetic neurons and the adrenal medulla. Sympathetic neurons release catecholamines onto effector cells from synapses. The adrenal medulla, by contrast, releases catecholamines into the bloodstream. The catecholamine primarily released by sympathetic neurons is norepinephrine; by the adrenal medulla, it is epinephrine. These two catecholamines bind B1AR equally well, whereas epinephrine binds B2AR more tightly than norepinephrine does. Consequently, B2AR is only weakly activated by norepinephrine released from sympathetic neurons (Hoffman, 2001; LeJemtel et al., 2001).

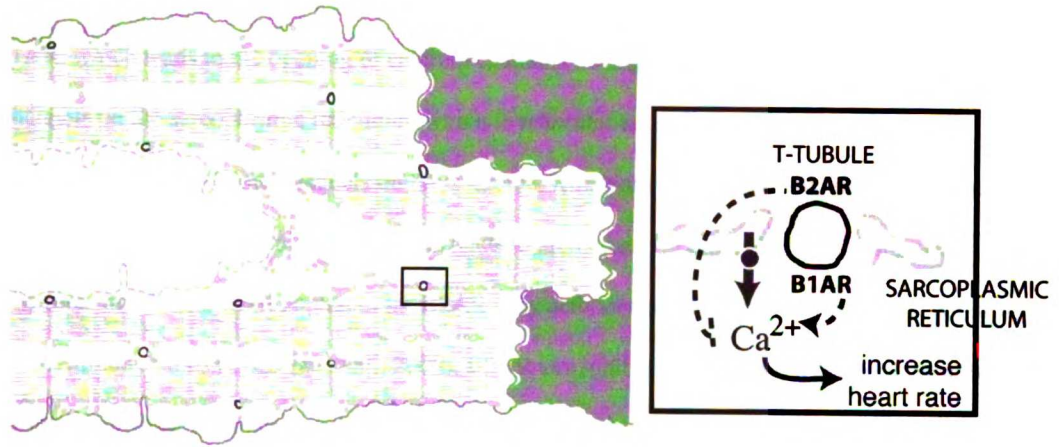
It is thought that activation of B2AR globally (by the adrenal medulla) and B1AR locally (by sympathetic neurons) provides complementary mechanisms to increase metabolic rate throughout the body. One well-known situation in which both the adrenal medulla and the sympathetic nervous system act in concert is in preparation for a “fight or flight” response. Given that B2AR and B1AR are thought of as acting in concert during the fight or flight response, it is interesting that these receptors are frequently found on the same cells. Indeed, these receptors have been found to have different

subcellular localizations and functions on many cell types. While B2AR is widely expressed, we will discuss the function of B2AR in the heart and kidney.

1.1.1 *Heart*

In the heart, catecholamines delivered either by sympathetic neurons or by the adrenal medulla increase the force and the rate of heart contractions (Figure 1) (Koch et al., 1996). Thus, the sympathetic nervous system, which primarily releases the potent B1AR agonist norepinephrine, and the adrenal medulla, which primarily releases the potent B2AR agonist epinephrine, indeed transmit complementary information to the heart. However, there is strong evidence that the increase in the rate of heart contractions caused by epinephrine in the bloodstream is primarily via B1AR signaling (Juberg et al., 1985). It has been proposed that B2AR has a distinct function from B1AR in the heart: to protect the heart from damage (Communal et al., 1999; Engelhardt et al., 1999; Xiao et al., 1999b; Zhu et al., 2001).

A. Cardiac Muscle



B. Epithelia of the Kidney Proximal Tubule

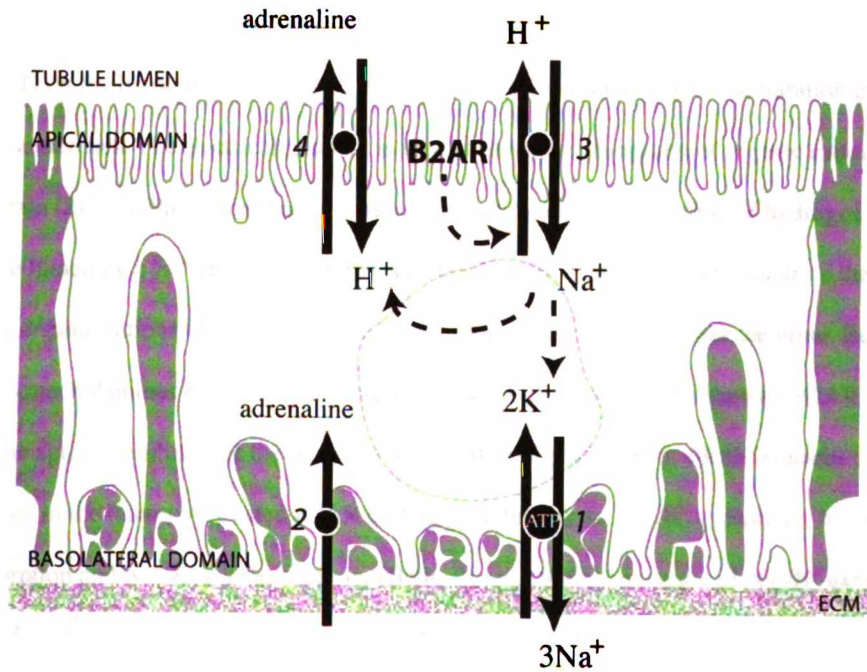


Figure 1

B2AR function in heart muscle and epithelial cells of the kidney proximal tubule. (Rennick, 1981; Vander et al., 1990; Wright and Dantzer, 2004) (A) In heart muscle cells, BAR agonists such as epinephrine activate B1AR, which leads to the opening of calcium channels throughout the cell (Bean et al., 1984). Calcium channels on the sarcoplasmic reticulum, which is muscular endoplasmic reticulum, are intracellular; there are also calcium channels on the T-tubule, which are specialized invaginations of the plasma membrane. Opening these calcium channels leads to an increase in intracellular calcium, which increases the force and rate of heart contractions. B2AR only activates adjacent calcium channels, perhaps channels that it directly binds (Chen-Izu et al., 2000). B2AR can inhibit the increase in heart rate caused by B1AR; this may contribute to protecting the heart from damage (Albrecht et al., 2000; Xiao et al., 1999b; Zhu et al., 2001). B2AR may in part do so by inhibiting calcium channels (Xiang and Kobilka, 2003b). (B) Epithelial cells in the proximal tubule secrete organic molecules from the body. Epinephrine secretion, which follows the path of other organic cations, is shown. This secretion is driven in part by a Na^+/K^+ ATPase (1) on the basolateral membrane, which creates an electrical and a concentration gradient across the cell membranes. The electrical gradient is used to drive the absorption of organic cations from the bloodstream (2). The Na^+ concentration gradient is used to drive the secretion of hydrogen ions (H^+) into the tubule lumen by a Na^+/H^+ exchanger (3). The resulting H^+ gradient in turn can drive the secretion of absorbed organic cations (4) into the tubule lumen, from which they can enter the urine. Before they are secreted, catecholamines can be metabolized into inactive compounds (not shown). B2AR is localized on or near the apical membrane of the proximal tubule (Boivin et al., 2001), which indicates that it is activated by agonists in the lumen. Activated B2AR probably stimulates the Na^+/H^+ exchanger; this in turn increases Na^+ absorption and Na^+/K^+ ATPase activity (Bello-Reuss, 1980). Activation of Na^+/H^+ exchange by B2AR agonists does not occur via a G_i signaling cascade (see text). Reprinted from Primer on Kidney Diseases, 3rd ed., Briggs, J.P., Kritiz, W., and Schnermann, J.B., "Overview of Renal Function and Structure," p. 10, Copyright (2001), with permission from Elsevier.

1.1.2 *Kidney Epithelia*

Beta-adrenergic receptor subtypes are also found together on epithelial cells, such as those in the kidney. In the kidney, the roles of B1AR and B2AR have not been separately defined. However, their subcellular distribution indicates at the least, a difference in regulation: in the proximal and distal tubules of kidney nephrons, B2AR is primarily at the apical membrane just below the microvilli, whereas B1AR is primarily intracellular (Boivin et al., 2001). Given this localization, B2AR may respond to catecholamines in the tubular lumen, where they are excreted from the body. Catecholamine activation of B2AR appears to stimulate a Na⁺/H⁺ exchanger, which establishes a H⁺ gradient that can lead to the transport of catecholamines and other organic cations into the tubular lumen (Besarab et al., 1977). This transport of organic cations is one mechanism to clear these signaling molecules from the bloodstream.

1.2 STRUCTURE

B2AR and B1AR are both G protein coupled receptors (GPCRs). GPCRs comprise a structurally related superfamily of proteins that signal to G proteins (reviewed in (Kobilka, 1992)). The most notable structural feature of this family is that these proteins span the plasma membrane seven times, with their amino terminus extracellular and their carboxy terminus intracellular (Figure 2). Mammalian GPCRs can be subdivided into three families; both B2AR and B1AR belong to family A. Receptors from family A typically bind their agonists in a crevice formed by the transmembrane domains. Residues lining the crevice result in distinct binding affinities for individual

catecholamines between the BARs. The amino acid sequence identity for BARs is higher in the transmembrane domains than other regions.

In general, for family A GPCRs, the proximal section of the cytoplasmic tail is less divergent than the distal section of the tail. This conservation ends at a conserved cysteine residue, which can be covalently bound to a lipid group, palmitate (Figure 2) (O'Dowd et al., 1989). In the inactive state, residues upstream of this cysteine may form an amphipathic alpha helix, helix 8, that lies along the membrane; large hydrophobic residues upstream of this cysteine are relatively conserved (Jung et al., 1996; Palczewski et al., 2000). It has been proposed that this amphipathic helix extends the cytoplasmic surface of the receptor, enabling it to interact with large cytoplasmic proteins such as $G\alpha\beta\gamma$ (Figure 3) (Bourne and Meng, 2000). Residues downstream of this amphipathic helix are not conserved. Both the amphipathic helix and the less conserved distal portion of the tail have been proposed to bind a number of cytosolic proteins (Figure 7 and Table 1).

TM H1

B2AR -----MGQPGN GSAFL LAPN-----RSHAP DHDVTQQRDEVVVVG MGIVMSLIVLAIVFG NVLIVITAIKFERLQ 65
 B1AR MGAGVIVIGASEPGN LSSAAPLPDGAATAA RLLVPASPASLLPP ASESEPELSQOWTAG MGLLMALIVLLIVAG NVLIVIVAIKTPRLQ 90
 B3AR -----MAPWPE NSSLAPWPDLP-----TLAPNT ANTSGLPGVPWEAAL AGALLALAVLATVGG NLLVIVIVAIKTPRLQ 69
 rhod -----MNGTEGPNF YVPFSNKTG-----VVRSPF EAPQYYLAEPPWQFSM LAAYMFLIMLGFPI NFLTLYVTVQHKKLR 69

TM H2

B2AR TVTNYFITSLACAL VMGLAVVPEFGAAHIL MKMWTFGNFWCFEFT SI VLVCVTASIEITC VIAVDYFAITSPFK YQSLLTKNKARVIL 155
 B1AR TLTNLFIMSLASADL VMGLLVVPEFGATIV WGRWEYGSFFCELTW SVDVLCVTASIEITC VIALDRYLAIITSPFR YQSLLTRARARGLVC 180
 B3AR TMTNVEVTSLAAADL VMGLLVVPPAATLAL TGHWPLGATGCELTW SVDVLCVTASIEITC ALAVDRYLAVTNPLR YGALVTKRCARTAVV 159
 rhod TPLNYILLNLAVADL FMVFGGTTTTLYTSL HGYPVFGPTGCNLEG FFATLGGEIALWSLV VLAIERVYVVVCKPMS NERFG-ENHAIMGVA 158

TM H3

B2AR TVTNYFITSLACAL VMGLAVVPEFGAAHIL MKMWTFGNFWCFEFT SI VLVCVTASIEITC VIAVDYFAITSPFK YQSLLTKNKARVIL 155
 B1AR TLTNLFIMSLASADL VMGLLVVPEFGATIV WGRWEYGSFFCELTW SVDVLCVTASIEITC VIALDRYLAIITSPFR YQSLLTRARARGLVC 180
 B3AR TMTNVEVTSLAAADL VMGLLVVPPAATLAL TGHWPLGATGCELTW SVDVLCVTASIEITC ALAVDRYLAVTNPLR YGALVTKRCARTAVV 159
 rhod TPLNYILLNLAVADL FMVFGGTTTTLYTSL HGYPVFGPTGCNLEG FFATLGGEIALWSLV VLAIERVYVVVCKPMS NERFG-ENHAIMGVA 158

TM H4

B2AR TVTNYFITSLACAL VMGLAVVPEFGAAHIL MKMWTFGNFWCFEFT SI VLVCVTASIEITC VIAVDYFAITSPFK YQSLLTKNKARVIL 155
 B1AR TLTNLFIMSLASADL VMGLLVVPEFGATIV WGRWEYGSFFCELTW SVDVLCVTASIEITC VIALDRYLAIITSPFR YQSLLTRARARGLVC 180
 B3AR TMTNVEVTSLAAADL VMGLLVVPPAATLAL TGHWPLGATGCELTW SVDVLCVTASIEITC ALAVDRYLAVTNPLR YGALVTKRCARTAVV 159
 rhod TPLNYILLNLAVADL FMVFGGTTTTLYTSL HGYPVFGPTGCNLEG FFATLGGEIALWSLV VLAIERVYVVVCKPMS NERFG-ENHAIMGVA 158

TM H4

B2AR MVWIVSGLTSFLPIQ MHWYRATHQ-EALNC YANETCCDFFTN-QA YAIASIVIVYVPLV IMVFVYSR-VFOEAKR QLOKIDKSEGRFH-- 241
 B1AR TVWAIASLVSEFLPIL MHWRAESD-EARRC YNDPKCCDFVTN-RA YAIASSVVSFYVPLC IMAFVYLR-VFREAOQ QVKKIDSCERRFLGG 268
 B3AR LVWVVSAAVSFAPIM SQWWRVGADAEAQRC HSNPRCCAFASN-MP YVLLSSSVSFYLPPL VMLFVYAR-VFVVATR QLRLLRGELGRFPPE 248
 rhod FTWVMALACAAPPLV G-WSRYIPEGMQCSC GIDYYTPHEETNNEF FVIYMFVVHFIIPLI VIFFCYGQLVFTV-KE AAAQQQESA----- 237

TM H5

B2AR MVWIVSGLTSFLPIQ MHWYRATHQ-EALNC YANETCCDFFTN-QA YAIASIVIVYVPLV IMVFVYSR-VFOEAKR QLOKIDKSEGRFH-- 241
 B1AR TVWAIASLVSEFLPIL MHWRAESD-EARRC YNDPKCCDFVTN-RA YAIASSVVSFYVPLC IMAFVYLR-VFREAOQ QVKKIDSCERRFLGG 268
 B3AR LVWVVSAAVSFAPIM SQWWRVGADAEAQRC HSNPRCCAFASN-MP YVLLSSSVSFYLPPL VMLFVYAR-VFVVATR QLRLLRGELGRFPPE 248
 rhod FTWVMALACAAPPLV G-WSRYIPEGMQCSC GIDYYTPHEETNNEF FVIYMFVVHFIIPLI VIFFCYGQLVFTV-KE AAAQQQESA----- 237

1. G protein activation

G protein activation

TM H6

B2AR -----VQNLS QVEQDGRGTGHGURRS SKFCLKEHKALKTLG IIMGFTTLCWLPPFI VIVHVIQD-NLIRK 305
 B1AR PARPPSPSPVPAP APPPGPRPAAAAAT APLANGRAGK-RRPS RLVALREQKALKTLG IIMGVFTLCWLPPFL ANVKAFHR-ELVPD 356
 B3AR E-----S----- PPAPSRSLAPAPVGT CAPPEGVPACGRRPA RLLPLREHRALCTLG LIMGTFTLCWLPPFL ANVLRALGGPSLVPG 325
 rhod -----TTQKAEKEVTRMVI IMVIAFLICWLPPYAG VAFYIFTHQGSDFGP 285

2. G protein specificity

H8

B2AR EVYILLNWIYVNSG FNPLIYCRS-PDEFRI AFQELLCRRSSLKA YNGYSSN-----GNTGEQSGYHVE QEKENKLLCEDLPGT 384
 B1AR RLFVFFNWLYGANS FNPDIYCRS-PDEFK AFQRLCCARRAARR RHATHGDRPRASGCL ARPGPPSPGAASDD DDDVVVGATPPARLL 445
 B3AR PAFALNWLGYANSA FNPLIYCRS-PDEFERS AFRRLLCRCG---R-----RLPPEPCAAA----- 376
 rhod IFMTIPAFFAKTSAV YNPVIYIMNMKQFRN CMVTTLCCGK-----

3. GRK2

GRK2

4. GRK2

4. GRK5 GRK2/5 GRK2/5 GRK2/5

B2AR EDFVGHQGTVPDNI DSQGRNCSTNDSLL- --- 413
 B1AR EPWAGCNGGAAADSD SSLDEPCRPGFASES KV- 477
 B3AR -PALFPSGVPAARSS PAQPRLCQLDGLASW GVS 408
 rhod ----NPLGDDEASTT VSKTETSQVAPA--- 348

Figure 2

Sequence alignment of B2AR, B1AR and B3AR with rhodopsin. (1) The crystal structure of inactive rhodopsin shows the location of eight alpha helical regions, transmembrane domains TM H1-7, and an amphipathic helix, H8 (Palczewski et al., 2000). The three cytoplasmic loops are in between TM1 and 2, 3 and 4, and 5 and 6, respectively; the carboxy terminus is also intracellular. Residues of B2AR that bind agonist are shaded, and the solvent accessible crevice is shown with a grey line (reviewed in (Gether, 2000)). Residues involved with G protein activation and specificity in the 3rd cytoplasmic loop are boxed (reviewed in (Ostrowski et al., 1992)). (2) PKA phosphorylates S236 within the 3rd cytoplasmic loop, which disrupts activation of G proteins (Kobilka, 1992). (3) GRK2 can phosphorylate T384, S396, S401, S407 of the carboxy terminal tail *in vitro* (Fredericks et al., 1996); GRK5 phosphorylates these sites as well as S411 and T393 (Fredericks et al., 1996). (4) However, S353, 356 and 364 are required for desensitization by GRK2 *in vivo* (Seibold et al., 1998; Seibold et al., 2000).

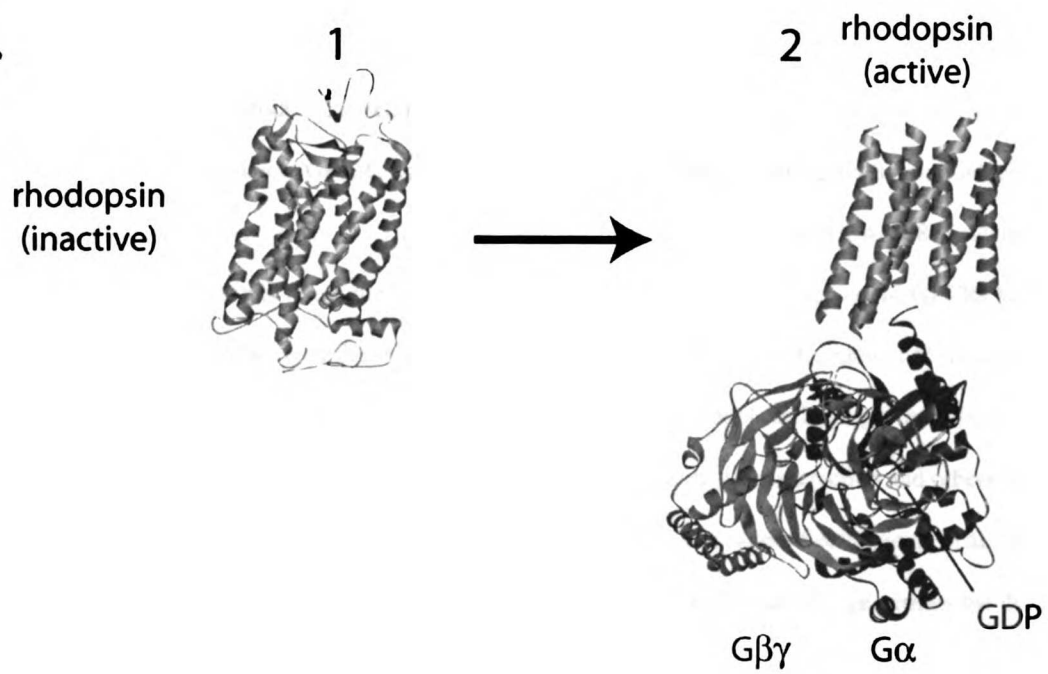
1.3 SIGNALING

Once BARs are activated by catecholamines, these receptors undergo a conformational change that allows them to activate the stimulatory G protein, G_s (Figure 2 and Figure 3). G proteins can bind to GDP or to GTP. BARs activate G_s by directly binding to them; this binding causes G_s to release GDP and to bind GTP. Activated G_s then stimulates adenylyl cyclase, an enzyme that generates cAMP (Figure 4). cAMP in turn activates the cAMP-dependent kinase, protein kinase A (PKA). PKA then phosphorylates effector proteins, which carry out the functional effects of B2AR activation. Each molecule on this signaling pathway (G_s , cAMP and PKA) can amplify the original signal by diffusing to and activating multiple downstream molecules (Stryer, 2002). For example,

each GTP-bound G_s protein could diffuse around the membrane and activate multiple adenylyl cyclase molecules.

In some cell types, the B2AR can also activate the inhibitory G protein, G_i (Xiao et al., 1995). In contrast to G_{α_s} , G_{α_i} inhibits adenylyl cyclase; this leads to a decrease in cAMP. The $\beta\gamma$ subunits of G_i , meanwhile, can directly bind to and activate ion channels (Neer and Smith, 1996). B1AR does not appear to share B2AR's ability to couple to multiple G proteins (Xiao et al., 1995).

A.



B.

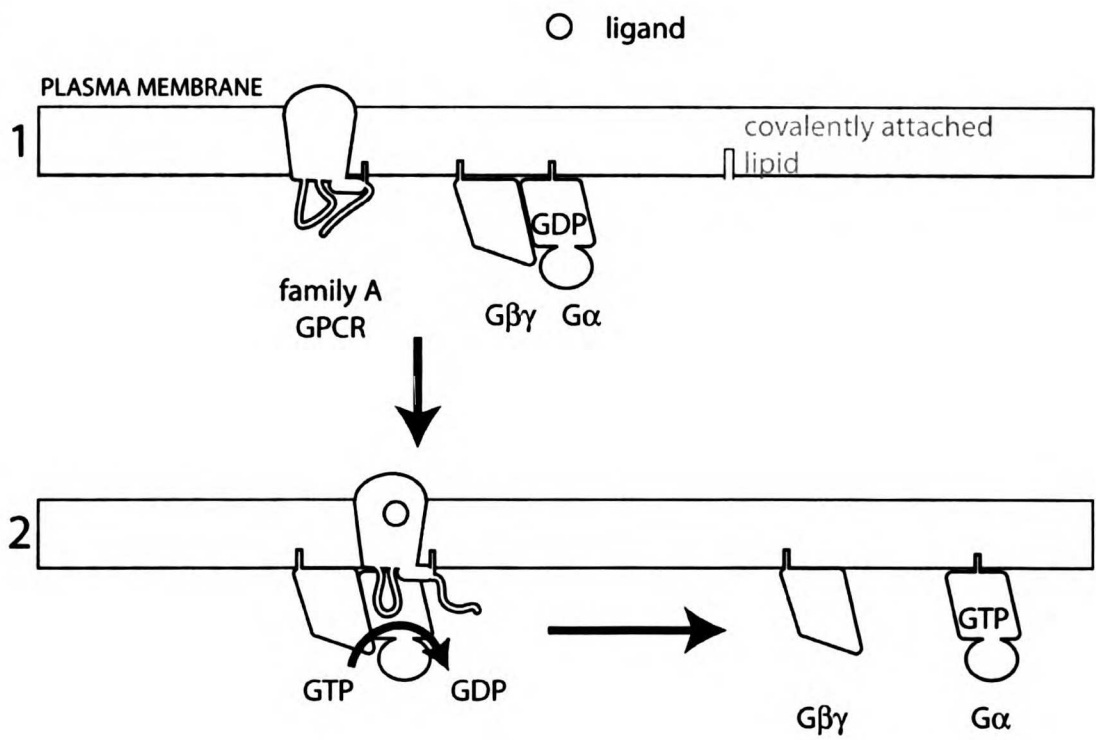


Figure 3

Activation of GPCRs. (A) Models derived from x-ray crystallography of rhodopsin, a family A GPCR, and its cognate G protein are shown. GPCRs undergo a conformational change after ligand binding which enables them to activate G proteins. (1) The inactive state of rhodopsin (PDB ID code #1F88 (Palczewski et al., 2000)). The cytoplasmic (here, the bottom) surface of GPCRs couples to G proteins. GPCRs have three cytoplasmic loops in between the seven transmembrane helices. The cytoplasmic tail of rhodopsin has a short helix that projects along the membrane, away from the receptor, anchored by lipid-modified cysteines. In the inactive state, the cytoplasmic tail covers the third loop; this interaction and others (not shown) are thought to prevent the cytoplasmic loops from binding to $G\alpha$ (Klein-Seetharaman et al., 2001; Meng and Bourne, 2001). (2) When ligand binds the receptor, a conformational change permits the distal portion of the tail to move away from the cytoplasmic loops; the cytoplasmic loops can then bind to and activate $G\alpha$. A proposed model for active rhodopsin bound to $G\alpha\beta\gamma$ is shown (Elaine Meng and Henry Bourne, personal communication); the loops and cytoplasmic tail of the receptor are not shown. (B) A model for Family A GPCR activation based on the crystal structure of rhodopsin. For simplicity, only one cytoplasmic loop is shown. (1) Inactive GPCR and G protein. (2) Upon activation, the GPCR binds its cognate G protein; the third loop of the receptor triggers the release of GDP from $G\alpha$. GTP can then bind and activate $G\alpha$. Active $G\alpha$ then releases the $G\beta\gamma$ subunit, which reveals effector-binding sites on $G\alpha$ and on $G\beta\gamma$. Both G protein subunits, and some family A GPCRs such as B2AR, have covalently attached lipid groups.

Gα signaling cascade

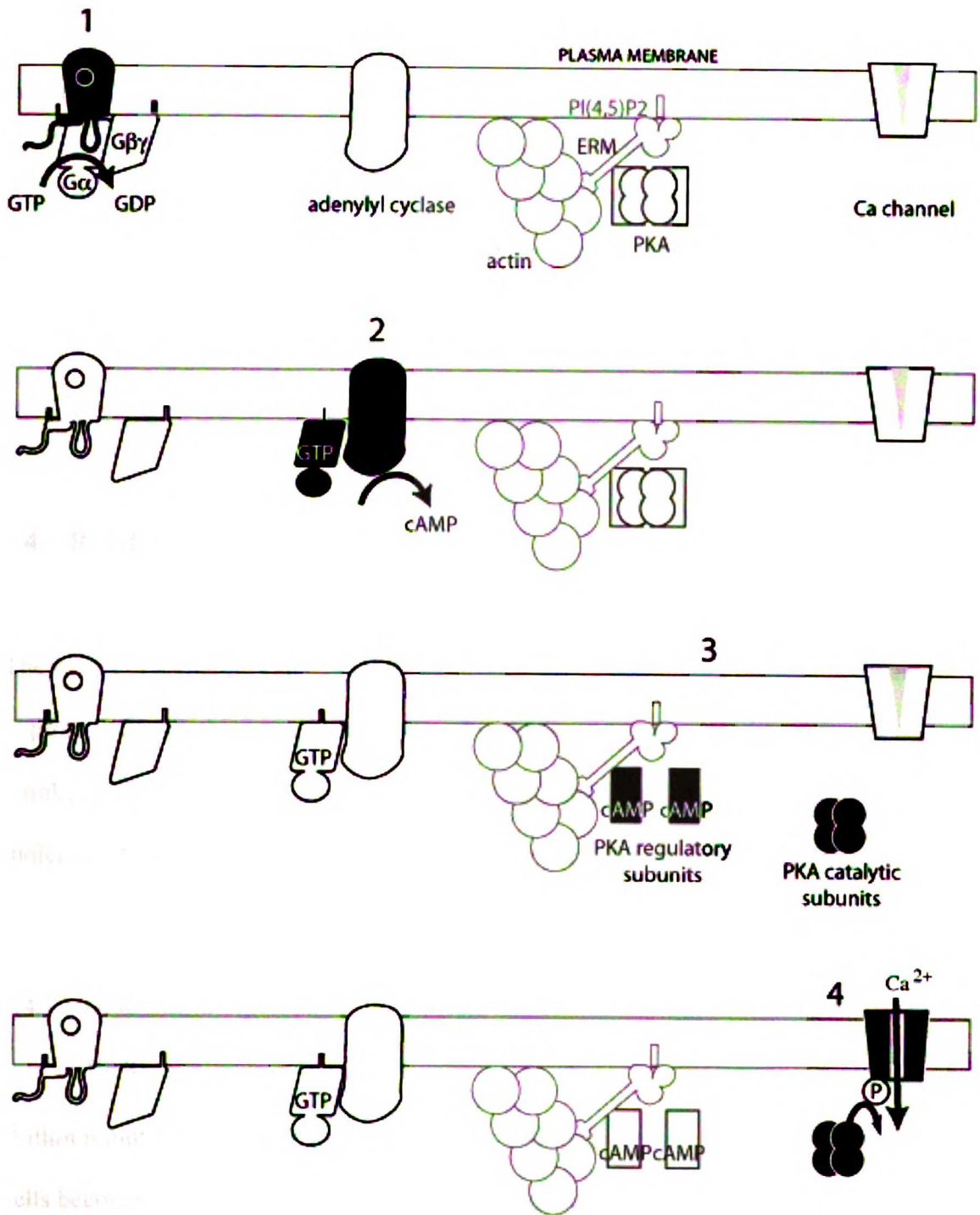


Figure 4

G_s signaling cascade (Stryer, 2002). (1) Upon ligand binding, the GPCR binds to $G\alpha_s$, which triggers the exchange of GTP for GDP on the G protein. (2) GTP bound $G\alpha_s$ releases the receptor and $G\beta\gamma$, and the exposed effector binding site on $G\alpha_s$ can bind to and activate adenylyl cyclase, a transmembrane protein that can generate cAMP. Released $G\beta\gamma$ can also bind effectors. (3) cAMP can bind to the regulatory subunits of PKA, which then release active PKA. These regulatory subunits can be tethered to the plasma membrane by anchoring proteins called AKAPs (Michel and Scott, 2002). ERM proteins (see text) are AKAPs which can bind both PI(4,5)P₂ and actin. (4) PKA can phosphorylate and activate downstream effectors such as calcium channels.

1.4 REGULATION OF SIGNALING

Both the timing and the location of signaling are controlled by a variety of mechanisms. The extent of signaling can be rapidly controlled by: 1) uncoupling the receptor from its G protein, 2) switching receptor signaling to inhibitory pathways, and 3) reducing the number of receptors at the cell surface. Signaling is also controlled by tethering molecules together and targeting them to specific subcellular locations.

1.4.1 *Desensitization*(Kobilka, 1992), Hein and Kobilka, 1995, (Krupnick and Benovic, 1998)

Within minutes of exposure to catecholamine, BAR signaling via G_s is turned off, and cells become less responsive to further catecholamine treatments. This decrease in responsiveness is a general feature of signaling cascades; this feature allows cells to adapt

to a particular level of stimulation. Adaptation enables cells to respond to increases in signal strength, rather than absolute signal levels. A decrease of signaling that is caused either by previous or chronic agonist treatment is called “desensitization”(Figure 6).

While desensitization is a commonly used term in signaling, it has no precise molecular definition. There are indeed many mechanisms to turn off GPCR signaling.

PKA One mechanism to decrease the signaling of GPCRs is to prevent them from activating G proteins. The third cytoplasmic loop of B2AR, which contains the binding site for G_s , can be phosphorylated by PKA, rendering the receptor unable to activate G_s (Kobilka, 1992) (Figure 2). PKA, which can be activated by agonist-bound receptors, can go on to phosphorylate other receptors. Inactivation of one receptor by the activity of another is called “heterologous desensitization.” The $t_{1/2}$ of PKA phosphorylation is rapid, about 2 min (Roth et al., 1991).

PKA activity can be regulated by AKAPs (A Kinase Anchoring Proteins), which anchor it to substrates, to specific membrane domains, and to other regulatory molecules. B2AR is thought to interact with a number of AKAPs, directly or indirectly (see Chapter 3).

GRKs Unlike PKA, which can phosphorylate either active or inactive receptors, GRKs only phosphorylate active receptors. Inactivation of a receptor by its own activity is called “homologous desensitization.” Homologous desensitization caused by GRKs proceeds more rapidly than heterologous desensitization caused by PKA: the $t_{1/2}$ of GRK phosphorylation of the B2AR has been estimated to be 15 sec (Roth et al., 1991).

Two classes of GRKs have been demonstrated to desensitize signaling from the BARs (reviewed by (Krupnick and Benovic, 1998; Pitcher et al., 1998a)). GRK2/BARK1 and GRK5 are mammalian GRKs that are broadly expressed; these two GRKs also have homologs in non-eukaryotic species. GRK2 is homologous to another mammalian protein, GRK3, which is predominantly found in the olfactory system. GRK5 is homologous to two other mammalian proteins, GRK4 and GRK6: GRK4 is exclusively in the testis while GRK6 is broadly expressed. While both GRK2 and GRK5 can bind the lipid $PI_{4,5}P_2$, GRK5 is stably associated with membranes whereas GRK2 is recruited to membranes by $G\beta\gamma$ after agonist activation of GPCRs (Figure 6).

The sites of phosphorylation of GRK2 and GRK5 have been mapped on purified, recombinant B2AR (Figure 2) GRK2 phosphorylates the carboxy terminus of B2AR on residues T384, S396, S401 and S407, whereas GRK5 also phosphorylates S411 and T393 (Fredericks et al., 1996). However, studies have indicated that these carboxy terminal sites are not required for desensitization via GRK2, and have instead implicated the more distal residues S355, 356, and 364 (Seibold et al., 1998; Seibold et al., 2000). Desensitization of mutant B2AR in cell lines expressing GRK5 was not investigated. Furthermore, these studies were performed using receptors epitope tagged at their carboxy terminus, a modification that may disrupt important interactions with cytosolic proteins.

	7. eIF2B α /GASP		4		6. SRC		3. GRK2		12. HRS		5. GRK5	
	1		H8								2. GRK2	
	9. H7				350						400	
MOUSE	NPLIYCRSP	DFRIAFQEIIL	CLRRSSSKTY	NGYSSNSNG	RTDYTGEPNT	COLGQEREQE	LLCEDPPGME	GFVNCQGTVP				
RAT	NPLIYCRSP	DFRIAFQEIIL	CLRRSSSKTY	NGYSSNSNG	RTDYTGEQSA	YQLGQEKENE	LLCEEAPGME	GFVNCQGTVP				
MACAQUE	NPLIYCRSP	DFRIAFQEIIL	CLRRSSLKAC	NGYSSNSNG	N...TGEQSG	YHLEQEKENK	LLCEDLPGTE	DFVGHQGTVP				
HAMSTER	NPLIYCRSP	DFRIAFQEIIL	CLRRSSSKAY	NGYSSNSNG	KTDYMGFASG	COLGQEKES	RLCEDPPGTE	SFVNCQGTVP				
CANFA	NPLIYCRSP	DFRIAFQEIIL	CLRRSSLKAY	NGYSSNSNS	RSDYAGEHSG	CHLGQEKDSE	LLCEDPPGTE	D...RQGTVP				
CAT	NPLIYCRSP	DFRIAFQEIIL	CLRRSSLKAY	NGYSSNSNS	RTDYAGEHSG	GPLGQEKDSE	VLCEDPPGTE	NLANRQGTVP				
HUMAN	NPLIYCRSP	DFRIAFQEIIL	CLRRSSLKAY	NGYSSNSNGTGEQSG	YHVEQEKENK	LLCEDLPGTE	DFVGHQGTVP				
HUMAN PROST	NPLIYCRSP	DFRIAFQEIIL	CLRRSSLKAY	NGYSSNSNGTGEQSG	YHVEQEKENK	LLCEDLPGTE	DFVGHQGTVP				
BOVIN	NPLIYCRSP	DFRIAFQEIIL	CLRRSSLKAY	NGGCSNSND	RTDYTGEQSG	YHLGEEKDSE	LLCEDPPGTE	NFVNQQTVP				
GUNEA PIG	NPLIYCRSP	DFRIAFQEIIL	CLRRSALKAY	GNDCCNSNG	KTDYTGEPNV	CHOGQEKERE	LLCEDPPGTE	DLVSCP GTVP				
PIG	NPLIYCRSP	DFRIAFQEIIL	CLRRSALKAY	NGYSSNSNG	RTDYTGEQSG	CYLGEEKDSE	RLCEDAPGPE	GCAHRQGTVP				
TROUT	NPLIYCRSP	EFRIYAFQEIIL	CLRGAAPTNP	GYIYRGHSLR	LSPKDKPG..	SLSNNVGTVE				
FUGU	NPLIYCRSP	EFRIYAFQEIIL	CMKRNRLTNP	gnGysRRHSWQSEQQGRSK	VSLEDSEANE				

10. G protein specificity 11. no G protein...

GRK5 (cont)

GRK2 (cont) 8. EBP50/N5F

	401		418
MOUSE	SLSVDSQGRN	CSTNDSPL	
RAT	SLSIDSQGRN	CNTNDSPL	
MACAQUE	SDNIDSQGRS	CSTNDSLL	
HAMSTER	SLSLDSQGRN	CSTNDSPL	
CANFA	SDSVDSQGRN	CSTNDSLL	
CAT	NDSIDSQGRN	GSTNDSLL	
HUMAN	SDNIDSQGRN	CSTNDSLL	
HUMAN PROST	SDNIDSQGRN	CSTNDSLL	
BOVIN	SDSIDSQGRN	CSTNDSLL	
GUNEA PIG	SDSIDSQGRN	YSTNDSLL	
PIG	DDSTDSQGRN	CSTNDSML	
TROUT	LGSLsstIN	GYCNPPL	
FUGU	DKTVDPNG.N	CntVTTVL	

Figure 5

Sequence alignment of the carboxy terminal tail of B2AR. (1) Proposed to be AP-2 binding sequence; L339 and L340 are highly conserved across GPCRs (Schulein et al., 1998). Mutation of LL inhibits endocytosis (Gabilondo et al., 1997). (3) and (5) GRK phosphorylation sites, see Figure 2. (4) C341 is covalently attached to the lipid palmitate (O'Dowd et al., 1989). (6) Co-immunoprecipitation of c-Src and related kinases with B2AR requires Y350 (Fan et al., 2001a). (7) eIF-2 β binds B2AR and other receptors sharing the DFRxxFxxxL sequence (Klein et al., 1997). GASP may bind a mutant B2AR at FR (332 and 333) (Simonin et al., 2004; Whistler et al., 2002) (8) *In vitro* binding of EBP50/NHERF to B2AR requires D(S/T)xL (Hall et al., 1998a; Hall et al., 1998b). *In vitro* binding of NSF to B2AR requires SLL (Cong et al., 2001a). (9) Helix 7 of inactive rhodopsin ends at the conserved NPxY motif. An amphipathic helix, helix 8, follows, ending before C341 (Palczewski et al., 2000). (10) Chimaeric receptors demonstrate that a region including helix 8 (327-339) is involved in G protein specificity (Liggett et al., 1991). Residues downstream of 343, by contrast, are probably not involved in G protein binding (Dixon et al., 1987). (12) HRS binds within this region of the B2AR tail, directly or indirectly; K380 is not required for this interaction (Aylin Hanyaloglu, personal communication).

GRKs may also phosphorylate cytosolic proteins: *in vitro*, GRK2 can phosphorylate tubulin (Pitcher et al., 1998b), and GRK6 can phosphorylate EBP50/NHERF, a protein that is associated with B2AR (Hall et al., 1999).

The increase in heart rate that is caused by B1AR signaling appears to be unaffected by either GRK2 or GRK5 (Koch et al., 1995). It is thought that GRKs are not involved in desensitization of B1AR: in numerous cell types, B1AR does not rapidly endocytose after agonist treatment (Xiang et al., 2002a). The effect of GRKs on B2AR *in vivo* is difficult to measure. Whether GRKs are involved in protecting the heart from

damage, the presumed function of B2AR, has not been directly tested. However, GRK2 mRNA is up-regulated in patients with heart damage, which suggests that desensitization of B2AR by GRK2 protects the heart from damage (Dzimiri et al., 2004; Ungerer et al., 1993).

Non-Visual Arrestins (Ferguson, 2001; Gurevich and Gurevich, 2004) Phosphorylation of the carboxy terminal tail by GRKs has been proposed to both activate arrestin and to make the third loop of the receptor accessible to bind this activated arrestin (Kim et al., 2004; Whistler et al., 2001). Bound arrestin, in turn, prevents the receptor from coupling to G protein by blocking the third cytoplasmic loop from binding to G α (Figure 2). There are two ubiquitously expressed (i.e. non-visual) arrestins in mammalian tissues, arrestin 2/ β arrestin and arrestin 3/ β arrestin 2, and only one each in *C. elegans* and *Drosophila* (*C.e.*: arrestin 1, *D.m.*: arrestin 2) (Fukuto et al., 2004; Klebes et al., 2002). The two mammalian non-visual arrestins are 80% identical in their receptor-binding domains, and they bind with similar affinities to family A receptors (Gurevich et al., 1995; Wu et al., 1997; but see Mukherjee et al., 2002). However, these arrestins are differently regulated *in vivo*. Only arrestin 3 is strongly recruited to the plasma membrane by activated B2AR in transfected cells, with a $t_{1/2}$ estimated to be 20-30 sec (Oakley et al., 2000). This difference in recruitment may explain why, in some cell lines, arrestin 3 is the primary arrestin that desensitizes cells in response to B2AR agonists (Ahn et al., 2003; Pippig et al., 1993; but see Kohout et al., 2001; Mundell et al., 1999).

Arrestin 3 may be strongly recruited to receptors such as the B2AR because of unique residues in its c-terminal domain. This so-called "R2" domain (regulatory domain

2) is highly divergent between the visual and non-visual arrestins, and is thought to associate the non-visual arrestins with clathrin-coated pits *in vivo* (Krupnick et al., 1997; Laporte et al., 2000). The R2 domain of arrestin 3 also binds to clathrin more tightly than arrestin 2 *in vitro*; however, it is not clear whether this binding occurs *in vivo* (reviewed by (Ferguson, 2001)). The R2 domains of arrestin 2 and 3, which are only about 50% identical, are both constitutively phosphorylated but on different residues. Mutational data suggests that phosphorylation of the R2 domain inhibits arrestin 2 but does not inhibit arrestin 3 (Kim et al., 2002; Lin et al., 1997). There is evidence that the inhibitory phosphorylation of arrestin 2 is caused by a MAP kinase (mitogen activated kinase, also called extracellular signal activated kinase or ERK) (Lin et al., 1999). There is evidence that the casein kinase II phosphorylates of arrestin 3, but the function of this phosphorylation is still unclear (Kim et al., 2002).

The increase in heart rate that is caused by B1AR signaling appears to be unaffected by either arrestin 2 or arrestin 3 (Conner et al., 1997; Walker et al., 1999). This is consistent with the findings that GRKs are not responsible for at desensitization of B1AR, with respect to control of heart rate (Koch et al., 1995). Unlike GRK2, arrestin 2 mRNA is not up-regulated in damaged hearts. Perhaps arrestin 3 acts with GRK2 to promote the endocytosis of B2AR in the heart (Ungerer et al., 1993).

Signaling to G_i Because G_i inhibits adenylyl cyclase, activation of G_i is a mechanism to rapidly turn off signaling from the G_s pathway. In myocytes, B2AR signaling to G_s is strongly inhibited by its signaling to G_i (Xiao et al., 1999a). Signaling of B2AR to G_i in cardiac myocytes appears to occur after a lag of several minutes,

theoretically enabling B2AR to stimulate G_s briefly (Devic et al., 2001). However, the downstream effect of B2AR stimulation in myocytes is independent of PKA, indicating that B2AR can somehow bypass PKA.

In the heart, it is thought that B2AR signaling to G_i is critical for its function. Stimulation of B2AR does not increase the rate of heart contractions, while activation of G_s by B1AR does (reviewed by (Lohse et al., 2003). Because B2AR can activate G_i in heart cells, and because excessive G_s signaling can damage the heart, is possible that B2AR inhibits G_s signaling from B1AR, thereby protecting the heart from excessive stimulation (Communal et al., 1999; Engelhardt et al., 1999; Zhu et al., 2001). However, the protective effects of B2AR appear to require signaling by the $\beta\gamma$ subunits of G_i (Zhu et al., 2001).

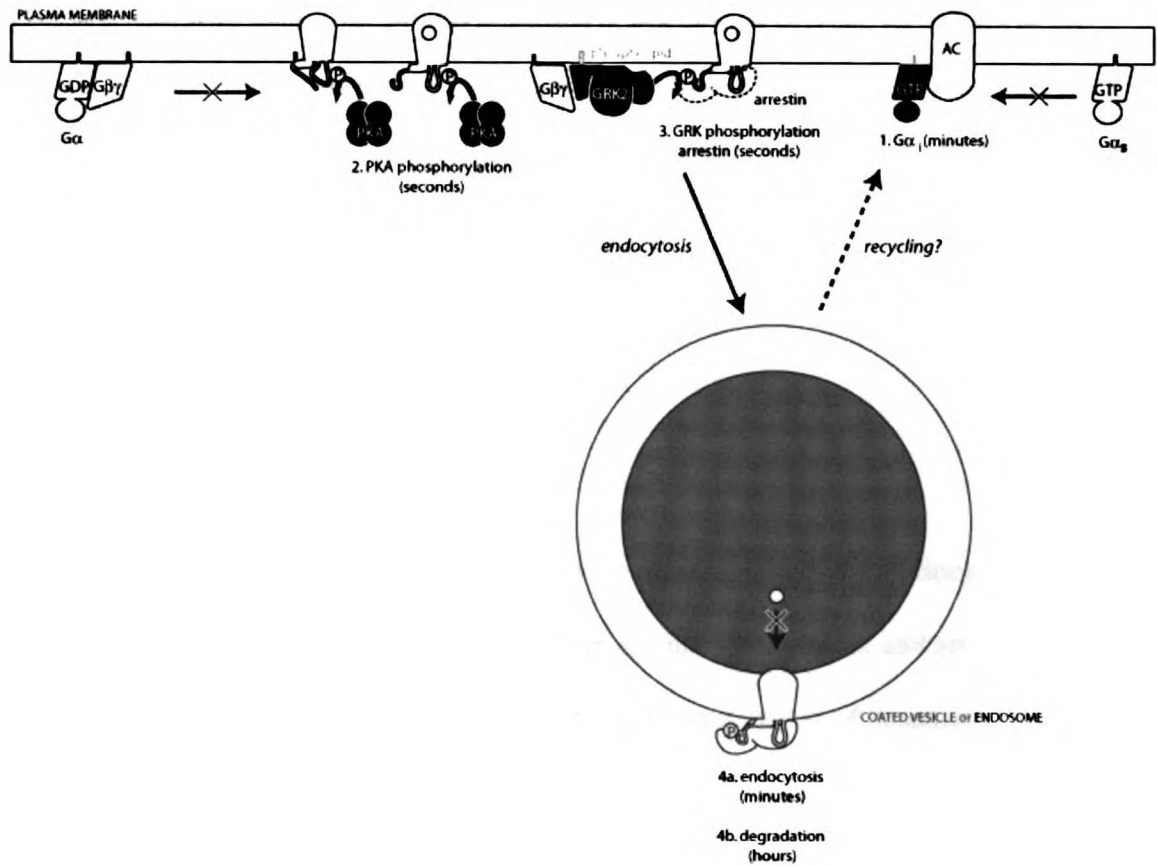


Figure 6

The signaling triggered by GPCR agonists can block signaling from further agonist treatments by a number of mechanisms. (1) Activated $G\alpha_i$ inhibits adenylyl cyclase (AC); this blocks $G\alpha_s$ signaling cascades. Agonist treated B2AR slowly activates $G\alpha_i$, with a lag of about 10 minutes (Devic et al., 2001). It has been proposed (dashed line) that B2AR must first be recycled from endosomes to signal to $G\alpha_s$. (2) PKA phosphorylation of active or inactive GPCRs in their third intracellular loop blocks them from coupling to G proteins. PKA is rapidly activated by $G\alpha_s$ signaling cascades, with a $t_{1/2}$ of about 2 minutes (Roth et al., 1991). (3) GRK phosphorylation of active GPCRs at sites in their carboxy terminal tail permits arrestin to bind (dotted outline); arrestin binding blocks GPCRs from coupling to G proteins. GRK itself is rapidly activated by GPCRs with a $t_{1/2}$ of about 15 seconds (Roth et al., 1991). Arrestin recruitment is slightly slower, with a $t_{1/2}$ of about 20–40 seconds (Oakley et al., 2000). GRK2, which is recruited to the

plasma membrane by phospholipids and by Gβγ, is shown. (4a) GRK phosphorylation and arrestin binding cause GPCRs to be endocytosed. In endosomes, low pH blocks agonists from binding; furthermore, agonists applied extracellularly cannot enter endosomes to activate these receptors. Endocytosis occurs with a $t_{1/2}$ of about 3 minutes, so in theory this process could contribute to desensitization (Yu et al., 1993). (4b) Endocytosed GPCRs can be degraded in the lysosomes; this leads to a decrease in the total number of GPCRs. Degradation occurs over several hours.

1.4.2 *Control of Receptor Number*

Because endocytosis removes receptors from the plasma membrane, endocytosis in theory should also cause desensitization. However, phosphorylation and arrestin binding, which precede receptor endocytosis, are the predominant causes of desensitization during short periods of agonist treatment (Pippig et al., 1995). Agonist-bound B2AR are rapidly endocytosed within minutes, whereas phosphorylation occurs within seconds. Arrestin can then potentially have a dual role in reducing cellular responsiveness: it both blocks G protein coupling and it links the receptor to the endocytic machinery, thereby triggering its endocytosis (Ferguson, 2001). Removal of receptors by endocytosis is transient; B2AR exogenously expressed in tissue culture cells is returned to the plasma membrane within minutes of endocytosis (reviewed in (Tsao et al., 2001)).

After many hours of continuous treatment with agonist, however, B2AR is degraded (Moore et al., 1999a). Under these conditions, this loss of total cellular B2AR can therefore lead to significant desensitization. Overexpression of GRK5 in tissue culture cells causes B2AR to degrade over a few hours, which indicates that in certain

cellular contexts, B2AR number may be controlled by degradation even during relatively short agonist treatment (Cao et al., 1999).

The process by which receptors return to the plasma membrane is called recycling. In the case of GPCRs, recycling can be accompanied by dephosphorylation, so the returned receptor can once again couple to G proteins (Figure 7). Recycling reverses desensitization caused by GRKs and by endocytosis. This reversal of desensitization is called “resensitization.”

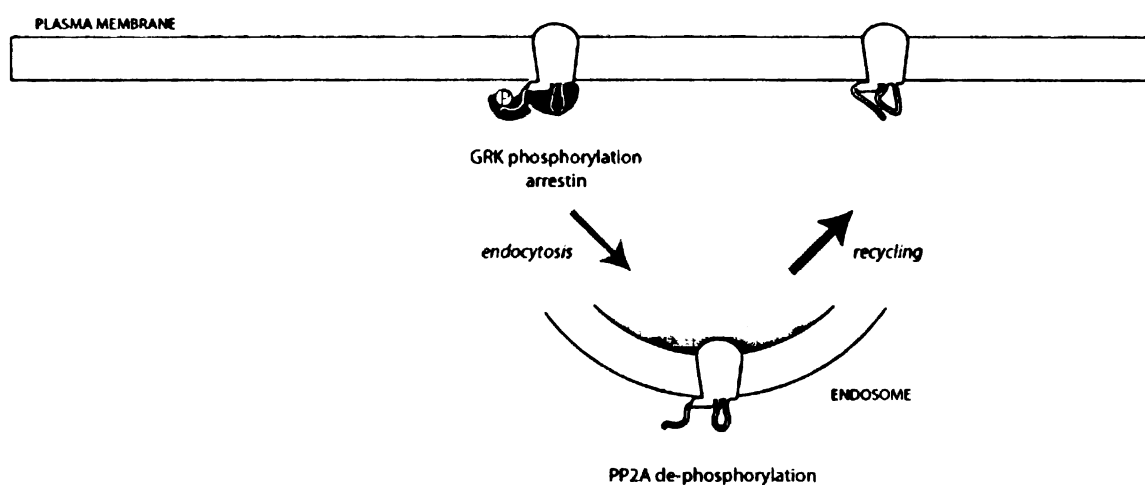


Figure 7

Trafficking of B2AR. At the plasma membrane, the carboxy-terminal tail of agonist-bound B2AR is phosphorylated by GRK, which enables arrestin to bind. Arrestin binding triggers endocytosis. In endosomes, PP2A de-phosphorylates B2AR. De-phosphorylated B2AR can be recycled to the plasma membrane in a conformation that can once again bind to ligand and activate G proteins.

1.5 TRAFFICKING

Endocytosis, recycling, and degradation are complicated processes that involve the formation and dissolution of large, multi-protein complexes on membranes. Relative to other organelle transport systems, we know relatively little about how proteins are moved through the endocytic system. The discovery that arrestin binds to components of clathrin coated pits at the plasma membrane has greatly aided our understanding of how GPCRs are endocytosed. However, the mechanism by which GPCRs are recycled or degraded is still largely unknown. The identification of a sequence on B2AR which is required for its recycling, and that this sequence can bind to EBP50/NHERF *in vitro*, may enable us to better understand how B2AR is recycled.

1.5.1 *Endocytosis*

To better understand the mechanism by which B2AR endocytoses, I will now contrast what is known of B2AR endocytosis with that of other well-studied receptors. Studies of exogenously expressed B2AR in mammalian cell lines have demonstrated that once B2AR binds agonist at the plasma membrane, it is rapidly internalized by the process of endocytosis, and then returned to the cell surface by a process called recycling. This itinerary of endocytic trafficking is very similar to the transferrin receptor, for which the details of trafficking have been extensively studied. One important difference between the endocytosis of these two receptors is that the transferrin receptor is continually and rapidly endocytosed (*review*), whereas B2AR endocytosis is regulated such that it

endocytosis is increased by binding agonist (Ferguson, 2001; Yu et al., 1993). Therefore, transferrin receptor is known as a “constitutively internalizing” receptor and B2AR as a “ligand-regulated” receptor.

Despite these differences, both agonist-bound B2AR and transferrin receptor enter coated pits, which are a major site of endocytosis in eukaryotes (Cao et al., 1998; Goodman et al., 1996; Santini et al., 2002; von Zastrow and Kobilka, 1994; Zhang et al., 1996). However, in at least some cell types, agonist-bound B2AR enters coated pits from specialized sub-domains of the plasma membrane that contain caveolar proteins (Ostrom et al., 2001; Rybin et al., 2000; Xiang et al., 2002b; but see also Odley et al., 2004). Transferrin receptor is not enriched in these “microdomains” (Harder et al., 1998; Montixi et al., 1998). Interestingly, a minority of coated pits that contain transferrin receptor appear to exclude B2AR, and vice versa (Cao et al., 1998). Agonist activation of B2AR triggers arrestin 3 to translocate to pre-existing coated pits on the plasma membrane (Santini et al., 2002; Scott et al., 2002). These pits presumably become competent to recruit B2AR, whereas transferrin receptor can enter coated pits that do not contain arrestin. To bind arrestin, B2AR must be phosphorylated, and receptor phosphorylation appears to be required for receptors to exit plasma membrane microdomains (Ostrom et al., 2001).

B2AR appears to require additional proteins that, along with arrestin, enable its endocytosis, which are not required for the endocytosis of transferrin receptor. The amount of endocytosed B2AR but not transferrin receptor decreases upon overexpressing an ARF GTPase activator, GIT1, and increases upon overexpressing the chaperone NSF (Claing et al., 2000; Cong et al., 2001a; Coppolino et al., 2001; McDonald et al., 1999). It

is not yet known whether GIT1 and NSF function before or after arrestin binding, or whether they allow entry into a subpopulation of coated pits. B2AR clustered in coated structures cannot internalize at temperatures below 16°C, while transferrin receptor can internalize at temperatures above 4°C (Cao et al., 1998; Ferguson, 2001; Santini et al., 2002; von Zastrow and Kobilka, 1994). It is not known what protein (or lipid) underlies this temperature sensitivity.

B2AR also appears to be ubiquitinated after agonist binding, but before endocytosis (Shenoy et al., 2001). Because ubiquitination is transient, it is difficult to know the degree to which the B2AR or the transferrin receptor may be ubiquitinated. Eps15, which has a ubiquitin-binding motif, may be required to promote endocytosis of the transferrin receptor (Carbone et al., 1997; but see also Confalonieri et al., 2000). However, lysine residues, generally the sites of ubiquitination, are not necessary for the rapid endocytosis of either the B2AR or the transferrin receptor (Jing et al., 1990; Shenoy et al., 2001). It has been proposed that ubiquitination of the B2AR plays a role later in endocytosis, perhaps in the long-term degradation of the receptor.

1.5.2 *Endocytosis sequences*

Differences between the endocytosis of B2AR and of transferrin receptor may result from specific sequences within their cytoplasmic domains. The sequences that have been identified on these receptors are thought to connect them to the same destination: to AP-2 and clathrin coated pits. But while transferrin receptor can constitutively associate with coated pits, the association of B2AR with pits is regulated by its association with arrestin.

B2AR can also bind to PDZ domain containing proteins, and these proteins may also influence receptor endocytosis.

Adaptor Protein Binding B2AR contains groups of basic residues within the third cytoplasmic loop; groups of basic residues within certain GPCRs have been shown to bind directly to arrestin (Figure 2) (DeGraff et al., 2002; but see Mukherjee et al., 2002). While phosphorylated peptides from the c-terminal tail of certain receptors can bind to arrestins in vitro, the c-terminal tail of B2AR is not absolutely required to bind arrestins (Ferguson et al., 1996). B2AR also contains a pair of cytoplasmic leucines in its cytoplasmic tail that are required for efficient endocytosis (Figure 5) (Gabilondo et al., 1997). It has been proposed that this sequence binds to AP-2 to promote endocytosis; however, it lacks an acidic amino acid or a serine at an upstream position that are found in other sequences that can bind AP-2 (Bonifacino and Traub, 2003; Pitcher et al., 1998a). Transferrin receptor, on the other hand, contains a Yxx ϕ motif which can bind to AP-2 and promote endocytosis of the receptor. These three possible AP-2 binding sequences (corresponding to the Yxx ϕ motif of transferrin receptor, the paired leucines of B2AR, and the AP-2 binding site of arrestin) should not interfere with each other because they bind at separate sites on AP-2 (Traub, 2003). Indeed, the endocytosis of B2AR does not interfere with the endocytosis of transferrin receptor (Marullo et al., 1999). It is not yet clear whether these identified endocytosis sequences can account for the observed differences between the endocytosis of B2AR and transferrin receptor.

PDZ Protein Binding The carboxy terminal tail of B2AR and B1AR can bind PDZ domains *in vitro*. The tail of B2AR binds to the PDZ domains of EBP50/NHERF (50 kDa ERM-binding phosphoprotein/Na⁺-H⁺ exchanger regulatory factor) and E3KARP/NHERF2 (Na⁺-H⁺ exchanger 3 kinase A regulatory protein). The tail of B1AR binds to the PDZ domains on PSD-95, MAGI-2, and CN-RasGEF (reviewed in (Hall, 2004)); PSD-95 inhibits B1AR endocytosis, whereas MAGI-2 enhances it. It is not known whether EBP50/NHERF affects the endocytosis of B2AR. However, indirect evidence suggests that EBP50/NHERF inhibits the endocytosis of B2AR. The tail of B2AR binds the chaperone NSF *in vitro* in a nucleotide-selective manner; the chaperone activity of NSF may help dissociate PDZ proteins from their ligands (Cong et al., 2001a; Gage et al., 2004; Whiteheart and Matveeva, 2004). Mutation of the NSF binding site on the B2AR tail appears to inhibit B2AR endocytosis, which suggests (to me) that B2AR release from PDZ proteins is required for endocytosis (Cong et al., 2001a). Michael Gage in our laboratory has confirmed that mutation of the NSF binding site inhibits the endocytosis of B2AR (personal communication).

1.5.3 *Recycling*

After endocytosis, B2AR and transferrin receptor efficiently return to the plasma membrane (Figure 6). This return of receptors is known as “recycling,” because the returned receptor is once again able to bind agonist. B2AR can recycle to the plasma membrane with a similar rate as transferrin receptor (B2AR $t_{1/2}$ =8-17 min, transferrin receptor $t_{1/2}$ =10min (Barak and Caron, 1995; Mayor et al., 1993; Moore et al., 1999b; Pippig et al., 1995). However, while transferrin receptor appears not to require a specific

recycling sequence, the carboxy terminus of B2AR is required for its recycling (Cao et al., 1999; Jing et al., 1990). To better understand the mechanism by which the B2AR recycling sequence operates, we will highlight the known differences between B2AR recycling and transferrin receptor recycling. Then we will discuss what is known about the B2AR recycling sequence.

1.5.4 *Endosomes*

After endocytosis, B2AR and transferrin receptor can enter the same endosomes (Marullo et al., 1999; von Zastrow and Kobilka, 1992). Early endosomes and recycling endosomes are two major endosome types in nonpolarized cells (Ghosh and Maxfield, 1995). Both transferrin receptor and B2AR enter early endosomes; for B2AR this has been determined by its extensive co-localization with endogenous Rab5 (Moore et al., 1995). Rab11, which is found on recycling endosomes, colocalizes well with transferrin but poorly with B2AR at steady state (Daro et al., 1996; Innamorati et al., 2001; Ren et al., 1998; Ullrich et al., 1996). Therefore, we feel that this data reflects that B2AR accumulates in early endosomes at steady state, in contrast with transferrin receptor, which accumulates in recycling endosomes. Furthermore, these studies suggest that endosomes that contain transferrin receptor but not B2AR are probably recycling endosomes (Marullo et al., 1999). Therefore, B2AR may require additional proteins, either to recycle from early endosomes or to be restricted from recycling endosomes.

Additional evidence suggests to us that B2AR recycles from early endosomes, whereas transferrin receptor recycles from both early and recycling endosomes. Rab4 is a GTPase that has been located on early endosomes and, more recently, on a subdomain of

recycling endosomes (Daro et al., 1996; Sonnichsen et al., 2000; van der Sluijs et al., 1992; van Der Sluijs et al., 1991). The Rab4-dependent step of recycling, proposed to be from early endosomes, may be easier to detect in cells where the transferrin has been endocytosed at 20°C, a condition that has been used to accumulate transferrin in the early endosome (Ren et al., 1998). In one study where transferrin was endocytosed at 20°C, overexpression of wild type Rab4 appeared to increase the amount of transferrin that recycles to the apical membrane in polarized cells (Mohrmann et al., 2002). In separate studies, overexpression of the Rab4 mutant N121I, which does not bind GTP, briefly increased the accumulation of B2AR but not transferrin (presumably exiting recycling endosomes) inside cells (Seachrist et al., 2000; van der Sluijs et al., 1992). Furthermore, in another experiment, a pulse of endocytosed B2AR recycled slower when Rab4 N121I was overexpressed (Seachrist et al., 2000). Therefore, efficient recycling of B2AR appears to require GTP-bound Rab4 briefly after endocytosis, presumably in early endosomes, whereas efficient recycling of transferrin receptor from recycling endosomes does not.

Complementary experiments have been performed that suggest to us that unlike transferrin receptor, the bulk of B2AR does not recycle from recycling endosomes. Rab11 is another endosomal GTPase; it is thought to control recycling from both the early endosome and the recycling endosome (Ren et al., 1998). As was shown with Rab4, transferrin receptor and B2AR appear to have different requirements for GTP-bound Rab11 during recycling. Overexpression of wild type Rab11 reduces the recycling of transferrin but not B2AR, whereas the recycling of both transferrin and B2AR are reduced by a mutant Rab11 that cannot bind GTP (Moore et al., 2004; Ren et al., 1998).

When transferrin is endocytosed at 20°C, overexpression of wild type Rab11 does not reduce the recycling of transferrin receptor (Ren et al., 1998). Therefore, it appears that efficient recycling of B2AR and of transferrin receptor in early endosomes requires GTP-bound Rab11, whereas transferrin in recycling endosomes requires both GTP-bound Rab11 and hydrolysis of the GTP on Rab11 (Moore et al., 2004; Ren et al., 1998). Together, the localization of B2AR and its sensitivity to mutant Rab proteins suggests to us that B2AR recycles predominantly from early endosomes and not from recycling endosomes.

However, that does not mean that B2AR cannot recycle from recycling endosomes. The recycling of transferrin from recycling endosomes is reduced by bafilomycin A1, an inhibitor of the vacuolar proton pump; bafilomycin A1 also inhibits the recycling of B2AR (Moore et al., 1999b; Presley et al., 1997).

1.5.5 *Recycling Sequences*

A basolateral recycling sequence has been identified on transferrin receptor that is required for its efficient recycling to the basolateral domain; this sequence may be involved in its exit from recycling endosomes. This sequence is thought to bind adaptor proteins. The PDZ binding domain at the carboxy terminus of B2AR, by contrast, has been identified as the recycling sequence of B2AR. Several proteins that bind this sequence, including EBP50/NHERF, have been implicated in B2AR recycling.

Adaptor Protein Binding A mutant transferrin receptor lacking a cytoplasmic domain recycles efficiently in nonpolarized cells (Jing et al., 1990), This result has been

interpreted either as recycling by “default,” or, less frequently (but with equal possibility), as recycling by a non-cytoplasmic recycling sequence. In polarized cells, transferrin does appear to contain a cytoplasmic recycling sequence: a sequence containing the Yxx ϕ motif, a possible beta-turn and a phosphorylated serine is required for efficient basolateral recycling of the receptor (Odorizzi and Trowbridge, 1997; Rothenberger et al., 1987). As Yxx ϕ can bind AP-2, transferrin receptor may bind to another adaptor protein (possibly AP-1) during recycling to the basolateral membrane in polarized cells (Traub and Apodaca, 2003). An ARF GTPase, some of which can bind to AP proteins, is also involved in efficient transferrin recycling in polarized cells (Futter et al., 1998; Nie et al., 2003; Wan et al., 1992). Recently, point mutants of the Yxx ϕ motif have been shown to decrease exit of receptors from the recycling endosome in non-polarized cells, indicating that transferrin receptor may utilize a recycling sequence in non-polarized cells as well (Dai et al., 2004).

It is not clear whether the adaptor protein linking sequences of B2AR -- the arrestin-binding sequence, and possibly the paired leucines -- are required for efficient recycling of this receptor. The carboxy terminal tail of B2AR, which is thought to contain an arrestin activation site but is not required for arrestin binding, is required for efficient recycling (Cao et al., 1999). Furthermore, arrestin does not co-localize with B2AR in endosomes (Ferguson, 2001). Therefore, in contrast to the recycling sequence of transferrin receptor, the recycling sequence of B2AR does not appear to interact with adaptor proteins.

Phosphorylation Like the cytoplasmic recycling sequence of the transferrin receptor, this recycling sequence of B2AR is phosphorylated. Dephosphorylation of the B2AR appears to be required for its recycling: B2AR is dephosphorylated before it recycles, and mutation of Ser411 prevents it from efficiently recycling in transfected cells (Cao et al., 1999). Dephosphorylation probably occurs after endosome pH drops but before exiting endosomes that contain Rab4, presumably early endosomes (Krueger et al., 1997; Pippig et al., 1995; Seachrist et al., 2000; Sibley et al., 1986).

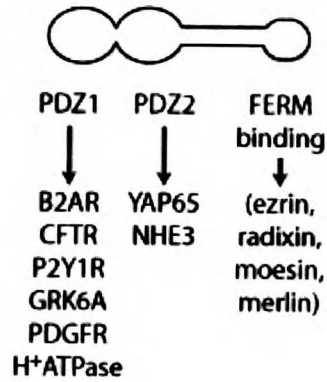
PDZ Domain Protein Binding and Actin Ser411 is part of a short sequence within B2AR that can bind to EBP50/NHERF, E3KARP/NHERF2 and to NSF (Figure 5) (Cao et al., 1999; Cong et al., 2001a; Hall et al., 1998a; Hall et al., 1998b). EBP50/NHERF, actin, and NSF have each been implicated in promoting B2AR recycling (Cao et al., 1999; Claing et al., 2001; Cong et al., 2001a; Gage et al., 2001; Xiang and Kobilka, 2003a). However, EBP50/NHERF binding but not NSF binding has been demonstrated to be sufficient to recycle a chimaeric receptor (Gage et al., 2004). EBP50/NHERF is thought to bind actin via an ERM, possibly ezrin, because cells that do not have apical ezrin mis-sort B2AR (Huang et al., 2003). It has been proposed that a complex of B2AR, EBP50/NHERF, ezrin and actin promotes B2AR recycling, and that the chaperone activity of NSF and/or phosphorylation by GRK5 disassembles this complex (Cao et al., 1999; Whiteheart and Matveeva, 2004).

While it is not known whether such a complex forms on endosomes, exogenously expressed NSF and EBP50/NHERF can be found on structures that contain agonist-treated B2AR (Cong et al., 2001a; Hall et al., 1998b). E3KARP/NHERF2, which is

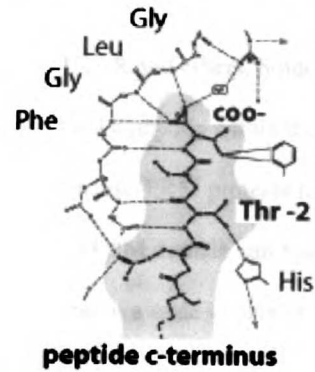
homologous to EBP50/NHERF, and merlin, an ERM, have each been localized to intracellular vesicles (LaJeunesse et al., 1998; Obremski et al., 1998; Scoles et al., 2000; Wade et al., 2003). EBP50/NHERF and ezrin are more closely apposed to the plasma membrane (Wade et al., 2003). These localizations predict that B2AR binds to a complex of EBP50/NHERF/ezrin at the plasma membrane but to E3KARP/NHERF2/merlin in endosomes.

It is still unclear whether B2AR recycling has a unique requirement for actin, or whether other proteins such as transferrin also require actin to recycle. The actin involved in B2AR recycling may be directly associated with the plasma membrane: mutants of Arf6, a protein that regulates actin assembly at the apical plasma membrane (Altschuler et al., 1999; Cavenagh et al., 1996; Macia et al., 2004; Peters et al., 1995), reduce the recycling of B2AR (Claing et al., 2001). By contrast, neither EBP50/NHERF nor actin appears to promote transferrin recycling, and a role for Arf6 in transferrin recycling is controversial (Altschuler et al., 1999). Overexpression of a mutant EPB50 gene or depolymerization of actin filaments does not inhibit the recycling of transferrin receptor, but does inhibit the recycling of B2AR (Cao et al., 1999; Durrbach et al., 1996). It should be noted, however, that in polarized cells depolymerization of actin inhibits the recycling of transferrin receptor to the basolateral plasma membrane (Sheff et al., 2002). Therefore, actin may play a general role in recycling, at least in polarized cells.

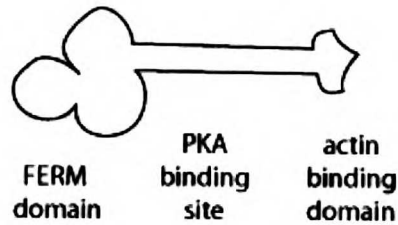
A.
EBP50 family



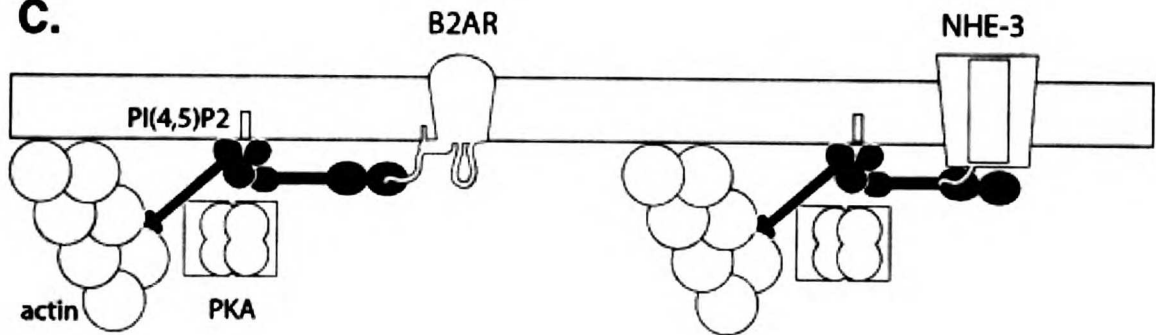
B. PDZ domain bound to c-terminus



ERM family



C.



D.

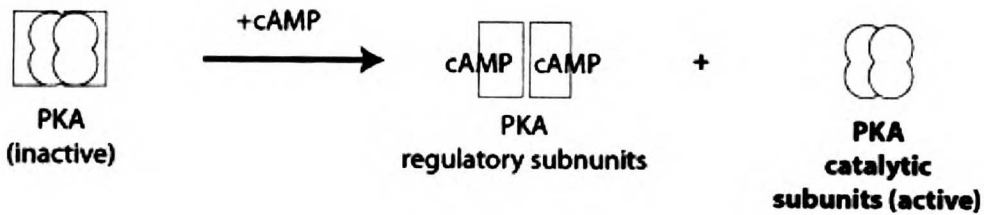


Figure 8

EBP50/NHERF and ERM proteins. (A) EBP50/NHERF has two N-terminal PDZ domains, an alpha helical region, and a carboxy terminal FERM binding domain. PDZ domains can bind the c-terminus of membrane proteins; PDZ1 can bind to the c-terminus of membrane proteins such as B2AR and others. Some PDZ domains can also bind peptides outside the carboxy terminus; PDZ2 can bind a peptide within the cytoplasmic domain of NHE3. PDZ domains may also bind other PDZ domains. ERM proteins have a FERM domain, an alpha helical region, and an actin-binding domain. The FERM domain can bind to lipids in the plasma membrane, such as phosphatidylinositol-4,5-bisphosphate, and to a wide variety of proteins, including EBP50/NHERF family members (Bretscher et al., 2002). The alpha-helical region can bind to the regulatory subunits of PKA. When the regulatory subunits bind cAMP, they release active PKA (Dransfield et al., 1997); Gronholm, 2003 #900}. (B) X-ray crystallography has demonstrated that PDZ domains bind directly to the carboxylate group at the carboxy terminus. Reprinted from Cell, Vol. 85, Doyle D. A., Lewis J., Kim. E., Sheng M. and MacKinnon R., "Crystal structures of complexed and peptide-free membrane protein-binding domain: molecular basis of peptide recognition by PDZ," p. 1071 Figure 4, Copyright (1996), with permission from Elsevier. (C) Model of two complexes of EBP50/NHERF, an ERM protein, actin, and PKA and PI(4,5)P2. In one, the carboxy terminus of B2AR is bound to PDZ1 of EBP50/NHERF. In the second, NHE3 is bound to PDZ2 of EBP50/NHERF. It has been postulated that both PDZ domains of EBP50/NHERF can be bound to receptors simultaneously. (D) The regulatory subunits of PKA can bind to ERM proteins and other AKAPs. cAMP binds the regulatory subunits of PKA, the kinase or catalytic subunits are released. Released catalytic subunits are active and able to phosphorylate target proteins.

HRS Recently, Aylin Hanyaloglu in our laboratory has discovered that the endosomal protein HRS (hepatocyte growth factor regulated tyrosine kinase substrate) promotes the recycling of certain GPCRs (irrespective of PDZ binding), but not transferrin receptor, in

transfected cells. It may be that HRS promotes recycling of receptors from the early endosome, but this has yet to be tested.

The mechanism by which HRS promotes the recycling of B2AR is also not understood. HRS may directly bind transmembrane proteins: transmembrane proteins may be transiently conjugated to ubiquitin on cytoplasmic lysine residues before they are endocytosed, and HRS may bind endocytosed proteins via its ubiquitin binding domain, and (Aguilar and Wendland, 2003; Raiborg et al., 2001). There is evidence that B2AR (or a co-precipitated protein) is transiently ubiquitinated after agonist stimulation but before endocytosis (Shenoy et al., 2001). However, the cytoplasmic lysines of B2AR are not necessary for HRS to promote B2AR recycling. Therefore, it is not clear whether HRS promotes B2AR recycling by directly binding to the receptor (Figure 5).

1.6 EBP50/NHERF

In considering the regulation of BARs in general, cytosolic proteins with PDZ domains are clearly important. The signaling of B2AR, as well as its endocytosis and recycling, is regulated by its PDZ ligand sequence *in vivo*, which binds tightly to EBP50/NHERF *in vitro*. The molecular details of this regulation, however, remain highly speculative.

1.6.1 Functions of EBP50/NHERF

1.6.1.1 *Binding B2AR in vivo*

The short EBP50/NHERF binding sequence at the carboxy terminus of B2AR is also required for B2AR signaling in the heart and kidney. In cell lines, B2AR activation of the kidney Na⁺/H⁺ exchanger, NHE3, requires its carboxy terminal EPB50 binding sequence (Hall et al., 1998b). In cardiac myocytes, B2AR signaling through G_i also depends on its carboxy terminal EPB50 binding sequence (Xiang and Kobilka, 2003a). Therefore, B2AR signaling NHE3 in the kidney and through G_i in the heart appears to require EBP50/NHERF binding, either directly or indirectly.

1.6.1.2 *Other functions of EBP50/NHERF and ERM proteins*

EBP50/NHERF and ERM proteins have many other functions that do not involve B2AR. These functions may help us understand the mechanism for how EBP50/NHERF functions in the heart and kidney, and how it promotes B2AR recycling. First, EBP50/NHERF can recruit cytosolic proteins to specific transmembrane proteins. For example, the second PDZ domain of EBP50/NHERF binds to a cytoplasmic sequence within NHE3. The coiled coil domain of ERMs can bind to the regulatory subunits of PKA (reviewed in (Shenolikar and Weinman, 2001)). NHE3 is a Na⁺/H⁺ exchanger that is localized to the apical plasma membrane of epithelial cells in the kidney and intestine. The function of this complex of EBP50/NHERF, PKA and NHE3 is likely to inactivate NHE3, and hence decrease H⁺ secretion, in response to hormones that activate PKA. A second function of EBP50/NHERF and ERM proteins is to recruit cytosolic proteins to specific membrane domains. A PDZ domain of EBP50/NHERF can also bind the cytosolic protein YAP65 (Yes-associated Protein 65). YAP65 binds to c-Yes, a kinase

that has a covalent lipid anchor and that is found in membrane “rafts”(McCabe and Berthiaume, 2001). There is evidence that EBP50/NHERF is responsible for the localization of YAP65 and c-Yes to the apical plasma membrane (Mohler et al., 1999). Some functions of this complex at the apical plasma membrane of airway epithelial cells may be to inactivate the ion channel CFTR there (Cystic Fibrosis Transmembrane conductance Regulator) (Fischer and Machen, 1996) and to close gap junctions (Huang et al., 2003) in response to infection. It is possible that EBP50/NHERF recruits Yes to B2AR, as c-Yes co-immunoprecipitates with B2AR in transfected cells; Yes and B2AR bind to different PDZ domains on EBP50/NHERF (Shumay et al., 2002). ERM proteins can also directly recruit cytosolic proteins to specific plasma membrane domains. The same domain on ERM proteins that binds to EBP50/NHERF can also bind to RhoGDI, a cytosolic protein that binds to and inhibits the activity of Rho. Rho, like c-Yes, has a covalent lipid anchor and is found in caveolae, which are a type of membrane microdomain (Michaely et al., 1999); c-Yes can also bind to and activate Rho kinase. A function of this complex may be to inhibit Rho activity, and therefore inhibit cell-cell or cell-substratum contacts during epithelial cell polarization (Speck et al., 2003).

1.6.2 Proposed Mechanism of Action on B2AR

While recruitment of cytosolic proteins has been a known function of EBP50/NHERF, in general other, more complex models have been proposed to explain the function of EBP50/NHERF in the kidney and in the heart.

1.6.2.1 Titration

EBP50/NHERF binding enables B2AR to signal to NHE3. Like B2AR signaling in the heart, B2AR activation of NHE3 in the proximal tubule of the kidney is independent of a G_i /PKA cascade (Singh and Linas, 1996). Catecholamines do not have the same effects as activation of PKA in these cells (Hall et al., 1998b; Kudo et al., 1991; Liu and Cogan, 1989; Moe et al., 1995). Indeed, PKA inactivates NHE3 *in vitro* (reviewed in (Shenolikar and Weinman, 2001)). NHE3 and B2AR can each bind to distinct regions of EBP50/NHERF via their PDZ binding motifs. *In vitro*, EBP50/NHERF is required for PKA to inactivate NHE3 (Shenolikar and Weinman, 2001). Therefore, the Lefkowitz lab has proposed that B2AR sequesters EBP50/NHERF away from NHE3, which becomes inaccessible to phosphorylation (and inactivation) by PKA (Figure 9). This would be a novel mechanism to regulate EBP50/NHERF function (Bretscher et al., 2002). We do not favor this model because EBP50/NHERF has a much higher stoichiometry than B2AR in cells (the cellular concentration of EBP50/NHERF is about 1 μ M and B2AR--when overexpressed--is about 200 nM; (Reczek et al., 1997), and because B2AR and NHE3 bind to separate sites on EBP50/NHERF (reviewed in (Shenolikar and Weinman, 2001)).

Another model, which I favor, is that (by analogy with the model proposed to explain its function in the heart) recycled B2AR activates G_i in the proximal tubule, and that the $\beta\gamma$ subunits activate NHE3 directly. There is evidence that $\beta\gamma$ subunits, which can activate channels in other cell types, activate NHE3 *in vitro*, and $\beta\gamma$ subunits of G_i are responsible for the protective function of B2AR in cardiac myocytes (Albrecht et al., 2000; Zhu et al., 2001).

1.6.2.2 *Phosphorylation*

While a possible role of oligomerization of EBP50/NHERF has not been elucidated, it has been pointed out that EBP50/NHERF likely has an additional effect on NHE3 other than recruiting an AKAP (Moe, 1999). *In vitro*, EBP50/NHERF is required for purified PKA catalytic subunits to inhibit NHE3 in the absence of either PKA regulatory subunits or AKAPs. Therefore, EBP50/NHERF binding can enable PKA phosphorylation of NHE3 in the absence of AKAPs. Perhaps binding to EBP50/NHERF causes a conformational change in NHE3 that makes sites accessible to phosphorylation.

This model can also be applied to B2AR function in the heart. There, as we have mentioned previously, it has been proposed that PKA phosphorylation of B2AR is required for B2AR to signal via G_i . EBP50/NHERF binding to B2AR could enhance PKA phosphorylation of B2AR, thus enabling B2AR to signal via G_i .

1.6.2.3 *Enabling G_i signaling*

Several models have been proposed to explain how EBP50/NHERF enables B2AR to signal through G_i . It was initially proposed that PKA phosphorylation of B2AR is required for B2AR to couple to G_i ; however, it is still not clear whether this phosphorylation is required *in vivo* (Daaka et al., 1997; Devic et al., 2001). It is possible that EBP50/NHERF recruits PKA (via ezrin) to B2AR, and that PKA then phosphorylates B2AR. Alternatively, because the EBP50/NHERF binding domain of B2AR is also required for B2AR to recycle, it has been proposed that recycled B2AR signals through G_i (Xiang and Kobilka, 2003a). Interestingly, monensin, which inhibits

recycling, appears to prevent B2AR from increasing Na⁺ absorption in cultured proximal tubule cells (Singh and Linas, 1996).

EBP50/NHERF and E3KARP/NHERF2 can simultaneously bind to B2AR and to proteins of the ERM family, and possibly also to NHE3 (Figure 8). ERM proteins, which generally localize to the apical membrane of polarized cells, in turn can also bind to the phospholipid PIP2 and to actin, and may form oligomers at membranes (Bretscher et al., 2002).

1.6.2.4 Oligomerization

Recently, the laboratory of Le-Yuan Liu-Chen has proposed yet another model for how binding to EBP50/NHERF activates NHE3. The kappa-opioid receptor, which signals through G_i, activates NHE3 in cultured cells (Huang et al., 2004). Because activation of NHE3 is insensitive to pertussis toxin, they concluded that NHE3 is not activated by G_i. Instead, they put forward a model where GPCRs that bind directly to EBP50/NHERF trigger its oligomerization, and oligomeric EBP50/NHERF activates NHE3. This model is based on still-controversial data that EBP50/NHERF can oligomerize *in vitro*. From certain assays, this oligomerization of EBP50/NHERF is stimulated by the carboxy terminus of receptors such as B2AR and the kappa-opioid receptor (Huang et al., 2004; Lau and Hall, 2001). However, data is still lacking on whether endogenous EBP50/NHERF oligomerizes *in vivo*. There is some evidence that Ser289 of EBP50/NHERF, which is constitutively phosphorylated, is required for oligomerization both *in vitro* and *in vivo* (Lau and Hall, 2001); however, mutation of Ser289 does not

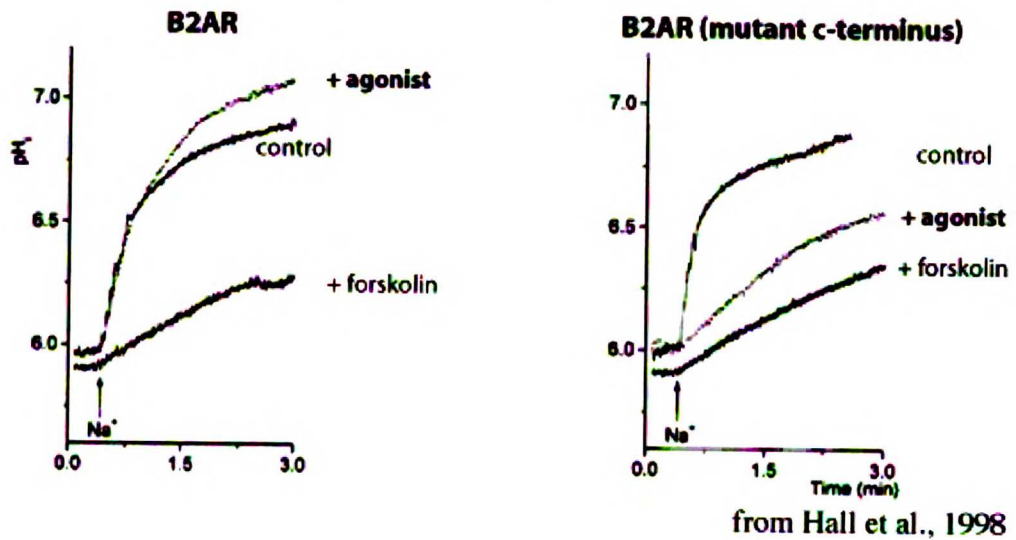
affect NHE3 regulation *in vitro* (Weinman et al., 1998) or *in vivo* (Zizak et al., 1999); this data does not support the “oligomerization” model.

1.6.3 *Testing these Models*

The “sequestration” model of EBP50/NHERF function, initially proposed by Hall and Lefkowitz, could be directly tested by analyzing whether B2AR agonists reduce the amount of EBP50/NHERF that associates with NHE3. The “ $\beta\gamma$ ” model of EBP50/NHERF function, proposed by this author, could initially be tested by confirming whether NHE3 can be activated by purified $\beta\gamma$, and then testing whether B2AR activates G_i in kidney cell lines (using a reporter of G_i activity). The “oligomerization” model proposed by Hall could be tested by discovering a functional effect of a mutation that inhibits the oligomerization of EBP50/NHERF.

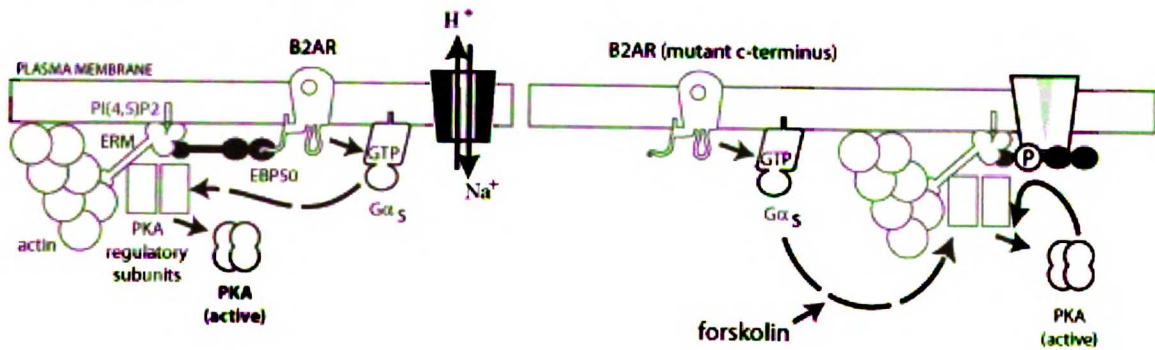
ERM proteins can connect protein complexes with actin in response to hormones and growth factors that cause the phosphorylation and activation of ERM proteins by PKC (protein kinase C) (Bretscher et al., 2002).

A. BAR inhibition of Na/H exchange requires intact c-terminus



B. Possible mechanisms

1. B2AR sequesters EBP50



2. B2AR activates Gi

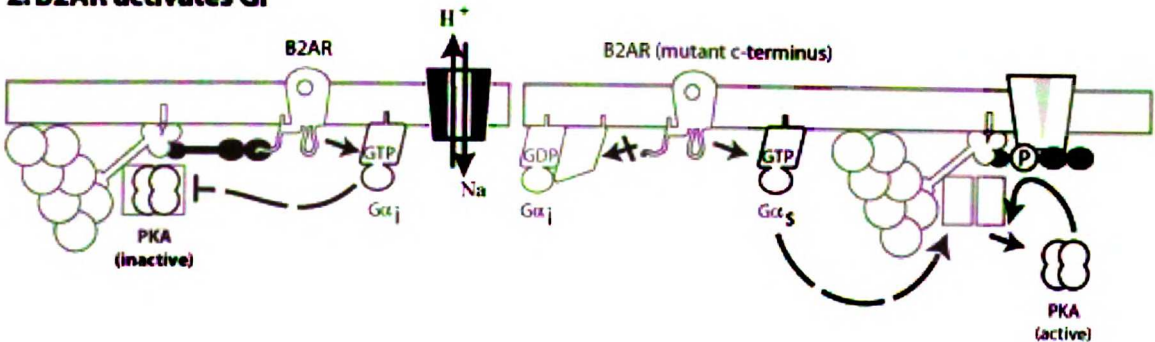


Figure 9

B2AR stimulation of Na⁺/H⁺ exchange in the kidney does not occur via G_s, and is dependent on the intact c-terminus, which can bind to EBP50/NHERF. A. (1) In tissue culture cells expressing B2AR and NHE3, B2AR ligands stimulate Na⁺/H⁺ exchange. Forskolin, which activates adenylyl cyclase, inhibits Na⁺/H⁺ exchange. Adenylyl cyclase is downstream of G_s. Therefore, B2AR does not stimulate Na⁺/H⁺ exchange by triggering a G_s signaling cascade. (2) When the c-terminus of B2AR is mutated, B2AR ligands inhibit Na⁺/H⁺ exchange. Therefore, stimulation of Na⁺/H⁺ exchange by B2AR requires its intact c-terminus. B. (1) The Lefkowitz lab has proposed that, upon activation by ligand, B2AR binds to a complex of EBP50/NHERF, an ERM protein, and PKA. The Na⁺/H⁺ exchanger NHE3 binds this complex, and the recruited PKA phosphorylates and inhibits the adjacent NHE3. In this model, B2AR activation displaces NHE3 from this complex, and activates PKA in a restricted area via a G_s signaling cascade (dashed line). When the c-terminus of B2AR is mutated, it activates PKA “at a distance”. This “EBP50/NHERF sequestration” model predicts that activated B2AR decreases (and a mutant B2AR increases) the amount of EBP50/NHERF that binds to NHE3. (2) Another model is that B2AR activates NHE3 by a G_i signaling cascade. G_i signaling cascade inhibits PKA (dashed line); PKA phosphorylates and inactivates NHE3. B2AR can switch from G_s signaling to G_i signaling in cardiac myocytes; this switch depends on the intact c-terminus of B2AR.

1.7 TETHERING

Another mechanism to control GPCR signaling is to tether signaling molecules together or to target them to specific membrane regions. A stable complex of signaling molecules would likely increase the speed, efficiency, and specificity of signaling at the expense of amplification (Ferrell and Cimprich, 2003). In some cells B2AR signaling via the G_s pathway is tightly localized, while B1AR signaling via G_s broadly diffuses (Xiao et al.,

1999a); Bean et al, 2001; (Chen-Izu et al., 2000). Indeed, B2AR may be in a stable complex with adenylyl cyclase, PKA, and downstream effectors in neurons and other cell types (see Chapter 3). PKA may be tethered to B2AR indirectly by anchoring proteins called AKAPs (A kinase anchoring proteins). As mentioned above, the c-terminal tail of B2AR binds to the AKAP binding proteins EBP50/NHERF and E3KARP/NHERF2 (Cao et al., 1999; Cong et al., 2001a; Hall et al., 1998a; Hall et al., 1998b). EBP50/NHERF and E3KARP/NHERF2 in turn can bind AKAPs of the ERM family (Ezrin, Radixin, Moesin) (Dransfield et al., 1997; Gronholm et al., 2003). Because ERM proteins can bind to EBP50/NHERF, PKA, and actin simultaneously, they may anchor B2AR to the actin cytoskeleton. Other AKAPs have also been co-immunoprecipitated with B2AR (see Chapter 3). It is therefore possible that PKA is tethered near B2AR. Furthermore, B2AR itself may homo-dimerize, which could create even more “rarefied” complexes of receptors and signaling molecules (Angers et al., 2002).

Anchoring of B2AR to PKA may control its function in heart cells. While both B1AR and B2AR can activate the L-type calcium channel, which triggers an increase in the contraction rate (Bean et al., 1984), the increase in the rate of heart contractions is primarily via B1AR (Chen-Izu et al., 2000). It is possible that the anchoring of B2AR to PKA and the actin cytoskeleton restricts the propagation of signaling of B2AR, such that activation of B2AR does not lead to an increase in the rate of heart contractions.

2 SUMMARY OF RESULTS

- **B2AR in lysates prepared from HEK293 cells treated with Tx-100 behaves as a monomer by sucrose gradient sedimentation.**
- **Unphosphorylated EBP50/NHERF in lysates prepared from HEK293 cells sediments at 5S by sucrose gradient sedimentation, while phosphorylated EBP50/NHERF sediments at 10S.**
- **In the presence of membrane-permeable crosslinker, phosphorylated EBP50/NHERF co-immunoprecipitates with B2AR. We estimate that at least 10% of B2AR is bound to EBP50/NHERF in the absence of agonist. This co-immunoprecipitation is abolished by the addition of residues to the B2AR tail, which have previously been demonstrated to disrupt direct *in vitro* binding.**
- **Treatment of cells with agonist slightly and variably reduces the amount of EBP50/NHERF that co-immunoprecipitates with B2AR.**
- **The ERM binding domain of EBP50/NHERF is not required for its co-immunoprecipitation with B2AR, but it may be required for normal agonist regulation.**
- **B2AR are in large vesicles that appear to move along or are constrained by the actin cytoskeleton. B2AR are also in small vesicles and tubules that have long**

bursts of extremely rapid microtubule-based movement, at speeds up to 4.7 $\mu\text{m}/\text{sec}$.

- **The recycling sequence of B2AR is required for B2AR to be found in rapidly moving endosomal tubules.**
- **We have developed a fixation protocol for indirect immunofluorescence that preserves endosomal tubules.**
- **B2AR is colocalized with transferrin in tubules by indirect immunofluorescence, and is colocalized with EEA1 in early endosomes. Latrunculin treatment, co-expression with delta-opioid receptor, and mutation of the recycling sequence of B2AR each disrupt the localization of B2AR in tubules.**
- **The recycling sequence of B2AR is not required for B2AR to be found in early endosomes. By contrast, DOR is rapidly sorted from early endosomes.**
- **Latrunculin treatment inhibits the number of B2AR clustered in deep clathrin-coated pits after agonist treatment at 16°C, observed by indirect immunofluorescence**
- **Latrunculin also inhibits the number of D2 dopamine receptor clusters, but not those of transferrin or D4 dopamine receptor.**

- **The EBP50/NHERF binding sequence of B2AR is not required for efficient clustering.**
- **Latrunculin induces a small but reproducible lag in the endocytosis of B2AR, measured by flow cytometry.**
- **Ilimaquinone, a drug that depolymerizes microtubules in cell extracts, does not depolymerize microtubules *in vitro*.**
- **The ilimaquinone-sensitive factor is heat and freeze-thaw sensitive, but is insensitive to NEM and trypsin. It is not a microtubule-associated protein. Gel filtration indicates that it is about 100 kDa. It is precipitated in a 40-50% ammonium sulfate cut but not by 0.1% polyethyleneimine. Anion and cation exchange chromatography inverted its activity from microtubule-destabilizing to microtubule-stabilizing.**
- **Analytical ultracentrifugation of recombinant material indicates that *Xenopus* Op18 is a monomer.**
- ***Xenopus* Op18 has a Stokes radius of 36Å measured by gel filtration, which increases to 60Å when added to purified tubulin *in vitro*. This result has**

subsequently been shown to indicate that Op18 is bound to tubulin dimers with 1:2 stoichiometry in a “T2S” complex.

- **Xenopus Op18 increases the catastrophe frequency and possibly the shrinkage rate of Xenopus tubulin at both the plus and minus ends observed by VE-DIC microscopy; Xenopus tubulin is a very stable form of tubulin.**
- **We have generated and purified an anti-Op18 antibody; this antibody inhibits catastrophe *in vivo*.**
- **Phosphorylated and unphosphorylated Op18 have an S-value of 1.4S in mitotic extracts and a Stokes radius of 40Å, indicating that they are monomers, not in a T2S complex. Phosphorylated and unphosphorylated Op18 in interphase extracts have an S-value of 2.5S and a Stokes radius of 40Å, indicating that they are a larger complex, but not a T2S complex.**
- **Tubulin in interphase and mitotic extracts has a Stokes radius of 40Å, which further indicates that it is not bound to Op18 in a T2S complex in extracts.**

3 BETA2-ADRENERGIC RECEPTOR BINDS EBP50/NHERF IN CELLS

Abstract. We have previously demonstrated that endogenous EBP50/NHERF co-immunoprecipitates with B2AR overexpressed in HEK293 cells, and that this co-immunoprecipitation relies upon the PDZ ligand sequence of B2AR. To our knowledge, this is one of the only examples where a binding site on B2AR has been established both *in vivo* and *in vitro*. Here we describe how we arrived at these co-immunoprecipitation conditions. Furthermore, we describe some unpublished features of this co-immunoprecipitation. Notably, it appears that only phosphorylated EBP50/NHERF co-immunoprecipitates with B2AR. Phosphorylated EBP50/NHERF migrates in a large complex by sucrose gradient sedimentation, providing further evidence that EBP50/NHERF is a phosphorylation-regulated homodimer *in vivo*. The co-immunoprecipitation of phosphorylated EBP50/NHERF with B2AR appears to be negatively regulated by B2AR agonist. However, a mutant EBP50/NHERF lacking an ERM binding domain co-immunoprecipitates well with agonist-treated B2AR, indicating that ERMs regulate the accessibility of EBP50/NHERF to B2AR.

WITH widespread use of the two-hybrid screen came an explosion in the number of documented protein-protein interactions. However, for proteins with low expression in general and for signaling proteins in particular, the ability to assess possible protein-

protein interactions *in vivo* can be a challenge. While co-immunoprecipitation of protein complexes have frequently been used to “verify” *in vitro* interactions, it is rare that papers demonstrate that the co-immunoprecipitation reflects a direct protein-protein interaction.

We are aware of nearly 30 cytoplasmic proteins, representing 20 different protein classes, which have been reported to co-immunoprecipitate with B2AR (Table 1). This is particularly impressive given that B2AR is a relatively compact protein composed of 418 amino acids, the bulk of which is embedded in the plasma membrane and hence inaccessible to cytoplasmic proteins. That each of these co-immunoprecipitations represents direct *in vivo* interactions has been accepted largely without question (Hall, 2004). For the majority of these interactions, the binding site has not been mapped either on B2AR or on the interacting protein. In nearly half of the cases where a binding domain has been identified on the receptor, this binding domain localizes to a region of the receptor that is highly conserved amongst GPCRs, and is therefore likely to be involved in receptor folding. Furthermore, of these 30 interactions, almost half have not been tested for agonist regulation, and only three appear to be strongly regulated by agonist. Finally, and most importantly, only one of these interactions has been demonstrated to alter the activity of wild-type B2AR, and an additional two are implicated by indirect evidence.

protein	category	cells	gene	expressed	time in agonist			on protein	binding domain on B2AR	other GPCRs	effect	effect abolished with blinding?
					X17	5'	15**					
AKAP250/gravin	AKAP	A431	endog		+	+	+		tail			
AKAP79	AKAP	HEK293	op		++	++	++	N-terminus	3rd loop, tail		antisen	decreased resensitization, decreased clathrin coilp
EBP50	AKAP associated	HEK293	endog		++			N-terminus	c term SxL		op full length	increased receptor phos; c term decreased GRK2 coilp
Cav1.2	channel	HEK293	op	DSP	+	x	x	N-terminus	tail		op full length	decreased recycling
CFTR	channel	COS	op	transient	+	x	+/-	N-terminus	tail xxxL		op full length	increased iodide efflux
NSF	chaperone	COS	op	transient	+	x	x	c-term TRL (indirect)	tail xxxxxSLL		op full length	increased endocytosis
arrestin 2	desensitization	A431	endog		+	+	+	N and C terminus	3rd loop, tail		op full length***	increased desensitization
arrestin 3	desensitization	A431	endog		0	+/-	+/-	N and C terminus	3rd loop, tail		op full length	increased internalization
clathrin	desensitization	A431	endog		0	+/-	+/-	indirect	indirect		op full length	increased desensitization
GRK2	desensitization	HEK293	op	stable	+	x	x	C-terminus	Stabilized FR ₃		op C-terminus***	decreased recycling
GASP	desensitization	HEK293	op	transient	+	+	+	S685 (indirect)	tail			
alpha2AR	GPCR	HEK293	op	transient	+	x	x	TM6	TM6 L155G	B1AR	xs TM6	decreased AC activation
B2AR	GPCR	CHW	op	transient	+	x	x	TM6	TM6 L155G	not M2 muscarinic KOR	op full length	etorphine-induced endo
DOR	GPCR	HEK293	op	transient	++	x	x					
Fyn	kinase	A431	endog		+	x	x					
Lyn	kinase	A431	endog		+	x	x					
PI3K	kinase	DDT MF1	endog		+/-	x	x		Y350		op (const act)	internal receptor (unstim)
Src	kinase	A431	endog		+	++	+++		Y350			
Yes	kinase	A431	endog		+	x	x					
Grd2	kinase associated	DDT MF1	endog		+/-	x	x					
PKC	resensitization	A431	endog		+/-	+/-	++		Y280		antisen	decreased desens, resens
PP2A	resensitization	HEK293	endog		0	x	+				antisen	decreased resensitization
PP2B	resensitization	A431	endog		+	+/-	+				antisen	decreased resensitization
Gas	signaling	HEK293	endog		0	++	0		nd			
PDE	signaling	A431	endog		+	++	++		3rd loop			
PKA	signaling	A431	endog		+++	x	x	C-terminus	3rd loop			
eIF2B-alpha	translation	HEK293	op		+++	x	x		3rd loop	many except V2	op full length	increased AC activity

* IPd from subcellular fraction
 ** or closest time
 *** effect on mutant receptor only

highly effluenced in GPCRs

Table 1. *Proteins that co-immunoprecipitate with B2AR.* Gene: source of the co-immunoprecipitated protein. op: overexpression. endog: endogenous. For overexpressed proteins, the type of expression, either transient or stable, is listed. DSP: di-succinopropionate, a membrane permeable crosslinker. time in agonist: qualitative assessment (e.g. +, ++, +++) of the amount of co-immunoprecipitated protein is listed either without agonist (O') or at 5 minutes or 15 minutes after agonist treatment. The binding sites, if identified, are also listed (see also Figure 5). other GPCRs: if the protein has been identified as interacting with other GPCRs. effect: functional effects of dominant negative, overexpression, or antisense knock-downs. abolished with binding: if the functional effect was eliminated with a control where the binding site was mutated. References: AKAP250 (Lin et al., 2000; Shih et al., 1999; Tao et al., 2003), AKAP79 (Cong et al., 2001b), EBP50/NHERF (Cao et al., 1999; Gage et al., 2004; Hall et al., 1998a; Hall et al., 1998b), Cav1.2 (Davare et al., 2001), CFTR (Naren et al., 2003), NSF (Cong et al., 2001a; Gage et al., 2004)}, arrestin 2, clathrin, GRK2 (Fan et al., 2001b; Lin et al., 2000), GASP (Simonin et al., 2004; Whistler et al., 2002), alpha-2 adrenergic receptor (Xu et al., 2003), B2AR (Hebert et al., 1996), delta-opioid receptor (DOR) (Jordan et al., 2001), Fyn, Lyn, Yes, Src (Luttrell et al., 1999; Shumay et al., 2002), PI3K, Grb2 (Karooor et al., 1998), PKC (Fraser et al., 2000), PP2A, PP2B (Krueger et al., 1997; Lin et al., 2000; Shih et al., 1999), G_α(Ostrowski et al., 1992), PDB, PKA (Lin et al., 2000), eIF2B-alpha (Klein et al., 1997).

The carboxy terminus of B2AR, which Tracy Cao had identified as being important for post-endocytic trafficking, had originally been reported to bind to the PDZ domains of EBP50/NHERF and the related protein, E3KARP/NHERF2 *in vitro* by Dr. Hall and colleagues (Hall et al., 1998a; Hall et al., 1998b). The sites on both B2AR and EBP50/NHERF responsible for this interaction had been identified, and the crystal structure of a related complex had been determined (Doyle et al., 1996). Therefore, I set out to determine whether EBP50/NHERF and B2AR could be co-immunoprecipitated

from cells, and whether this co-immunoprecipitation was due to the direct binding of EBP50/NHERF to B2AR. Finally, we discovered that this interaction may be regulated *in vivo*.

While not widely accepted, there is data that EBP50/NHERF also binds to itself, forming higher-order oligomers. Because this literature has not yet been reviewed, I will take the opportunity to do so here. The N-terminal PDZ domain of EBP50/NHERF appears to be sufficient to bind full length EBP50/NHERF or an isolated N-terminal PDZ domain *in vitro* by far-Western (Fouassier et al., 2000; Shenolikar et al., 2001). However, other labs have failed to detect this interaction (Reczek and Bretscher, 2001), or have reported that it is the second PDZ domain, and not the N-terminal one, that is sufficient to bind EBP50/NHERF *in vitro* (Lau and Hall, 2001). Exogenously expressed EBP50/NHERF has been reported to co-immunoprecipitate EBP50/NHERF in the absence (Fouassier et al., 2000) or in the presence (Lau and Hall, 2001) of crosslinker; Shenolikar, Weinman and colleagues have reported similar findings, but did not report the immunoprecipitation conditions used (Shenolikar et al., 2001). While the possible role of oligomerization *in vivo* has not been elucidated, *in vitro*, PDZ ligands such as the PDGFR tail (Maudsley et al., 2000), B2AR tail (Lau and Hall, 2001) and the kappa-opioid receptor tail (Huang et al., 2004) increase the amount of oligomerization detected by far-Western, indicating that oligomerization of EBP50/NHERF is involved in its role as a B2AR binding protein.

It is thought that EBP50/NHERF oligomerization is regulated by phosphorylation. Ser298, a residue after the second PDZ domain, is constitutively phosphorylated *in vivo*. *In vitro*, Ser298 can be phosphorylated by GRK6A (Hall et al., 1999). Phosphorylation of

EBP50/NHERF may also promote the oligomerization of EBP50/NHERF (Lau and Hall, 2001). However, mutation of Ser298 does not disrupt binding to ezrin or to NHE3 (see (Figure 8), nor does it disrupt regulation of NHE3 *in vivo*, so its function -- beyond promoting oligomerization of EBP50/NHERF -- is still a mystery (Zizak et al., 1999).

While we were not explicitly investigating EBP50/NHERF oligomerization, we uncovered evidence that endogenous EBP50/NHERF may indeed oligomerize *in vivo*. Because EBP50/NHERF oligomerization has been linked to binding membrane proteins such as B2AR *in vitro*, a future direction from this research would be to use our procedures to determine how EBP50/NHERF-B2AR complexes and EBP50/NHERF-EBP50/NHERF oligomers are regulated *in vivo*.

3.1 *Materials and Methods*

Cell Lines

HEK293 cells stably transfected with B2AR or BAR and EBP50/NHERF were maintained and passaged in DMEM supplemented with 10% fetal bovine serum (Cell Culture Facility, UCSF). Human EBP50/NHERF and EBP50/NHERF Δ 61c, which have HA tags at their carboxy termini, have been described elsewhere (sequence data of EBP50/NHERF is available from GenBank under accession number AF015926) (Cao et al., 1999). EBP50/NHERF Δ 61c lacks 61 amino acids at its carboxy terminus. Cells stably expressing human B2AR with FLAG tags at their amino terminus have also been described elsewhere (von Zastrow and Kobilka, 1992).

Sucrose Gradient Sedimentation

Sucrose gradients were prepared as step gradients (five 400 μ L steps) of MBS from 10-50% sucrose (MBS = 100 mM NaCl, 1 mM CaCl₂, 50 mM Tris pH 7.4, 0.2% triton, 1 mM beta-mercaptoethanol, with a protease inhibitor cocktail of leupeptin, pepstatin, and aprotinin), similarly to a previously published protocol (Moritz et al., 1998). Solutions were carefully layered with cut-off pipet tips (Eppendorf) and incubated at 4°C overnight to form the continuous gradient. Low-speed supernatants of HEK293 cells stably expressing Flag-B2AR were carefully layered onto the gradient and spun 50,000 rpm for 4 hours in a TLS-55 rotor (Beckman). Twelve 166 μ L fractions were carefully collected from the top of the gradient with a cut-off pipet tip (Eppendorf). Fractions were precipitated by mixing 1:1 with 20% trichloroacetic acid (TCA precipitation). 0.5 mg/mL each of two protein standards (BSA, 4.4S, and porcine thyroglobulin, 19.4S) were run in parallel over identical gradients.

Antibodies

The rabbit polyclonal anti-EBP50/NHERF antibody “61”, a gift from Anthony Bretscher and David Reczek, was raised against the carboxy terminus of EBP50/NHERF; it cross-reacts with E3KARP/NHERF2. This affinity purified antibody was used for immunoblotting at a dilution of 1:5000. Polyclonal rabbit anti-B2AR antibody “86” was raised against a carboxy-terminal epitope of B2AR by Mark von Zastrow. The mouse monoclonal antibody HA.11 was used to detect HA (HA.11, Berkeley Antibody Company).

Immunoblotting

Proteins were resuspended 1:1 in sample buffer (125 mM Tris pH 6.8, 20% v/v glycerol, 4.6% SDS, 0.01% bromophenol blue), 30 min at 25°C or 10 min at 37°C, then separated by SDS-PAGE and transferred to nitrocellulose. Dye-coupled proteins were used to identify molecular weights (Prestained Broad Range Markers, New England Biolabs). Blots were incubated for 20 minutes in block (TBS + 0.1% Tween-20, 3% nonfat dry milk). A chemiluminescent substrate system (Vectastain ABC, Vector Laboratories) was used to detect HRP-conjugated secondary antibodies. Blots were exposed onto film (Xomat or BioMax, Kodak).

Receptor Biochemistry

The standard lysis buffer was 0.5% (v/v) Tx-100, 50 mM TrisCl pH 7.5, 120 mM NaCl, 25 mM KCl and 1 mM CaCl₂. The SDS high stringency wash was included 0.1% SDS. The high salt buffer was the standard lysis buffer with an additional 1 mM NaCl. The low salt buffer was 10 mM Tris pH 7.5, 2 mM EDTA pH 8.0. The digitonin-tris lysis buffer had 1.2% digitonin instead of Tx-100. The digitonin-phosphate lysis buffer also had 10 mM phosphate pH 7.2 instead of Tris. The CHAPS buffer had 0.1% CHAPS instead of Tx-100. RIPA buffer had 0.5% deoxycholate and 0.2% Tx-100. Protease inhibitors (leupeptin, pepstatin and aprotinin) and 1 mM DTT were included freshly to all buffers. Immunoprecipitates were washed in lysis buffer 3x and 40 µL SDS sample buffer was added for 30 min before freezing. 10 µL of extract was then separated on an 8% SDS-PAGE gel.

Co-immunoprecipitation

To adhere cells firmly during room temperature incubations, 5 mL of Poly-L-lysine diluted 1:200 in PBS was added to each culture dish for 10 minutes and rinsed well with water before plating the cells. HEK293 cells stably expressing Flag-B2AR with an n-terminal signal sequence were then plated onto these dishes. Fresh DMEM+10% fetal calf serum was added to each dish of cells for 30 min. Then the dishes were washed with 3 changes of 5 mL PBS+30 mM HEPES (pH 7.5) at room temperature and rocked gently for 30 min. The crosslinker di-succinopropionate (DSP) was added freshly to PBS+30 mM HEPES (pH 7.5) to a final concentration of 0.3 mM, or as indicated. 5 mL of this crosslinking solution was added to each dish and incubated for 30 min. The crosslinker was removed and 5 mL of PBS+HEPES+50 mM glycine (pH 7.4) was added to quench the DSP. The cells were incubated a further 10 minutes on the rotator, and this quenching step was repeated. 1 mL of ice cold lysis buffer was added to each dish and the cells were rotated a further 15 min at 4°C. The standard lysis buffer was 0.5% (v/v) Tx-100, 50 mM TrisCl pH 7.5, 120 mM NaCl, 25 mM KCl and 1 mM CaCl₂; Tx-100 was added freshly. Protease inhibitors (leupeptin, pepstatin and aprotinin) and 1 mM DTT were also included freshly. The cells were removed by scraping with a rubber policeman into clear microcentrifuge tubes (USA-Scientific Plastics) and spun 10,000 rpm for 10 min. The supernatant, between 2.5-3.5 mg/mL by Bradford (Pierce) using bovine serum albumin (Sigma) as a standard, were removed and incubated in 7 mL of packed beads covalently attached to the anti-FLAG monoclonal antibody, M2 (Sigma). The beads were rotated gently for 1 hour at 4°C and then spun to pellet. The beads were washed in 0.8 mL lysis buffer 3x and proteins were incubated with sample buffer containing 100 mM DTT and

200 mM beta-mercaptoethanol, to reduce the crosslinker. The proteins were incubated in this solution at room temperature for 30 minutes before separation by 10% PAGE.

Occasionally immunoprecipitates were left at 4°C in SDS sample buffer overnight, but were never frozen, as that lead to aggregation of the purified B2AR.

To analyze proteins in low speed pellets, pellets were triturated with a 20 gauge needle (to break up DNA) in 200 μ L of sample buffer supplemented with 200 mM DTT and 400 mM BME, boiled 10 minutes and immediately loaded into PAGE wells with a pipet.

Quantitative Western Immunoblotting

Immunoblots were quantified by the technique of (Moritz et al., 1998). Briefly, dilutions of low speed supernatants were included on immunoblots adjacent to experiments.

Developed film was scanned into a computer (scanner, UMAX) and band intensities were quantified with software (Adobe Photoshop, Adobe). The values of the diluted low speed supernatant were then used to generate a standard curve, from which we converted the intensities to a percentage.

3.2 Results and Discussion

Biochemistry of exogenously expressed B2AR in HEK293 cells

Because B2AR is a membrane protein, it may be difficult to preserve its interactions with other proteins upon lysing the cell for immunoprecipitation. Therefore, we surveyed several lysis conditions and investigated the solubility of B2AR. By SDS-PAGE of low

speed supernatants from HEK293 cells exogenously expressing FLAG-B2AR, B2AR migrates as a monomer. It has previously been seen that B2AR from cells lysed by mechanical disruption migrates predominantly as a monomer under similar conditions (Salahpour et al., 2003). By contrast, purified B2AR can migrate as a dimer; this may be enhanced by freezing B2AR after denaturing with SDS. We found that immunopurified, denatured B2AR from cells lysed in CHAPS, RIPA, and Tx-100 buffers migrates as a dimer by PAGE after freezing (Figure 10A). In a digitonin-TRIS buffer, denatured B2AR migrates primarily as a monomer by PAGE. It has previously been seen that non-denatured B2AR purified from cells lysed by digitonin is a monomer, whereas a fraction of non-denatured B2AR purified from cells lysed by dodecyl maltoside is a dimer (Salahpour et al., 2003; Shorr et al., 1985).

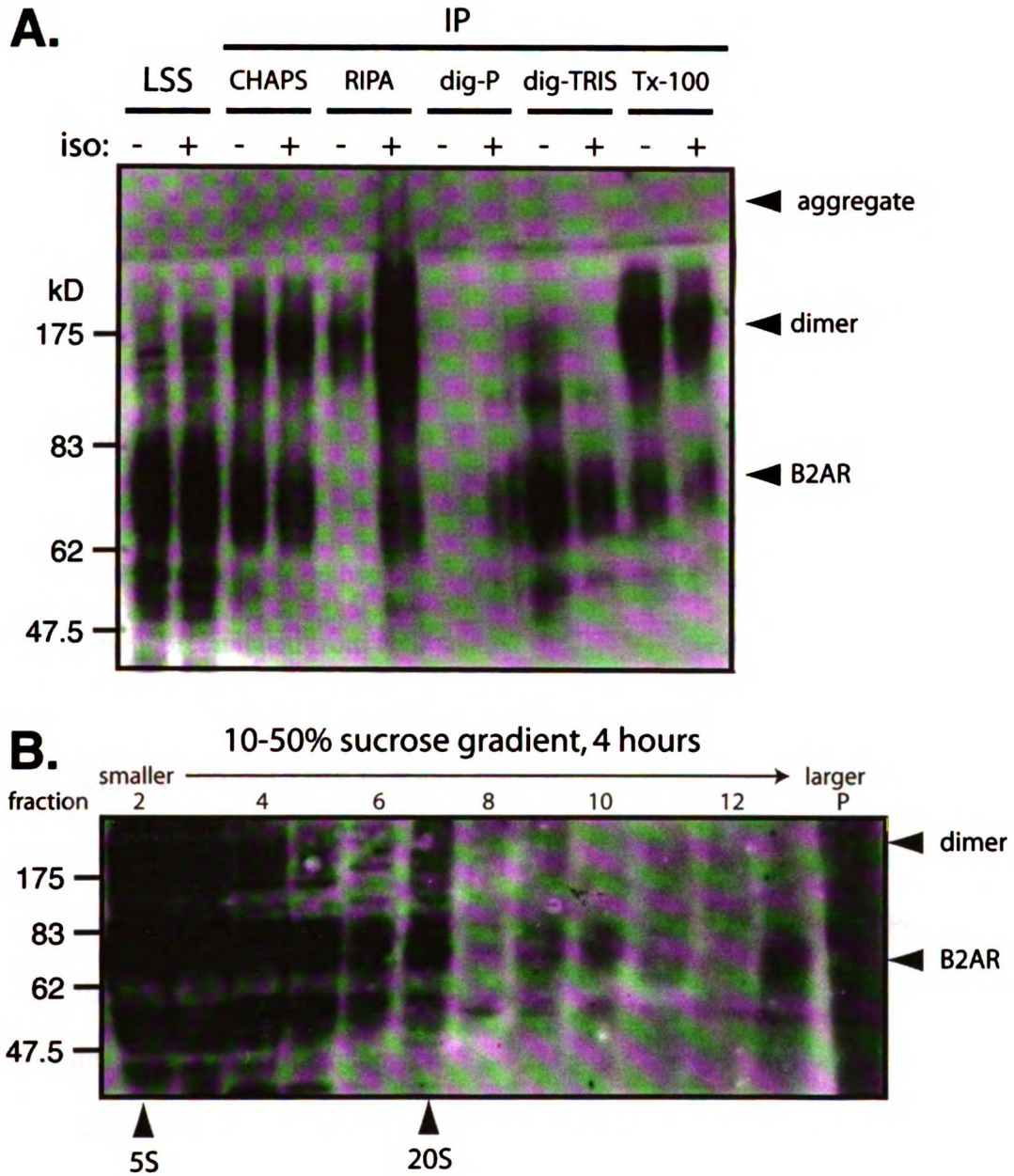


Figure 10 *Biochemistry of B2AR in Extracts*

A. HEK293 cells expressing exogenous FLAG-B2AR were treated with the agonist isoproterenol to drive endocytosis, lysed in various detergents (see Methods), and proteins were separated by SDS-PAGE on 8% gels. The gels were transferred to nitrocellulose and immunoblotted for FLAG. (B) Behavior of B2AR during sucrose gradient sedimentation of HEK293 cell lysates expressing FLAG-B2AR. Extracts were

sedimented over 5-20% sucrose gradients for 4 hours. Each fraction was TCA precipitated, separated by PAGE on a 12.5% gel, and immunoblotted for FLAG. Standards were run in parallel over identical gradients, and the location of the peak for each standard is indicated by an arrowhead and its S value. Identical dishes of cells was treated with isoproterenol 30 minutes before lysis; the migration of B2AR was similar under these conditions (not shown).

In immunoprecipitates from TRIS-buffered digitonin, Tx-100 and CHAPS, less B2AR was immunoprecipitated from cells that had been treated with isoproterenol. In either RIPA or digitonin-phosphate buffer, both of which contain bile acids, more B2AR was immunoprecipitated from cells treated with isoproterenol.

We detected a small amount of EBP50/NHERF in immunoprecipitates from cells lysed with Tx-100 and TRIS-buffered digitonin (not shown). We arbitrarily selected Tx-100 to use in our lysis buffers.

We next analyzed the behavior of B2AR by sucrose gradient sedimentation. The majority of B2AR sediments around 5S, at the top of the gradient (Figure 10B). This indicates that B2AR is a monomer in Tx-100 lysates. The “dimers” observed by PAGE also sediment around 5S, which indicates that these dimers are formed after SDS is added. Previous studies have demonstrated that purified BARs prepared from tissues lysed with digitonin sediments as a monomer, between 8.5-10S (Shorr et al., 1981; Shorr et al., 1982). Digitonin, which is a bile acid derived from cholesterol, binds directly to B2AR and increases its sedimentation (Shorr et al., 1985).

Indeed, we did not detect a pool of B2AR that sediments as a dimer, although a small fraction of B2AR sediments >20S. It has been previously demonstrated that a minority of purified B2AR from cells lysed with dodecyl maltoside are oligomers by ultrafiltration; however, these dimers also migrate as a dimer by SDS-PAGE (Salahpour et al., 2003). To resolve dimers from monomers, I recommend running the gradients for 8 hours rather than 4 hours.

Biochemistry of endogenous EBP50/NHERF in HEK293 cells

In HEK293 cells, a band of about 50 kDa by PAGE is detected with an antibody against EBP50/NHERF (Figure 11A). While EBP50/NHERF has a predicted molecular weight of 38.6 kDa, recombinant EBP50/NHERF migrates at 50 kDa by PAGE (Reczek et al., 1997).

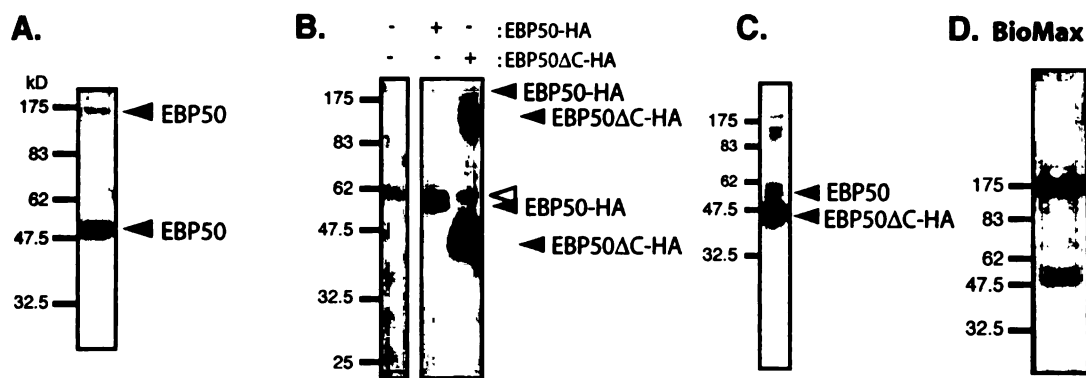


Figure 11. *Detection of EBP50/NHERF*

A. HEK293 cell lysates were separated by PAGE on 10% gels, transferred to nitrocellulose, and immunoblotted for endogenous EBP50/NHERF. B. 15 μ L HEK293 cell lysates or lysates from cells expressing HA-tagged EBP50/NHERF or EBP50/NHERF Δ 61c were immunoblotted for HA. C. 15 μ L lysates from cells expressing EBP50/NHERF Δ 61c were immunoblotted with antibodies against EBP50/NHERF. D. 10 μ L lysate separated by 10% PAGE, 6x1.5 mm² well area (all others, 4x1.5 mm²), exposed onto BioMax film.

In tissues, EBP50/NHERF migrates as a 50 kDa/53 kDa doublet (Reczek et al., 1997). The 53 kDa band represents constitutively phosphorylated EBP50/NHERF. We saw that in HEK293 cells, the 53 kDa band of this doublet, corresponding to phosphorylated EBP50/NHERF, was less intense than the 50 kDa band. This decrease in intensity is also true of EBP50/NHERF in many mammalian tissues (Reczek et al., 1997). However, under certain conditions the majority of EBP50/NHERF may be phosphorylated (Cong et al., 2001a; Hall et al., 1999).

We also detected another band of about 200 kDa with this antibody (Figure 11A). This band is weakly detected by an antibody that was also raised against the carboxy terminal half of EBP50/NHERF, “60;” this antibody does not cross-react with E3KARP/NHERF2. This band is not detected by an antibody raised against full-length EBP50/NHERF, “62” (Tracy Cao, personal communication), which suggests that this protein is not EBP50/NHERF. This high molecular weight band has not been previously been observed with these antibodies, which have been used to detect EBP50/NHERF in many mammalian tissues (Reczek et al., 1997).

Sucrose gradient analysis of epitope-tagged EBP50/NHERF in cells also suggests that this band is not EBP50/NHERF. We stably expressed EBP50/NHERF with an HA tag in HEK293 cells, separated the proteins by PAGE, and performed Western analysis using antibodies against HA. We detected a 50 kDa band and multiple bands around 100 kDa, neither of which were detected in control HEK293 cells (Figure 11B). This antibody also detects a 60 kDa band in HEK293 cells that did not express the HA-tagged EBP50/NHERF, therefore the 60 kDa band is nonspecific. We also stably expressed a carboxy-terminally truncated EBP50/NHERF with an HA tag, EBP50/NHERF Δ 61c. Antibodies against HA specifically detected a 40 kDa band and a group of high molecular weight bands which appear to be about 100, 150, and 200 kDa; these appear as doublets when probed with antibodies against EBP50/NHERF (Figure 11B, C; Figure 12A, B). When HA-EBP50/NHERF was analyzed by sucrose gradient sedimentation, the 100, 150, and 200 kDa bands detected by antibodies against HA did not co-fractionate with the 200 kDa band that is detected by antibodies against EBP50/NHERF (Figure 12A,B).

The majority of endogenous EBP50/NHERF, exogenously expressed EBP50/NHERF, and EBP50/NHERF Δ 61c sediments at 5-6S (Figure 12A, C).

A. 10-50% sucrose gradients, 4 hours

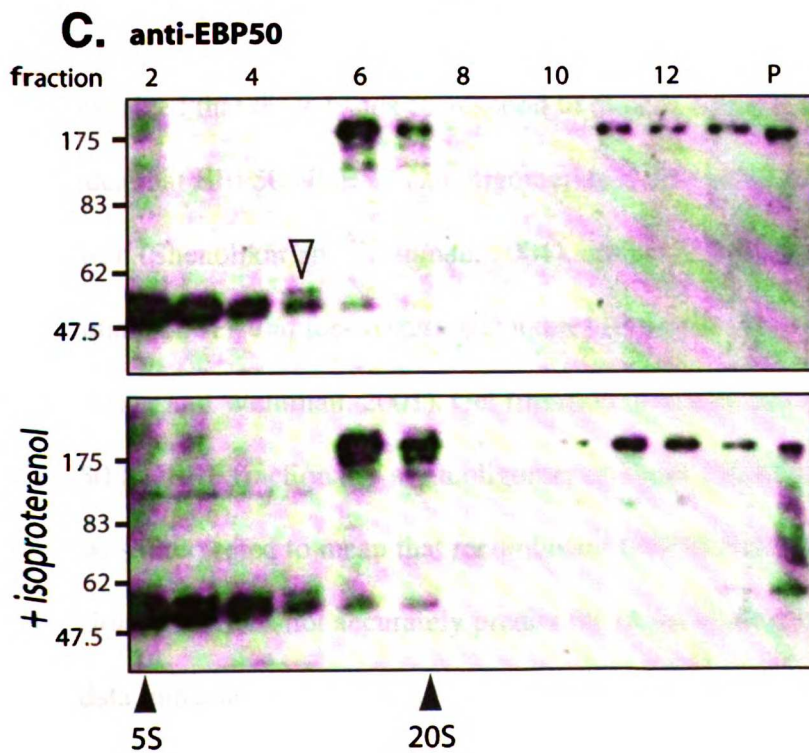
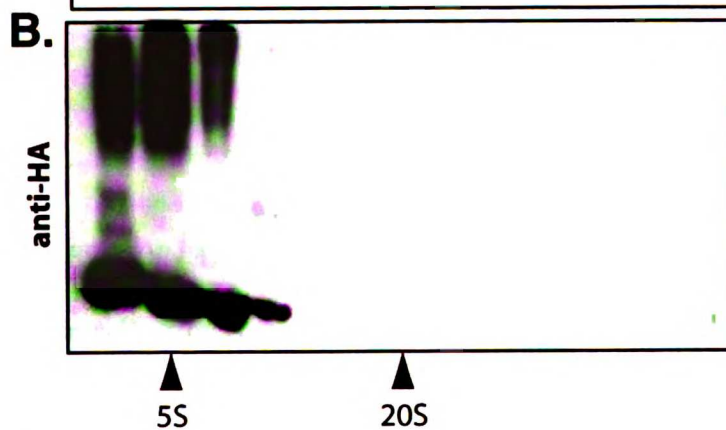
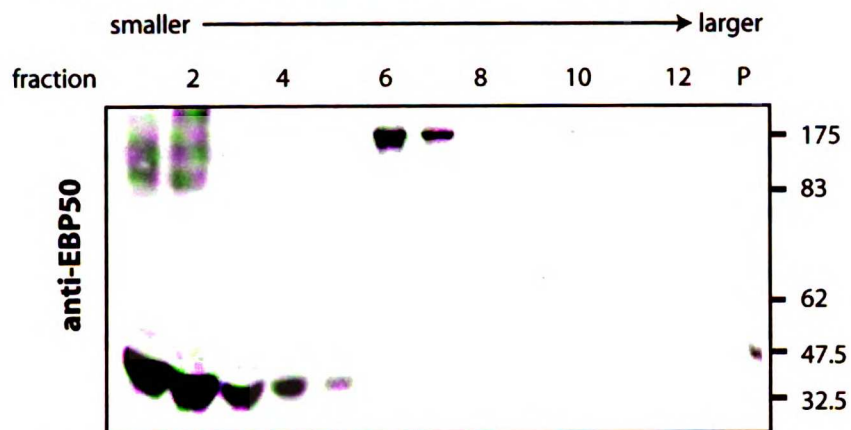


Figure 12. *Sucrose gradient of EBP50/NHERF in HEK293 cell extracts.*

Behavior of EBP50/NHERF Δ 61c (A, B) and endogenous EBP50/NHERF (C) during sucrose gradient sedimentation of HEK293 cell lysates expressing FLAG-B2AR. To see the effect of B2AR activation, some cells were treated with isoproterenol 30 minutes before lysis (C). Extracts were sedimented over 5-20% sucrose gradients for 4 hours. Each fraction was TCA precipitated, separated by PAGE on a 12.5% gel, and immunoblotted for either EBP50/NHERF (A, C) or HA (B). Standards were run in parallel over identical gradients, and the location of the peak for each standard is indicated by an arrowhead and its S value.

EBP50/NHERF has not been previously observed to migrate above 50 kDa by PAGE in cell extracts, nor does recombinant EBP50/NHERF (Reczek et al., 1997). However, when recombinant EBP50/NHERF is incubated with crosslinker, it migrates as 100 kDa, 150 kDa and 200 kDa by PAGE (Fouassier et al., 2000). It has been hypothesized that these bands correspond to dimers, trimers, and tetramers, respectively. The idea that EBP50/NHERF can oligomerize is also supported by experiments using gel filtration (Shenolikar and Weinman, 2001), optical affinity biosensor (Shenolikar and Weinman, 2001), and far-western techniques (Fouassier et al., 2000; Lau and Hall, 2001; Shenolikar and Weinman, 2001). Gel filtration indicates that the majority of purified EBP50/NHERF fractionates as an oligomer of about 150 kDa. While the gel filtration data was interpreted to mean that recombinant EBP50/NHERF is primarily trimeric, gel filtration alone does not accurately predict the molecular weight of elongated proteins. Our data indicates that these high molecular weight bands are formed after SDS is added, because the bands migrate at 5S with the 50 kDa form.

Notably, the 53 kDa phosphorylated band sediments in a complex, heavier than non-phosphorylated EBP50/NHERF (Figure 12C). The 50 kDa band peaks in fraction 2 and 3 (~5S), the 53 kDa band in fraction 5 (~10S). To better separate the 50 and 53 kDa bands, I recommend increasing the spin time for the sucrose gradient from 4 to 8 hours. Previous studies both *in vitro* and *in vivo* have also indicated that EBP50/NHERF can oligomerize. Mutation of Ser298 from rabbit EBP50/NHERF or treatment with okadaic acid both reduce the amount of exogenously expressed EBP50/NHERF that co-immunoprecipitates with endogenous EBP50/NHERF in HEK293 cells (Lau and Hall, 2001; Weinman et al., 2001). Furthermore, mutation of Ser298 to Asp increases the amount of recombinant EBP50/NHERF-EBP50/NHERF binding measured by a solid-phase plate assay (Lau and Hall, 2001). Therefore, to confirm that the 9S fraction represents oligomeric EBP50/NHERF, a purified Asp298 mutant could be analyzed by sedimentation.

While it is not known whether phosphorylated EBP50/NHERF binds to B2AR *in vivo*, *in vitro* addition of the carboxy terminal B2AR tail increases the amount of EBP50/NHERF oligomerization detected by far-Western (Lau and Hall, 2001). However, because B2AR in cell lysates fractionates at 5S, the majority of B2AR is not bound to phosphorylated EBP50/NHERF, at least under these conditions. Furthermore, while agonist treatment of B2AR appears to increase the amount of phosphorylated EBP50/NHERF (Error! Reference source not found.D), agonist treatment does not affect its sedimentation (Figure 12C)

Immunoprecipitation of EBP50/NHERF with B2AR

In order to see whether EBP50/NHERF could be cleanly immunoprecipitated using antibody-bound beads, we first incubated HEK293 cell lysate with M1 anti-FLAG antibody, and immunoprecipitated M1 with protein A beads. The FLAG tag does not interfere with the trafficking of B2AR. We found that the 53 kDa band could be immunoprecipitated from a control HEK293 cell extract that was not expressing FLAG-tagged B2AR (Figure 13A). This band was not washed from beads by SDS, high salt, or low salt (not shown). This immunoprecipitation with M1 indicated that the 53 kDa band bound nonspecifically to either M1 or Protein A beads, or both. We were unable to block this nonspecific binding with BSA, or pre-clearing with Protein A beads, or increasing the salt concentration to 0.5 M (not shown).

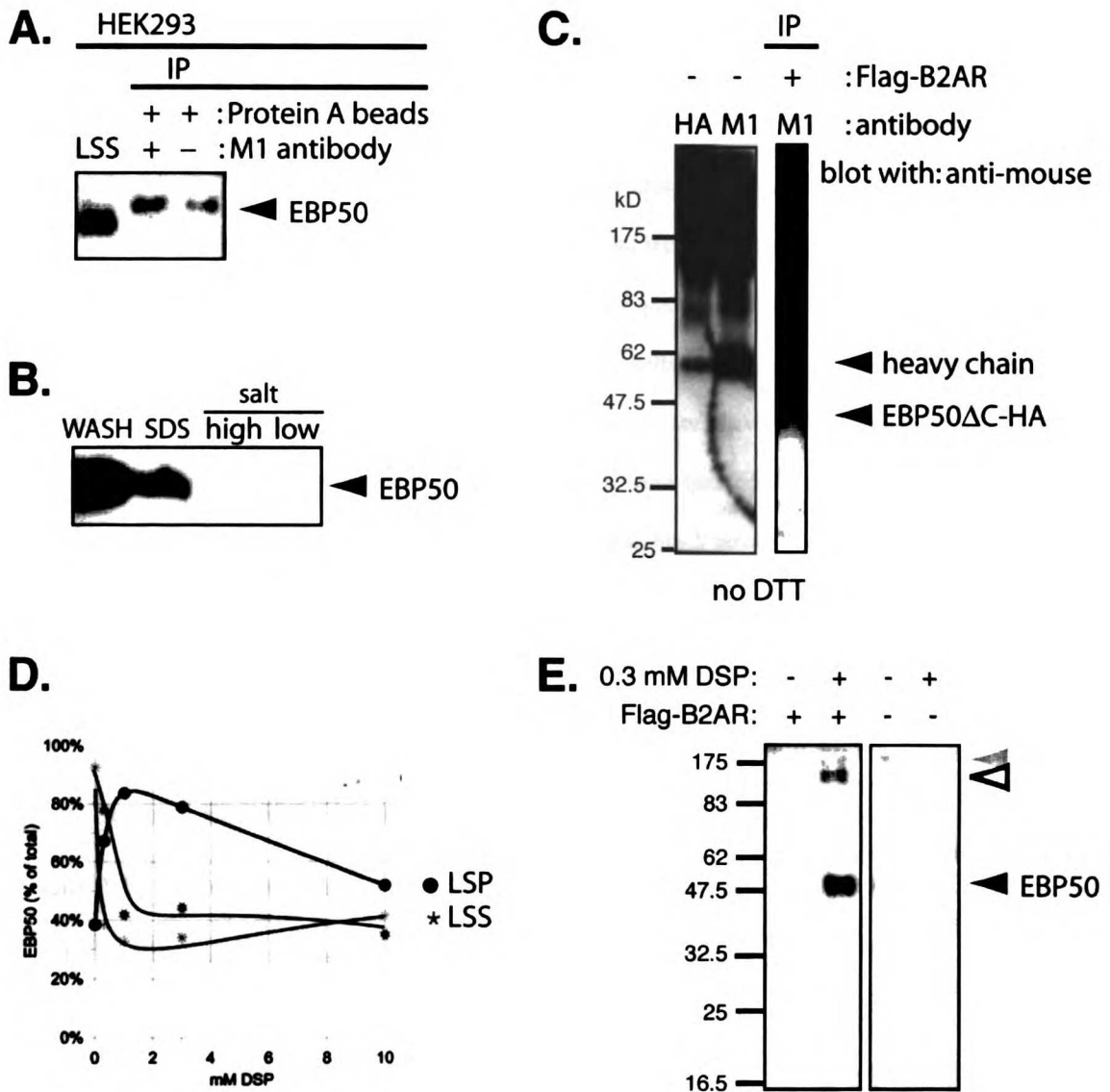


Figure 13. Co-immunoprecipitation of EBP50/NHERF with B2AR in the presence of crosslinker

A. Immunoprecipitation pellets from low speed supernatants of HEK293 cells (IP). M1 anti-FLAG antibodies and Protein A beads were used to immunoprecipitate nonspecific proteins, which were subject to PAGE on a 10% gel, transferred to nitrocellulose, and immunoblotted for endogenous EBP50/NHERF. LSS = low speed supernatant (HEK293 cell lysate). A 53 kDa band, corresponding to phosphorylated EBP50/NHERF, was detected in immunoprecipitates. B. Immunoprecipitation pellets from low speed supernatants of cells expressing FLAG-B2AR were washed with lysis buffer (WASH), SDS, 1M salt

(high), and low salt (low). M2-beads were used to immunoprecipitate FLAG-B2AR. C. Immunoprecipitation pellets from HEK293 cells and HEK293 cells co-expressing FLAG-B2AR and EBP50/NHERF Δ 61c (+) were subject to PAGE under non-reducing conditions (no DTT). EBP50/NHERF Δ 61c was detected with anti-HA antibodies. Secondary antibodies used in immunoblotting cross-reacted with the mouse antibodies in the immunoprecipitates (heavy chain), but no EBP50/NHERF Δ 61c was detected. D. Lysates and pellets from HEK293 treated with crosslinker (DSP) were subjected to PAGE, and EBP50/NHERF was detected by quantitative immunoblotting. E. Immunoprecipitation pellets from HEK293 cells and HEK293 cells expressing FLAG-B2AR previously treated with 0.3 mM DSP. M2-beads were used to immunoprecipitate FLAG-B2AR; endogenous EBP50/NHERF was detected by immunoblotting. Two bands were specifically co-immunoprecipitated with B2AR in the presence of DSP (open arrowhead, ~100 kDa; black arrowhead, ~53 kDa).

Because EBP50/NHERF could not be cleanly immunoprecipitated with M1 and protein A beads, we next asked whether exogenously expressed EBP50/NHERF could be cleanly immunoprecipitated. We therefore expressed HA tagged EBP50/NHERF Δ 61c in cells containing FLAG-B2AR, and immunoprecipitated B2AR with M1 antibodies as before. We did not detect EBP50/NHERF Δ 61c, which runs below the heavy chain of M1, in the immunoprecipitate (Figure 13B). This may be because EBP50/NHERF Δ 61c does not bind well to B2AR in the absence of agonist, or because crosslinker is required, below.

Membrane-permeable crosslinkers have been used in co-immunoprecipitation protocols of GPCRs with cytosolic proteins. Most frequently with B2AR, DSP -- a lipophilic, amine-reactive, thiol-cleavable crosslinker -- has typically been added to cells at 3-10 mM before they are lysed with detergent (Table 1). With the cadherin/catenin

complex, representing another membrane protein/cytoskeleton interaction, use of 0.5 μ M DSP increased the amount of co-immunoprecipitation in the low-speed cellular supernatant (Hinck et al., 1994). Detergent solubilizes membrane components while rendering the actin cytoskeleton insoluble, and pre-adding crosslinker may prevent this biochemical separation. Alternatively, these interactions could be of low affinity or weak, and crosslinker could stabilize such interactions. We found that 1 mM DSP greatly increases the amount of EBP50/NHERF that pellets during a low speed spin (40% no DSP, 80% + DSP) (Figure 13D). Therefore, we chose to treat cells with 0.3 mM DSP, which leaves about 40% of EBP50/NHERF in the low speed supernatant. For the immunoprecipitations, we used M2 antibody covalently coupled to agarose gel (M2-beads), because unlike Protein A-agarose, the M2-beads did not pellet EBP50/NHERF non-specifically (Figure 13E). Two bands reactive with the EBP50/NHERF antibody were seen to co-immunoprecipitate with B2AR, one at 100 kDa (open arrowhead) and another around 53 kDa (black arrowhead) (Figure 13E). A 150 kDa band was non-specifically immunoprecipitated from HEK293 cell lysate (grey arrowhead). Therefore, only the phosphorylated form of EBP50/NHERF co-immunoprecipitates with B2AR. Phosphorylation of EBP50/NHERF is probably not required for binding to B2AR *per se*, as it is not required for binding *in vitro*. Instead, it may be required indirectly: for example, it may be required to recruit EBP50/NHERF to B2AR. Interestingly, both binding to B2AR *in vitro* and phosphorylation of EBP50/NHERF appear to promote the oligomerization of EBP50/NHERF, suggesting that these properties are linked (Huang et al., 2004; Lau and Hall, 2001).

By quantitative immunoblotting, we estimate that our conditions immunoprecipitated 80% of B2AR and 4% of EBP50/NHERF from low speed supernatants. Correcting for EBP50/NHERF that was pelleted from low speed supernatants, we estimate that 2% of total cellular EBP50/NHERF is co-immunoprecipitated under our conditions. It has been previously estimated that the cellular concentration of EBP50/NHERF is 1 μM , which corresponds to 1×10^4 molecules per cell, given a cell volume of $1000 \mu\text{m}^3$ (Anthony Bretscher, personal communication). We have estimated that our expression of B2AR is around 1×10^5 molecules per cell (Mark von Zastrow, personal communication), therefore approximately 10% of B2AR is bound to EBP50/NHERF under our crosslinking conditions, assuming 1:1 stoichiometry. We have not estimated the percentage of phosphorylated EBP50/NHERF in HEK293 cells.

Using these crosslinking conditions, we next asked whether this co-immunoprecipitation was specific to B2AR. We looked at two other GPCRs from family A, MOR and DOR, which share homology upstream of the palmitoylated cysteine, a region that is implicated in binding to a variety of cytosolic proteins (Figure 5 and Table 1). These GPCRs are not homologous at the carboxy terminus, the site of EBP50/NHERF binding to B2AR *in vitro*. Neither MOR nor DOR could co-immunoprecipitate the ~50 kDa or the 100 kDa band using our crosslinking conditions, indicating that endogenous EBP50/NHERF specifically interacts with B2AR in transfected cells (Figure 14A).

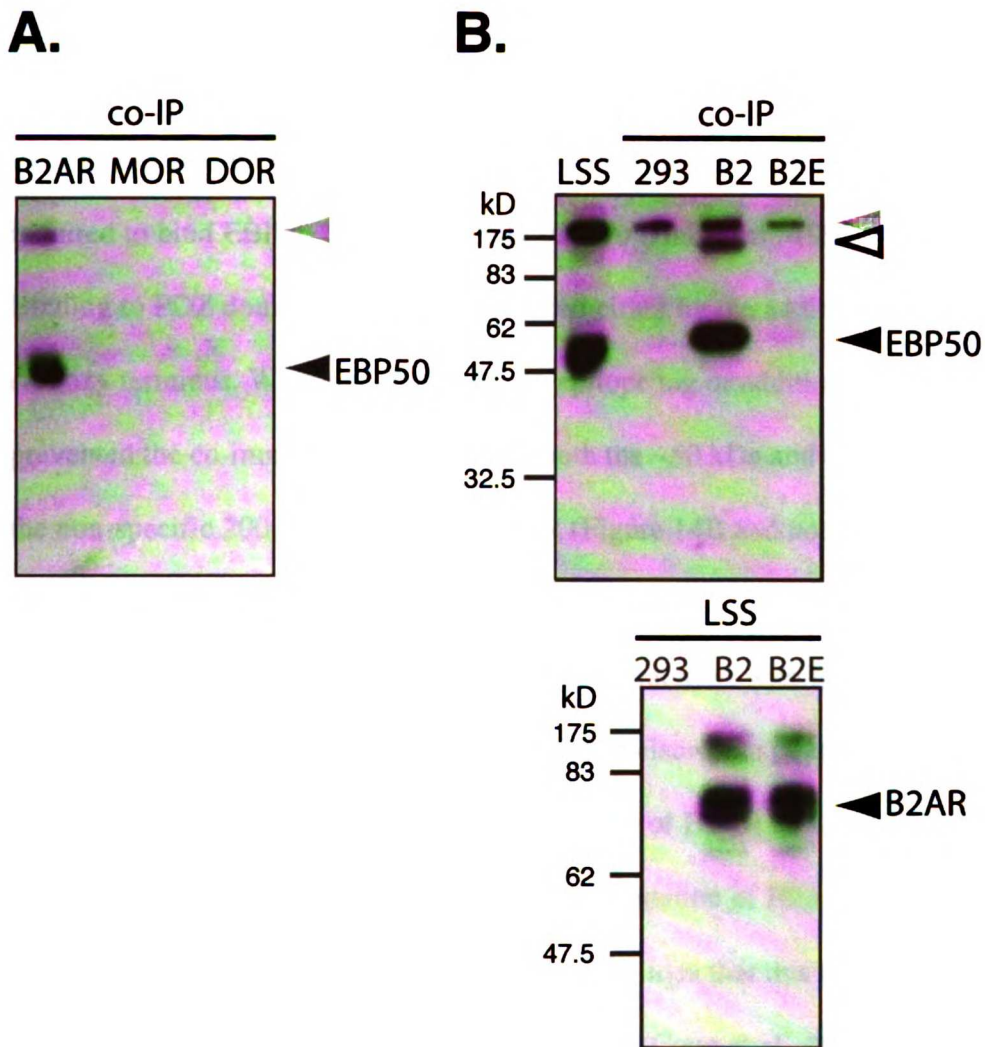


Figure 14. *EBP50/NHERF specifically co-immunoprecipitates with B2AR*

A. Immunoprecipitation pellets from HEK293 cell lysates expressing FLAG-B2AR, FLAG-MOR, or FLAG-DOR. Immunoprecipitated proteins were separated by PAGE on a 10% gel, transferred to nitrocellulose, and immunoblotted for endogenous EBP50/NHERF. EBP50/NHERF was co-immunoprecipitated only with B2AR. **B.** Immunoprecipitation pellets from HEK293 cells lysate or HEK293 cells expressing FLAG-B2AR or carboxy-terminally tagged B2AR, FLAG-B2EE (co-IP). Endogenous EBP50/NHERF was co-immunoprecipitated only with B2AR. Immunoblots of lysates (LSS) with M1 antibody demonstrates the receptors were expressed at equivalent levels.

We next asked whether the co-immunoprecipitation required the carboxy terminal PDZ ligand domain of B2AR. The carboxy terminal PDZ ligand domain of B2AR is required to bind EBP50/NHERF directly *in vitro* (Hall et al., 1998a; Hall et al., 1998b). Binding to PDZ domains can also be blocked either by the addition of residues to the carboxy terminus. We found that either an epitope tag or addition of an alanine residue prevented the co-immunoprecipitation of both the ~50 kDa and the 100 kDa band, but not the non-specific 200 kDa band, with B2AR (Figure 14B and not shown). This indicates that the co-immunoprecipitation of the ~50 kDa and the 100 kDa species of EBP50/NHERF with B2AR are due to direct interactions with the tail of the receptor. This result has in part been previously published elsewhere (Cao et al., 1999). More recently, additional mutations in the PDZ domain of B2AR (D410, S411, L413) have been demonstrated to block the co-immunoprecipitation of B2AR with exogenously expressed EBP50/NHERF, further supporting the idea that this co-immunoprecipitation reflects a direct interaction with the PDZ domain (Cong et al., 2001a).

Regulation of EBP50/NHERF/B2AR interaction by agonist

Because the immunoprecipitations were performed in the absence of isoproterenol, it appears that EBP50/NHERF binds to B2AR at the plasma membrane. We next wondered whether EBP50/NHERF binding to B2AR is regulated by ligand activation of B2AR. To answer this question, we performed co-immunoprecipitations in the presence of the BAR agonist isoproterenol. Under these conditions, it appeared that the amount of endogenous

and exogenous (not shown) EBP50/NHERF co-immunoprecipitating with the receptor was reduced (Figure 15A). We then repeated these experiments using HEK293 cells transfected with exogenous EBP50/NHERF and EBP50/NHERF Δ 61c. Again, the amount of endogenous EBP50/NHERF co-immunoprecipitating with the receptor was reduced when cells were treated with isoproterenol (Figure 15B). However, the amount of EBP50/NHERF Δ 61c that co-immunoprecipitated with the receptor increased. Furthermore, a different subset of the high molecular weight bands co-immunoprecipitated when cells were treated with isoproterenol. Given their sensitivity to agonist, it may be that the second high-molecular weight band represents endogenous EBP50/NHERF, and the third high-molecular weight band represents EBP50/NHERF Δ 61c. The difference in agonist regulation between full length and EBP50/NHERF Δ 61c suggests that the c-terminus of EBP50/NHERF is required for its regulation *in vivo*. For example, EBP50/NHERF could be restricted to the plasma membrane, while EBP50/NHERF Δ 61c could interact with B2AR in the cytosol, i.e. on endosomes.

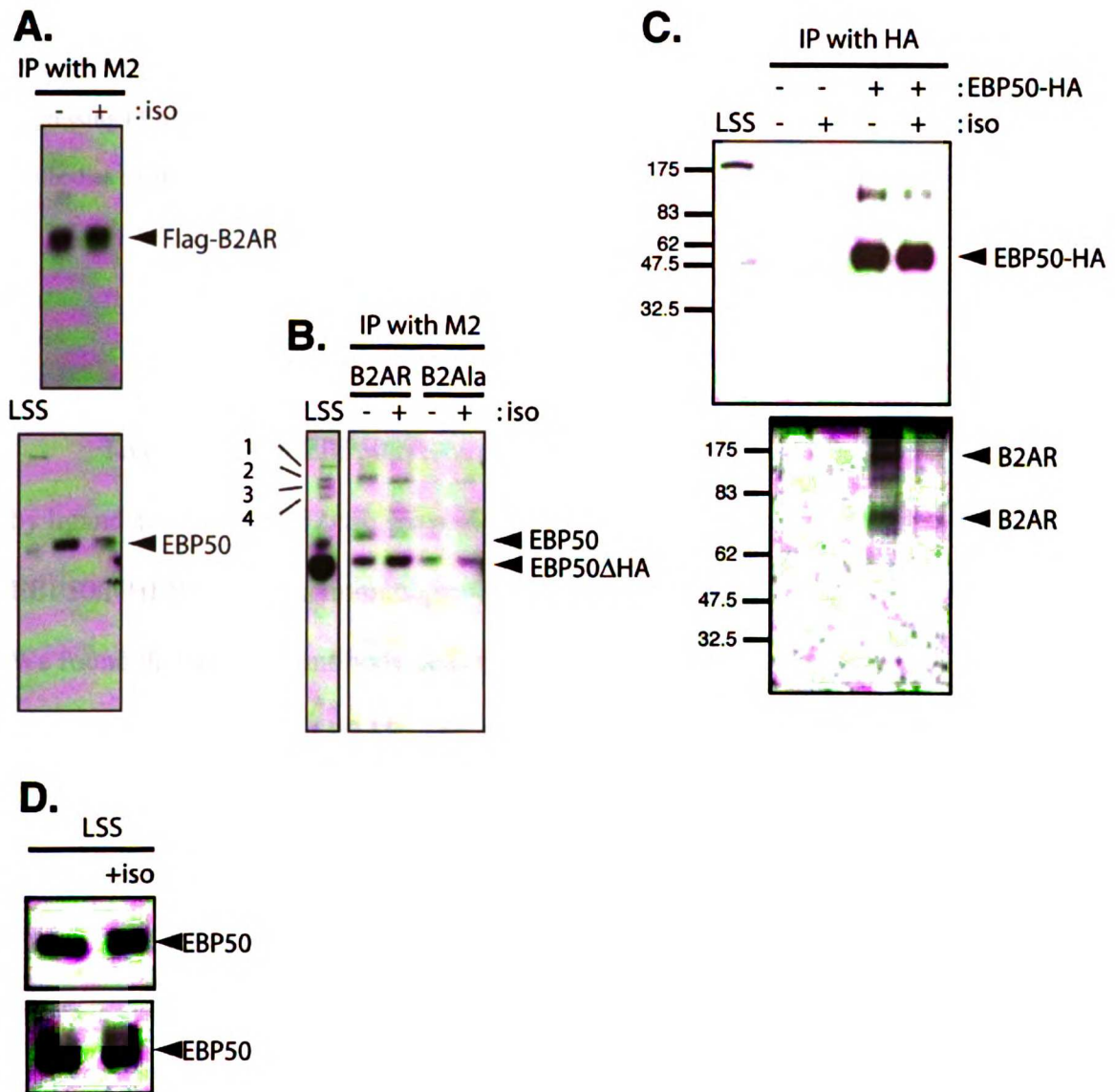


Figure 15. *Effects of B2AR agonist on EBP50/NHERF co-immunoprecipitation*

(A) Immunoprecipitation pellets from HEK293 cell lysates expressing FLAG-B2AR; some cells were treated with isoproterenol before lysis. Lysates and immunoprecipitated proteins were separated by PAGE and transferred to nitrocellulose. Lysates were immunoblotted with anti-FLAG or anti-EBP50/NHERF antibodies; immunoprecipitates were immunoblotted with anti-EBP50/NHERF antibodies. (B) Lysate (LSS) and immunoprecipitation pellets from HEK293 cells expressing FLAG-B2AR or FLAG-B2Ala and HA-tagged EBP50/NHERFΔ61c were immunoblotted with anti-EBP50/NHERF antibodies. Endogenous

EBP50/NHERF and EBP50/NHERFΔ61c-HA are indicated. (C) Lysates (LSS) or immunoprecipitation pellets from HEK293 cells expressing FLAG-B2AR and HA-tagged EBP50/NHERF were immunoblotted with antibodies against EBP50/NHERF (top) or FLAG (bottom). (D) Lysates from HEK293 cells expressing FLAG-B2AR, which had been treated with isoproterenol or not, were immunoblotted with antibodies against EBP50/NHERF.

To confirm that EBP50/NHERF co-immunoprecipitation with B2AR was reduced by ligand activation of B2AR, we performed a “reverse” co-immunoprecipitation where EBP50/NHERF-HA was immunoprecipitated from extracts using anti-HA antibodies. We found that a B2AR antibody detects two bands in the immunoprecipitate, corresponding to purified B2AR. The amount of B2AR that co-immunoprecipitates with EBP50/NHERF-HA was reduced after cells were treated with isoproterenol (Figure 15C). Therefore, B2AR agonist decreases the amount of B2AR that associates with full-length EBP50/NHERF in cells. Furthermore, neither exogenous expression nor the HA tag interferes with ligand regulation of the co-immunoprecipitation.

The localization of EBP50/NHERF and its close homolog E3KARP/NHERF2 suggests that B2AR binds to EBP50/NHERF at the plasma membrane but to E3KARP/NHERF2 in endosomes. E3KARP/NHERF2 has been localized to a vesicle-rich area underneath the apical surface of kidney epithelia, whereas EBP50/NHERF is more closely apposed to the plasma membrane (Wade et al., 2003). Interestingly, E3KARP/NHERF2 is not constitutively phosphorylated. Possibly, phosphorylation of EBP50/NHERF controls its association with the plasma membrane and plasma

membrane proteins such as B2AR. It would therefore be interesting to do localization and/or cell fractionation studies of a mutant EBP50/NHERF that is not phosphorylated *in vivo*. Furthermore, to more precisely identify where EBP50/NHERF (and E3KARP/NHERF2) binds to B2AR in cells, it would be useful to co-immunoprecipitate under conditions where plasma membrane B2AR or endosomal B2AR are precisely immunoprecipitated.

In preparing low-speed supernatants, we consistently saw that treatment of cells with isoproterenol increased the amount of EBP50/NHERF in the supernatant (Figure 15D). It appears that this represents an increase in phosphorylated 53 kDa EBP50/NHERF, although the fact that the bands were not clearly resolved. An increase in phosphorylated EBP50/NHERF could mean a number of things: it could, for instance, mean that EBP50/NHERF is more soluble after agonist treatment, or that more EBP50/NHERF is phosphorylated after agonist treatment. We did not analyze the amount of phosphorylated EBP50/NHERF in the low speed pellet, so we do not know whether B2AR activation increases the total level of EBP50/NHERF or whether it increases its solubility in detergent. Agonist activation of GPCRs activates GRKs, and GRK6A can phosphorylate EBP50/NHERF *in vitro*.

4 SORTING BETA2-ADRENERGIC RECEPTOR INTO DYNAMIC ENDOSOMAL TUBULES IS DEPENDENT ON ITS RECYCLING SEQUENCE AND ON ACTIN

Abstract. Endosomes are cellular organelles that rapidly receive proteins, lipids, and fluids from the plasma membrane surface and then sort this cargo to various cellular destinations. In endosomes, proteins returning to the plasma membrane are sorted from proteins traveling to lysosomes, organelles where proteins are degraded. We are interested in understanding how endosomes sort a particular class of transmembrane proteins, the g-protein coupled receptors (GPCRs), to the plasma membrane or to lysosomes. The GPCRs we have chosen for this study are the beta2-adrenergic receptor (B2AR), which travels from endosomes to the plasma membrane, and the delta-opioid receptor, which travels from endosomes to lysosomes. We have developed a fixation protocol for indirect immunofluorescence that retains endosomal structures that are observed in living cells. Using this new protocol, we have demonstrated that B2AR unlike the delta-opioid receptor, are seen in membrane tubules as long as 2 microns. Because of the limitations of previous methods used to visualize endosome tubules, there is little data on how endosomal proteins are distributed along tubules, and therefore little is known about the mechanism of protein sorting into tubules. Most of the tubules we observed using our immunofluorescence protocol contain transferrin, a protein that travels from several types of endosomes to the plasma membrane, and EEA1, a protein that promotes fusion of certain endosomes. In living cells, we have shown that these tubules are highly mobile and detach from enlarged vesicular endosomes. The vesicular

endosomes contain both transferrin and B2AR, but the two proteins appear to be in different sub-domains of the same endosome. We provide evidence that binding of B2AR to the actin cytoskeleton allows the receptor to enter tubules from a subdomain in the vesicular endosome, and we propose that association of B2AR with this subdomain is a mechanism by which the cell can regulate the trafficking of this receptor between the plasma membrane and lysosomes.

Endocytosed membrane proteins are targeted to the lysosomes by specific sequences in their cytoplasmic domain. By contrast, cytoplasmic sequences are typically not required for recycling membrane proteins from endosomes to the plasma membrane. The cytoplasmic domain of the transferrin receptor, a nutrient receptor that constitutively endocytoses, is not required for its recycling (Marsh et al., 1995; Odorizzi and Trowbridge, 1997; Rothenberger et al., 1987). Endocytosed proteins can recycle by following bulk membrane flow into endosomal tubules that contain little endocytosed fluid (Maxfield and McGraw, 2004; Mellman, 1996). However, cytoplasmic sequences are required to recycle proteins to specific sub-domains of the plasma membrane, for example to either the apical or basolateral domains of epithelial cells (Apodaca and Mostov, 1993; Odorizzi and Trowbridge, 1997). These sequences may function to bind adaptor protein subunits on endosomes (Gan et al., 2002).

The cytoplasmic domain of the beta-2 adrenergic receptor (B2AR) is required for its efficient recycling in nonpolarized cells. B2AR is a mammalian signaling receptor of the GPCR superfamily that is expressed in many tissues, whose signaling and endocytosis is activated by catecholamines (Tsao et al., 2001). During recycling, B2AR is

returned to its unstimulated state, perhaps with altered g-protein specificity (Lefkowitz, 1998; Pippig et al., 1995; Xiang and Kobilka, 2003a). This return of B2AR enables cells to repeatedly respond or “resensitize” to agonists. A sequence at the carboxy terminus of B2AR is necessary for its recycling and is sufficient to recycle a chimaeric receptor (Cao et al., 1999; Gage et al., 2001). This recycling signal, which can be inactivated by phosphorylation, appears to mask an upstream sequence that efficiently targets B2AR and other GPCRs to lysosomes within hours of agonist treatment (Cao et al., 1999; Whistler et al., 2002). Inactivation of this recycling signal will therefore reduce or “desensitize” cellular responsiveness to catecholamines. Therefore, the recycling signal of B2AR plays a central role in regulating catecholamine signaling via B2AR in cells.

The recycling signal of B2AR can directly bind to PDZ domains in the EBP50/NHERF family, and can also bind to the chaperone NSF (N-ethyl maleimide sensitive factor) (Cao et al., 1999; Cong et al., 2001a; Gage et al., 2004; Hall et al., 1998a; Hall et al., 1998b). EBP50/NHERF family members may link B2AR to the actin cytoskeleton by also binding proteins of the ERM family (Ezrin, Radixin, Moesin) (Bretscher et al., 2002; Huang et al., 2003; Murthy et al., 1998; Nguyen et al., 2001; Reczek et al., 1997; Yun et al., 1998). EBP50/NHERF, actin, and NSF have each been implicated in promoting B2AR recycling (Cao et al., 1999; Claing et al., 2001; Cong et al., 2001a; Gage et al., 2001; Gage et al., 2004). The identification of these protein interactions has not, however, revealed the mechanism by which the recycling signal of B2AR operates.

In order to understand the mechanism by which the recycling signal of B2AR sorts B2AR to the plasma membrane, we have attempted to more precisely identify the

sub-domains of endosomes where the recycling signal functions. To that end, we have looked at the dynamics and sub-structure of endosomes containing various GPCRs. Analysis of endosome dynamics by live cell imaging has enabled us to identify endosomal transport intermediates in the recycling pathway of B2AR. After identifying these endosomal transport intermediates, we surveyed fixation conditions whereby the sub-structure of these endosomes was preserved during indirect immunofluorescence. These conditions enabled us to identify these endosomes with endosomal markers. We then analyzed the localization within these endosomes of various GPCRs: GPCRs with the wild-type recycling signal of B2AR, and inactive recycling signal, or no recycling signal. We also studied the effect of adding latrunculin, which depolymerizes actin, on the localization of B2AR within these endosome sub-structures. These techniques have enabled us to determine where the recycling signal of B2AR and the actin cytoskeleton act in directing B2AR to the plasma membrane.

4.1 *Materials and Methods:*

Buffers

RPMI: RPMI, L-glutamine, no phenol red (Invitrogen); RPMIH: RPMI, 30 mM HEPES (pH 7.5); BRB80: 80 mM PIPES (pH 6.8), 1 mM MgCl₂, 1 mM CaCl₂; TBS: 25 mM Tris, 137 mM NaCl, 3 mM KCl, pH 7.6; TBST_x: TBS 0.05% Tx-100 added freshly; AbDil: TBST_x, 2% bovine serum albumin, 0.1% NaN₃.

Cell Lines and Cell Culture

Human embryonic kidney (HEK293) cells were maintained and passaged in Dulbecco's modified Eagle's medium (DMEM) containing 10% fetal bovine serum and 100 units/mL penicillin/streptomycin (Cell Culture Facility, UCSF). HEK293 cells stably transfected with wild type receptors containing an N-terminal signal sequence and FLAG epitope have been previously described (Tsao and von Zastrow, 2000). B2Ala receptors contain the B2AR sequence with an additional carboxy-terminal alanine as previously described (Cao et al., 1999). DORcB2 contain the DOR sequence with the last 6 residues from its carboxy terminus deleted and replaced with the last 10 residues of B2AR; DORcBAla contain the DORcB2 sequence with an additional carboxy-terminal alanine as previously described (Gage et al., 2001). Cells were plated onto poly-L lysine (Sigma-Aldrich Co.) coated coverslips before imaging.

Live Cell Imaging

Cells were plated onto 22 mm round coverslips for 48 hours. A heat-controlled perfusion chamber (Brook Industries, Lake Villa, IL) was placed on a Nikon Diaphot 300 inverted microscope with a 60X, 1.4NA PlanApo objective (Nikon Inc.) and pre-warmed to 37°C. Surface receptors were labeled with M1 anti-FLAG antibody (Sigma Chemical Co.) covalently conjugated to Alexa 594 (Molecular Probes) in RPMIH at 37°C for 30 min. This antibody binds to receptors but does not inhibit their post-endocytic trafficking (Tsao and von Zastrow, 2000). The cells were washed 3x in RPMIH and placed into the perfusion chamber with 200 μ L RPMIH. After 5 minutes, 250 μ L of 20 μ M isoproterenol in RPMIH was added to the chamber to drive endocytosis of B2AR. Alternatively, to label transferrin receptors, cells were incubated with RPMIH for 30 min and then with 50

$\mu\text{g/mL}$ transferrin covalently conjugated to Alexa 488 (Molecular Probes) in RPMIH immediately before imaging. The samples were illuminated with a 100W mercury arc lamp using appropriate filters (Chroma Technology Corp., Rockingham, VT). Cells were imaged up to 30 min after application of agonist, but each field of cells was imaged for no more than 1 min, under minimal illumination intensity. Images were acquired on a CCD camera (Princeton Scientific Instruments, Inc., Monmouth Junction, NJ) and recorded with IP Lab Spectrum software (Scanalytics, Fairfax, VA) onto S-VHS video tape (Sony Corp.) The images were continuously integrated over 0.3 sec. To measure position, video tape frames were digitized at a rate of 2 frames per second with a Scion AG-5 frame grabber, and endosomes were identified by hand in Scion Image software (Scion Corp., Frederick, MD).

Data Analysis

After acquiring the coordinates of fluorescent structures, we calculated the distance traveled, r , by each particle over various time intervals, Δt . Plotting the mean square displacement (MSD) as a function of Δt , for a diffusion in a two-dimensional plane:

$$\text{MSD}(\Delta t) = \langle (r(t) - r_0)^2 \rangle$$

particle motion can be categorized as simple Brownian diffusion, directed motility, or confined diffusion (Saxton and Jacobson, 1997). For simple diffusion,

$$\text{MSD}(\Delta t) = 4D\Delta t$$

where D is the diffusion coefficient. For directed motility,

$$\text{MSD}(\Delta t) = (v\Delta t)^2$$

where v is velocity. If a diffusing particle drifts with constant velocity, these two equations are summed:

$$\text{MSD}(\Delta t) = 4D\Delta t + (v\Delta t)^2$$

For a diffusing particle that is trapped within a domain or is tethered,

$$\text{MSD}(\Delta t) \approx r_c^2(1 - 1/A_1 \exp((4A_2 D \Delta t)/r_c^2))$$

$A_1 = 0.99$ and $A_2 = 0.85$ are constant coefficients determined by the geometry of a circular cage in which the particle can freely diffuse (Steyer and Almers, 1999). r_c is the radius of a circular cage (minus the radius of the particle), or is the length of the flexible tether on the particle.

Immunofluorescence

To visualize tubular endosomes, surface receptors were labeled with M1 anti-FLAG antibody (Sigma-Aldrich Co., St. Louis, MO) covalently conjugated to Alexa-594 (Molecular Probes) in RPMIH at 37°C for 30 min. The cells were then washed with RPMIH. For latrunculin experiments, 0.025-25 μM latrunculin B (Alexa C, San Diego, CA) or a control DMSO solution was added to each coverslip for 15 min to depolymerize actin. A solution of 10 μM agonist (DADLE or isoproterenol), 50 $\mu\text{g}/\text{mL}$ Alexa-488 conjugated transferrin (Molecular Probes) and latrunculin in RPMIH was added to the cells, which were then incubated for 15 min. Cells were then rapidly washed in RPMIH+10% fetal bovine serum (Cell Culture Facility, UCSF) and fixed in BRB80+4% EM grade formaldehyde (Ted Pella, Redding, CA). This fixative was critical to preserve morphology of tubules. Cells were washed 3x for 5 min each in TBS and mounted in VectaShield (Vector Laboratories Inc., Burlingame, CA). Staining was imaged with the

microscope and camera above; digital images were saved to a computer. Tubular structures longer than 0.2 μm were identified by eye and measured with IP Lab Spectrum software.

To visualize early endosomes, surface receptors were labeled with M1 anti-FLAG antibody (Sigma-Aldrich Co.) in RPMIH at 37°C for 30 min. Cells were then washed in RPMIH and then incubated in RPMIH containing 50 $\mu\text{g}/\text{mL}$ Alexa-647 conjugated transferrin (Molecular Probes, Eugene, OR). After 15 min, cells were rapidly washed with RPMIH containing 10% fetal bovine serum (Cell Culture Facility, UCSF) to remove surface transferrin. Cells were then immediately fixed at room temperature in BRB80+4% EM grade formaldehyde (Ted Pella, Redding, CA). After 20 minutes, fixed cells were placed in TBS. After 20 minutes, cells were permeablized in TBSTx for 5 minutes and then rinsed 3x in TBSTx. Low Tx-100 (0.05%) was used to preserve endosomal staining of receptors. Cells were blocked in AbDil for 10 minutes. Subsequent antibodies were added in the following order for 45 min each, followed by 3 5 min washes in TBSTx: Alexa 555-conjugated anti-mouse IgG2b (Molecular Probes) at 1:1000, mouse IgG1 anti-EEA1 (BD Biosciences-PharMingen, San Diego, CA) at 1:50, Alexa 488-conjugated goat anti IgG1 at 1:1000 (Molecular Probes). All antibodies were diluted in AbDil. Cells were incubated with 10 $\mu\text{g}/\text{mL}$? Hoechst 33342 in TBSTx for 10 min to stain nuclei and then washed in TBSTx. Cells were mounted in ProLong (Molecular Probes).

Confocal Microscopy

Confocal laser scanning microscopy was performed on a Zeiss LSM 510 with a Plan-Neofluar 100x 1.3NA oil immersion objective (Carl Zeiss Inc.) To visualize Alexa 555 fluorescence, a 543 nm laser was used with the dichroic filters HFT KP 700/543 and NFT 545, and the bandpass filter BP 565-615R. To visualize Alexa 488 staining, a 488 nm laser was used with the dichroic filter HFT 488 and the bandpass filter BP 500-550IR. To visualize Alexa 647 fluorescence, a 633 nm laser was used with dichroic filter HFT 488 and a tunable bandpass filter from 644-719nm. All settings (such as camera gain and laser intensity) were selected such that no bleed-through was observed with control samples prepared in parallel lacking one of the three Alexa dyes. Individual z-sections were filtered 3 times using a 3x3 hybrid median filter in Adobe Photoshop (Adobe Systems Inc., Mountain View), and sections were stacked using maximum projection in Zeiss LSM Image Examiner (Carl Zeiss Inc.) (Hammond and Glick, 2000; Russ, 1999).

4.2 Results

Dynamics of endosomes that contain GPCRs in living cells

Structures containing fluorescently labeled GPCRs exhibit many types of movements in HEK293 cells within 30 minutes of treatment with agonist. To track endocytosed GPCRs, we incubated cells with monoclonal antibodies against an epitope engineered onto the extracellular N-terminus of exogenously expressed receptors. This incubation of live cells with monoclonal antibodies allows receptors at the plasma membrane to be specifically labeled, and does not alter the intracellular trafficking of GPCRs. Some labeled structures had so-called “directed” movements that covered long distances (>1 μm)

(Figure 16A). Such directed movements followed either straight, smoothly curved or stuttering paths. Structures that followed straight or smoothly curved paths moved faster than structures that followed stuttering paths. By contrast, diffusing structures followed random paths (Figure 16B). Some diffusing structures also exhibited brief periods of directed movements that covered short distances (between 0.5 and 1 μm) that rapidly reversed (Figure 16B). We call this type of rapidly reversing motion “recoil.” Finally, a small number of structures exhibited very little or no movement, which we have termed “stationary.”

We analyzed the movements by plotting the slope of the mean squared displacement of these structures versus time (see methods). The slope of this plot is linear for objects that move by simple diffusion, curves upward for objects that have directed movements, and curves downward for objects that are constrained (Figure 16C). We found that for structures that have slow movements, the slope of this plot fits a formula that includes both diffusive and active movement. For structures that recoil, we found that the slope of this plot curves sharply in both directions, while the overall slope of the plot is linear. This sharply curving slope suggests that while this motion is predominantly diffusive, this motion also consists of brief active movements that are constrained and can reverse.

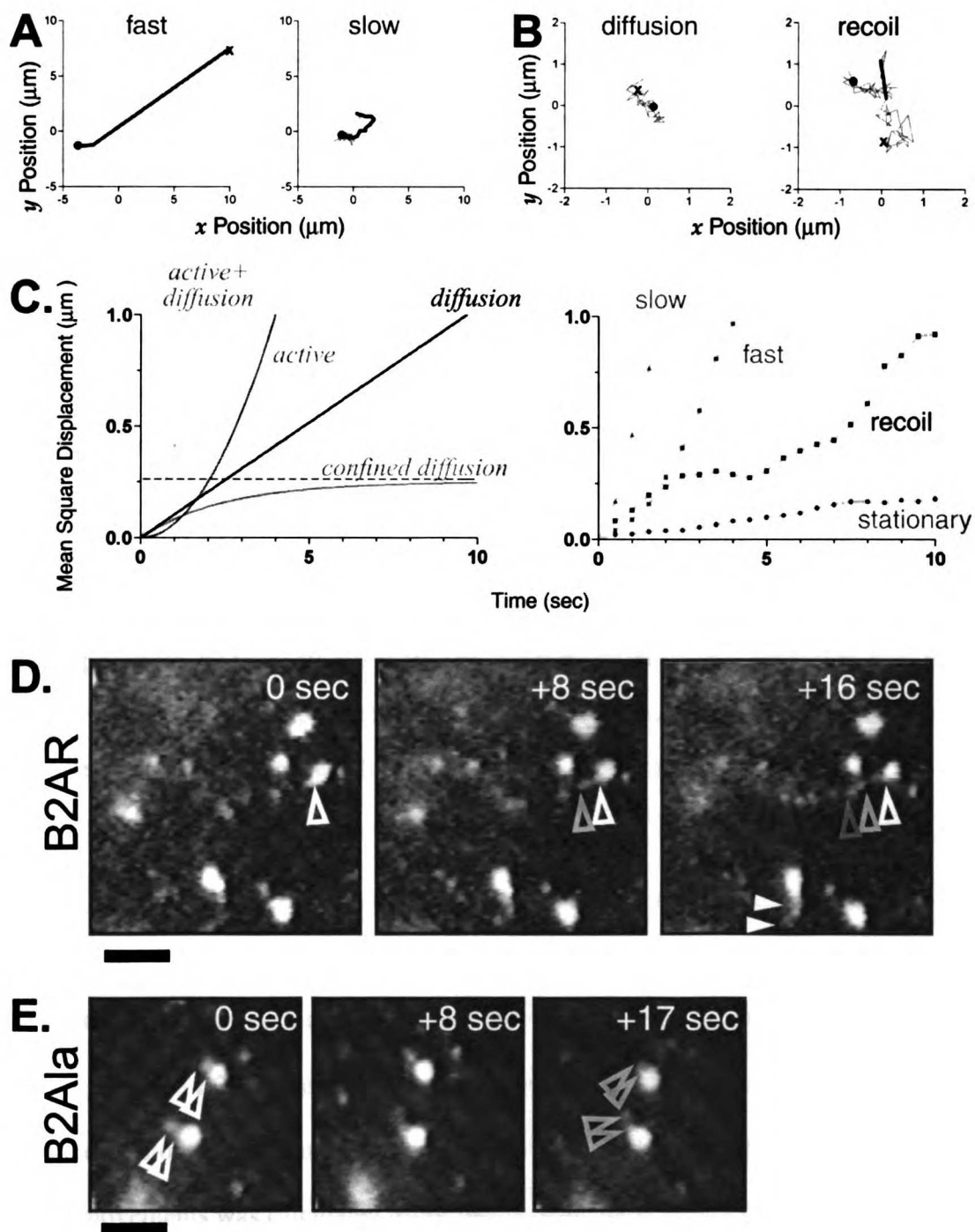


Figure 16

Live cell imaging of B2AR, B2AlaR, DOR. (a-d) Structures containing B2AR were made visible in HEK293 cells that had been stably transfected with plasmids containing FLAG-B2AR. These cells were

first incubated in serum-free media containing a fluorochrome-conjugated antibody, M1, which will bind to the FLAG epitope on surface B2AR. Coverslips containing treated cells were then placed within a heated chamber on an epi-fluorescent microscope, treated with media containing agonist, and recorded with a CCD camera. (a-b) Plots represent the positions of representative fluorescent particles recorded at 0.5 second intervals. X=first position, 0= last position, grey line= diffusive motility, black line= directed movement (a) left panel: particle with fast movement; right panel: particle with diffusion and slow movement. During the phase of slow movement, there were frequent pauses. (b) (note scale change from (a)) left panel: particle with diffusive motility; right panel: particle with diffusive motility, directed motility and recoil. (c) Mean squared displacement $MSD(\Delta t)$ for three particles is plotted. These particles represent three different types of particle movements. Theoretical curves are also shown: active, $v = 0.04 \mu\text{m}/\text{sec}$, active+diffusion, $D = 0.06 \mu\text{m}^2/\text{sec}$, $v = 0.4 \mu\text{m}/\text{sec}$; diffusion, $D = 0.03 \mu\text{m}^2/\text{sec}$; confined diffusion, $r_c = 500 \text{ nm}$, $D = 0.03 \mu\text{m}^2/\text{sec}$. (d) The position of a tubule that emerges from an enlarged fluorescent structure (arrowhead) is shown at three different times. Bar=5 μm . This tubule later detaches and has fast movement. A slight gap appears in the tubule (16 sec, middle arrowhead); the tubule detaches, however, from the base of the vesicular structure (right arrowhead) (e) Live imaging of cells containing B2A1a. The position of two short tubules (arrowheads) are shown at three different times; white=0 sec, black=17 sec.

To characterize each of the different movements observed for structures containing labeled B2AR, we determined the speed of directed movements and the apparent diffusion coefficient of diffusive movements. The instantaneous speed of directed movements was calculated using the point-to-point distance between data measurements from successive frames (see methods). Structures with fast movements along linear or curved paths were twice the speed of structures that move with slow movements along stuttering paths (Table 2). The apparent diffusion coefficient for

diffusing structures was calculated from the average of the initial slopes of the plots of mean squared displacement. The apparent diffusion coefficient of structures with recoil determined by this method was four times larger than that the apparent diffusion coefficient of stationary structures (Table 2).

fast movements			
instant speed (d/t) at 0.5 frame/sec			
average +/- SD	2.5 +/- 1		um/sec
maximum	4.7		um/sec
<v > (slope msd/t)			
average +/- SD	0.5 +/- 0.3		um/sec
slow movements			
instant speed (d/t) at 0.5 frame/sec			
	0.8 +/- 0.3		um/sec
recoil movements			
initial slope msd/t +/- SD	0.103 +/- 0.004		um ² /sec
diffusion coefficient +/- SD	1.03E-10 +/- 0.1E-10		cm ² /sec
stationary			
initial slope msd/t +/- SD	0.018 +/- 0.002		um ² /sec
diffusion coefficient (1/4*slope msd/t) +/- SD	2.68E-11 +/- 0.5E-11		cm ² /sec

Table 2. vesicle movements

Some of the round or “vesicular” structures that contained B2AR protruded narrow, extended domains; we call these narrow structures “tubules.” Tubules that detached from a vesicular structure could move over long distances with fast speeds (Figure 16D and Table 2), whereas tubules that remained attached to a vesicular structure generally exhibited rebounds. Rarely, tubules remained attached to a vesicular structure

while moving over long distances (not shown). Therefore, tubules generally move faster than the vesicular structures from which they emerge.

While labeled structures exhibiting fast, slow, and diffusive motility were also observed in HEK293 cells expressing B2A1a or DOR, tubules were much more frequently observed in cells expressing B2AR. Vesicular structures that contained B2A1a occasionally formed short protrusive structures; however, these structures did not elongate and did not detach during the viewing period (1 min; Figure 16E). Therefore, while a subset of structures that contain fluorescently labeled B2AR are in tubules that exhibit fast movements, B2A1a and DOR do not appear in similar structures.

Quantification of tubules within fixed cells

To quantitatively determine the extent to which endosomes that contain B2AR form tubules, we needed to visualize tubular structures in fixed cells. To assess fixation conditions, we first drove receptor endocytosis to steady state by incubating cells in agonist for 15 minutes. Next, we replaced the media with a fixative, and then visualized structures with an epi-fluorescent microscope. However, with many fixative buffers, we did not observe elongated, tubular structures. In the end, we were best able to visualize tubules when cells labeled for B2AR were fixed by formaldehyde in a buffer commonly used to preserve microtubules (Figure 17A, open arrowheads). Transferrin receptor, which rapidly recycles from endosomes, has been previously shown in living cells to exit vesicular structures in elongated tubules by epi-fluorescence microscopy (Sonnichsen et al., 2000). In our fixative, fluorescent transferrin added to cells for 15 minutes was also observed in elongated, tubular structures (Figure 17B). By contrast, shorter tubular

structures were visualized in cells that were labeled for DOR and B2A1a (Figure 17C and D, closed arrowheads). Therefore, using conditions that preserve microtubule structure, we were able to specifically visualize elongated tubules in fixed cells that had been labeled for B2AR or for transferrin receptor, but not in cells labeled for DOR or B2A1a.

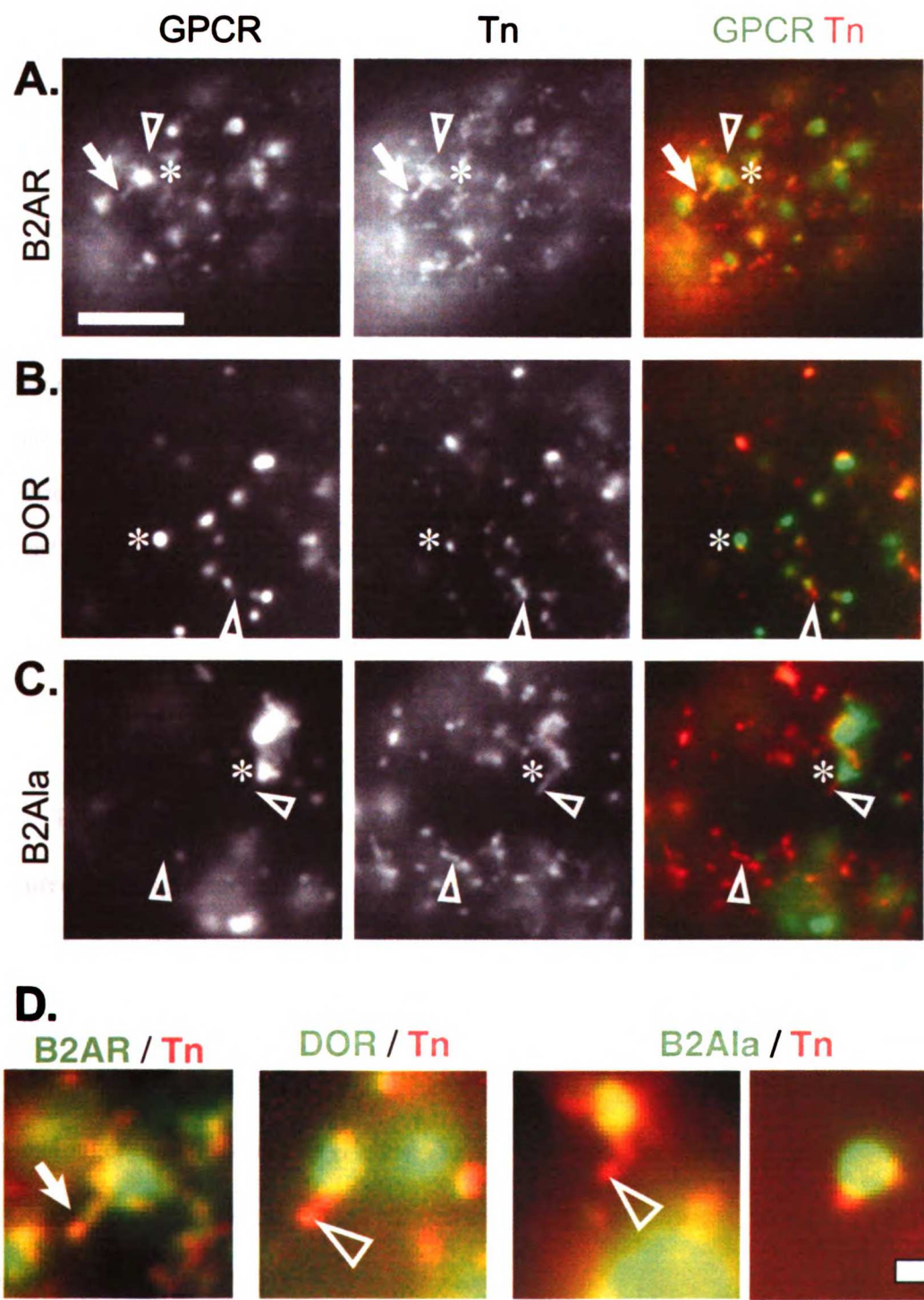


Figure 17

Epi-fluorescence microscopy of transferrin receptor with GPCRs. Structures containing GPCRs and transferrin receptor (Tn) were made visible in HEK293 cells that had been stably transfected with plasmids containing FLAG-GPCRs: (a) B2AR, (b) DOR, (c) B2A1a. These cells were first incubated with serum-free media containing a fluorochrome-conjugated antibody, M1, that will bind to the FLAG epitope on surface GPCRs. Next, cells were incubated for 15 minutes in media containing agonist. To label transferrin receptor, cells were incubated for 15 minutes in media containing fluorochrome-conjugated transferrin. Cells were then fixed with formaldehyde and imaged on an epi-fluorescent microscope. In the merged images, the fluorescence from the GPCR is colored green and the transferrin, red. In (a) and enlarged in (d), there are elongated tubules containing B2AR and transferrin (arrows). In (a) there are also enlarged structures that contain both B2AR and transferrin; in these structures, the two receptors are not perfectly colocalized. In (b), (c) and (d) there are elongated Tn tubules that do not contain the degrading GPCRs DOR and B2A1a (open arrowheads). (a) Bar = 10 μm , (d) Bar=1 μm .

To determine the extent to which endocytosed GPCRs are found in tubules, we measured the length and number of labeled tubules in fixed cells. To measure tubule length, elongated structures were measured from end to end, or from end to a junction with an enlarged vesicular structures (Figure 17D, arrows). We found that cells labeled for B2AR or transferrin, but not in cells labeled for DOR or B2A1a, contained many tubules longer than 0.6 microns (Figure 18). The overall distribution of tubule lengths for B2AR was significantly longer than that for DOR ($P < 0.0001$, 3 experiments, by Mann-Whitney) and B2A1a ($P < 0.0001$, 3 experiments, by Mann-Whitney). The median length was 30% longer for B2AR tubules than both DOR and B2A1a tubules (0.6 microns versus

0.4 microns). However, we feel that median lengths are less useful to compare receptors than the overall distribution of lengths, because tubules are dynamic structures that are constantly formed on endosomes (Figure 16D). To quantify the number of labeled tubules, we counted the average number of tubules (see methods) observed in individual cells within a 13 x 13 μm region. By this approach, we estimated that B2AR are in three fold more tubules per cell than either DOR or B2Ala. (Figure 19A, green + yellow bars). Together these results demonstrate that under steady state conditions, endocytosed B2AR is found in tubules that are significantly longer and more numerous than either DOR or B2Ala. The finding that B2Ala is not observed in elongated tubules suggests that the c-terminus is necessary for B2AR to be found in tubules.

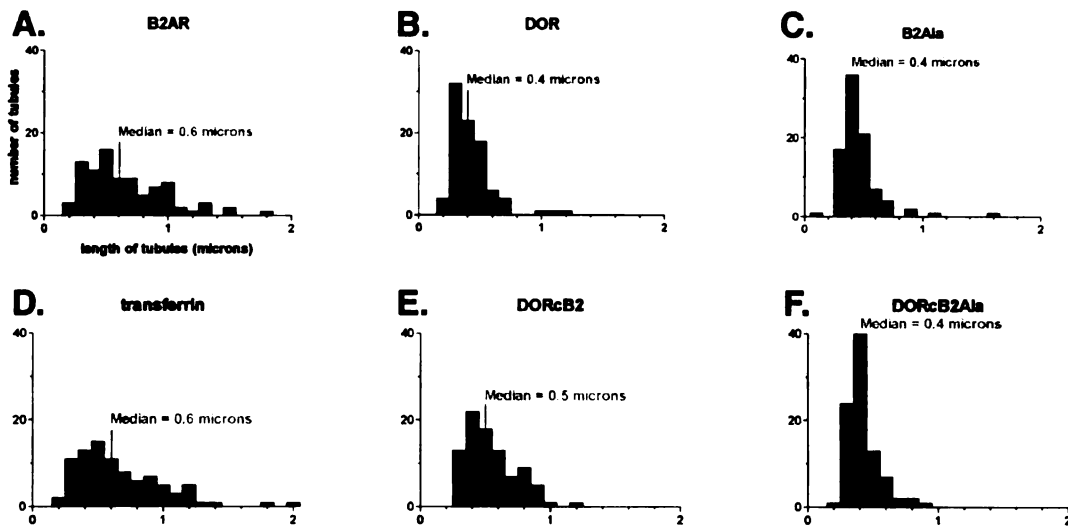


Figure 18

Histogram of tubule length for GPCRs. For each histogram, the lengths of 90 individual fluorescent tubules from about 20 cells prepared as in Figure 2 are plotted and the median tubule length was calculated. The GPCRs were: (a) B2AR (b) DOR (c) B2A1a (d) transferrin (e) DORcB2 (f) DORcB2A1a.

To investigate whether the c-terminus of B2AR is also sufficient to cause receptor to be found in tubules, we measured the number and the length of labeled tubules in cells expressing the chimaeric receptor, DORcB2. DORcB2 has the c-terminal 11 residues of B2AR appended onto those of DOR. We chose the c-terminal region of B2AR because this region comprises a recycling sequence that is sufficient to rapidly target the receptor from endosomes to the plasma membrane (Gage et al., 2001). This recycling sequence can be inactivated by adding additional residues to the c-terminus, such as alanine. We found that cells labeled for DORcB2, but not cells labeled for DORcB2A1a, contained a

large number of tubules longer than 0.6 microns (Figure 18). The overall distribution of tubule lengths for DORcB2 was significantly longer than that for DORcBA1a (0.0001, 2 experiments, by Mann-Whitney). The median length was 20% longer for DORcB2 tubules than both DORcBA1a tubules (0.5 microns versus 0.4 microns). Again, we feel that median lengths are less useful to compare receptors than the overall distribution of lengths, because tubules are dynamic structures that are constantly formed on endosomes. Together these results indicate that GPCRs with the intact recycling sequence of B2AR are found in longer and more numerous tubules than GPCRs that do not recycle, and that these tubules are similar in length to those of transferrin receptor, which also recycles.

Co-localization of tubules with transferrin

To determine whether the tubules that contained B2AR or DORcB2 were part of the same endosomal pathway utilized by the transferrin receptor, we co-localized B2AR with fluorescent transferrin. Transferrin receptor, which is found in early endosomes and recycling endosomes, has previously been shown to broadly co-localize with the B2AR. We found that tubular structures that contained B2AR frequently co-localized with transferrin (Figure 17A and D, arrow). With all GPCRs studied, it was common to see transferrin tubules that did not contain detectable GPCR (Figure 17, open arrowheads).

To determine the extent to which tubules that contained different GPCRs were co-localized with transferrin receptor, we quantified the number structures containing labeled GPCRs co-localized with transferrin. We found that 90% of B2AR tubules and 70% of DORcB2 tubules co-localized with transferrin, whereas only 50% of the rare, short tubules that contain DOR and B2A1a (and only 10% for DORcB2A1a) co-localize

with transferrin (Figure 19A, yellow bars). The number of B2AR tubules that did not co-localize with transferrin (Figure 19A, green bars) was not significantly different from the number of DOR tubules that did not co-localize ($P=0.5$, 3 experiments, Welch's t-test). The data presented, from cells that were incubated in agonist for 15 minutes, is similar to data from cells that were incubated in agonist for 5 minutes, which presumably labels early endosomes (not shown). B2AR and DORcB2, both recycling receptors, are in at least twice the number of endosomal tubules as DOR, B2A1a, and DORcB2A1a, and most of these tubules co-localized with transferrin. Therefore, we conclude that most of the tubules that contain B2AR and DORcB2 are co-localized with transferrin, in contrast with those of DOR, B2A1a, and DORcB2A1a. This indicates that GPCRs with the intact recycling sequence of B2AR are found in tubules that are part of the same endosomal pathway as transferrin receptor – that is, early and/or recycling endosomes. Furthermore, this result suggests that the recycling sequence of B2AR is required for this receptor to enter these endosomal tubules.

Co-localization of endosomes and tubules with EEA1

To determine whether B2AR tubules likely emerge from either early or recycling endosomes, we co-localized the B2AR with the early endosomal protein EEA1. We chose EEA1 because this protein is restricted to a subset of early endosomes (Mu et al., 1995; Wilson et al., 2000). To locate endogenous EEA1 in cells that express GPCRs, we modified our fixation protocol to include detergent (Figure 21). As has been demonstrated before, EEA1 is often concentrated at one or more locations on endosomes (Figure 21A, arrows) (Raiborg et al., 2002). The location of EEA1 relative to both

GPCRs and transferrin was determined by confocal microscopy. In enlarged structures contiguous with a tubule that contained B2AR, EEA1 often was concentrated primarily at a small area away from the tubule. Therefore, endocytosed B2AR was located with EEA1 in early endosomes. This result suggests that early endosomes extend tubules that contain B2AR.

To determine the extent to which B2AR is found in early endosomes, we counted the number of labeled structures containing endocytosed B2AR that were co-localized with EEA1. For comparison, we also co-localized EEA1 with labeled structures containing DOR. While it has been previously demonstrated that DOR sorts away from B2AR after prolonged agonist treatment, the sorting of DOR at early stages has not been investigated (Keith et al., 1996; Tsao and von Zastrow, 2000). We found that after 15 minutes of agonist treatment, 75% of labeled structures containing B2AR, but only 40% of labeled structures containing DOR, co-localized with EEA1 (Figure 19B). This indicates that after 15 minutes of agonist treatment, B2AR is mostly in early endosomes, whereas a majority of DOR is not. Therefore, B2AR likely enters tubules from early endosomes.

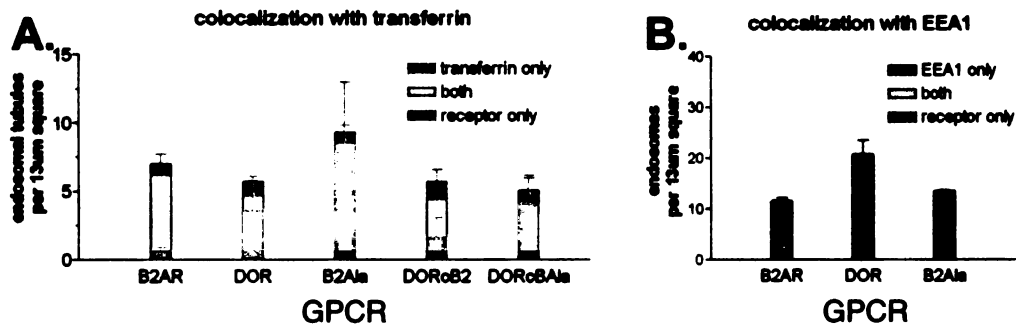


Figure 19

Quantification of co-localization of transferrin and EEA1 with GPCRs. The samples from Figure 3 were imaged on an epi-fluorescent microscope and displayed in PhotoShop. Structures within squares of 13x13 microns that were placed on cells were counted; 20 cells were counted per experiment, and the experiment was repeated three times and over 400 structures were counted for each cell line. (a) Tubules were counted as containing either transferrin or the GPCR. The green bars represent the average number of tubules per square that contain only the GPCR and the red bars represent the number that contain only transferrin. The yellow bar represents the average number of GPCR tubules that are co-localized with transferrin receptor. (b) To measure co-localization of GPCR endosomes with EEA1, EEA1 was made visible in cells expressing Flag-B2AR by indirect immunofluorescence; this procedure was done in the presence of detergent. The quantification was performed as described above. The blue bars represent the average number of EEA1 structures which do not co-localize with a GPCR. The pink bar represents the average number of GPCR structures that co-localize with EEA1.

To determine whether B2AR and DOR are in the same early endosomes, we co-expressed B2AR and DOR in the same cells. However, in these cells we found that B2AR was not found in endosomal tubules (not shown). It has previously been

demonstrated that B2AR can co-immunoprecipitate with DOR, which could explain why B2AR was unable to enter endosomal tubules (Jordan et al., 2001).

If DOR is rapidly sorted from early endosomes, which are capable of forming elongated tubules, then this rapid sorting could explain why DOR is found in fewer, shorter tubules. To see whether other degrading receptors are rapidly sorted from early endosomes, we co-localized B2A1a with EEA1. We chose B2A1a because, like DOR, it is not found in elongated tubules, and because it is degraded after endocytosis. We found that, like B2AR but unlike DOR, the majority B2A1a structures co-localize with one or more small spots of EEA1. The percentage co-localization of B2A1a structures with EEA1 is not significantly different than was seen for B2AR (Figure 19B), ($P=0.8$, 3 experiments, Welch's t-test). This result indicates that receptors not observed in elongated tubules may still be found in early endosomes that can extend tubules. Furthermore, it suggests that the recycling sequence of B2AR is required to enter tubules from early endosomes.

Latrunculin treatment

Unlike transferrin receptor, B2AR recycling in non-polarized cells is sensitive to actin-depolymerizing drugs such as latrunculin (Cao et al., 1999; Durrbach et al., 1996). We therefore asked whether actin is selectively required for endocytosed B2AR to be found in tubules. We treated cells with latrunculin and then separately measured the length of B2AR tubules and transferrin tubules. We found that latrunculin treatment resulted in significantly shorter tubules that contain B2AR, whereas tubules that contain transferrin are still elongated (Figure 20). When cells expressing B2AR were treated with $2.5 \mu\text{M}$

latrunculin to depolymerize actin, the length of B2AR tubules was significantly shorter than controls ($P < 0.0001$, 3 experiments, by Wilcoxon) but the transferrin tubules did not ($P = 0.8$, 3 experiments, by Wilcoxon) (Figure 20B and C). The median tubule length for the B2AR was 30% shorter than the median transferrin tubule length in these cells (0.5 microns versus 0.7 microns), and 20% shorter than the median B2AR tubule length in untreated cells (0.6 microns). While statistical tests did not reveal a significant difference in transferrin tubule length between the latrunculin treated and control cells, the median tubule length increased slightly (0.7 microns latrunculin treatment, versus 0.6 microns control) and the shape of the histogram was slightly different. This different histogram shapes for transferrin tubules with and without latrunculin may be due to the effect of latrunculin on cell shape, which in turn could change the length of the tubules visualized by standard epi-fluorescent microscopy. Alternatively, this difference in lengths could be due to a subtle effect of latrunculin on transferrin tubule length. The length of B2AR tubules also decreased when cells were treated with either 25 or 0.25 μM latrunculin, (not shown). We conclude from these results that the length of B2AR tubules is more sensitive than transferrin tubules to latrunculin. Therefore, it appears that B2AR requires actin to exit early endosomes in tubules, whereas transferrin receptor does not.

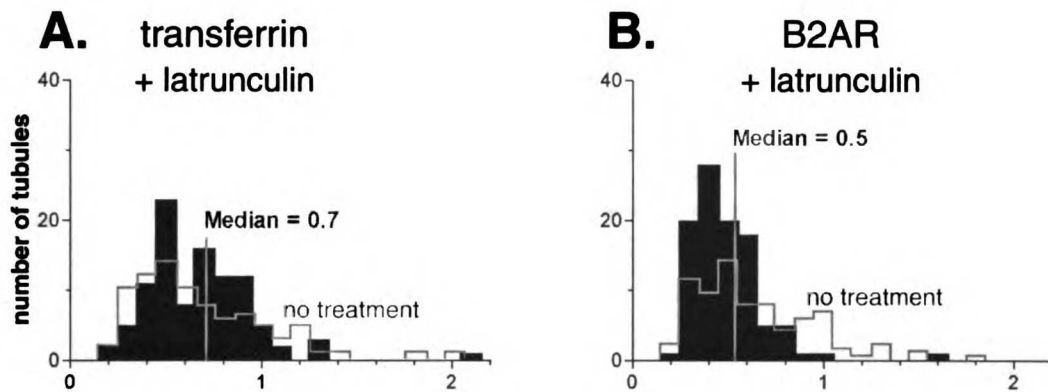


Figure 20

Actin is necessary for B2AR to be found in elongated tubules. (a) latrunculin prevents B2AR from being found in tubules containing Tn (picture of fixed cells) (b) The median lengths of 100 tubules are plotted as a histogram. The median lengths of B2AR tubules and transferrin tubules in cells treated with 2.5 mM latrunculin are significantly different from each other, $P < 0.0001$ by Mann-Whitney. The median lengths of B2AR tubules in latrunculin treated cells are also significantly different than those of B2AR tubules in untreated cells, $P < 0.0001$ by Wilcoxon.

Enlarged vesicular structures

Many early endosomes appear as enlarged vesicular structures; these large structures have been seen before using epi-fluorescence (Barak et al., 1997; Sonnichsen et al., 2000). Vesicular structures greater than 0.4 microns in diameter contained both transferrin and GPCR, for all of the GPCRs in this study (Figure 17, asterisks).

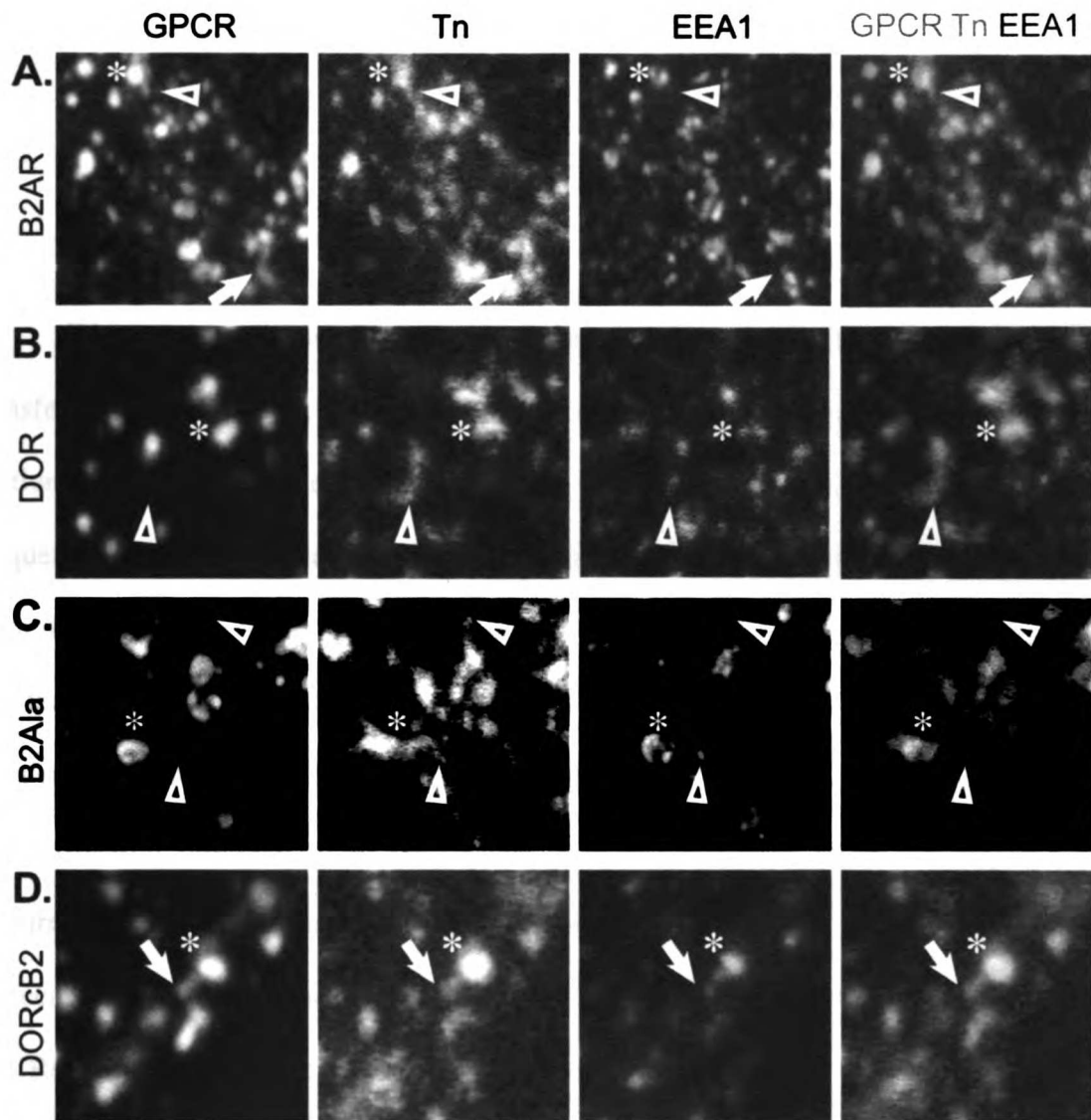


Figure 21

Confocal microscopy of transferrin and EEA1 with GPCRs. Structures containing GPCRs and transferrin receptor (Tn) were made visible in cells that had been stably transfected with plasmids containing FLAG-GPCRs. The GPCRs used were: (a) B2AR, (b) DOR, (c) B2AlaR (d) DOR-cB2AR. These cells were first incubated in serum-free media containing M1 antibody and then in media containing both agonist and fluorochrome-conjugated transferrin; this second incubation lasted 15 minutes. Cells were then fixed with

formaldehyde, permeabilized with detergent, and then processed for indirect immunofluorescence to detect M1 and endogenous EEA1. The cells were then imaged on a confocal microscope and displayed as a maximum projection. In the merged images, the fluorescence from the GPCR is colored green, from transferrin, red and from EEA1, blue. In (a) EEA1 (arrows) is located both on endosomes that contain B2AR (filled arrow) and on elongated endosomal tubules that contain B2AR (lower open arrow).

We noticed a couple of interesting differences between the fluorescence of the transferrin receptor and the GPCRs in enlarged endosomes. When comparing the tubular section with the enlarged section of a structure, the brightness of the fluorescence frequently decreases. This decrease in brightness is more pronounced for the fluorescence from the B2AR than for transferrin (Figure 17A and D, asterisks). A second difference was that the distribution of GPCRs and of transferrin within an enlarged structure was frequently distinct (Figure 17A and C, asterisks). For example, when DOR and transferrin were observed on the same structure, transferrin was restricted to discrete foci (Figure 17B). In some cases, transferrin appeared to form a narrow “bridge” between two adjacent enlarged endosomes (not shown). This distinct distribution likely reflects that GPCRs, even those that recycle, can be in a different sub-domain of an endosome than transferrin receptor.

Structured Illumination

To better visualize endosomal sub-domains, we used structured illumination microscopy, a technique that provides two-fold better resolution than standard epi-fluorescent

microscopy. Using structured illumination microscopy on fixed cells, we found that in enlarged structures B2AR and transferrin clearly concentrate in distinct domains (Figure 22). Therefore, in the vesicular portion of early endosomes, in contrast to the tubular portion, B2AR concentrates in a different sub-domain than transferrin receptor.

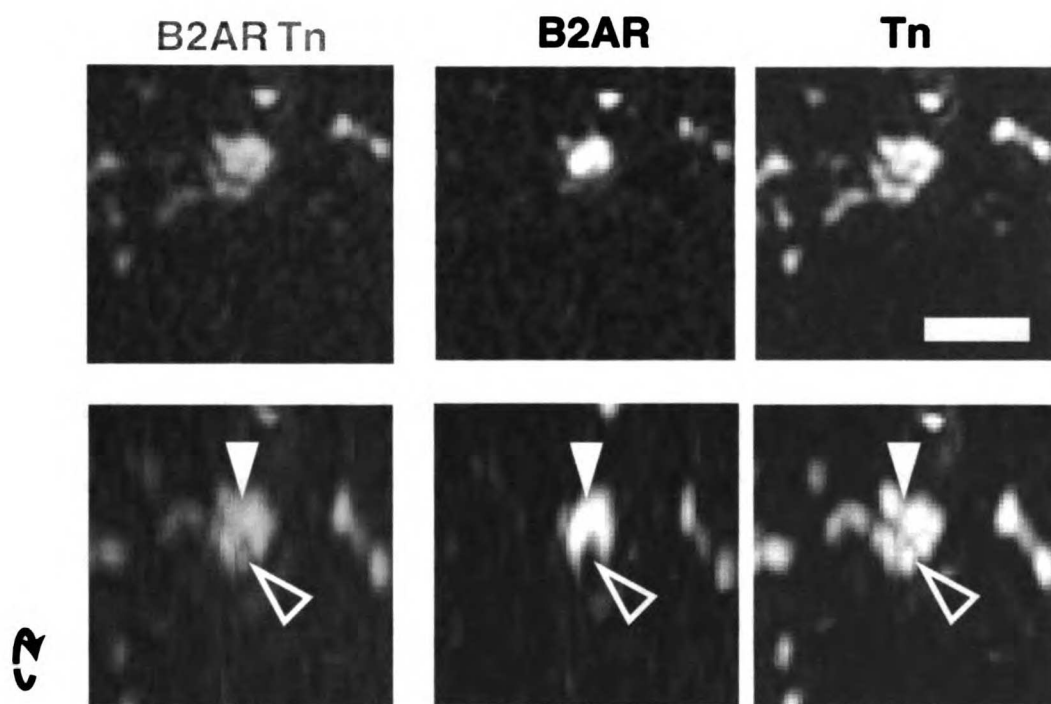


Figure 22

Structured illumination pictures of enlarged structure and tubule. Samples prepared as in Figure 2a were imaged on a structured illumination microscope. Digital images were taken at different focal planes, and the images were superimposed using maximum projection. A rotated maximum projection is also shown

below the original. Note within this structure, transferrin (open arrowhead) and B2AR (closed arrowhead) are not completely co-localized. A tubule containing Tn is to the left. Bar = 1 μ m.

4.3 Discussion

We have used live cell imaging to identify endosomal transport intermediates in the recycling pathway of B2AR, a pathway that is central in controlling the cellular response to catecholamines via B2AR in cells. We found that endocytosed GPCRs are found in a variety of structures with different sizes and motilities. Tubular transport intermediates containing B2AR rapidly emerged from slower vesicular endosomes, whereas DOR, a degrading GPCR, did not appear in elongated tubules. We developed fixation conditions to preserve these tubular transport intermediates. Quantification of tubule length in fixed cells confirmed that endocytosed B2AR is found with transferrin receptor in numerous elongated tubules that emerge from early endosomes. We present evidence that the recycling signal of B2AR enables it to enter these tubules from a sub-domain of early endosomes. Actin, which may be recruited to B2AR indirectly via the recycling sequence, is also important in enabling B2AR to enter tubules.

Motility of endosomes in the B2AR recycling pathway

Transport intermediates between organelles are best identified in living cells, where origin and/or destination structures can also be observed. We observed small vesicles and elongated tubules containing labeled GPCRs that rapidly emerged from enlarged vesicular endosomes. These transport intermediates moved at speeds greater than 1

$\mu\text{m}/\text{sec}$ along gently curving paths greater than $2 \mu\text{m}$. Both the speed and path of these structures are characteristic of microtubule-based motility (Cramer et al., 1997; Odde et al., 1999; Vorobjev et al., 1997). However, some vesicles and tubules had a maximum “instantaneous speed” of $4.7 \mu\text{m}/\text{sec}$, which is almost twice as fast as the maximum speeds previously reported for endosomes (De Brabander et al., 1988; Matteoni and Kreis, 1987)). Endocytic vesicles have been reported to move up to $5 \mu\text{m}/\text{sec}$ after a block in cholesterol trafficking is released (Ko et al., 2001; Zhang et al., 2001), and vesicles have been observed to move at similar speeds in tissue culture cells and in neurons (Allen et al., 1982; Breuer et al., 1988; Lasek et al., 1984; Rebhun, 1972) (Burdwood 1965). Because vesicle movements greater than $2.5 \mu\text{m}/\text{sec}$ are rarely reported (Current Biology or Trends review), fast movements may be a rare property of unique vesicles (e.g. cholesterol-rich vesicles). Alternatively, fast vesicle movements may be underreported. For structures that move along curving paths, such as vesicles that move along cellular microtubules, instantaneous velocity increases with the frequency of position measurement (Lackie, 1986). In addition, tracking vesicles becomes more difficult with increasing vesicle displacement between position measurements. Therefore, fast vesicle movements may be underreported in papers that measure vesicle position less frequently than we did.

A different type of directed motion in these cells is exhibited by large endosomes, revealing that they interact differently with the cytoskeleton. These endosomes diffuse or have slow movements. We estimate that large endosomes have a diffusion coefficient of $2.7 \times 10^{-11} \text{ cm}^2/\text{sec}$, which is smaller than that seen for secretory granules in PC12 cells ($3.9 \times 10^{-11} \text{ cm}^2/\text{sec}$) (Abney et al., 1999). These vesicles can also move slowly with an

average instantaneous velocity of $0.8 \mu\text{m}/\text{sec}$, and they occasionally recoil. That large vesicles move slowly has previously been demonstrated for endosomes (De Brabander et al., 1988), and for vesicles in axons (Allen et al., 1982; Breuer et al., 1988). That large vesicles can also exhibit recoil has been described in axons (Allen et al., 1982). Recoil and slow movements reveal that large endosomes have different interactions with the cytoskeleton than the fast vesicles. Recoil may result from a “failed” tubule formation from an endosome firmly attached to the cytoskeleton. Segregation of “slow” and “rapid” motors on endosomal sub-domains could provide the force to elongate membrane tubules from vesicular endosomes (Bananis et al., 2000).

These tubular transport intermediates were observed when endocytosed B2AR but not DOR was labeled. Because endocytosed B2AR efficiently recycles, whereas DOR does not, these tubules may recycle B2AR to the plasma membrane. Indeed, rapidly moving endosomal tubules are thought to recycle other receptors (Dunn et al., 1989; Geuze et al., 1987; Sonnichsen et al., 2000).

Tubular intermediates in the B2AR recycling pathway

In order to further characterize these tubular endosomes, we developed a fixation protocol that preserves endosomal tubules in fixed cells. The length distribution of tubules that contain transferrin was 0.3 to $2 \mu\text{m}$. A broader length distribution, 0.1 to $3 \mu\text{m}$, was previously observed for endosomal tubules containing transferrin in A431 cells with transmission electron microscopy (Stoorvogel et al., 1996). We occasionally observed tubules longer than $2 \mu\text{m}$, but these were rare(not shown). Our median tubule length of $0.6 \mu\text{m}$ is four times longer than the mean tubule length reported for early

endosomes in PC12 cells (0.14 μm (de Wit et al., 2001)). However, because that study used electron microscopy, tubules smaller than our detection limit (0.2 μm) were measured. Furthermore, conventional electron microscopy generates smaller z-slices than epi-fluorescence, shortening the apparent length of tubules grazing the z-section. Indeed, we limited our measurements to tubule projections observed in a single image (i.e. single xy section); this biases our median towards shorter lengths. These sources of error, however, should be constant between the various receptors that are compared within this study.

In both live and fixed cells, we found that B2AR is found in longer and more numerous tubules than DOR, a GPCR from the same family as B2AR, which is degraded in lysosomes. This is similar to previous epi-fluorescent studies with EGF receptor, a signaling receptor from the receptor tyrosine kinase family, which is also degraded. In these studies, endosome tubulation was promoted by various treatments, and EGF receptor was found in vesicular endosomes adjacent to elongated tubules (Carlton et al., 2004; McCaffrey et al., 2001). Under our conditions, where tubulation was not stimulated, DOR was generally not observed adjacent to elongated tubules labeled with transferrin receptor. In agreement with our data from live cells, this indicates late endosomes containing DOR do not normally extend elongated tubules (containing transferrin receptor).

Tubules emerging from the early endosome

Previous studies have demonstrated that DOR is sorted away from transferrin into late endosomes within 45 minutes of treatment with agonist (Tsao and von Zastrow, 2000;

Whistler et al., 2002). We have determined that within 15 minutes of treatment with agonist, DOR is significantly sorted away from early endosomes. To identify early endosomes, we labeled fixed cells with antibodies against EEA1, a protein that binds to the Rab5 (Chavrier et al., 1990; Gillingham and Munro, 2003; Mu et al., 1995; Wilson et al., 2000). We found that EEA1 co-localized with only 40% of structures containing DOR.

By contrast, B2AR is predominantly in early endosomes after 15 minutes of agonist treatment. EEA1 co-localized with 75% of labeled structures containing B2AR. This result agrees with a previous study showing that B2AR can extensively co-localize with endogenous Rab5 (Moore et al., 1995). Also consistent with our study, early endosomes have been previously observed to extend tubules, in live cells. Specifically, tubules containing labeled transferrin emerged from vesicular structures containing Rab5 (Sonnichsen et al., 2000). Indeed, when we stained for endocytosed B2AR in this study, 90% of tubular structures observed in fixed cells co-localized with transferrin, indicating that B2AR emerges from early endosomes in those same structures.

In non-polarized cells, membrane proteins can recycle from both the early endosome and the recycling endosome. Interestingly, studies with Rab4 and Rab11, two endosomal GTPases, also indicate that B2AR recycles predominantly from early endosomes. Rab11, which is found on recycling endosomes, co-localizes poorly with B2AR at steady state (Daro et al., 1996; Innamorati et al., 2001; Ren et al., 1998; Ullrich et al., 1996). Along with our co-localization data, this demonstrates that B2AR accumulates in early endosomes at steady state. Furthermore, B2AR is sensitive to perturbations that affect recycling from early endosomes but not from recycling

endosomes (Daro et al., 1996; Ren et al., 1998; Sonnichsen et al., 2000). Specifically, overexpression of a Rab4 mutant can inhibit B2AR recycling (Seachrist, 2000 #508; van der Sluijs et al., 1992; van Der Sluijs et al., 1991), while overexpression of Rab11 (which appears to inhibit endogenous Rab11) does not (Moore et al., 2004). Together, we feel that these studies reveal that B2AR recycles predominantly from early endosomes.

Role of the recycling signal

Like DOR, B2A1a is degraded and is not found on endosomal tubules. However, we found that, unlike DOR, B2A1a is predominantly in early endosomes after 15 minutes of agonist treatment. Therefore, we believe that the recycling signal is not required to target B2AR to the early endosome, but is required for B2AR to enter endosomal tubules and to recycle.

To determine whether the recycling signal of B2AR influences the ability of B2AR to enter membrane tubules, we measured the number and length of tubules in receptors containing an intact or mutated recycling signal. We found that the PDZ ligand sequence is necessary for B2AR to be found in tubules, because the mutant B2A1a was not found in elongated tubules. The recycling signal is also sufficient to locate a receptor in tubules, because the chimaeric receptor DORcB2AR was also found in elongated tubules.

To determine whether actin is required for B2AR to enter endosomal tubules, we treated cells with the actin-depolymerizing drug, latrunculin. Because the recycling signal of B2AR is thought to link it to the actin cytoskeleton and to promote recycling, we predicted that latrunculin would reduce the number of B2AR-labeled tubules. Indeed,

latrunculin decreased the number of elongated tubules labeled with B2AR without affecting the length of tubules labeled with transferrin. Therefore, a latrunculin-sensitive pool of actin is specifically required for B2AR, but not transferrin receptor, to be found in elongated tubules.

B2AR is in a transferrin-poor sub-domain of the early endosome

Several sub-domains of vesicular early endosomes have been defined, the largest and most well studied of which are the clathrin-rich and clathrin-poor sub-domains. The clathrin-rich domain has an approximate diameter of 0.1-0.5 microns on lymphocyte endosomes (Murk et al., 2003). The clathrin-poor sub-domain co-localizes with transferrin receptor, whereas the clathrin-poor sub-domain co-localizes with receptors fused to ubiquitin (Raiborg et al., 2002). We have observed that B2AR is clearly segregated from transferrin receptor in early endosomes, indicating that it is in the clathrin-rich sub-domain. Indeed, B2AR appears to be ubiquitinated after agonist binding (Shenoy et al., 2001), a modification which could target it to this sub-domain.

Despite the fact that B2AR is segregated from transferrin receptor in the vesicular portion of the early endosome, both proteins are found in the tubular portion of the early endosome. Therefore, we propose a model where the recycling sequence of B2AR binds cytosolic proteins that allow it to enter the tubule from the clathrin-poor sub-domain. We propose that ubiquitination of B2AR targets B2AR to the clathrin-rich sub-domain, but that binding to an EBP50/NHERF family member prevents it from moving inside of the early endosome with other proteins destined for lysosomal degradation (Raiborg et al., 2003). By contrast, transferrin receptor recycles “by default” because it is

not targeted to the clathrin-rich sub-domain. It is known that B2AR is ubiquitinated after ligand binding, and that binding to an EBP50/NHERF family member is necessary and sufficient to prevent its rapid degradation (Cao et al., 1999; Gage et al., 2001; Gage et al., 2004; Shenoy et al., 2001). We propose that the EBP50/NHERF family member tethers B2AR to the surface of the early endosome via its association with the actin cytoskeleton (Figure 23). The actin cytoskeleton around the plasma membrane contacts the early endosome and restricts the motility of this structure during separation of tubules. The chaperone activity of NSF, which binds to B2AR in a nucleotide-selective manner, has been proposed to disassemble the complex of EBP50/NHERF and B2AR (Gage et al., 2004; Whiteheart and Matveeva, 2004). We propose that dissociation of B2AR from EBP50/NHERF after de-ubiquitination enables B2AR to enter the tubule.

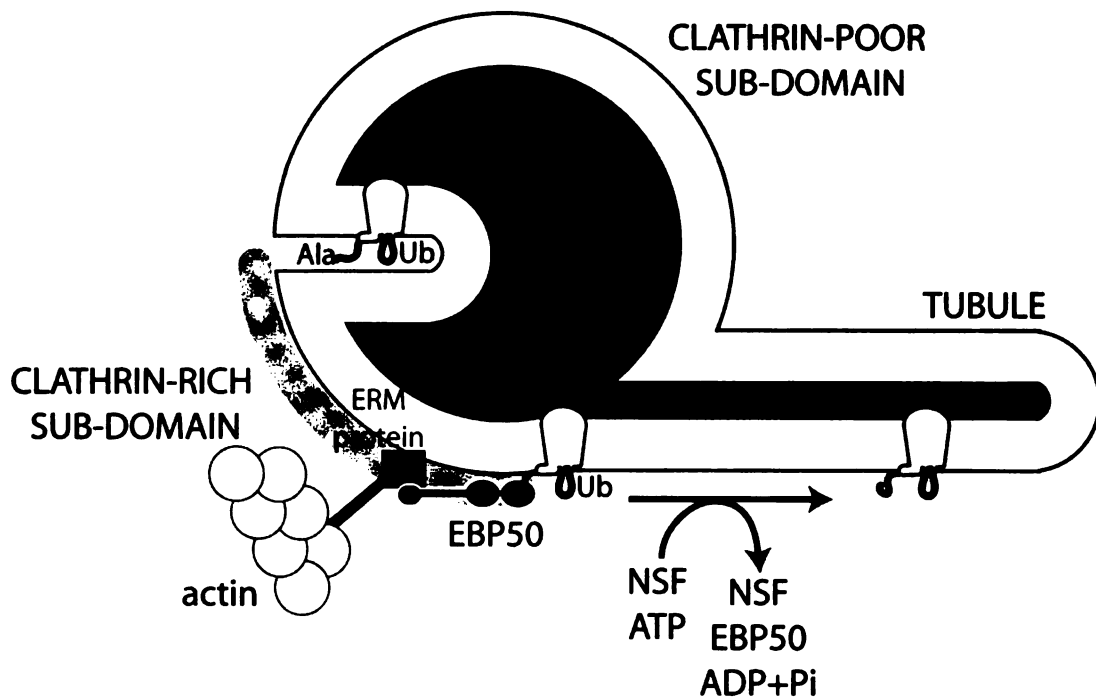


Figure 23

Model for the role of EBP50/NHERF in B2AR recycling. The early endosome can both extend tubules to sort membrane proteins such as transferrin for recycling and involute membrane to sort other membrane proteins such as EGF receptor for degradation. Ubiquitin, which can be covalently conjugated to membrane proteins, is thought to target proteins to the clathrin-rich sub-domain of early endosomes and then target these proteins for involution. B2AR is ubiquitinated, which may target it to the clathrin-rich sub-domain, but it also able to enter tubules. We propose that association with EBP50/NHERF, an ERM protein, NSF and actin prevents ubiquitinated B2AR from involuting, and allows B2AR to enter tubules; transferrin receptor, which does not localize to the clathrin-rich sub-domain, targets to tubules by default.

While transmembrane proteins can follow bulk membrane flow in order to recycle from endosomes, specific targeting sequences can control receptor recycling. To

understand the mechanisms by which the B2AR is recycled, we have demonstrated that this receptor enters transferrin-rich tubules of early endosomes from a specialized, transferrin-poor vesicular sub-domain. We also provide evidence that the PDZ domain at the c-terminus of B2AR and actin are necessary and sufficient for B2AR to enter these tubules. We propose a model whereby the PDZ ligand domain of B2AR recruits actin to the receptor, which allows it to move out of the clathrin-rich sub-domain of early endosomes, where receptors are targeted for degradation.

Future Directions

A future direction is to investigate the role of trafficking signals in other transmembrane proteins on distribution of these receptors into endosomal sub-domains. There are novel recycling signals on several GPCRs that do not appear to bind EBP50/NHERF (Tanowitz and von Zastrow, 2003; Vargas and Von Zastrow, 2004). Transferrin receptor contains a cytoplasmic sequence that is required for it to efficiently recycle to the basolateral surface in polarized cells (Dai et al., 2004; Odorizzi and Trowbridge, 1997). There is evidence that transferrin receptor targets to a specific transport intermediate from recycling endosomes, but the role of its recycling signal in this targeting is not known (Lampson et al., 2001). There also appear to be two separate degradation signals in B2AR, which target it to lysosomes under different cellular conditions (Cao et al., 1999; Moore et al., 1999a; Moore et al., 1999b; Shenoy et al., 2001; Whistler et al., 2002). It will be interesting to discover whether such sequences direct proteins into or out of endosomal sub-domains. It will also be useful to know whether EBP50/NHERF, or a related protein

5 ACTIN-DEPENDENT CLUSTERING OF BETA2-ADRENERGIC RECEPTOR

Abstract. Actin is involved in several stages of B2AR trafficking at the plasma membrane. The actin-associated protein EBP50/NHERF appears to prevent endocytosis of inactive B2AR. While wild-type B2AR is only endocytosed after activation by ligand, mutants of B2AR that do not bind to EBP50/NHERF appear to be endocytosed constitutively. We believe that actin is also required for B2AR to cluster into clathrin-coated pits after activation by ligand. Latrunculin, a drug that depolymerizes the actin cytoskeleton, inhibits the clustering of activated B2AR. EBP50/NHERF, however, is not necessary for efficient clustering. The D2 receptor, which does not bind EBP50/NHERF, also does not cluster in the presence of latrunculin. Meanwhile, a mutant of B2AR that does not bind EBP50/NHERF clusters efficiently. Inhibition of clustering may explain why latrunculin inhibits B2AR endocytosis by inducing a 5-10 minute lag. As arrestin 3 is rapidly recruited to B2AR and is required for B2AR endocytosis, we speculate that latrunculin inhibits arrestin 3 recruitment.

WHILE binding to EBP50/NHERF (or a related protein) clearly is involved in B2AR recycling from endosomes, our data from co-immunoprecipitations suggests a role for EBP50/NHERF, perhaps in a complex with actin, at the plasma membrane rather than in endosomes. Actin has previously been implicated at many stages of membrane trafficking. There is evidence that actin promotes the budding -- or restricts re-absorption

-- of transport intermediates such as clathrin-coated vesicles from the plasma membrane (Fujimoto et al., 2000; Moskowitz et al., 2003) and secretory tubules from the golgi (Hirschberg et al., 1998; Musch et al., 1997). Actin can restrict the motility of organelles (Smith and Simmons, 2001), or drive the movement of others (Qualmann et al., 2000), and can restrict the motility of proteins within those membranes (Gaidarov et al., 1999; Sako and Kusumi, 1995). Actin appears to bind the membrane microdomain, caveolae (Fujimoto et al., 2000). Actin binding proteins that bind to receptors at the plasma membrane could therefore have several possible functions. With B2AR, we anticipate that such proteins could maintain inactive B2AR in microdomains, maintain inactive B2AR away from sites of constitutive endocytosis, promote the exit of ligand-activated B2AR from microdomains, or promote the entry of B2AR into a sub-population of coated pits (see Introduction).

Initially, we asked whether a complex of EBP50/NHERF/ezrin/actin was involved in retaining B2AR at the plasma membrane, i.e. away from sites of constitutive endocytosis. Next, we asked whether a complex of EBP50/NHERF/ezrin/actin controls entry of B2AR into coated pits.

5.1 Materials and Methods

Constitutive Endocytosis

We chilled HEK293 cells stably expressing FLAG-tagged B2AR or B2A1a for 15 minutes in ice cold, fresh, buffered media (DMEM, 30 μ m HEPES pH 7.4). We then added fluorochrome-labeled M1 anti-FLAG antibody (Sigma) to cells for 30 minutes. We

then warmed cells to 37°C to allow constitutive endocytosis. At various times, we fixed cells and mounted them for epi-fluorescence as described in Chapter 3.

Isolating Plasma Membrane Fragments

Isolation of plasma membrane fragments for visualization by epi-fluorescent microscopy is a technique developed by Sanan and Anderson (Sanan and Anderson, 1991). To firmly adhere cells, coverslips were treated with poly-L-lysine (Sigma) as described in Chapter 3. HEK293 cells expressing HA-B2AR or HA-B2A1a were then grown on these coverslips. To prevent endocytosis of receptors, cells were chilled to 16°C for 15 minutes. To label surface receptors, cells were incubated in media containing fluoresceine-conjugated M1 anti-FLAG antibody (M1 antibody, Sigma; fluorescein conjugation kit, Molecular Probes). After 30 minutes, cells were treated with 10 μ M isoproterenol (Research Biochemicals) and then incubated a further 15 minutes. Cells were then chilled to 4°C to block constitutive endocytosis, To measure shallow pits, cells were further treated with rhodamine-conjugated anti-mouse antibodies. To isolate plasma membrane sheets, the plasma membrane was removed by the procedure described previously (Cao et al., 1998). Poly-L-lysine coated coverslips were firmly placed on top of the cells and then removed. After fixation, exposed plasma membrane edges were labeled with wheat germ agglutinin conjugated to rhodamine (Vector Labs). These coverslips were then fixed and mounted using standard fixation protocols. Plasma membrane sheets were identified by their intense staining with wheat germ agglutinin, which concentrates around the rims of the sheets.

Endocytosis assay

First, we chilled HEK293 cells stably expressing Flag-tagged B2AR for 15 minutes in ice cold, fresh, buffered media (DMEM, 30 μ m HEPES pH 7.4). We then added agonist (10 μ m isoproterenol) to the cells for 1 hour, maintaining the cells on ice. We also included 5 μ m latrunculin or an equivalent amount of DMSO (control), which we diluted into warm media that was then chilled to 4°C before adding it to the cells. We then incubated cells at 37°C to permit endocytosis. This temperature shift may have caused variability at early time points (endocytosis less than 5 minutes, see text). At various time points, the cells were then returned to an ice bath to arrest endocytosis. Cells were washed in ice-cold buffer containing EDTA to dissociate the cells from the Petri dishes (PBS, 0.04% EDTA). After 30 minutes, the dissociated cells and buffer were spun gently to pellet. The buffer was removed and cells were resuspended in buffered media and spun again. The buffer was again removed and the cells were incubated in buffered media containing fluorescein-cojugated M1 anti-FLAG antibody (2.5 μ g/mL). The cells were incubated in antibody while rotating for 45 minutes at 4°C and then propidium iodide was added to stain the nuclei of dead cells. The cells were imaged on a flow cytometer (FACScan, Beckton Dickinson), and mean intensity of fluorescence for each timepoint of cells was quantified using Cellquest software (Beckton Dickinson). Dead cells were removed from all calculations.

Radioactive Ligand Binding

10 cm dishes of confluent HEK293 cells stably expressing HA-B2AR were grown and treated with various concentrations of latrunculin B (Alexis) or DMSO (Sigma) as a

control. Cells were lifted at 4°C for 30 minutes in a cell dissociation buffer (CDB) of PBS-EDTA to lift cells, and supplemented with 10% fetal calf serum to block nonspecific binding (Cell Culture Facility, University of California, San Francisco). The cells were then dispersed with transfer pipets fitted with 200 μ L tips (Eppendorf) and then pelleted gently. The supernatant was removed and cells were resuspended in a drop of cell dissociation buffer, resuspended gently, and then diluted in 5 mL of CDB. The cells were washed three times in this manner. Cells were then diluted to a volume of 300 μ L with 3×10^5 cells per tube. Latrunculin or DMSO was then added again to each vial of cells. Cell suspensions were further incubated with a saturating concentration (10 μ M; K_D is sub-nM) of radioactive ligand, [3 H]-dihydroalprenolol, to measure total ligand binding, or both [3 H]-dihydroalprenolol and a non-radioactive antagonist, alprenolol, to measure non-specific binding. Cells were placed on a shaker for 1 hour, and filter binding was performed by standard methods (filter binding apparatus, Millipore)(Hulme, 1990).

5.2 Results and Discussion

Role of EBP50/NHERF in Constitutive Endocytosis

First, we asked whether EBP50/NHERF is involved in retaining the B2AR at the plasma membrane. To address this question, we labeled exogenously expressed FLAG-tagged receptors at the plasma membrane of HEK293 cells by incubating them with fluorescently labeled M1 antibody. We labeled receptors at 4°C to block endocytosis, and then shifted the temperature to 37°C to permit constitutive endocytosis. Cells labeled for surface B2A1a, but not wild type B2AR, contained small, internal, labeled structures

(Figure 24). Therefore, we concluded that binding to EBP50/NHERF prevents constitutive endocytosis of B2AR. However, it is possible that EBP50/NHERF is required to promote recycling of constitutively endocytosed B2AR. This would be consistent with the previously demonstrated role of EBP50/NHERF in promoting recycling of ligand-stimulated B2AR. Further analysis will be required to address this question.

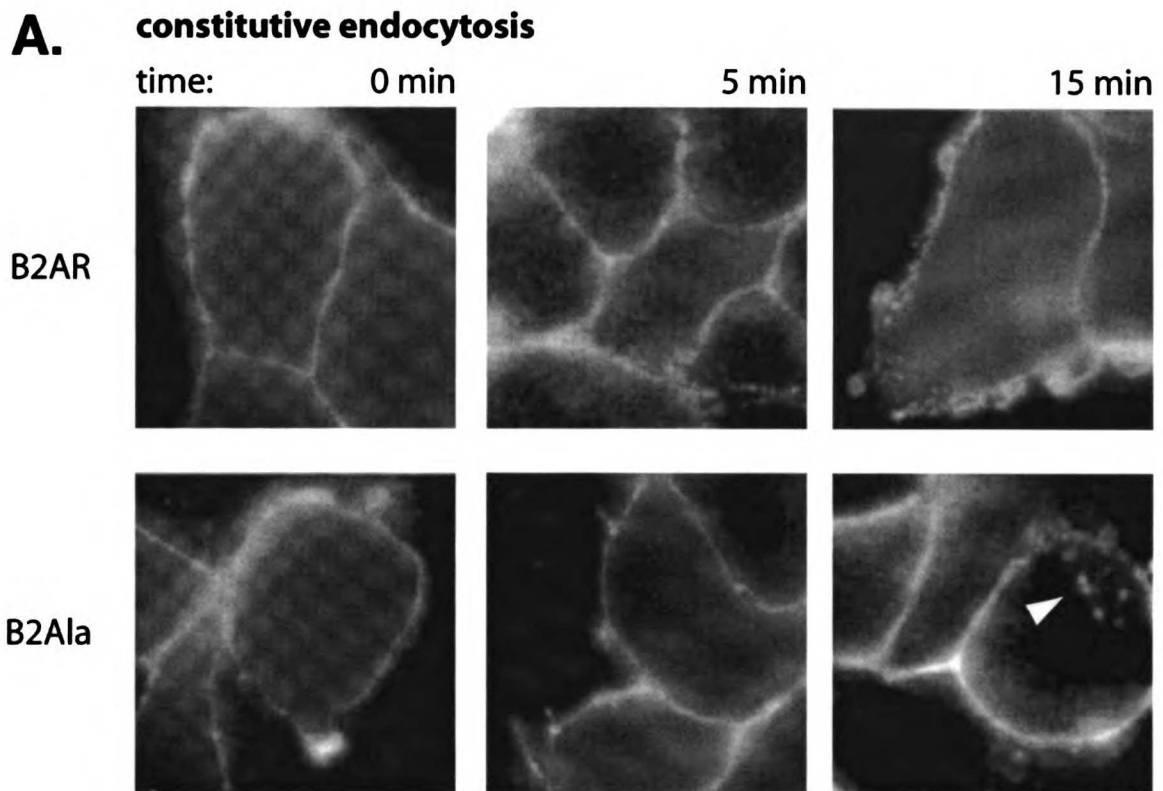


Figure 24. *The EBP50/NHERF binding site is required to inhibit constitutive endocytosis*

FLAG-B2AR or the mutant B2A1a were stably expressed in HEK293 cells and cells were incubated at 4°C with M1 anti-FLAG antibody to label surface receptors. Cells were warmed to 37°C to allow constitutive endocytosis and fixed at the times indicated. M1 antibodies were detected by indirect immunofluorescence and imaged on an epi-fluorescent microscope. B2A1a, but not B2AR, was found in internal vesicles after 15 minutes, arrowhead.

Role of Actin in Clustering of Ligand-Activated Receptors

We next asked whether actin is involved in clustering of ligand-activated B2AR. To induce clustering of B2AR, we added the ligand isoproterenol at a saturating

concentration to surface-labeled HEK293 cells expressing FLAG-B2AR. To block endocytosis, we labeled the cells at 16°C. To depolymerize the actin cytoskeleton, we incubated cells in 5 μ M latrunculin. When these cells were visualized by epi-fluorescent microscopy, we found that latrunculin treatment dramatically reduced the number of labeled B2AR puncta (Figure 25A). This was also observed at 2.5 and at 15 μ M latrunculin (not shown).

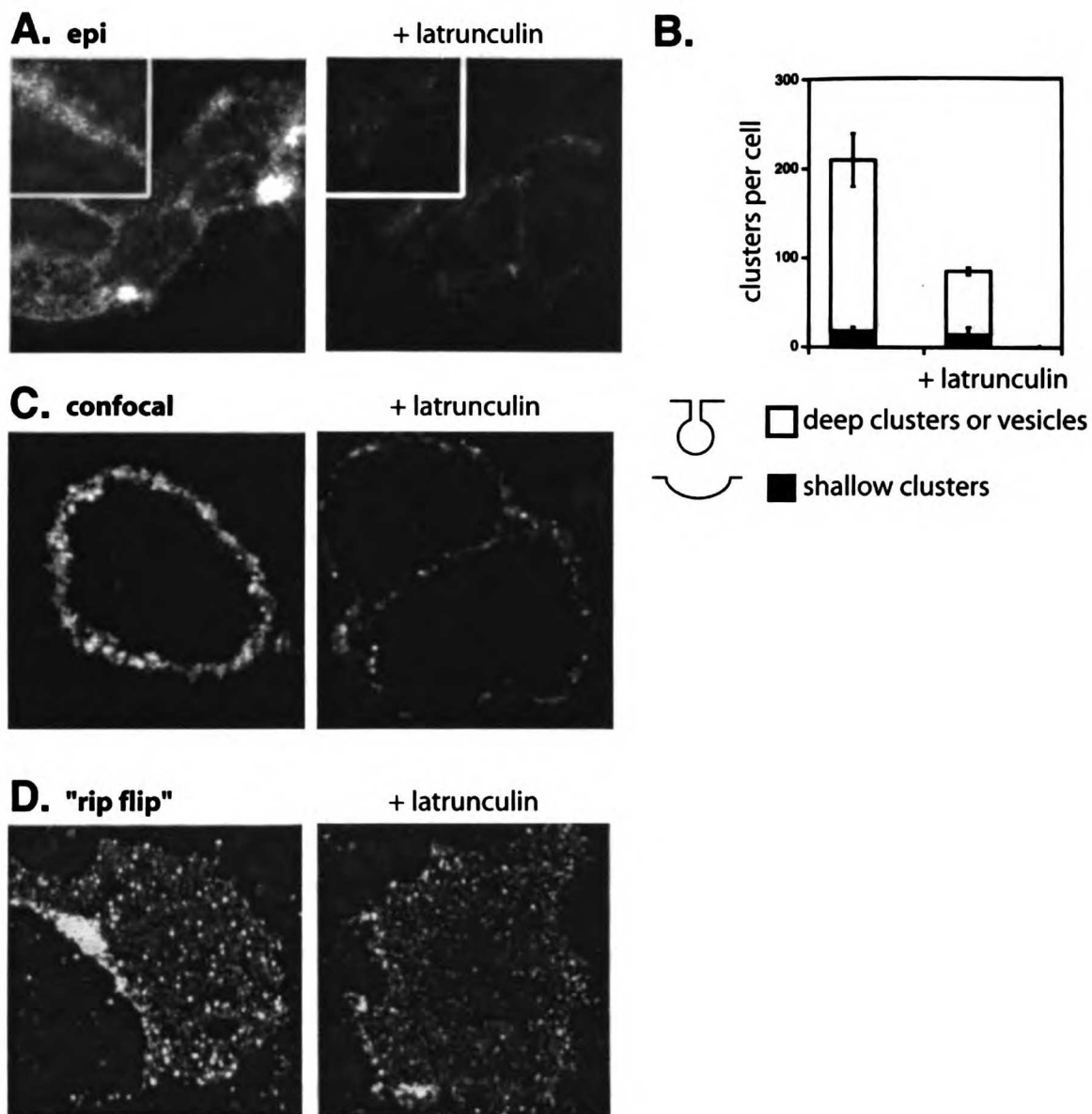


Figure 25. *Latrunculin inhibits clustering of B2AR*

Cells labeled for surface B2AR with fluorochrome-conjugated M1 antibodies were held at 16°C, which inhibits endocytosis of B2AR while allowing it to cluster with clathrin-coated structures. Some cells were treated with 5 μ M latrunculin to depolymerize the actin cytoskeleton. Cells were then treated with agonist and fixed. A. Epi-fluorescence microscopy demonstrates that cells treated with latrunculin do not have B2AR puncta. B. After treatment with agonist, cells were chilled to 4°C and incubated with fluorochrome-conjugated secondary antibodies to detect shallow clusters. The number of shallow clusters does not appear

to be affected by latrunculin treatment. C. Confocal microscopy demonstrates confirms that latrunculin reduces the number of B2AR puncta. D. Plasma membrane sheets were isolated by the “rip-flip” method, which further confirms that latrunculin inhibits the number of B2AR puncta.

A small number of puncta were observed in latrunculin-treated cells. These puncta, which are clustered receptors, could be several types of structures. For example, receptors can cluster with clathrin in shallow pits, deep pits, or small vesicles that are closely associated with the plasma membrane. Additionally, it is possible that GPCRs could cluster at the plasma membrane before being associated with clathrin. To determine the identity of the puncta, we took cells that had been incubated with fluorescein-conjugated mouse anti-Flag M1 antibodies at 16°C and subsequently incubated them with rhodamine-conjugated anti-mouse antibodies. Under these conditions, the anti-mouse antibodies will not be able to penetrate into deep clusters or vesicles. We then counted the number of structures labeled with M1 only (representing deep pits or vesicles) and those labeled both with M1 and the anti-mouse antibodies (representing shallow pits). We found that latrunculin treatment decreases the number of deep clusters or vesicles by over 50%, but does not affect the number of shallow clusters (Figure 25B). Only about 10% of all puncta at 16°C correspond to shallow clusters. These structures did not co-localize with clathrin (not shown). Clathrin-free puncta have been demonstrated to account for 10% of all B2AR puncta at the plasma membrane, when endocytosis is blocked (Cao et al., 1998).

To confirm that the puncta observed were on the cell surface, we also imaged cells by confocal microscopy and isolated plasma membrane sheets. By both of these procedures, it was clear that latrunculin treatment dramatically reduced the number of puncta at the plasma membrane at 16°C (Figure 25C). By counting the number of puncta observed on plasma membrane sheets, we found that latrunculin reduces the number of clusters by about 5-fold (0.5 vs. 0.1 puncta/ μm^2 when cells were treated with 5 μm latrunculin) (Figure 26A). The number of puncta in the absence of latrunculin is similar to what has previously been observed with B2AR using this technique (0.6 puncta/ μm^2 (Cao et al., 1998)).

Our results are different than that of the Keen lab, who stated –based on qualitative observations – that latrunculin reduces the size but not the number of B2AR clusters in cells overexpressing arrestin 3 (Santini et al., 2002). A difference between the methodologies of our two studies was in *how* we identified clustered receptor on the plasma membrane. In our study, we counted clusters in cells held at 20°C, a condition that inhibits endocytosis of B2AR. In the Keen study, plasma membrane clusters were identified based on their co-localization with AP-2; cells were held at 37°C. It is our feeling that in the Keen study, large clusters cannot be distinguished from endosomes. Indeed, these large clusters did not form at 16°C, a condition which inhibits endocytosis. Both studies would of course benefit greatly from quantitative use of electron microscopy.

The decrease in clustering is specific to B2AR, because the number of transferrin clusters was unchanged by latrunculin treatment (0.3 puncta/ μm^2). This observation is similar to that of the Schmid lab, who observed using immuno-electron microscopy that,

qualitatively, latrunculin does not inhibit transferrin receptor from clustering in coated pits (Lamaze et al., 1997). Furthermore, latrunculin does not appear to strongly inhibit the number of D4 dopamine receptor puncta (Figure 26C). However, latrunculin does appear to inhibit the number of D2 receptor puncta (Figure 26D). The D2 receptor does not have an EBP50/NHERF binding sequence at its carboxy terminus, and does not bind strongly to EBP50/NHERF *in vitro* (Heydorn et al., 2004). This indicates that EBP50/NHERF is not required for latrunculin-sensitive clustering. However, it has been suggested based on *in vitro* binding studies that D2 receptor binds to APB-280 (actin binding protein, 280 kDa) (Li et al., 2000). ABP-280, also called non-muscle filamin, is a flexible actin cross-linking protein that can bind to other transmembrane proteins and perhaps to microdomains, and is required in lamellae (Stossel et al., 2001). Therefore, it is possible that actin association with receptors, which can occur via various actin-binding proteins in the cell cortex, is involved in the clustering of certain GPCRs at the plasma membrane.

To find out whether actin promotes B2AR clustering as a part of a complex with EBP50/NHERF, we asked whether mutating the EBP50/NHERF binding site similarly blocks B2AR clustering. We found that surface-labeled B2A1a was observed in the same number of puncta as wild-type B2AR (0.5 puncta/ μm^2) (Figure 26A, B). Therefore, we believe that actin, but not a complex of EBP50/NHERF/ezrin/actin, promotes clustering of B2AR and D2 receptor at the plasma membrane.

A.

receptor	condition	clusters/ μm^2
		0.1 +/- 0.1
B2AR	+ iso	0.5 +/- 0.2
	+ iso + lat	0.1 +/- 0.0
B2Ala	+ iso	0.5 +/- 0.1
TnR		0.3 +/- 0.3
	+ lat	0.3 +/- 0.2

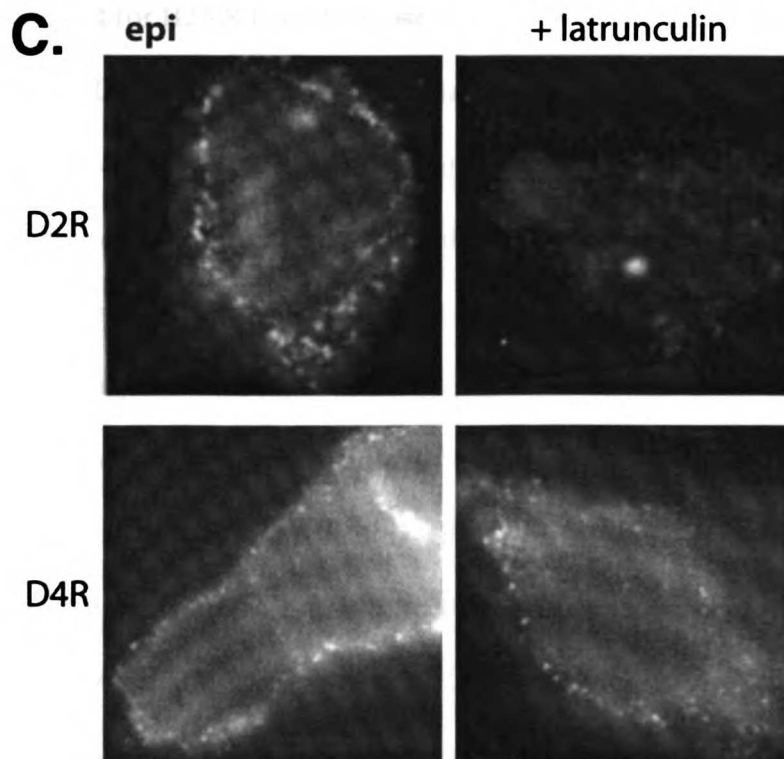
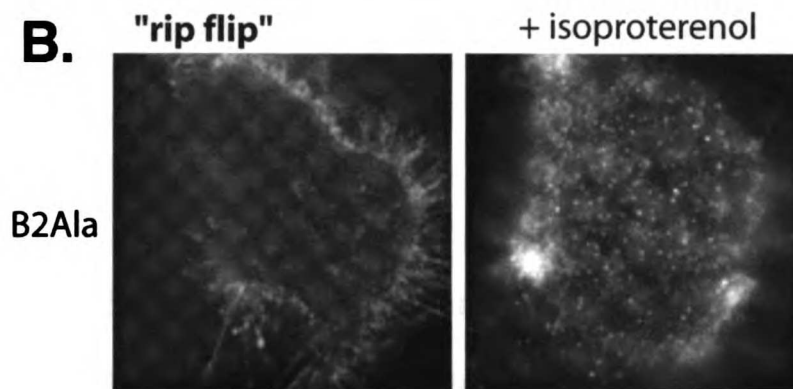


Figure 26. *Dependence of GPCR clustering on actin is not due to EBP50/NHERF binding*

(A) The number of clusters observed in isolated plasma membrane sheets was quantified. The mutant receptor B2Ala has the same number of puncta as wild type B2AR, indicating that EBP50/NHERF is not involved in clustering the receptor. The constitutively internalizing transferrin receptor (TnR) also appears to cluster well in the presence of latrunculin. (B) Latrunculin does not qualitatively inhibit the number of B2Ala puncta observed in isolated plasma membrane sheets ("rip flip). (C) Latrunculin qualitatively inhibits the number of D2 receptor puncta but not the number of D4 receptor puncta observed by epi-fluorescent microscopy ("epi").

Several studies indicate that latrunculin inhibits clustering of receptors by inhibiting the recruitment of arrestin. As mentioned in the introduction, arrestin 3 is required for B2AR to endocytose in clathrin-coated vesicles after agonist treatment (Ahn et al., 2003; Menard et al., 1997); arrestin binds to proteins such as AP-2 in the coated pits (Goodman et al., 1996; Laporte et al., 2002; Laporte et al., 2000). Our preliminary evidence suggests that latrunculin does not qualitatively reduce the amount of clathrin puncta at the plasma membrane (not shown). This fits with previous data from our laboratory showing that activation of B2AR does not increase the number of clathrin structures at the plasma membrane (Cao et al., 1998). However, we do not know if arrestin recruitment to receptors inhibited by latrunculin. Arrestin 3 apparently translocates from the cytosol directly to clathrin structures at the plasma membrane (Oakley et al., 2000; Santini et al., 2002; Scott et al., 2002). It is also known that actin acts upstream of arrestin 3. Overexpression of arrestin 3 increases the size of AP-2 structures in cells treated with B2AR agonists, whereas latrunculin treatment blocks this

effect (Santini et al., 2002). Interestingly, it was recently discovered that visual arrestin (arrestin 1) moves to the plasma membrane on myosin-driven vesicles. Therefore, arrestin 3 may also move to the plasma membrane along actin filaments. Actin-based movement could increase the speed at which arrestin translocates to activated B2AR.

Role of Actin in Endocytosis of B2AR

Because latrunculin inhibits B2AR clustering at the plasma membrane, we wondered whether latrunculin also inhibits B2AR endocytosis. To measure endocytosis, we labeled surface B2AR with antibodies after various times of agonist treatment. A decrease in labeled B2AR therefore indicates a decrease in surface receptor due to endocytosis. To label surface receptors, we held cells at 4°C before treating them with agonist; however, this 4°C step alters the early kinetics of endocytosis (Michael Tanowitz, personal communication). Surface receptor was measured with a flow cytometer. We found that latrunculin treatment inhibits early stages of endocytosis, within 5-10 minutes of agonist treatment (Figure 27A). This inhibition of endocytosis is not due to a gross inhibition of ligand binding, at least at the concentration of ligand we used (Figure 27B). An early inhibitory effect on endocytosis is consistent with the model where latrunculin inhibits arrestin translocation, as translocation maximally occurs one minute after agonist stimulation. Translocation of arrestin occurs even at 16°C, where endocytosis of B2AR is blocked (Cao et al., 1998; Oakley et al., 2000). However, the inhibitory effect of latrunculin on endocytosis showed extreme variability beyond 10 minutes of agonist treatment, and was difficult to quantify. We attempted to measure the effect of latrunculin on the rate constant for endocytosis, but were unsuccessful.

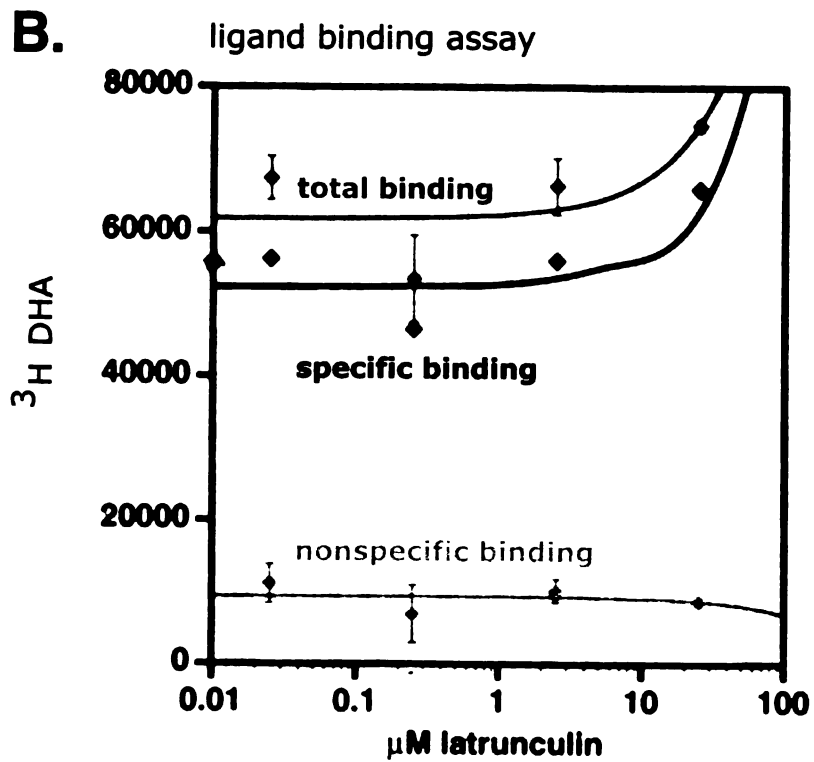
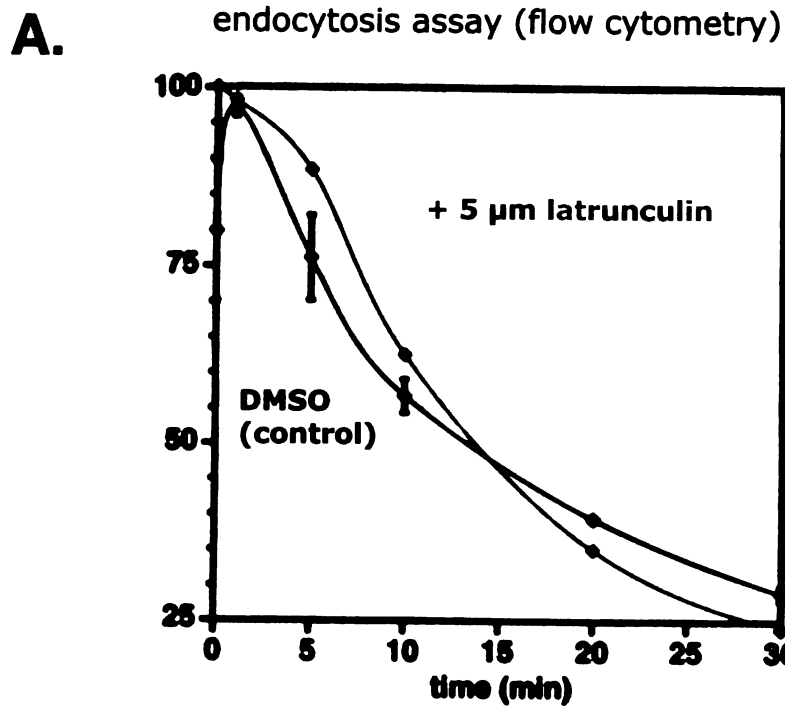


Figure 27. Latrunculin inhibits endocytosis of B2AR but not ligand binding

(A) Cells were treated with agonist in the presence or absence of latrunculin at 4°C, and cells were then warmed to 37°C for various times to allow endocytosis. Surface B2AR was detected with fluorochrome-conjugated M1 antibodies, and cell fluorescence was measured by flow cytometry. Error bars reveal the standard deviation between multiple experiments; only one experiment is shown for latrunculin-treated cells. The lag induced by latrunculin between 5-10 minutes was reproducible. (B) Cells expressing B2AR were incubated with saturating concentrations of the radioactive ligand [3H]-dihydroalprenolol (³H DHA) at 4°C in the presence of various concentrations of latrunculin, and binding was measured by the filter binding method. 5 μM latrunculin does not inhibit ligand binding.

Interestingly, we observed that the slope of the curve for B2AR endocytosis (ignoring the “bump” at early timepoints) has an inflection at about 10 minutes. This sharply curving slope confounded our attempts to estimate the endocytosis rate constant by the method outlined by Koenig and Edwardson (Koenig and Edwardson, 1997). An inflection has also been observed for the endocytosis of the delta-opioid receptor (which does not rapidly recycle) (Tanowitz and Von Zastrow, 2002) and the somatostatin receptor (Koenig et al., 1997), but not the muscarinic acetylcholine receptor (Koenig and Edwardson, 1996). Activation of muscarinic receptor, B2AR and delta-opioid receptors recruits arrestin 3 to coated pits, and B2AR and muscarinic receptor bind arrestin 3 equally well *in vitro* (Gurevich et al., 1995; Santini et al., 2002; Zhang et al., 1999). However, unlike the other receptors, muscarinic receptor is probably not co-internalized with its agonists because the agonists have low affinity for the receptor. The endocytosis of delta-opioid receptor switches to a simple exponential when its cytoplasmic lysines are

mutated to alanine, although these residues should not affect ligand binding (Tanowitz and Von Zastrow, 2002). Mutation of these lysine residues should, however, block ubiquitination of these receptors; both B2AR and delta-opioid receptors are ubiquitinated after agonist treatment (Chaturvedi et al., 2001; Shenoy et al., 2001). It is not known whether the endocytosis of B2AR switches to a simple exponential when its cytoplasmic lysines are mutated. Other plasma membrane proteins are ubiquitinated after endocytosis, and this ubiquitination is thought to link them to components of the clathrin-coated pits such as Eps15, which have ubiquitin-binding motifs (Carbone et al., 1997). While in mammalian cells, ubiquitination does not appear to be required for endocytosis of transmembrane proteins, it is not known whether it changes the kinetics of internalization (Duan et al., 2003; Jing et al., 1990; Shenoy et al., 2001).

From our data, it appears that latrunculin does not convert the endocytosis of B2AR to a simple exponential slope (Figure 27A). However, the effect of latrunculin on endocytosis was highly variable at timepoints after 10 minutes, so the effect of latrunculin on the kinetics of endocytosis is difficult to address. In our opinion, cells should not be shifted to 4°C until the experiment is completed, if at all: fixation could be used to arrest endocytosis before flow cytometry. Holding cells at 4°C inhibits the attachment of cells to the substrate, and substrate attachment alters the effects of latrunculin on endocytosis of other receptors in some cell lines (Fujimoto et al., 2000).

Depending on the cell line used, it appears from other studies that latrunculin can inhibit either the rate of endocytosis or the extent (Fujimoto et al., 2000; Lamaze et al., 1997).. With B2AR, however, it appears that latrunculin has a severe effect on endocytosis at early times. This could perhaps be interpreted as B2AR inducing a 5 min

lag before endocytosis rather than (or in addition to) the rate or extent of endocytosis. This lag has not been observed with the transferrin receptor (Fujimoto et al., 2000). Such a lag would be consistent with a model by which latrunculin does not inhibit the activation of arrestin, but rather inhibits its rapid recruitment to the plasma membrane.

We have demonstrated that actin is utilized by B2AR at two stages of endosomal trafficking. In this chapter, I have demonstrated that B2AR requires actin at a stage where B2AR exits a plasma membrane microdomain and clusters into clathrin-coated pits (see Introduction). In Chapter 4, I have described a role for actin at a stage where B2AR exits an early endosome microdomain and enters endosomal tubules. In both stages, B2AR is initially in a unique microdomain that does not contain other endocytosed receptors such as transferrin, but then moves into a common domain with transferrin. Therefore, while the molecular details (i.e. EBP50/NHERF or arrestin binding) of this interaction may be different, the general role of actin may be to enable B2AR to move out of specialized lipid domains. Indeed, actin associates with caveolar microdomains, but not with clathrin coated pits (Chung et al., 1999).

6 ACTIVITY OF ILIMAQUINONE ON MICROTUBULES

Abstract. We have demonstrated that ilimaquinone, a sea sponge metabolite that stimulates microtubule catastrophe *in vivo*, does not stimulate catastrophe with purified tubulin. We have partially purified a ~100 kDa factor from high speed supernatants of interphase and mitotic *Xenopus* eggs which renders pure tubulin sensitive to ilimaquinone *in vitro*.

ILIMAQUINONE and a related compound, avarol, break down the Golgi into mitotic-like vesicles (Takizawa et al., 1993). *In vitro*, ilimaquinone inhibits ADP-ribosyltransferase, which adds ATP-ribose groups to proteins such as G α (Radeke et al., 1999; Weigert et al., 1997). It is thought that *in vivo*, ilimaquinone triggers the activation of a G α and release of a G $\beta\gamma$, which in turn vesiculates golgi (Jamora et al., 1997). Interestingly, ilimaquinone, but not avarol, also depolymerizes microtubules *in vivo* and in cell extracts. Together, this data suggested to us that ilimaquinone may act upon a non-tubulin factor to depolymerize microtubules.

After discovering that ilimaquinone does not act on purified tubulin, we attempted to purify the intracellular target of ilimaquinone from *Xenopus* egg extracts.

6.1 *Materials and Methods*

Microtubule Dynamics

Sea urchin axonemes were a gift from Ron Vale. The *Xenopus* extracts and bovine brain tubulin used in the early characterization experiments were a gift from Josh Nicklas.

Axonemes were adhered to coverslips for 3 minutes in a 5-8 μL flow cell prepared as described in (Vale, 1991). Loose axonemes were washed out with PBS and clarified extract was flowed into the chamber. Assembly of microtubules on axonemes was made visible by video-enhanced differential interference contrast microscopy (VE-DIC) (63x 1.4 NA Plan-Apochromat objective, Axioplan microscope, Zeiss). Images were captured on a video camera (Newvicon, Hamamatsu) and enhanced with an image processor (Argus 20, Hamamatsu). The images were recorded onto S-VHS videotape (Maxell) and analyzed with a position-tracking program (W. Marshall and R.W. Vale).

Xenopus Egg Extracts

Crude “mitotic” extracts were derived from spin-crushing CSF arrested *Xenopus* eggs; technically, these eggs are arrested at metaphase of meiosis II. These extracts were prepared essentially as described (Murray, 1991) with the modifications of (Walczak et al., 1996). “50K” high speed supernatants were then prepared as in (Hirano and Mitchison, 1991) and frozen in small aliquots.

Microtubule stability assay

To measure microtubule stability, we added rhodamine-labeled bovine brain tubulin to unlabeled bovine brain tubulin in a ratio of 1:5 to a final concentration of 1.3 mg/mL tubulin. To this we added 1 mM GTP and sea urchin axonemes on ice for 15 minutes, and

ilimaquinone, avarol or DMSO (control) at various concentrations of extract (1:2, 1:10, 1:30). The dilution buffer was BRB80 (80 mM PIPES, pH 6.8 with KOH, 1 mM MgCl₂, 1 mM EGTA, 1 mM DTT). We then fixed the solution in 3x the original volume of 1% glutaraldehyde in BRB80 for 15 minutes, and then added 10x the original volume of 60% glycerol for mounting. 2 μ L of this solution was then added to a coverslip and microtubule polymerization was assessed qualitatively.

Heat and Trypsin Sensitivity

To measure heat sensitivity, extract was heated for 5 minutes in a water bath at various temperatures and then spun 15,000 rpm in a centrifuge. To measure trypsin sensitivity of the heat-stable activity, Xenopus egg supernatant was treated at 55°C for 5 minutes, then diluted 1:10 at 4°C in BRB80 and treated with 0.2 mg/mL trypsin.

Purification

Gel filtration was performed on a high molecular weight TSK-G300SW column (TosoHaas) equilibrated with BRB80 containing an additional 4 mM MgCl₂ (5 mM total). Anion exchange was performed on DEAE cellulose with 20 mM Tris pH 8.0. Cation exchange was performed on SP Sepharose fast flow with 20 mM MES, pH 6.2. Both buffers also contained 0.1 mM DTT, 1 mM EGTA, 1 mM GTP and 20 mM KCl. After purification steps, fractions were dialyzed into BRB80+1 mM GTP+1 mM DTT.

MAP Enrichment

Interphase extract was diluted 1:1 in BRB80, and DMSO was added to 3% by volume . The extract was spun at 40,000 in a TLA 100 rotor at 4°C (Beckman). The supernatant was removed and left at 25°C for 30-45 min to allow microtubule polymerization. The supernatant was layered onto 1.5 mL 1M sucrose cushions containing BRB80+1 mM ATP at 25°C. The cushions were spun 40,000 rpm in a TSL55 rotor for 20 min at 22°C (Beckman). The cushion was aspirated and the pellet resuspended in ice-cold BRB80 in 3/4 the initial volume of extract. To prepare microtubule depleted extracts, DMSO was omitted from the initial step and the supernatant was reserved after the 40,000 rpm spin.

6.2 Results and Discussion

Characterization of Ilimaquinone Activity in vitro and in Extracts

Because ilimaquinone is a potent microtubule destabilizing protein, to study its activity in *Xenopus* egg extracts we pre-polymerized microtubules off of axonemes and then perfused in extracts containing ilimaquinone (Figure 28A). Microtubules immediately switched to rapid shrinking, or catastrophe, sometimes with short pauses during shrinking. By contrast, a control wash of DMSO does not alter microtubule dynamics in *Xenopus* egg extracts. Pauses may indicate that the microtubule tip is “capped” such that it cannot accept additional tubulin subunits. Therefore, it appears that ilimaquinone increases the catastrophe frequency and can cap microtubules at plus ends, but does not reduce rescue frequency. As little as 0.1 μ M ilimaquinone caused a noticeable effect.

7. **Task 1**
1. **Task 1**
2. **Task 2**
3. **Task 3**
4. **Task 4**
5. **Task 5**
6. **Task 6**
7. **Task 7**
8. **Task 8**
9. **Task 9**
10. **Task 10**

Task 11

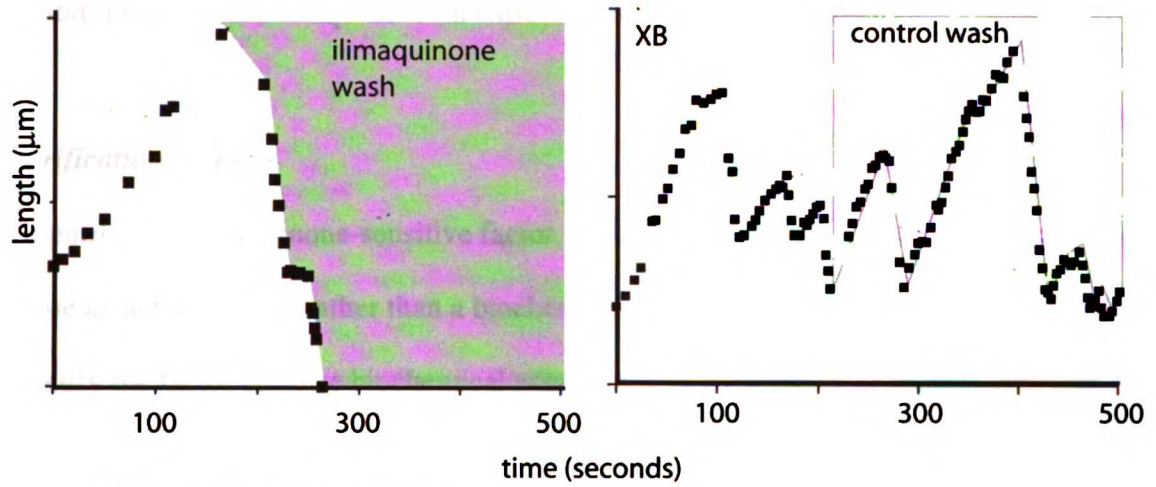
1. **Task 11**
2. **Task 12**
3. **Task 13**
4. **Task 14**
5. **Task 15**
6. **Task 16**
7. **Task 17**
8. **Task 18**
9. **Task 19**
10. **Task 20**

When we added ilimaquinone to purified bovine brain tubulin, we did not detect an increase in catastrophe frequency. Therefore, we concluded that a factor in high speed supernatant confers ilimaquinone sensitivity on microtubules (Figure 28B).

1. The first step is to identify the problem or goal. This involves understanding the current situation and what you want to achieve.

2. Next, you need to gather information and resources. This could involve research, consulting experts, or identifying the tools and materials you need.

A. Xenopus extracts



B. purified microtubules

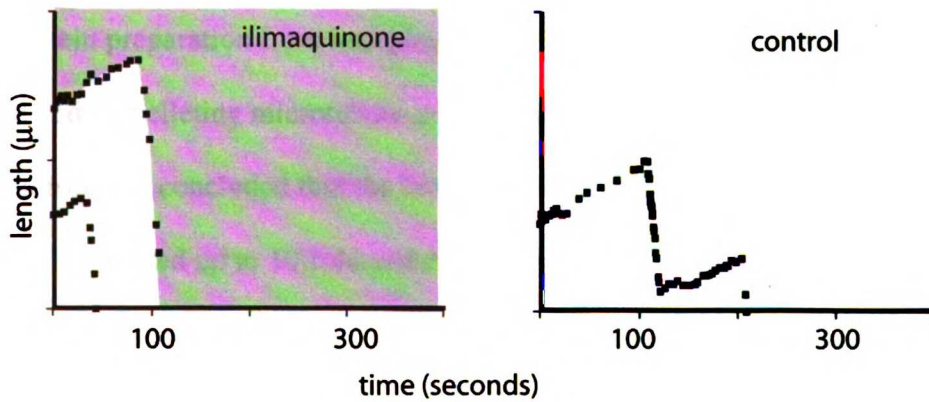


Figure 28. *Effect of ilimaquinone on microtubule polymerization in extracts and in vitro*

Ilimaquinone treatment of growing microtubules in *Xenopus* extracts and pure microtubules. (A)

Microtubules in *Xenopus* extracts were treated with ilimaquinone and their growth was followed with DIC

microscopy and position tracking software. (B) Purified bovine brain microtubules polymerized in XB

were also treated with ilimaquinone or a control wash of DMSO.

To probe whether the factor was a GTP binding protein, we pre-incubated extracts in 100 μ M GTP γ S for 1-3 hours before adding ilimaquinone. GTP γ S pretreatment did not inhibit the effect of ilimaquinone on extract microtubules (not shown).

Purification Steps

To purify the ilimaquinone-sensitive factor, we chose an activity-based visual assay. We chose an activity assay rather than a biochemical assay (i.e. ilimaquinone binding) to identify the factor because biochemical assays require nanomolar, or ideally, covalent target binding (King, 1999). The ilimaquinone-sensitive factor was stable at 55°C and was NEM- and trypsin-insensitive. The factor did not co-purify with a microtubule-associated protein preparation from interphase *Xenopus* egg extracts. Similarly, the factor was not depleted by pelleting microtubule-associated proteins (MAPs) from a mitotic egg extract. Therefore, we concluded that the factor is not a MAP. Concentrated extracts (8 mg/mL) could be diluted up to 10-fold and demonstrate ilimaquinone-stimulated activity, therefore we fractionated the extracts by gel filtration. Gel filtration indicated that the factor was around 100 kDa, and present in both interphase and mitotic high speed supernatants. When the factor was purified by gel filtration from interphase high speed supernatant, the fraction behaved normally, but after freeze-thaw the fraction stimulated microtubule polymerization in the presence of ilimaquinone. From mitotic egg extracts, the factor migrated slightly smaller by gel filtration. When a 20-80% ammonium sulfate cut of interphase high speed supernatant was placed on a gel filtration column, the factor was in a fraction containing 0.1 mg/mL protein, containing a prominent band at around 80 kDa by SDS-PAGE (Figure 29).

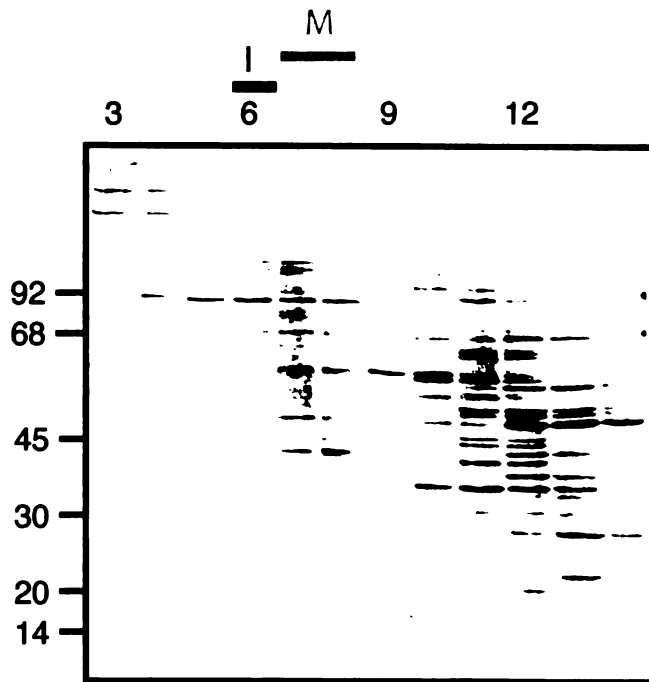


Figure 29. *Sizing column of interphase high speed supernatant*

Xenopus interphase or mitotic arrested extracts were separated by gel filtration chromatography, treated with ilimaquinone, and then added to microtubules. The extracts were also subjected to SDS-PAGE (interphase extract is shown) and proteins were stained with Coomassie dye. The fractions that tested positive for ilimaquinone-stimulated activity are indicated (I=interphase activity, M=mitotic activity).

The factor was stable at room temperature in high speed supernatants for 24 hours. However, after fractionation by gel filtration from mitotic Xenopus egg extracts,

1. **Introduction**
2. **Background**
3. **Methodology**
4. **Results**
5. **Discussion**
6. **Conclusion**
7. **References**
8. **Appendix**
9. **Index**
10. **Table of Contents**

11. **Abstract**
12. **Summary**
13. **Key Words**
14. **Keywords**
15. **Subject Headings**
16. **Classification**
17. **Indexing**
18. **References**
19. **Appendix**
20. **Index**

after three hours the activity “flipped”, i.e. it stimulated microtubule polymerization in the presence of ilimaquinone. This “flipped” activity was insensitive to salt up to 600 mM NaCl. We could detect only ilimaquinone-dependent, microtubule-stimulating activity after anion or cation exchange chromatography; this activity bound to Q at 600 mM NaCl, DEAE at 150 mM NaCl, and S at 300 mM NaCl.

The factor did not pellet with 0.1% polyethyleneimine, and was isolated with a 40-50% ammonium sulfate cut.

Ilimaquinone also inhibits s-adenosylhomocysteinase, which is involved in activated methyl chemistry (Radeke et al., 1999; Radeke and Snapper, 1998; Weigert et al., 1997). Beta-tubulin is isoaspartylated *in vivo* (Lanthier et al., 2002), and mice knocked out for the protein L-isoaspartyl methyltransferase have abnormal microtubule arrays (Yamamoto et al., 1998). Therefore it is possible that ilimaquinone exerts its activity on microtubules by inhibiting an s-adenosylhomocysteinase; we have not tested this possibility.

7 CHARACTERIZATION OF ONCOPROTEIN 18

Abstract. While bovine brain tubulin forms dynamic microtubules that rapidly switch between growth and shrinkage, tubulin in cells typically requires cytoplasmic factors to trigger microtubule “catastrophe.” Op18 (Oncoprotein 18 kDa) represents a family of proteins that stimulates microtubule catastrophe. We have recombinantly expressed and purified Xenopus Op18 and demonstrated that this protein can stimulate microtubule catastrophe at both ends of otherwise stable microtubules. This lends more support to the idea that Op18 stimulates catastrophe by preventing proper protofilament packing. Op18 has also been shown to sequester tubulin *in vitro*. However, we do not see evidence that Op18 binds tightly to tubulin in extracts. Extracts from interphase Xenopus eggs, specialized cells with enormous microtubule arrays, contain Op18 in a 40 kDa particle of unknown composition.

DRAMATIC microtubule rearrangements are required to form the mitotic spindle and, later, to reassemble the interphase microtubule array (further discussed in Appendix I). Individual microtubules can switch between growth and rapid shrinkage by a process termed “catastrophe,” enabling the rapid disassembly of microtubule structures. However, due to the widespread use of bovine brain tubulin to measure microtubule dynamics, it is sometimes overlooked that tubulin purified from other cell types is actually quite stable, and requires additional proteins to stimulate catastrophes (Simon et

1. The first part of the document discusses the importance of maintaining accurate records of all transactions and activities. It emphasizes that proper record-keeping is essential for ensuring transparency and accountability in financial reporting.

2. The second part of the document outlines the various methods and techniques used to collect and analyze data. It highlights the need for consistent and reliable data collection processes to ensure the validity of the results.

3. The third part of the document describes the different types of data that can be collected and analyzed. It includes information on both quantitative and qualitative data, as well as the various sources and methods used to gather this information.

4. The fourth part of the document discusses the importance of data analysis and interpretation. It explains how data analysis can help identify trends, patterns, and relationships, and how these insights can be used to make informed decisions and predictions.

5. The fifth part of the document provides a summary of the key findings and conclusions of the study. It highlights the main results and discusses their implications for future research and practice.

al., 1992). The catastrophe frequency of microtubules increases during prometaphase, as the mitotic spindle assembles, and is highest during mitosis (Rusan et al., 2001).

Op18, also known as stathmin, and related proteins form one family of “catastrophe factors,” proteins that along with the members of the kinesin-13 family (also known by MCAK, mitotic centromere-associated kinesins, or kif2, kinesin family 2) stimulate microtubule catastrophe *in vitro* (further discussed in Appendix II). Inhibition of Op18 reduces the number of microtubule catastrophes in interphase cells by half and in mitotic extracts by an unquantified amount (Belmont and Mitchison, 1996; Howell et al., 1999a). Because inhibition of kinesin-13/MCAK in interphase cells reduces the number of microtubule catastrophes by half and inhibition of kinesin-13/XKCM1 in mitotic extracts reduces catastrophes by four fold, it is likely that kinesin-13 is the predominant catastrophe factor at mitosis (Walczak et al., 2002; Walczak et al., 1996). Indeed, Op18 is at least partially inactivated during mitosis by multiple phosphorylations (reviewed in Appendix I, II and Cassimeris, 2002).

Kinesin-13 members have a curved microtubule binding surface relative to other kinesins, and they bind preferentially to microtubule ends (reviewed in Wordeman, 2005). Consequently, a model emerged where kinesin-13 binding peels apart protofilaments at microtubule ends, which naturally curve during depolymerization (Desai et al., 1999). Structural analysis of a fragment of RB3 that is homologous to Op18 has indicated that Op18 also attacks protofilaments. A structure of an RB3/tubulin complex indicates that the carboxy terminal sub-domain of Op18 causes two bound tubulin dimers (a so-called “T2S” complex refers to 2 tubulin dimers and one Op18/stathmin molecule) to rotate and pull away from adjacent protofilaments (Figure

1. The first part of the document is a list of names and titles, including the names of the authors and the titles of their works. This list is organized in a structured manner, likely serving as a table of contents or a reference list for the document.

2. The second part of the document contains a series of numbered entries, each corresponding to a specific item or topic. These entries are arranged in a list format, providing a clear and organized overview of the content.

3. The third part of the document consists of a series of paragraphs, each discussing a different aspect of the subject matter. These paragraphs are written in a formal and academic style, providing detailed information and analysis.

4. The fourth part of the document is a series of numbered entries, similar to the second part, but with more detailed descriptions and references. These entries provide a comprehensive overview of the topics discussed in the document.

5. The fifth part of the document is a series of paragraphs, each discussing a different aspect of the subject matter. These paragraphs are written in a formal and academic style, providing detailed information and analysis.

6. The sixth part of the document is a series of numbered entries, similar to the second part, but with more detailed descriptions and references. These entries provide a comprehensive overview of the topics discussed in the document.

7. The seventh part of the document is a series of paragraphs, each discussing a different aspect of the subject matter. These paragraphs are written in a formal and academic style, providing detailed information and analysis.

8. The eighth part of the document is a series of numbered entries, similar to the second part, but with more detailed descriptions and references. These entries provide a comprehensive overview of the topics discussed in the document.

9. The ninth part of the document is a series of paragraphs, each discussing a different aspect of the subject matter. These paragraphs are written in a formal and academic style, providing detailed information and analysis.

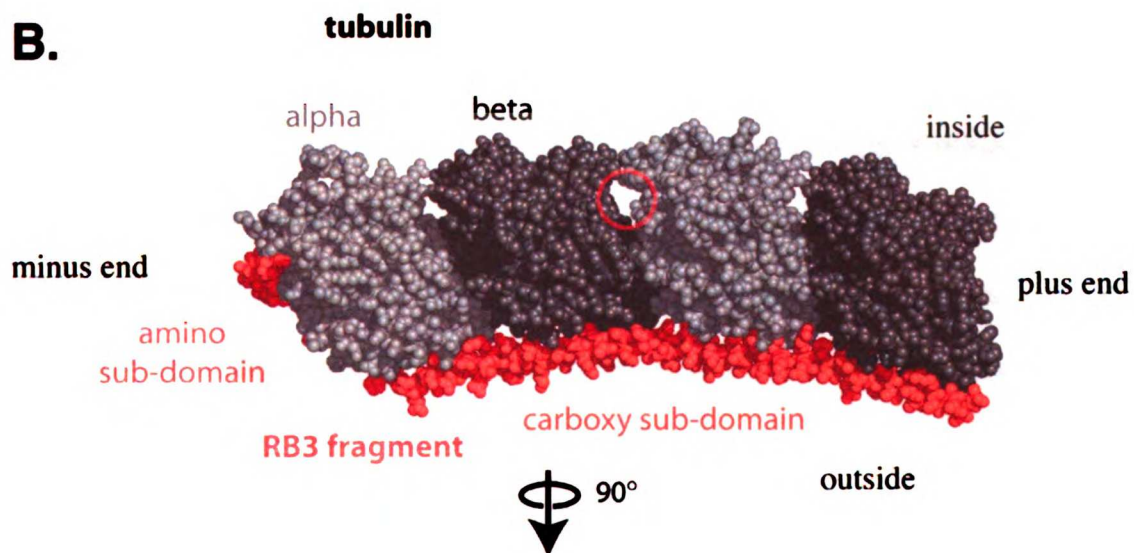
10. The tenth part of the document is a series of numbered entries, similar to the second part, but with more detailed descriptions and references. These entries provide a comprehensive overview of the topics discussed in the document.

30B,C). Thus, Op18 binding should cause protofilaments to pack inefficiently, which could cause catastrophe at either end of the microtubule (Gigant et al., 2000; Meurer-Grob et al., 2001). However, the amino-terminal sub-domain of Op18 wraps around an α tubulin subunit, which should prevent it from binding to another tubulin subunit (Muller et al., 2001; Ravelli et al., 2004). Therefore, Op18-bound tubulin subunits should not incorporate into the plus ends of microtubules, and should “cap” the minus ends of microtubules (Cassimeris, 2002).

A.

		amino sub-domain		linker	
<i>X.l.</i>	4	SDIKVKQLEKRASGQAFELILSPPS	-----	MDAAPDLSITSPKKKECSLEEIQKLEA	
<i>H.s.</i>	4	SDIQVKELEKRASGQAFELILSPRSKESVPEF	----	P-LS--PPKKKDLSEEEIQKLEA	
<i>X.l.</i>	57	AEERRKQHEAEILKQLAEKREHEKEVQLQKAIENN	NNNFSKMAEEKLTTKMETIKENREAQI		
<i>H.s.</i>	57	AEERRKSHAEVLKQLAEKREHEKEVQLQKAIENN	NNNFSKMAEEKLTHKMEANKENREAQM		
<i>X.l.</i>	117	AAKLERLREKDKKVEEIRKGKECKEP			
<i>H.s.</i>	117	AAKLERLREKDKHIEEVRKNKESKDP			
		carboxy sub-domain			

B.



C.

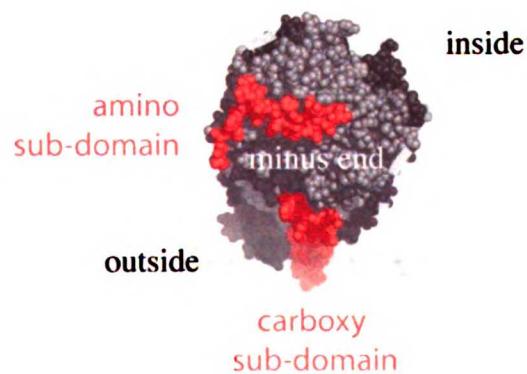


Figure 30. *Op18 sequence and structure*

A. The sequences of Op18 from *Xenopus laevis* and *Homo sapiens* are aligned; identical residues are identified with a line. Sub-domains of Op18 are boxed; the phosphorylated residues are bold. One phosphorylated residue is not conserved in *Xenopus*; this residue is outlined. B. The structure of an RB3 fragment bound to two tubulin dimers (from PDB ID code 1SA0 (Ravelli et al., 2004; Sussman et al., 1998)). C. The same structure, rotated 90°, looking down the protofilament axis from the minus end. Two adjacent protofilaments are also shown (dashed outlines) (Gigant et al., 2000; Meurer-Grob et al., 2001). In both (B) and (C), the outside (facing the cytoplasm) and the inside of the microtubule are indicated.

This structure-based model therefore does not explain how Op18 stimulates catastrophe at the plus ends of microtubules. The amino terminal sub-domain (and linker region) of Op18, which binds α tubulin, increases catastrophe frequency at plus ends *in vitro*, and quite likely *in vivo* (Howell et al., 1999b; Larsson et al., 1999). Meanwhile, the carboxy terminal sub-domain, which binds along the protofilament axis, does not increase catastrophe frequency. GTP hydrolysis at the tip can cause catastrophe at the plus end of microtubules. Ironically, it is the carboxy terminal sub-domain that increases the basal GTPase rate of tubulin. Therefore GTP hydrolysis *per se* does not appear to be the mechanism of Op18-induced catastrophes (Larsson et al., 1999).

To further understand the mechanism by which Op18 causes microtubule catastrophe, we assembled recombinant Op18 with a *Xenopus* egg tubulin and measured microtubule catastrophe. *Xenopus* Op18 is 80% identical to human Op18, and it can increase the catastrophe frequency at the plus ends of microtubules in interphase extracts,

when added in high amounts (3 μ M Op18) (Arnal et al., 2000; Maucuer et al., 1993) (Figure 30A).

To understand how Op18 is regulated in cells, we also looked at the association of Op18 with proteins in interphase and mitotic extracts.

7.1 *Materials and Methods*

Expression and purification of Op18

The gene for *Xenopus laevis* Op18 (sequence data of XO35A (Maucuer et al., 1993) is available from GenBank under accession number X71431) was cloned and expressed as previously described (Howell et al., 1999a). The composition of the expressed protein was confirmed by amino acid analysis (below). Proteins were separated on a 7-20% SDS-polyacrylamide gel (Novex).

Concentration of Op18

To measure the concentration of purified *Xenopus* Op18, we compared results from using Bradford reagent (Pierce “Coomassie Plus”), Ellman’s reagent (Pierce) and amino acid analysis (Protein and Nucleic Acid Facility, Beckman Center, Stanford University Medical Center).

Analytical Ultracentrifugation

3 mg/mL of purified, recombinant *Xenopus* Op18 in a HEPES buffer (10 mM HEPES pH 7.7, 50 mM NaCl, 1 mM DTT) was diluted to an OD₂₂₀ of 0.35 (30-fold) into a

1. The first step is to identify the problem or goal. This involves understanding the current situation and what you want to achieve. It's important to be clear and specific about your objectives.

2. Next, you need to gather information. This could involve research, talking to experts, or looking at data. The more you know, the better you can plan.

3. Once you have the information, you can start to develop a plan. This should outline the steps you need to take, the resources you need, and the timeline for completion.

4. It's also important to consider potential risks and challenges. Think about what could go wrong and how you can avoid or mitigate those risks.

5. Finally, you need to implement the plan. This is where you put your ideas into action. It's important to stay focused and motivated, and to be flexible if things don't go as planned.

phosphate buffer (50 mM NaPO₄, 100 mM NaCl, 1 mM DTT). Blanks were prepared with HEPES buffer diluted in phosphate buffer. Samples were run on an analytical ultracentrifuge (XLA, Beckman) under sedimentation equilibrium conditions at 20°C, 25,000 rpm, for at least 7 hours and measured at a wavelength of 230 nm. Apparent weight-averaged molecular weight (M_{wapp}) was calculated with $\nu\text{-bar}=0.716$.

Microtubule Assembly

Bovine brain tubulin conjugated to the fluorochrome rhodamine was mixed 1:5 with unconjugated tubulin and used at a final concentration of 2 mg/mL in BRB80+1 mM GTP on ice was incubated with stable microtubule seeds (GMPCPP-tubulin) and visualized by epi-fluorescence.

Purification of Xenopus Tubulin

Purified tubulin from Xenopus eggs was prepared by cycles of glutamate polymerization and depolymerization and perfused into these chambers in BRB80+GTP+DTT (pH with KOH to 6.8). 18 mL of high speed supernatant prepared as above were diluted in half volume of BRB80+4 mM MgCl₂ (5 mM total MgCl₂)+7.5 mM Creatine Phosphate+1 mM ATP. The extract was spun at 80,000 rpm in two TLA 100.3 rotors (Beckman) at 4°C for 15 min. The supernatant was removed, pooled on ice, and then warmed to 25°C for 2 min. DMSO (Sigma) was rapidly added, to 7.2% and mixed well by gentle inversion. Microtubules were thus polymerized over 30 min. The supernatant was then layered onto a BRB80-40% glycerol cushion and spun at 50,000 rpm in a 70 Ti rotor at 25°C (Beckman). The supernatant was aspirated and the pellet was resuspended in 4 mL

ice cold CB for 30–40 min (50 mM PIPES, pH 6.8, 0.2 mM MgCl₂, 1 mM EGTA), using only one pipet tip to resuspend all pellets. A water sonicator at 4°C was also used to disrupt aggregates. Depolymerized tubulin was then spun in a TLA 100.3 at 55,000 rpm for 15 min at 2°C. Tubulin was then loaded onto a phosphocellulose column equilibrated in CB. Fractions greater than 1 mg/mL by Bradford were pooled and salts were added to convert the mixture to BRB80. GTP was added to 0.5 mM and solid monosodium glutamate was added to 1 M with mixing in an ice water bath. The mixture was then warmed to 37°C for 20 min. The microtubules were then placed on a 1.4 mL BRB80–40% glycerol cushion in a TLA 100.3 and spun at 80,000 rpm, 30°C for 15 min. The supernatant was aspirated and the pellet was depolymerized in enough ice cold BRB80 to yield 2–4 mg/mL tubulin, about 1 mL. The depolymerized tubulin was clarified in a TLA 100.3 at 55,000 rpm for 10 min at 4°C. Tubulin concentration was estimated with a spectrophotometer, using $\epsilon_{227}=80,000 \text{ M}^{-1}\text{cm}^{-1}$. Tubulin was frozen in small aliquots.

Live imaging of Microtubule Dynamics

Sea urchin axonemes were bound to glass coverslips in a heated chamber as described (Govindan and Vale, 2000). Purified, recombinant Xenopus Op18 in BRB80+DTT was then perfused into these chambers. Microtubules were recorded on a video-enhanced DIC microscope using S-VHS (microscope, Nikon; S-VHS, Maxell).

Sucrose Gradients

Xenopus egg extracts were sedimented over a 5–20% sucrose gradient. Fractions were TCA precipitated and then separated on 10–20% Tris-tricine SDS-polyacrylamide gels.

The gels were then transferred to nitrocellulose and immunoblotted with anti-Op18 or anti-tubulin antibodies (anti-tubulin antibody, DM1alpha, Sigma). Protein standards were loaded in an equivalent volume and run in parallel over identical gradients.

Gel filtration Chromatography

Gel filtration chromatography was carried out on a TSK-300 PWxl column by HPLC (TosoHaas) in XB (0.1 M KCl, 1 mM MgCl₂, 0.1 mM CaCl₂, 10 mM HEPES pH 7.5, 1 mM DTT). The column was calibrated with standards of known Stokes radii according to (Siegel and Monty, 1966). We loaded 200 μg of bovine brain tubulin ($\epsilon_{280}=115000 \text{ M}^{-1} \text{ cm}^{-1}$) and 6 μg of recombinant *Xenopus* Op18 onto the column. To detect tubulin, absorbance at 280nm was recorded. To detect Op18, fractions were collected, processed by SDS-PAGE and immunoblotted for Op18. Quantitative immunoblotting was performed as described in an earlier chapter. The peak elution volume of the tubulin-Op18 complex was determined by subtracting the graph of tubulin or Op18 alone from the graph of the complex. The column was calibrated with standards of known Stokes radii. The sizes of protein complexes were estimated by the method of (Siegel and Monty, 1966).

7.2 Results and Discussion

Expression of Xenopus Op18

We expressed Op18 from the *Xenopus laevis* as a GST fusion in bacteria (Figure 31A). Purified Op18 was generated by isolating the fusion protein on a GSH

column, cleaving the GST tag with thrombin, and removing the GST tag with an anion exchange column.

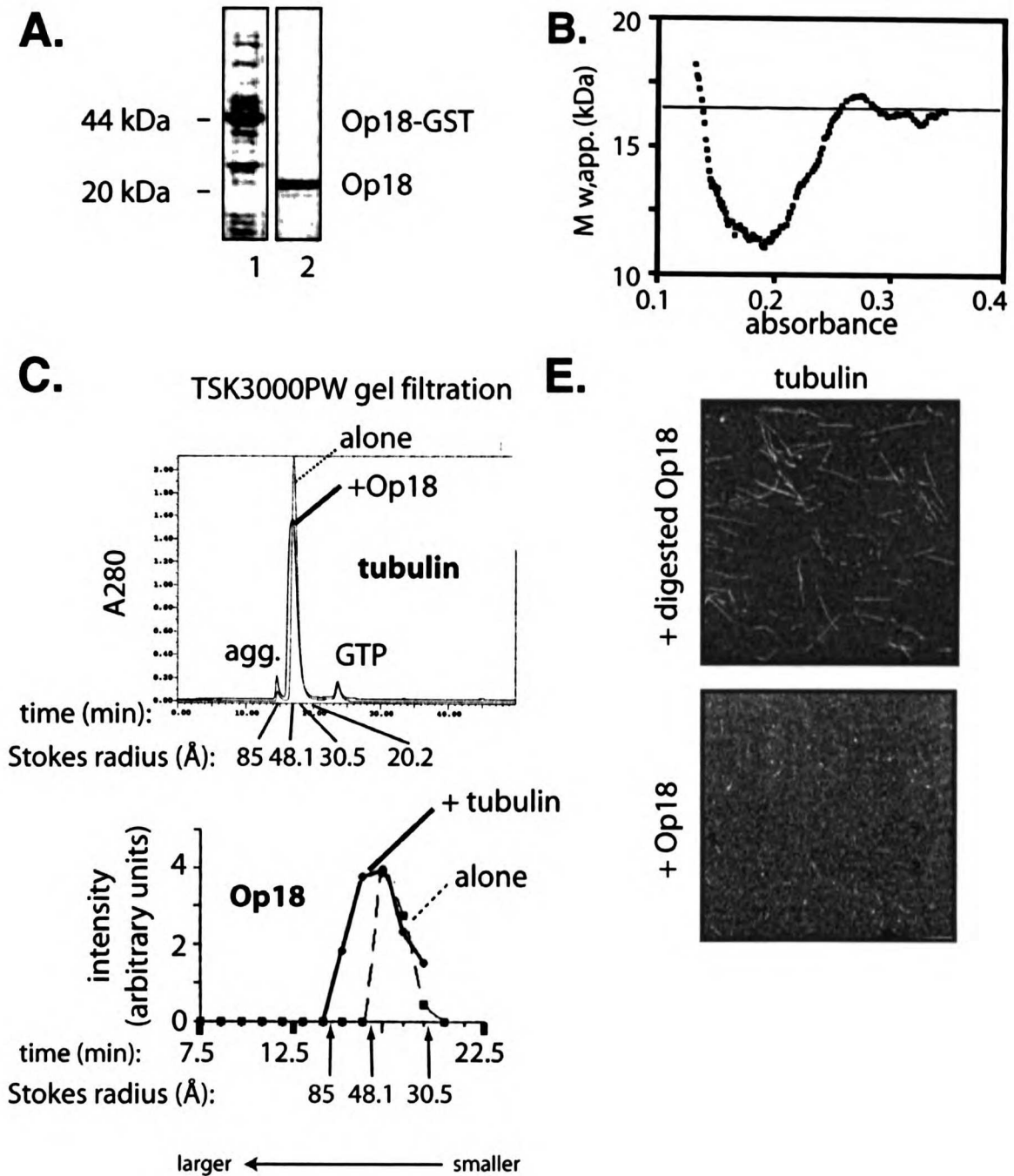


Figure 31. Characterization of *Xenopus Op18*

(A) Cell lysate from bacteria expressing GST-Op18 from *Xenopus laevis* (1) was bound to a GSH column and bound protein was cleaved with thrombin; cleaved Op18 flows through an anion exchange column (2).

(B) The native molecular mass of purified *Xenopus Op18* was analyzed by analytical ultracentrifugation

1. The first part of the document discusses the importance of maintaining accurate records of all transactions and activities related to the business. It emphasizes the need for transparency and accountability in financial reporting.

2. The second part of the document outlines the various methods and techniques used to collect and analyze data. It covers both qualitative and quantitative research approaches, highlighting the strengths and limitations of each.

under equilibrium sedimentation conditions. (C) Bovine brain tubulin was analyzed by gel filtration in the absence (alone) or presence (+Op18) of purified *Xenopus* Op18. A280 reflects the location of tubulin; Op18 was identified by immunoblotting individual fractions. Protein standards were loaded onto the gel filtration column before each experiment; the position and Stokes radius of several standards are indicated (and see next figure). (E) Purified *Xenopus* Op18 (+Op18), but not protease-treated Op18 (+ digested Op18) inhibits the polymerization of fluorochrome-conjugated tubulin.

Determining the Concentration of Op18

Because Op18 has no tryptophans or tyrosines, its protein concentration cannot be determined by measuring its absorbance at 280 nm; from its amino acid composition, we estimate $\epsilon_{280}=337.5 \text{ M}^{-1}\text{cm}^{-1}$. To determine the accuracy of the Bradford assay in measuring the concentration of Op18, we also estimated its concentration by the Edman method for cysteine accessibility and by amino acid analysis. Comparing denaturing with non-denaturing conditions, we determined that Op18 contains one free cysteine (and two buried cysteines) per molecule. Compared to amino acid analysis, the Edman method overestimates the concentration of Op18 by 1.5 fold, whereas Bradford (using BSA as a standard) overestimates the concentration of Op18 by 1.2-fold. We used the conversion factor of 1.2 fold when reporting the concentration of Op18 measured by Bradford.

Physical Characteristics of *Xenopus* Op18

To determine the physical characteristics of *Xenopus* Op18, we performed analytical ultracentrifugation on our purified material under sedimentation equilibrium conditions

(Figure 31B). The apparent molecular weight by analytical ultracentrifugation indicated that our recombinant *Xenopus* Op18 is 17 kDa in solution, corresponding to a monomer. Op18 has been previously demonstrated to be a monomer *in vivo* and *in vitro*. (Marklund et al., 1994; Schubart et al., 1987).

Activity of Xenopus Op18

To determine whether our recombinant *Xenopus* Op18 was active, we tested whether it could bind to tubulin and inhibit microtubule polymerization. Op18 has previously been demonstrated to bind to two tubulin dimers *in vitro* (reviewed in Cassimeris, 2002). This binding shifts the size of tubulin on a gel filtration column (Belmont and Mitchison, 1996; Curmi et al., 1997). We found that addition of *Xenopus* Op18 to bovine brain tubulin increases the gel filtration peak of tubulin from a Stokes radius of 47Å (corresponding to tubulin dimer) to 58Å, indicating that our recombinant Op18 binds tubulin. The Stokes radius of *Xenopus* Op18 also increased when added to tubulin, from 36Å to 60Å. 37Å and 60Å are the published Stokes radii of Op18 and the tubulin/Op18 complex, respectively, which agrees well with our data (Curmi et al., 1997).

To determine whether our recombinant *Xenopus* Op18 inhibits microtubule polymerization, we added it to fluorochrome-conjugated tubulin. As a control, we digested our recombinant material with protease before adding it to tubulin. We found that Op18, but not digested Op18, inhibits microtubule polymerization. Therefore, our recombinant *Xenopus* Op18 is active in binding to tubulin and in inhibiting microtubule polymerization.

Action of Xenopus Op18 on Xenopus Microtubules

To understand the mechanism by which Xenopus Op18 inhibits microtubule polymerization, we looked at the polymerization dynamics of purified tubulin from Xenopus egg extracts. We chose Xenopus egg tubulin because it more homogeneous than bovine brain tubulin. Bovine brain tubulin contains a large mixture of tubulin isoforms, which could explain why it is much more dynamic than other tubulin preparations (Simon et al., 1992). The critical concentration of our Xenopus tubulin preparation was estimated to be 2 μM at the plus end and 5 μM at the minus end in BRB80. By contrast, sea urchin tubulin has a critical concentration of 1.5 μM at the plus end in a similar buffer (Simon et al., 1992).

To polymerize microtubules at both plus and minus ends, 5 and 10 μM Xenopus egg tubulin was incubated at room temperature using sea urchin axonemes as nucleation sites. The resulting microtubules were then perfused with 0.3 or 0.9 μM of purified Xenopus Op18. At 10 μM tubulin and 0.9 μM Op18, 1.8 μM tubulin could be sequestered in a T2S complex. Op18 binds tubulin with micromolar affinity, or even tighter (reviewed by Cassimeris, 2002).

After perfusion with 0.3 μM Xenopus Op18, microtubules grew at similar velocities (not shown). With 0.9 μM Xenopus Op18, the plus ends grew slowly, did not grow or were “paused” (Figure 32A). This is a stronger inhibitory effect on elongation velocity than has previously been seen on bovine brain microtubules or on microtubules from Xenopus egg extracts under similar conditions (Arnal et al., 2000; Howell et al., 1999b). Furthermore, we occasionally observed minus ends slowly shrinking before rescue (Figure 32A, gray arrowhead; -0.5 $\mu\text{m}/\text{min}$). Somewhat slow shrinkage rates (-5

1. The first part of the document is a list of names and titles, including the names of the authors and the titles of their respective works. This list is organized in a structured manner, likely serving as a table of contents or a reference list for the document.

2. The second part of the document contains a series of numbered entries, each corresponding to a specific item or topic. These entries are arranged in a list format, providing a clear and organized overview of the content.

$\mu\text{m}/\text{min}$) has previously been seen for the plus ends of sea urchin microtubules in PIPES buffer, which does not allow more rapid disassembly (Simon et al., 1992). However, we observed rapid shrinkage of both plus and minus ends in the presence of Op18, even in PIPES buffer. The rate of rapid shrinkage in the presence of $0.9 \mu\text{M}$ Op18 was $-10 \mu\text{m}/\text{min}$ (plus end) or $-30 \mu\text{m}/\text{min}$ (minus end) at both tubulin concentrations. We did not measure shrinkage in the absence of Op18, because we could not observe any shrinking microtubules under these conditions. The rapid shrinkage velocity of plus ends in the presence of Op18 are similar to that previously reported for plus ends of *Xenopus* tubulin in extracts ($-13 \mu\text{m}/\text{min}$) (Belmont et al., 1990). *Xenopus* Op18 does not increase the microtubule shrinkage rate of bovine brain tubulin (Howell et al., 1999b). However, it is possible that Op18 enables rapid shrinkage in the presence of PIPES, which does not support rapid shrinkage of egg tubulin. This would imply that either Op18 incorporates into microtubules, which is not supported by data from microtubule pelleting assays, or that Op18 alters the nature of the catastrophe itself.

As with tubulin in *Xenopus* egg extracts (Parsons and Salmon, 1997), but in contrast to bovine brain tubulin, *Xenopus* tubulin rarely exhibits catastrophe in PIPES buffer (Figure 32C and D). Op18 increases the frequency of catastrophes (Figure 32C and D). This increase in catastrophe frequency is more dramatic than the effects seen with Op18 on bovine brain tubulin and microtubules in *Xenopus* extracts (Arnal et al., 2000; Belmont and Mitchison, 1996; Howell et al., 1999b). However, it is possible that we were not able to accurately count catastrophes in the absence of tubulin because PIPES inhibits rapid disassembly.

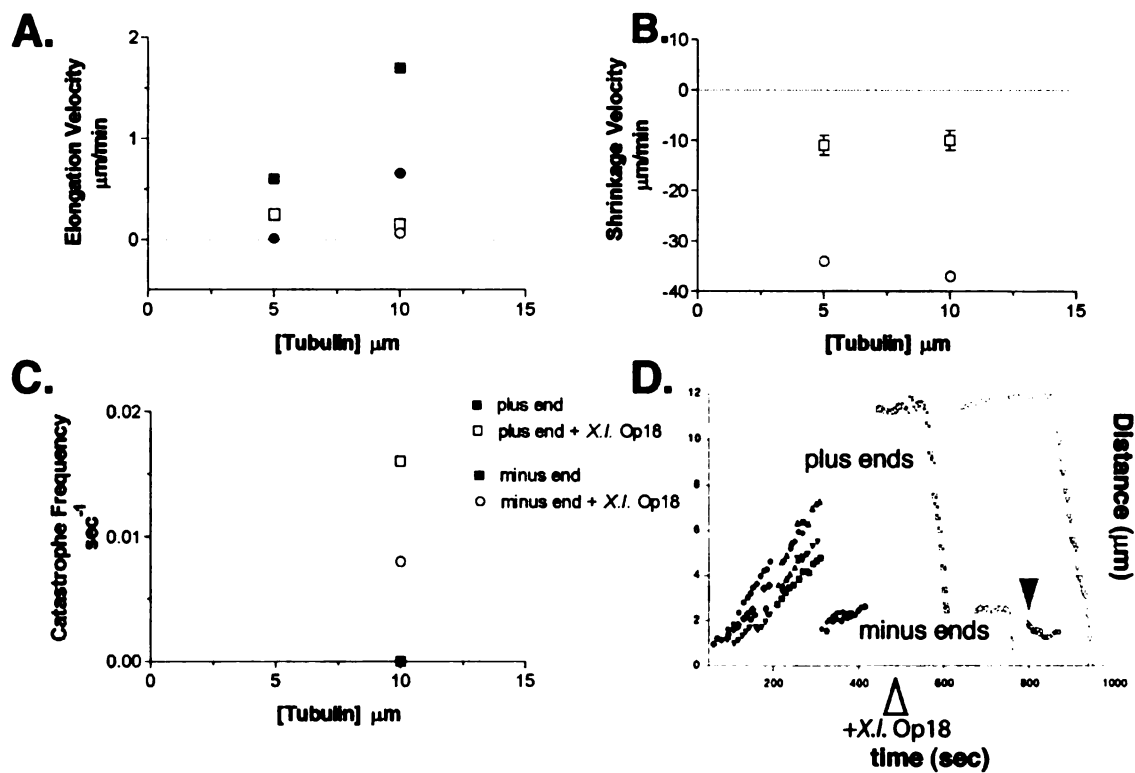


Figure 32. Microtubule polymerization dynamics influenced by *Xenopus Op18*

Microtubules were grown in perfusion chambers and visualized by video-enhanced DIC microscopy (A-C).

filled = + 0.9 μM *Xenopus Op18*, open = no *Op18*. squares = microtubule plus ends, circles = minus ends.

(A) Elongation velocity of *Xenopus* microtubules +/- *Xenopus Op18*. (B) Shrinkage velocity of *Xenopus*

microtubules + 0.9 μM *Op18*. (C) Catastrophe frequency of *Xenopus* microtubules +/- *Xenopus Op18*. (D)

Traces of the growing ends of individual microtubules. *Xenopus Op18* was perfused at 500 sec (open

arrowhead). Some minus ends shrank slowly (filled arrowhead).

1. The first part of the document discusses the importance of maintaining accurate records of all transactions and activities. It emphasizes that this is crucial for ensuring transparency and accountability in the organization's operations.

2. The second part of the document outlines the various methods and tools used to collect and analyze data. It highlights the need for consistent and reliable data collection processes to support informed decision-making.

This preliminary data suggests a model for Op18 action. A catastrophe factor that causes pausing at the plus ends of microtubules is consistent with a mechanism where the plus end is capped, such that it cannot accept additional tubulin subunits. This model also predicts that the critical concentration for assembly at the minus end would be lowered. We were unable to measure the critical concentration of the minus end because the elongation velocities at the concentrations of tubulin we used were very small. A catastrophe factor that causes catastrophes at the minus ends of microtubules as well as the plus ends is consistent with a mechanism where the protofilaments are kept apart. Furthermore, Op18 may increase the rate of rapid shrinkage observed in the presence of PIPES. Perhaps the type of catastrophe stimulated by Op18 in PIPES buffer is different than the intrinsic catastrophes under these conditions. Therefore, from our data we anticipated that Op18 acts as a cap at plus ends and as a protofilament destabilizer at both ends of microtubules.

While our data is qualitatively (if not quantitatively) similar to what has previously been seen with bovine brain tubulin, others have variously attributed the effect of Op18 on catastrophe (at one or both ends) as an indirect effect of inhibiting tubulin-Op18 assembly, also called sequestration (Curmi et al., 1997; Howell et al., 1999b; Jourdain et al., 1997). However, it is known that Op18 causes microtubule catastrophe at plus ends *in vivo*, where sequestration of tubulin is not sufficient to increase catastrophe. Furthermore, in this *in vitro* study we used a stable, physiologically relevant source of tubulin, where microtubule catastrophes do not occur at even low levels of tubulin (Parsons and Salmon, 1997; Simon et al., 1992). Therefore, we feel that the increase in

catastrophe we observed was due to Op18 binding to the microtubule itself, at both ends, and not due to sequestration.

We propose a model whereby the amino terminal sub-domain of Op18 can bind the both ends of microtubules, and thereby cause catastrophe. Perhaps the gap between tubulin dimers seen in the crystal structure permits the amino terminus to bind (Figure 30B). The growing end of microtubules has more outward curvature than the rest of the microtubule, which could increase the accessibility of the plus ends of microtubules to Op18 (Meurer-Grob et al., 2001). Given that we saw catastrophes at both ends, it would be useful to determine which sub-domain of Op18 can cause catastrophe at the minus end of microtubules.

Regulation of Op18 in Xenopus egg extracts

To understand how Op18 is regulated in high-speed supernatants of *Xenopus* egg extract, we raised antibodies to Op18 as previously described (Howell et al., 1999a). Op18 is phosphorylated in both interphase and mitotic *Xenopus* egg extracts (Andersen et al., 1997; Kuntziger et al., 2001). Our antibodies recognize three prominent bands from 20-24 kDa, corresponding to unphosphorylated and phosphorylated forms of Op18 (*Xenopus* Op18 is probably phosphorylated on Ser16 or 25 and 38 (Andersen et al., 1997; Curmi et al., 1997), and a 50 kDa band. These bands are also recognized by the peptide antibody SLEEIQ (not shown). Op18 in mitotic extract sediments with a peak at 1.4S and has a Stokes radius of 40Å (Figure 33). This is similar to the hydrodynamic properties of pure Op18 (1.4S/33Å, (Schubart et al., 1987); 37Å (Curmi et al., 1997)), and is smaller than the tubulin/Op18 complex *in vitro* (7.7S/60Å (Curmi et al., 1997)). Therefore, the

majority of Op18 in mitotic extracts behaves as a monomer, not bound to tubulin. Indeed, the hydrodynamic properties of tubulin are 5.6S/40Å, which is also smaller than the tubulin/Op18 complex (Figure 33B). Therefore, the majority of tubulin and Op18 in mitotic extract are not in a complex. This is consistent with the finding that some cell types contain enough Op18 that, theoretically, could sequester all cellular tubulin in a T2S complex, but still have large microtubule arrays (Larsson et al., 1999).

Op18 in interphase extracts, by contrast, is in a complex. Here, Op18 sediments with a peak at 2.5S and has a Stokes radius of 40Å (Figure 33). These hydrodynamic values predict a protein complex of about 40 kDa, about 20 kDa larger than monomeric Op18 (Siegel and Monty, 1966). We do not know what other proteins may be in this complex. However, we believe that this complex does not contain tubulin because tubulin binding to Op18 *in vitro* generates a complex with a Stokes radius of 60Å (Figure 31C, D and (Curmi et al., 1997). Furthermore, phosphorylated Op18 binds tubulin weakly (Di Paolo et al., 1997; Holmfeldt et al., 2001), yet the phosphorylated forms of Op18 migrate together at 2.5S. Further experimentation will be required to determine the identity of the proteins in the 2.7S complex of Op18. Perhaps *Xenopus* eggs, which to assemble huge microtubule arrays (up to 600 μm) during interphase, sequester Op18 in an inactive complex (Parsons and Salmon, 1997). However, 10 μM but not 3 μM Op18 inhibits microtubule catastrophe in interphase extracts, and shrinks microtubules in mitotic extracts, suggesting exogenously added Op18 is equally active at interphase and mitosis in egg extracts (Andersen et al., 1997; Arnal et al., 2000).

Because we did not detect a large amount of the Op18/tubulin complex in high-speed supernatants, it appears that Op18 does not sequester a large amount of non-

polymerized tubulin in extracts. Instead, it appears that Op18/tubulin association in extracts is inhibited. To verify this model, the tubulin/Op18 complex should be looked for in extracts from other cell types. Based on analysis of microtubule assembly in crude supernatants, we suspect that Op18 is at least partially active in mitotic egg extracts (Belmont and Mitchison, 1996). Therefore, Op18 activity in eggs likely does not involve sequestration of a large amount of non-polymerized tubulin by Op18. It will be important in other cell types where the activity of Op18 has been verified to determine whether Op18 is in a 60Å complex with tubulin.

1. The first part of the document is a list of names and addresses of the members of the committee. The names are listed in alphabetical order. The addresses are listed in the order in which they appear in the list.

MEMBERS OF THE COMMITTEE

2. The second part of the document is a list of the names and addresses of the members of the committee. The names are listed in alphabetical order. The addresses are listed in the order in which they appear in the list.

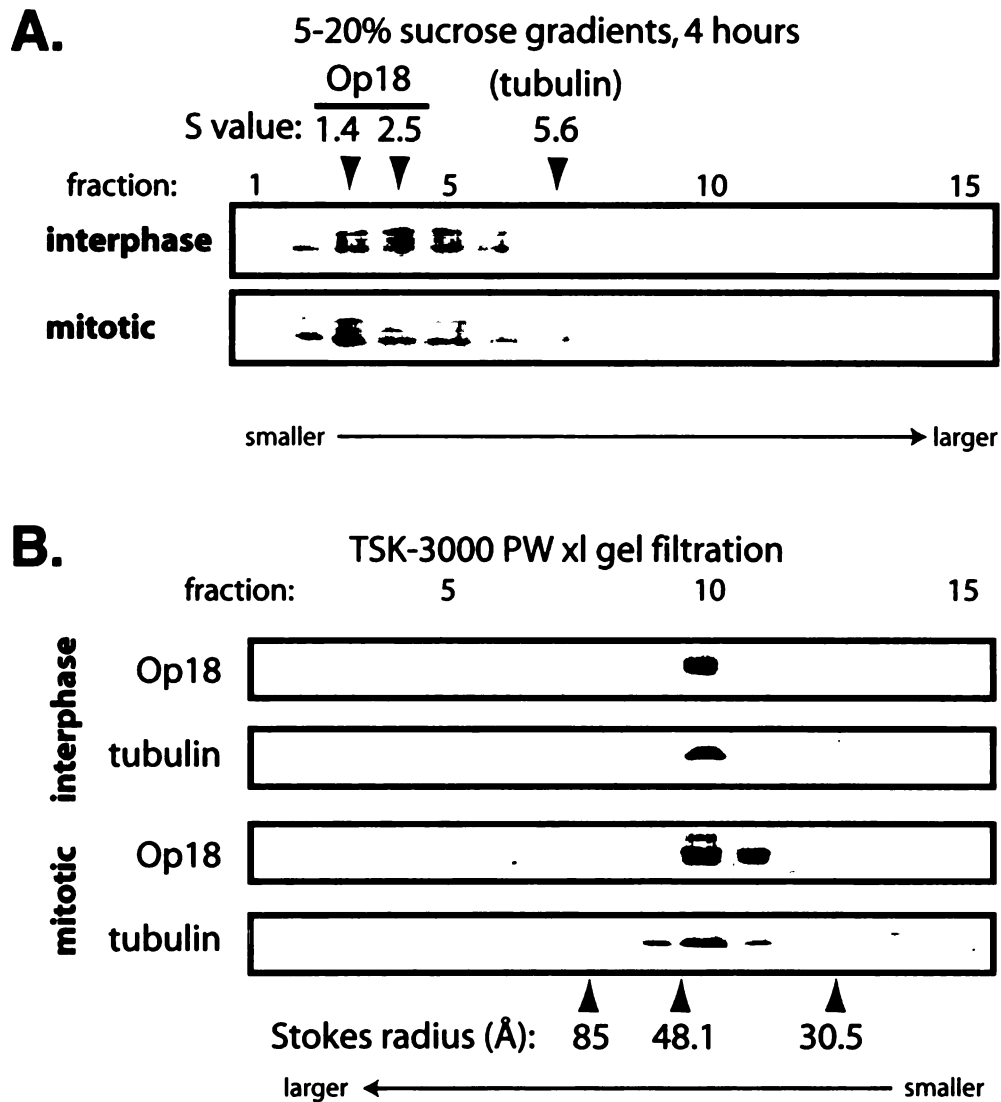


Figure 33. *Op18* in *Xenopus* egg extracts

High speed supernatants of interphase or mitotic *Xenopus* egg extracts were separated by sucrose gradient sedimentation or gel filtration chromatography. Extracts were sedimented on a 10-50% sucrose gradient for 4 hours (A) or fractionated by TSK-3000 PW xl gel filtration chromatography. Sucrose gradient fractions were collected from the top of the gradient. Each fraction was immunoblotted for Op18 or tubulin (not shown) after separation by SDS-PAGE on a 10-20% gradient gel. Standards with known S value or Stokes radius were run in parallel over identical gradients or columns, respectively. The gel filtration column was

1. The first part of the document is a list of names and titles, including the names of the authors and the titles of their respective works. This list is organized in a structured manner, likely serving as a table of contents or a reference list for the document.

2. The second part of the document contains a series of numbered entries, possibly representing a list of items or a sequence of events. These entries are organized in a structured manner, likely serving as a table of contents or a reference list for the document.

8 APPENDIX I: DISCOVERY OF OP18 FUNCTION

Reprinted from Trends in Cell Biology, Belmont L., Mitchson T. J. and Deacon H.,
Catastrophic Revelations About Op18/Stathmin, pages 197-198, Copyright (1996) with
permission from Elsevier.

Catastrophic revelations about Op18/stathmin

A 17 kDa phosphoprotein, variously termed Op18, stathmin, p19, 19K, pp17, p18, pp20-pp21-pp23, lap18 and prosolin has caught the attention of many investigators for many different reasons. This protein, which we will refer to as Op18/stathmin, is phosphorylated in response to numerous extracellular signals and is present in increased levels in many types of cancer cells¹. Here, we review recent advances in the understanding of Op18/stathmin function and regulation, and discuss them in light of a recent report that purified Op18/stathmin regulates microtubule polymer dynamics *in vitro*.

Op18/stathmin regulation and function

Op18/stathmin first attracted attention because its abundance and isoelectric point change dramatically in response to changes in cellular physiology. This protein was subsequently found to be a major substrate of several kinase signaling pathways². The phosphorylation sites of Op18/stathmin have now been mapped to four serine residues: S16, S25, S38 and S63. S25 and S38 were first identified as residues phosphorylated in Op18/stathmin purified from bovine brain³ and Jurkat T cells⁴. Beretta *et al.*⁵ identified all four phosphorylation sites and determined that, *in vivo* (in brain tissue and PC12 cells), all of the observed phosphoisomers could be accounted for by phosphorylation on some combination of these four sites. These sites can be phosphorylated *in vitro* by mitogen-activated protein (MAP) kinase (S25), p34^{cdc2} (S25 and S38), protein kinase A (S16, S63) and Ca²⁺-calmodulin kinase type Gr (S16) (Refs 5-7).

Other work has focused on the cell-cycle regulation of phosphorylation of Op18/stathmin. Strahler *et al.*⁸ first reported that Op18/stathmin phosphorylation changes throughout the cell cycle. Using drugs to block cells in S phase or in mitosis, they observed a very small increase in phosphorylation between G1 and S, and a large increase in phosphorylation at mitosis. Luo *et al.*⁹ used flow cytometry to separate leukemia cells with different DNA content and observed a major increase in phosphorylation during G2 or M, primarily resulting

from an increase in phosphorylation on S25 and S38. Brattsand *et al.*¹⁰ reported an increase of Op18/stathmin phosphorylation on S16, S25 and S38 when the mitotic index is highest in synchronized Jurkat cells. They found a similar phosphorylation pattern in a mitotic shake-off of HeLa cells. When Jurkat cells were blocked in M phase, the phosphorylation levels of Op18/stathmin increased until phosphorylation on all four sites was observed.

Recent studies of Op18/stathmin using antisense RNA inhibition and overexpression of phosphorylation site mutants have shed light on its function (Table I). Overexpression of antisense RNA causes an increase in cellular doubling time and an increase in the number of cells with a 4N (G2-M) DNA content⁹. Overexpression of the gene encoding Op18/stathmin with both S25 and S38 mutated to alanine (S25,38A) results in a large number of cells with a 4N and 8N DNA content, while overproduction of wild-type Op18/stathmin causes only a slight increase¹¹. Synthesis of Op18/stathmin with all four phosphorylation sites mutated to alanine (S16,25,38,63A), as well as an S16,63A variant, resulted in a similar phenotype.

While the S16,63A variant is phosphorylated on S25 and S38, the S25,38A variant is primarily nonphosphorylated¹². The authors propose that overproduction of Op18/stathmin, which cannot be phosphorylated on S16 and S63, results in the G2-M block, and that phosphorylation of S25 and S38 is necessary for phosphorylation of S16 and S63. Despite this elegant biochemical analysis, the function of Op18/stathmin remained obscure.

Cell-cycle regulation of microtubule dynamics

Research on Op18/stathmin has recently collided head-on with another field, the regulation of microtubule (MT) dynamics. MTs are long protein polymers composed of subunits of α and β tubulin. These polymers are essential for cellular organization, polarization and the movement of the chromosomes during mitosis. Microtubule polymers interconvert between phases of slow

growth or rapid shortening, with abrupt transitions between the two phases, *in vitro* and *in vivo*¹³. Transitions from growing to shrinking are called 'catastrophes', and transitions from shrinking to growing are called 'rescues' (see Fig. 1a). It has been known for some time that MTs turn over more quickly in mitosis¹⁴, probably owing to an increase in the frequency of catastrophes¹⁵. Recent studies have demonstrated that there are also changes in MT dynamics within different phases of mitosis. Microtubule-associated proteins (MAPs) and their regulation by phosphorylation probably account for some of the cell-cycle regulation of MT dynamics. However, the high frequency of MT catastrophes in mitosis suggests the presence of factors that destabilize MTs¹⁶. Such factors are also present during interphase, as interphase MTs *in vivo* have a higher catastrophe frequency than purified MTs.

Recently, two proteins have been identified that destabilize MTs by increasing the catastrophe frequency: XKCM1 (a kinesin-related protein¹⁷) and Op18/stathmin¹⁸. The physiological roles of these two factors are still unclear, although both molecules regulate MT polymerization dynamics in *Xenopus* egg extracts. The identification of Op18/stathmin as a MT dynamics regulator allows us to re-examine the previous studies on this protein discussed above. Microtubule dynamics change throughout the cell cycle (Fig. 1b), and the multiple phosphorylations of Op18/stathmin might reflect these changes. In particular, the change in MT dynamics

Table I. Phosphorylation site mutants of Op18/stathmin*

Variant	Block in	
	G2-M	Endoreduplication
Wild type	+/-	-
S16A	+/-	-
S25A	+	+/-
S38A	+	+/-
S63A	+	+
S25,38A	++	+
S16,63A	++	+
S16,25,38,63A	++	+
Antisense RNA	+	-

*Summary of the results of overproducing Op18/stathmin phosphorylation-site mutants^{11,12}. Cell cycle is determined by FACS analysis to measure DNA content. A G2-M block reflects a higher percentage of cells with 4N DNA content and endoreduplication reflects a higher percentage of cells with 8N DNA content. Analysis of the residues phosphorylated indicates that the S25,38A mutants are not phosphorylated on S16 or S63, suggesting that inhibition of phosphorylation on both S16 and S63 results in the strongest cell-cycle block.

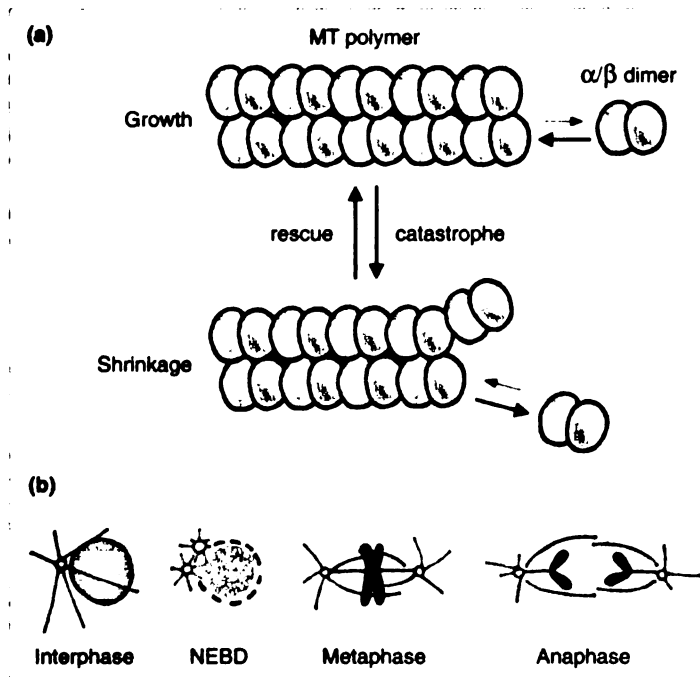


Figure 1

(a) Microtubule (MT) polymerization dynamics at both ends is described as dynamic instability. The polymer stochastically transits between periods of growth, where α/β tubulin dimers add onto the ends of the MT, and periods of shrinkage where subunits are lost. The transition from a period of growth to a period of shrinkage is called a 'catastrophe', and the transition from a period of shrinkage to growth is called a 'rescue'. Dramatic changes in MT polymer mass can therefore result from the modulation of catastrophe and rescue frequencies. (b) MT dynamics change throughout the cell cycle. These changes in MT dynamics are reflected by the changes in turnover^{1,5} and lengths^{2,6} of MT populations. The MTs of a PTK cell are schematized as follows: MTs with low turnover (stable MTs) are shown in green; MTs with rapid turnover are shown in red; DNA is shown in blue; the nuclear envelope in black. Abbreviation used: NEBD, nuclear envelope breakdown.

at nuclear envelope breakdown (NEBD) is thought to allow rapid disassembly of the interphase MT array and construction of the mitotic spindle. It is tempting to speculate that phosphorylations on S25 and S38 activate Op18/stathmin at NEBD; the phosphorylations on S16 and S63 might then inactivate or alter the activity of this protein on MTs at later stages of mitosis. At present, however, there is no evidence demonstrating that Op18/stathmin activity as a catastrophe factor is regulated by phosphorylation.

The identification of Op18/stathmin as a catastrophe factor might also explain the seemingly contradictory findings that both antisense RNA inhibition and overproduction of Op18/stathmin cause mitotic arrests. We know that mitotic cells monitor MT dynamics, and drugs that either stabilize or destabilize microtubules arrest cells in mitosis¹⁹. Therefore, if Op18/stathmin is acting as a regulator

of MT dynamics during mitosis, either an increase or decrease in its activity might result in a mitotic arrest. This hypothesis leads to the testable prediction that antisense inhibition of the expression of the gene encoding Op18/stathmin would lead to an increase in MT polymer, whereas overexpression would result in decreased polymer levels. The mitotic arrest phenotype of the serine mutants could similarly be explained if these mutants were active as catastrophe factors. These predictions can be tested by analysis of tubulin immunofluorescence in cells where the Op18/stathmin level and phosphorylation state have been manipulated: injection of fluorescently labeled tubulin will allow direct observation of MT dynamics and measurements of turnover rates. Overproduction of the S25,38A form of Op18/stathmin has been reported to prevent spindle formation in tissue culture¹¹, and

antibody depletion of Op18/stathmin in *Xenopus* extracts causes an increase in MT polymer mass. If future studies extend these observations *in vivo*, we might wish to consider renaming this protein. We would like to propose the name catastrophin.

Note added in proof

The overproduction of Op18/stathmin *in vivo* has recently been shown to cause a decrease in MT polymer levels (M. Gullberg, unpublished).

Acknowledgement

We thank A. Desai for helpful discussions and comments on the manuscript.

References

- 1 Sobel, A. (1991) *Trends Biochem. Sci.* 16, 301-305
- 2 Marklund, U. et al. (1993) *J. Biol. Chem.* 268, 25671-25680
- 3 Laodon, J., Nieves, E. and Schubart, U. K. (1992) *J. Biol. Chem.* 267, 3506-3513
- 4 Wang, Y. K. et al. (1993) *J. Biol. Chem.* 268, 14269-14277
- 5 Beretta, L., Dobransky, T. and Sobel, A. (1993) *J. Biol. Chem.* 268, 20076-20084
- 6 Marklund, U., Brattsand, G., Shingler, V. and Gullberg, M. (1993) *J. Biol. Chem.* 268, 15039-15047
- 7 Marklund, U. et al. (1994) *Eur. J. Biochem.* 225, 53-60
- 8 Strahler, J. R. et al. (1992) *Biochem. Biophys. Res. Commun.* 185, 197-203
- 9 Luo, X-N. et al. (1994) *J. Biol. Chem.* 269, 10312-10318
- 10 Brattsand, G. et al. (1994) *Eur. J. Biochem.* 220, 359-368
- 11 Marklund, U. et al. (1994) *J. Biol. Chem.* 269, 30626-30635
- 12 Larsson, N. et al. (1995) *J. Biol. Chem.* 270, 14175-14183
- 13 Mitchison, T. and Kirschner, M. (1984) *Nature* 312, 237-242
- 14 Saxton, W. M. et al. (1984) *J. Cell Biol.* 99, 2175-2186
- 15 Belmont, L. D., Hyman, A. A., Sawin, K. E. and Mitchison, T. J. (1990) *Cell* 62, 579-589
- 16 McNally, F. (1996) *Cur. Opin. Cell Biol.* 8, 23-29
- 17 Walczak, C. E., Mitchison, T. J. and Desai, A. (1996) *Cell* 84, 37-47
- 18 Belmont, L. D. and Mitchison, T. J. (1996) *Cell* 84, 623-631
- 19 Wilson, L. and Jordan, M. A. (1994) in *Microtubules* (Hyams, J. S. and Lloyd, C. W., eds.), pp. 59-83. Wiley-Liss
- 20 Mastroratte, D. N., McDonald, K. L., Ding, R. and McIntosh, J. R. (1993) *J. Cell Biol.* 123, 1475-1489

LISA BELMONT AND TIMOTHY MITCHISON

Department of Cellular and Molecular Pharmacology, University of California-San Francisco, San Francisco, CA 94143-0450, USA.

HEATHER W. DEACON

Department of Biochemistry and Biophysics, Box 0448, University of California-San Francisco, San Francisco, CA 94143-0448, USA.

9 APPENDIX 2: SUMMARY OF OP18 PROPERTIES

(published in Deacon et al., 1999)

10 APPENDIX 3: ENDOSOMAL MOTOR PROTEINS

Certain guesses as to the identity of the motor proteins responsible for endosomal vesicle movements can be made from our data. We wondered whether the “slow” movements of enlarged structures may represent actin based motility. Endosomes that contain B2AR are about four times faster than several types of actin-polymerization dependent movements of organelles in animal cells (Taunton et al., 2000; Wu et al., 1998). But another type of actin-dependent movement may be involved; motors in the myosin V family can move along actin at this rate (Mehta et al., 1999; Sakamoto et al., 2000; Tabb et al., 1998); in addition, vesicles moved by these motors move along tortuous paths *in vivo*, as our enlarged B2AR vesicles do. Frequent pauses occur when the myosin V motors bind to actin filaments. However, these slow movements are also the same speed as the movements of kinesin family members (Orozco et al., 1999; Vale and Fletterick, 1997) and a little slower than the movements of dynein (Howard, 1997); it bears mentioning that vesicle movements *in vivo* can be slowed by many factors. While the tortuous path indicates actin-based motility, their slow speed does help us narrow down the list of candidate motor proteins (Goldstein and Yang, 2000). This model predicts that depolymerization of actin filaments or inactivation of myosin V would decrease the frequency of pauses and increase the run length of small vesicles, and could therefore be tested by adding latrunculin to cells. Furthermore, it will be interesting to see if motors such as myosin V are restricted to the vesicular domain of tubulo-vesicular endosomes, in a similar fashion as Rab5 (Sonnichsen et al., 2000).

What motor is driving fast transport of B2AR particles, of up to 5 $\mu\text{m}/\text{sec}$? While speeds of up to 5 $\mu\text{m}/\text{sec}$ have been occasionally observed *in vivo*, no motor has been identified that operates at such fast speeds, and there is scant discussion in the literature on this topic. Organelle motors move at speeds no faster than about 1.25 $\mu\text{m}/\text{sec}$ (average) *in vitro* (Howard, 1997). However, these *in vitro* measurements are invariably performed at room temperature, and actual motor speeds may be higher *in vivo*. In addition, there may be endogenous factors *in vivo* that stimulate motility. The Unc104 family of motors is the fastest within the kinesin superfamily; they are required to move endosomes at a speed of 3 $\mu\text{m}/\text{sec}$ (average) in *Ustilago* (Wedlich-Soldner et al., 2002), and they can move *Dictyostelium* vesicles at a speed of 2.6 $\mu\text{m}/\text{sec}$ (average) *in vitro* (Pollock et al., 1999). However, motor speeds can vary from organism to organism (e.g. conventional kinesin from *Neurospora* moves at a speed of 2.5 $\mu\text{m}/\text{sec}$ *in vitro*; from mammals, this kinesin moves at 0.5 $\mu\text{m}/\text{sec}$) so it is not clear if these rates will be similar with human Unc104. Human Unc104 has a PH domain, which can bind to the phospholipid PI(4,5)P₂.

Fast organelle speeds can also be generated by the coordinated activity of multiple non-processive motors (Howard, 1997). Myosin I is a motor that can generate fast movements by the cooperation of multiple motors, and this motor has been located on tubules and vesicles that contain transferrin (Raposo et al., 1999). People generally assume that myosins cannot support long-range transport (greater than 2.5 μm) in most regions of the cell, because long actin structures can be composed of bundles of short actin filaments (about 0.8 μm) that have alternating polarity (Cramer et al., 1997). However, it should be appreciated that there are in fact many actin bundles with long

stretches of uniform polarity in migrating fibroblasts. However, these so-called “graded polarity” bundles appear to be specific to migrating cells, and are straight rather than curvy, therefore we do not believe that the fast vesicle movements we have observed are occurring on actin filaments.

Dynein is also a candidate for driving fast movement of B2AR particles. While so-called “cytoplasmic” dynein, an organelle motor, moves at a speed of 1.25 $\mu\text{m}/\text{sec}$ *in vitro* (Paschal et al., 1987), dynein can move particles 3.5 $\mu\text{m}/\text{sec}$ (average) in *Chlamydomonas* flagella. The *in vivo* speed of “cytoplasmic dynein,” which is an organelle motor, may be affected by the number of dyneins on a vesicle; multiple dyneins may be able to act co-operatively to generate faster speeds than individual motors under certain conditions, in an analogous fashion to myosin I (Howard, 1997; Mallik et al., 2004). Dynein is recruited to endosomes by active Rab7, which is in turn recruited to cholesterol-rich endosomes (Lebrand et al., 2002).

We propose that dynein is recruited to early endosomes by cholesterol. We surmise that when this motor is clustered on a small structure with low drag, such as a severed tubule multiple dyneins cooperate to move the structure with high speed. Because they have different motility properties, segregation of dynein and myosin V could therefore provide the force for separation of tubules, and associated receptors, from endosomes.

1. The
2. The
3. The
4. The
5. The
6. The
7. The
8. The
9. The
10. The

Details of the

1. The
2. The
3. The
4. The
5. The
6. The
7. The
8. The
9. The
10. The

11 BIBLIOGRAPHY

Abney, J.R., C.D. Meliza, B. Cutler, M. Kingma, J.E. Lochner, and B.A. Scalettar. 1999.

Real-time imaging of the dynamics of secretory granules in growth cones.

Biophys J. 77:2887-95.

Aguilar, R.C., and B. Wendland. 2003. Ubiquitin: not just for proteasomes anymore.

Curr Opin Cell Biol. 15:184-90.

Ahn, S., C.D. Nelson, T.R. Garrison, W.E. Miller, and R.J. Lefkowitz. 2003.

Desensitization, internalization, and signaling functions of beta-arrestins

demonstrated by RNA interference. *Proc Natl Acad Sci U S A.* 100:1740-4.

Albrecht, F.E., J. Xu, O.W. Moe, U. Hopfer, W.F. Simonds, J. Orlowski, and P.A. Jose.

2000. Regulation of NHE3 activity by G protein subunits in renal brush-border membranes. *Am J Physiol Regul Integr Comp Physiol.* 278:R1064-73.

Allen, R.D., J. Metzals, I. Tasaki, S.T. Brady, and S.P. Gilbert. 1982. Fast axonal

transport in squid giant axon. *Science.* 218:1127-9.

Altschuler, Y., S. Liu, L. Katz, K. Tang, S. Hardy, F. Brodsky, G. Apodaca, and K.

Mostov. 1999. ADP-ribosylation factor 6 and endocytosis at the apical surface of Madin-Darby canine kidney cells. *J Cell Biol.* 147:7-12.

Andersen, S.S., A.J. Ashford, R. Tournebize, O. Gavet, A. Sobel, A.A. Hyman, and E.

Karsenti. 1997. Mitotic chromatin regulates phosphorylation of Stathmin/Op18.

Nature. 389:640-3.

- Angers, S., A. Salahpour, and M. Bouvier. 2002. Dimerization: an emerging concept for G protein-coupled receptor ontogeny and function. *Annu Rev Pharmacol Toxicol.* 42:409-35.
- Apodaca, G., and K.E. Mostov. 1993. Transcytosis of placental alkaline phosphatase-polymeric immunoglobulin receptor fusion proteins is regulated by mutations of Ser664. *J Biol Chem.* 268:23712-9.
- Arnal, I., E. Karsenti, and A.A. Hyman. 2000. Structural transitions at microtubule ends correlate with their dynamic properties in *Xenopus* egg extracts. *J Cell Biol.* 149:767-74.
- Bananis, E., J.W. Murray, R.J. Stockert, P. Satir, and A.W. Wolkoff. 2000. Microtubule and motor-dependent endocytic vesicle sorting In vitro. *J Cell Biol.* 151:179-86.
- Barak, L.S., and M.G. Caron. 1995. Modeling of sequestration and down regulation in cells containing beta2-adrenergic receptors. *J Recept Signal Transduct Res.* 15:677-90.
- Barak, L.S., S.S. Ferguson, J. Zhang, C. Martenson, T. Meyer, and M.G. Caron. 1997. Internal trafficking and surface mobility of a functionally intact beta2-adrenergic receptor-green fluorescent protein conjugate. *Mol Pharmacol.* 51:177-84.
- Bean, B.P., M.C. Nowycky, and R.W. Tsien. 1984. Beta-adrenergic modulation of calcium channels in frog ventricular heart cells. *Nature.* 307:371-5.
- Bello-Reuss, E. 1980. Effect of catecholamines on fluid reabsorption by the isolated proximal convoluted tubule. *Am J Physiol.* 238:F347-52.
- Belmont, L., T. Mitchison, and H.W. Deacon. 1996. Catastrophic revelations about Op18/stathmin. *Trends Biochem Sci.* 21:197-8.

1. The first part of the document is a list of names and titles, including the names of the authors and the titles of their works. This list is organized in a structured manner, likely serving as a table of contents or a reference list for the document.

2. The second part of the document contains a series of numbered entries, each corresponding to a specific item or topic. These entries are arranged in a list format, providing a clear and organized overview of the content.

3. The third part of the document consists of a series of paragraphs, each discussing a different aspect of the subject matter. These paragraphs are written in a formal and academic style, providing detailed information and analysis.

4. The fourth part of the document is a series of footnotes or references, providing additional information and sources for the reader. These references are organized in a list format, following a standard academic convention.

5. The fifth part of the document is a series of appendices or supplementary material, providing additional data and information related to the main text. These appendices are organized in a list format, providing a clear and organized overview of the supplementary content.

- Belmont, L.D., A.A. Hyman, K.E. Sawin, and T.J. Mitchison. 1990. Real-time visualization of cell cycle-dependent changes in microtubule dynamics in cytoplasmic extracts. *Cell*. 62:579-89.
- Belmont, L.D., and T.J. Mitchison. 1996. Identification of a protein that interacts with tubulin dimers and increases the catastrophe rate of microtubules. *Cell*. 84:623-31.
- Bercovy, E. All About Erich. Vol. 2004.
- Besarab, A., P. Silva, L. Landsberg, and F.H. Epstein. 1977. Effect of catecholamines on tubular function in the isolated perfused rat kidney. *Am J Physiol*. 233:F39-45.
- Boivin, V., R. Jahns, S. Gambaryan, W. Ness, F. Boege, and M.J. Lohse. 2001. Immunofluorescent imaging of beta 1- and beta 2-adrenergic receptors in rat kidney. *Kidney Int*. 59:515-31.
- Bonifacino, J.S., and L.M. Traub. 2003. Signals for sorting of transmembrane proteins to endosomes and lysosomes. *Annu Rev Biochem*. 72:395-447.
- Bourne, H.R., and E.C. Meng. 2000. Structure. Rhodopsin sees the light. *Science*. 289:733-4.
- Bretscher, A., K. Edwards, and R.G. Fehon. 2002. ERM proteins and merlin: integrators at the cell cortex. *Nat Rev Mol Cell Biol*. 3:586-99.
- Breuer, A.C., P.A. Eagles, M.P. Lynn, M.B. Atkinson, S.P. Gilbert, L. Weber, J. Leatherman, and J.M. Hopkins. 1988. Long-term analysis of organelle translocation in isolated axoplasm of *Myxococcus xanthus*. *Cell Motil Cytoskeleton*. 10:391-9.

- Cao, T.T., H.W. Deacon, D. Reczek, A. Bretscher, and M. von Zastrow. 1999. A kinase-regulated PDZ-domain interaction controls endocytic sorting of the beta2-adrenergic receptor. *Nature*. 401:286-90.
- Cao, T.T., R.W. Mays, and M. von Zastrow. 1998. Regulated endocytosis of G-protein-coupled receptors by a biochemically and functionally distinct subpopulation of clathrin-coated pits. *J Biol Chem*. 273:24592-602.
- Carbone, R., S. Fre, G. Iannolo, F. Belleudi, P. Mancini, P.G. Pelicci, M.R. Torrisi, and P.P. Di Fiore. 1997. eps15 and eps15R are essential components of the endocytic pathway. *Cancer Res*. 57:5498-504.
- Carlton, J., M. Bujny, B.J. Peter, V.M. Oorschot, A. Rutherford, H. Mellor, J. Klumperman, H.T. McMahon, and P.J. Cullen. 2004. Sorting nexin-1 mediates tubular endosome-to-TGN transport through coincidence sensing of high-curvature membranes and 3-phosphoinositides. *Curr Biol*. 14:1791-800.
- Cassimeris, L. 2002. The oncoprotein 18/stathmin family of microtubule destabilizers. *Curr Opin Cell Biol*. 14:18-24.
- Cavenagh, M.M., J.A. Whitney, K. Carroll, C. Zhang, A.L. Boman, A.G. Rosenwald, I. Mellman, and R.A. Kahn. 1996. Intracellular distribution of Arf proteins in mammalian cells. Arf6 is uniquely localized to the plasma membrane. *J Biol Chem*. 271:21767-74.
- Chaturvedi, K., P. Bandari, N. Chinen, and R.D. Howells. 2001. Proteasome involvement in agonist-induced down-regulation of mu and delta opioid receptors. *J Biol Chem*. 276:12345-55.

- Chavrier, P., R.G. Parton, H.P. Hauri, K. Simons, and M. Zerial. 1990. Localization of low molecular weight GTP binding proteins to exocytic and endocytic compartments. *Cell*. 62:317-29.
- Chen-Izu, Y., R.P. Xiao, L.T. Izu, H. Cheng, M. Kuschel, H. Spurgeon, and E.G. Lakatta. 2000. G(i)-dependent localization of beta(2)-adrenergic receptor signaling to L-type Ca(2+) channels. *Biophys J*. 79:2547-56.
- Chung, K.-N., R. Roth, H. Morisaki, and J. Heuser. 1999. Dynamics of GFP/caveolin in living cells. *Molecular Biology of the Cell*. 10.
- Claing, A., W. Chen, W.E. Miller, N. Vitale, J. Moss, R.T. Premont, and R.J. Lefkowitz. 2001. beta-Arrestin-mediated ADP-ribosylation factor 6 activation and beta 2-adrenergic receptor endocytosis. *J Biol Chem*. 276:42509-13.
- Claing, A., S.J. Perry, M. Achiriloaie, J.K. Walker, J.P. Albanesi, R.J. Lefkowitz, and R.T. Premont. 2000. Multiple endocytic pathways of G protein-coupled receptors delineated by GIT1 sensitivity. *Proc Natl Acad Sci U S A*. 97:1119-24.
- Communal, C., K. Singh, D.B. Sawyer, and W.S. Colucci. 1999. Opposing effects of beta(1)- and beta(2)-adrenergic receptors on cardiac myocyte apoptosis : role of a pertussis toxin-sensitive G protein. *Circulation*. 100:2210-2.
- Confalonieri, S., A.E. Salcini, C. Puri, C. Tacchetti, and P.P. Di Fiore. 2000. Tyrosine phosphorylation of Eps15 is required for ligand-regulated, but not constitutive, endocytosis. *J Cell Biol*. 150:905-12.
- Cong, M., S.J. Perry, L.A. Hu, P.I. Hanson, A. Claing, and R.J. Lefkowitz. 2001a. Binding of the beta2 adrenergic receptor to N-ethylmaleimide-sensitive factor regulates receptor recycling. *J Biol Chem*. 276:45145-52.

1. The first part of the document is a list of names and titles of the members of the committee. The names are listed in alphabetical order, and each name is followed by a title or position. The list includes names such as John F. Kennedy, Lyndon B. Johnson, and Hubert H. Humphrey.

2. The second part of the document is a list of the names of the members of the committee who were present at the meeting. The names are listed in alphabetical order, and each name is followed by a title or position. The list includes names such as John F. Kennedy, Lyndon B. Johnson, and Hubert H. Humphrey.

- Cong, M., S.J. Perry, F.T. Lin, I.D. Fraser, L.A. Hu, W. Chen, J.A. Pitcher, J.D. Scott, and R.J. Lefkowitz. 2001b. Regulation of membrane targeting of the G protein-coupled receptor kinase 2 by protein kinase A and its anchoring protein AKAP79. *J Biol Chem.* 276:15192-9.
- Conner, D.A., M.A. Mathier, R.M. Mortensen, M. Christe, S.F. Vatner, C.E. Seidman, and J.G. Seidman. 1997. beta-Arrestin1 knockout mice appear normal but demonstrate altered cardiac responses to beta-adrenergic stimulation. *Circ Res.* 81:1021-6.
- Coppolino, M.G., C. Kong, M. Mohtashami, A.D. Schreiber, J.H. Brumell, B.B. Finlay, S. Grinstein, and W.S. Trimble. 2001. Requirement for N-ethylmaleimide-sensitive factor activity at different stages of bacterial invasion and phagocytosis. *J Biol Chem.* 276:4772-80.
- Cramer, L.P., M. Siebert, and T.J. Mitchison. 1997. Identification of novel graded polarity actin filament bundles in locomoting heart fibroblasts: implications for the generation of motile force. *J Cell Biol.* 136:1287-305.
- Curmi, P.A., S.S. Andersen, S. Lachkar, O. Gavet, E. Karsenti, M. Knossow, and A. Sobel. 1997. The stathmin/tubulin interaction in vitro. *J Biol Chem.* 272:25029-36.
- Daaka, Y., L.M. Luttrell, and R.J. Lefkowitz. 1997. Switching of the coupling of the beta2-adrenergic receptor to different G proteins by protein kinase A. *Nature.* 390:88-91.

- Dai, J., J. Li, E. Bos, M. Porcionatto, R.T. Premont, S. Bourgoïn, P.J. Peters, and V.W. Hsu. 2004. ACAP1 promotes endocytic recycling by recognizing recycling sorting signals. *Dev Cell*. 7:771-6.
- Daro, E., P. van der Sluijs, T. Galli, and I. Mellman. 1996. Rab4 and cellubrevin define different early endosome populations on the pathway of transferrin receptor recycling. *Proc Natl Acad Sci U S A*. 93:9559-64.
- Davare, M.A., V. Avdonin, D.D. Hall, E.M. Peden, A. Burette, R.J. Weinberg, M.C. Horne, T. Hoshi, and J.W. Hell. 2001. A beta2 adrenergic receptor signaling complex assembled with the Ca²⁺ channel Cav1.2. *Science*. 293:98-101.
- De Brabander, M., R. Nuydens, H. Geerts, and C.R. Hopkins. 1988. Dynamic behavior of the transferrin receptor followed in living epidermoid carcinoma (A431) cells with nanovid microscopy. *Cell Motil Cytoskeleton*. 9:30-47.
- de Wit, H., Y. Lichtenstein, R.B. Kelly, H.J. Geuze, J. Klumperman, and P. van der Sluijs. 2001. Rab4 regulates formation of synaptic-like microvesicles from early endosomes in PC12 cells. *Mol Biol Cell*. 12:3703-15.
- Deacon, H.W., T.J. Mitchison, and M. Gullberg. 1999. Op18/stathmin. *In* Guidebook to the Cytoskeletal and Motor Proteins. T. Kreis and R. Vale, editors. Oxford University Press, New York. 222-5.
- DeGraff, J.L., V.V. Gurevich, and J.L. Benovic. 2002. The third intracellular loop of alpha 2-adrenergic receptors determines subtype specificity of arrestin interaction. *J Biol Chem*. 277:43247-52.

1. The first part of the document discusses the importance of maintaining accurate records of all transactions and activities. It emphasizes the need for transparency and accountability in financial reporting.

2. The second part of the document outlines the various methods and techniques used to collect and analyze data. It includes a detailed description of the experimental procedures and the statistical tools employed.

- Desai, A., H.W. Deacon, C.E. Walczak, and T.J. Mitchison. 1997. A method that allows the assembly of kinetochore components onto chromosomes condensed in clarified *Xenopus* egg extracts. *Proc Natl Acad Sci U S A.* 94:12378-83.
- Desai, A., S. Verma, T.J. Mitchison, and C.E. Walczak. 1999. Kin I kinesins are microtubule-destabilizing enzymes. *Cell.* 96:69-78.
- Devic, E., Y. Xiang, D. Gould, and B. Kobilka. 2001. Beta-adrenergic receptor subtype-specific signaling in cardiac myocytes from beta(1) and beta(2) adrenoceptor knockout mice. *Mol Pharmacol.* 60:577-83.
- Di Paolo, G., B. Antonsson, D. Kassel, B.M. Riederer, and G. Grenningloh. 1997. Phosphorylation regulates the microtubule-destabilizing activity of stathmin and its interaction with tubulin. *FEBS Lett.* 416:149-52.
- Dixon, R.A., I.S. Sigal, E. Rands, R.B. Register, M.R. Candelore, A.D. Blake, and C.D. Strader. 1987. Ligand binding to the beta-adrenergic receptor involves its rhodopsin-like core. *Nature.* 326:73-7.
- Doyle, D.A., A. Lee, J. Lewis, E. Kim, M. Sheng, and R. MacKinnon. 1996. Crystal structures of a complexed and peptide-free membrane protein- binding domain: molecular basis of peptide recognition by PDZ. *Cell.* 85:1067-76.
- Dransfield, D.T., A.J. Bradford, J. Smith, M. Martin, C. Roy, P.H. Mangeat, and J.R. Goldenring. 1997. Ezrin is a cyclic AMP-dependent protein kinase anchoring protein. *Embo J.* 16:35-43.
- Duan, L., Y. Miura, M. Dimri, B. Majumder, I.L. Dodge, A.L. Reddi, A. Ghosh, N. Fernandes, P. Zhou, K. Mullane-Robinson, N. Rao, S. Donoghue, R.A. Rogers, D. Bowtell, M. Naramura, H. Gu, V. Band, and H. Band. 2003. Cbl-mediated

1. The first part of the document discusses the importance of maintaining accurate records of all transactions. It emphasizes that proper record-keeping is essential for the integrity of the financial system and for the ability to detect and prevent fraud.

2. The second part of the document outlines the specific procedures for recording transactions. It details the steps involved in the accounting cycle, from identifying the transaction to posting it to the appropriate ledger account.

- ubiquitylation is required for lysosomal sorting of epidermal growth factor receptor but is dispensable for endocytosis. *J Biol Chem.* 278:28950-60.
- Dunn, K.W., T.E. McGraw, and F.R. Maxfield. 1989. Iterative fractionation of recycling receptors from lysosomally destined ligands in an early sorting endosome. *J Cell Biol.* 109:3303-14.
- Durrbach, A., D. Louvard, and E. Coudrier. 1996. Actin filaments facilitate two steps of endocytosis. *J Cell Sci.* 109 (Pt 2):457-65.
- Dzimiri, N., P. Muiya, E. Andres, and Z. Al-Halees. 2004. Differential functional expression of human myocardial G protein receptor kinases in left ventricular cardiac diseases. *Eur J Pharmacol.* 489:167-77.
- Engelhardt, S., L. Hein, F. Wiesmann, and M.J. Lohse. 1999. Progressive hypertrophy and heart failure in beta1-adrenergic receptor transgenic mice. *Proc Natl Acad Sci U S A.* 96:7059-64.
- Fan, G., E. Shumay, C.C. Malbon, and H. Wang. 2001a. c-Src tyrosine kinase binds the beta 2-adrenergic receptor via phospho-Tyr-350, phosphorylates G-protein-linked receptor kinase 2, and mediates agonist-induced receptor desensitization. *J Biol Chem.* 276:13240-7.
- Fan, G., E. Shumay, H. Wang, and C.C. Malbon. 2001b. The scaffold protein gravin (cAMP-dependent protein kinase-anchoring protein 250) binds the beta 2-adrenergic receptor via the receptor cytoplasmic Arg-329 to Leu-413 domain and provides a mobile scaffold during desensitization. *J Biol Chem.* 276:24005-14.
- Ferguson, S.S. 2001. Evolving concepts in G protein-coupled receptor endocytosis: the role in receptor desensitization and signaling. *Pharmacol Rev.* 53:1-24.

2. The
3. The
4. The
5. The
6. The
7. The
8. The
9. The
10. The
11. The
12. The
13. The
14. The
15. The
16. The
17. The
18. The
19. The
20. The
21. The
22. The
23. The
24. The
25. The
26. The
27. The
28. The
29. The
30. The
31. The
32. The
33. The
34. The
35. The
36. The
37. The
38. The
39. The
40. The
41. The
42. The
43. The
44. The
45. The
46. The
47. The
48. The
49. The
50. The
51. The
52. The
53. The
54. The
55. The
56. The
57. The
58. The
59. The
60. The
61. The
62. The
63. The
64. The
65. The
66. The
67. The
68. The
69. The
70. The
71. The
72. The
73. The
74. The
75. The
76. The
77. The
78. The
79. The
80. The
81. The
82. The
83. The
84. The
85. The
86. The
87. The
88. The
89. The
90. The
91. The
92. The
93. The
94. The
95. The
96. The
97. The
98. The
99. The
100. The

- Ferguson, S.S., W.E. Downey, 3rd, A.M. Colapietro, L.S. Barak, L. Menard, and M.G. Caron. 1996. Role of beta-arrestin in mediating agonist-promoted G protein-coupled receptor internalization. *Science*. 271:363-6.
- Ferrell, J.E., Jr., and K.A. Cimprich. 2003. Enforced proximity in the function of a famous scaffold. *Mol Cell*. 11:289-91.
- Fischer, H., and T.E. Machen. 1996. The tyrosine kinase p60c-src regulates the fast gate of the cystic fibrosis transmembrane conductance regulator chloride channel. *Biophys J*. 71:3073-82.
- Fouassier, L., C.C. Yun, J.G. Fitz, and R.B. Doctor. 2000. Evidence for ezrin-radixin-moesin-binding phosphoprotein 50 (EBP50) self-association through PDZ-PDZ interactions. *J Biol Chem*. 275:25039-45.
- Fraser, I.D., M. Cong, J. Kim, E.N. Rollins, Y. Daaka, R.J. Lefkowitz, and J.D. Scott. 2000. Assembly of an A kinase-anchoring protein-beta(2)-adrenergic receptor complex facilitates receptor phosphorylation and signaling. *Curr Biol*. 10:409-12.
- Fredericks, Z.L., J.A. Pitcher, and R.J. Lefkowitz. 1996. Identification of the G protein-coupled receptor kinase phosphorylation sites in the human beta2-adrenergic receptor. *J Biol Chem*. 271:13796-803.
- Fujimoto, L.M., R. Roth, J.E. Heuser, and S.L. Schmid. 2000. Actin assembly plays a variable, but not obligatory role in receptor-mediated endocytosis in mammalian cells. *Traffic*. 1:161-71.
- Fukuto, H.S., D.M. Ferkey, A.J. Apicella, H. Lans, T. Sharmeen, W. Chen, R.J. Lefkowitz, G. Jansen, W.R. Schafer, and A.C. Hart. 2004. G protein-coupled

1. The first part of the document discusses the importance of maintaining accurate records of all transactions. This is essential for ensuring the integrity of the financial statements and for providing a clear audit trail.

2. The second part of the document outlines the various methods used to collect and analyze data. These methods include direct observation, interviews, and the use of specialized software tools.

- receptor kinase function is essential for chemosensation in *C. elegans*. *Neuron*. 42:581-93.
- Futter, C.E., A. Gibson, E.H. Allchin, S. Maxwell, L.J. Ruddock, G. Odorizzi, D. Domingo, I.S. Trowbridge, and C.R. Hopkins. 1998. In polarized MDCK cells basolateral vesicles arise from clathrin-gamma-adaptin-coated domains on endosomal tubules. *J Cell Biol.* 141:611-23.
- Gabilondo, A.M., J. Hegler, C. Krasel, V. Boivin-Jahns, L. Hein, and M.J. Lohse. 1997. A dileucine motif in the C terminus of the beta2-adrenergic receptor is involved in receptor internalization. *Proc Natl Acad Sci U S A.* 94:12285-90.
- Gage, R.M., K.A. Kim, T.T. Cao, and M. von Zastrow. 2001. A transplantable sorting signal that is sufficient to mediate rapid recycling of G protein-coupled receptors. *J Biol Chem.* 276:44712-20.
- Gage, R.M., E.A. Matveeva, S.W. Whiteheart, and M. von Zastrow. 2004. Type I PDZ ligands are sufficient to promote rapid recycling of G protein-coupled receptors independent of binding to NSF. *J Biol Chem.*
- Gaidarov, I., F. Santini, R.A. Warren, and J.H. Keen. 1999. Spatial control of coated-pit dynamics in living cells. *Nat Cell Biol.* 1:1-7.
- Gan, Y., T.E. McGraw, and E. Rodriguez-Boulau. 2002. The epithelial-specific adaptor AP1B mediates post-endocytic recycling to the basolateral membrane. *Nat Cell Biol.* 4:605-9.
- Gether, U. 2000. Uncovering molecular mechanisms involved in activation of G protein-coupled receptors. *Endocr Rev.* 21:90-113.

- Geuze, H.J., J.W. Slot, and A.L. Schwartz. 1987. Membranes of sorting organelles display lateral heterogeneity in receptor distribution. *J Cell Biol.* 104:1715-23.
- Ghosh, R.N., and F.R. Maxfield. 1995. Evidence for nonvectorial, retrograde transferrin trafficking in the early endosomes of HEP2 cells. *J Cell Biol.* 128:549-61.
- Gigant, B., P.A. Curmi, C. Martin-Barbey, E. Charbaut, S. Lachkar, L. Lebeau, S. Siavoshian, A. Sobel, and M. Knossow. 2000. The 4 A X-ray structure of a tubulin:stathmin-like domain complex. *Cell.* 102:809-16.
- Gillingham, A.K., and S. Munro. 2003. Long coiled-coil proteins and membrane traffic. *Biochim Biophys Acta.* 1641:71-85.
- Goldstein, L.S., and Z. Yang. 2000. Microtubule-based transport systems in neurons: the roles of kinesins and dyneins. *Annu Rev Neurosci.* 23:39-71.
- Goodman, O.B., Jr., J.G. Krupnick, F. Santini, V.V. Gurevich, R.B. Penn, A.W. Gagnon, J.H. Keen, and J.L. Benovic. 1996. Beta-arrestin acts as a clathrin adaptor in endocytosis of the beta2-adrenergic receptor. *Nature.* 383:447-50.
- Govindan, B., and R.D. Vale. 2000. Characterization of a microtubule assembly inhibitor from *Xenopus* oocytes. *Cell Motil Cytoskeleton.* 45:51-7.
- Gronholm, M., L. Vossebein, C.R. Carlson, J. Kuja-Panula, T. Teesalu, K. Alftan, A. Vaheri, H. Rauvala, F.W. Herberg, K. Tasken, and O. Carpen. 2003. Merlin links to the cAMP neuronal signaling pathway by anchoring the R1beta subunit of protein kinase A. *J Biol Chem.* 278:41167-72.
- Gurevich, V.V., S.B. Dion, J.J. Onorato, J. Ptasienski, C.M. Kim, R. Sterne-Marr, M.M. Hosey, and J.L. Benovic. 1995. Arrestin interactions with G protein-coupled receptors. Direct binding studies of wild type and mutant arrestins with rhodopsin,

beta 2-adrenergic, and m2 muscarinic cholinergic receptors. *J Biol Chem.* 270:720-31.

Gurevich, V.V., and E.V. Gurevich. 2004. The molecular acrobatics of arrestin activation. *Trends Pharmacol Sci.* 25:105-11.

Hall, R.A. 2004. Beta-adrenergic receptors and their interacting proteins. *Semin Cell Dev Biol.* 15:281-8.

Hall, R.A., L.S. Ostedgaard, R.T. Premont, J.T. Blitzer, N. Rahman, M.J. Welsh, and R.J. Lefkowitz. 1998a. A C-terminal motif found in the beta2-adrenergic receptor, P2Y1 receptor and cystic fibrosis transmembrane conductance regulator determines binding to the Na⁺/H⁺ exchanger regulatory factor family of PDZ proteins. *Proc Natl Acad Sci U S A.* 95:8496-501.

Hall, R.A., R.T. Premont, C.W. Chow, J.T. Blitzer, J.A. Pitcher, A. Claing, R.H. Stoffel, L.S. Barak, S. Shenolikar, E.J. Weinman, S. Grinstein, and R.J. Lefkowitz. 1998b. The beta2-adrenergic receptor interacts with the Na⁺/H⁺-exchanger regulatory factor to control Na⁺/H⁺ exchange. *Nature.* 392:626-30.

Hall, R.A., R.F. Spurney, R.T. Premont, N. Rahman, J.T. Blitzer, J.A. Pitcher, and R.J. Lefkowitz. 1999. G protein-coupled receptor kinase 6A phosphorylates the Na⁽⁺⁾/H⁽⁺⁾ exchanger regulatory factor via a PDZ domain-mediated interaction. *J Biol Chem.* 274:24328-34.

Hammond, A.T., and B.S. Glick. 2000. Raising the speed limits for 4D fluorescence microscopy. *Traffic.* 1:935-40.

- Harder, T., P. Scheiffele, P. Verkade, and K. Simons. 1998. Lipid domain structure of the plasma membrane revealed by patching of membrane components. *J Cell Biol.* 141:929-42.
- Hebert, T.E., S. Moffett, J.P. Morello, T.P. Loisel, D.G. Bichet, C. Barret, and M. Bouvier. 1996. A peptide derived from a beta2-adrenergic receptor transmembrane domain inhibits both receptor dimerization and activation. *J Biol Chem.* 271:16384-92.
- Heydorn, A., B.P. Sondergaard, N. Hadrup, B. Holst, C.R. Haft, and T.W. Schwartz. 2004. Distinct in vitro interaction pattern of dopamine receptor subtypes with adaptor proteins involved in post-endocytotic receptor targeting. *FEBS Lett.* 556:276-80.
- Hinck, L., I.S. Nathke, J. Papkoff, and W.J. Nelson. 1994. Dynamics of cadherin/catenin complex formation: novel protein interactions and pathways of complex assembly. *J Cell Biol.* 125:1327-40.
- Hirano, T., and T.J. Mitchison. 1991. Cell cycle control of higher-order chromatin assembly around naked DNA in vitro. *J Cell Biol.* 115:1479-89.
- Hirschberg, K., C.M. Miller, J. Ellenberg, J.F. Presley, E.D. Siggia, R.D. Phair, and J. Lippincott-Schwartz. 1998. Kinetic analysis of secretory protein traffic and characterization of golgi to plasma membrane transport intermediates in living cells. *J Cell Biol.* 143:1485-503.
- Hoffman, B. 2001. Catecholamines, Sympathomimetic Drugs, and Adrenergic Receptor Agonists. *In Goodman and Gilman's The Pharmacological Basis of Therapeutics.* J. Hardman and L. Limbird, editors. McGraw-Hill. 215-268.

- Holmfeldt, P., N. Larsson, B. Segerman, B. Howell, J. Morabito, L. Cassimeris, and M. Gullberg. 2001. The catastrophe-promoting activity of ectopic Op18/stathmin is required for disruption of mitotic spindles but not interphase microtubules. *Mol Biol Cell*. 12:73-83.
- Howard, J. 1997. Molecular motors: structural adaptations to cellular functions. *Nature*. 389:561-7.
- Howell, B., H. Deacon, and L. Cassimeris. 1999a. Decreasing oncoprotein 18/stathmin levels reduces microtubule catastrophes and increases microtubule polymer in vivo. *J Cell Sci*. 112 (Pt 21):3713-22.
- Howell, B., N. Larsson, M. Gullberg, and L. Cassimeris. 1999b. Dissociation of the tubulin-sequestering and microtubule catastrophe-promoting activities of oncoprotein 18/stathmin. *Mol Biol Cell*. 10:105-18.
- Huang, P., D. Steplock, E.J. Weinman, R.A. Hall, Z. Ding, J. Li, Y. Wang, and L.Y. Liu-Chen. 2004. kappa Opioid receptor interacts with Na(+)/H(+)-exchanger regulatory factor-1/Ezrin-radixin-moesin-binding phosphoprotein-50 (NHERF-1/EBP50) to stimulate Na(+)/H(+) exchange independent of G(i)/G(o) proteins. *J Biol Chem*. 279:25002-9.
- Huang, T., Y. You, M.S. Spoor, E.J. Richer, V.V. Kudva, R.C. Paige, M.P. Seiler, J.M. Liebler, J. Zabner, C.G. Plopper, and S.L. Brody. 2003. Foxj1 is required for apical localization of ezrin in airway epithelial cells. *J Cell Sci*. 116:4935-45.
- Hulme, E.C. 1990. Receptor binding studies, a brief outline. *In* Receptor-Effector Coupling, A Practical Approach. E.C. Hulme, editor. Oxford University Press, New York. 203-15.

- Innamorati, G., C. Le Gouill, M. Balamotis, and M. Birnbaumer. 2001. The long and the short cycle. Alternative intracellular routes for trafficking of G-protein-coupled receptors. *J Biol Chem.* 276:13096-103.
- Jamora, C., P.A. Takizawa, R.F. Zaarour, C. Denesvre, D.J. Faulkner, and V. Malhotra. 1997. Regulation of Golgi structure through heterotrimeric G proteins. *Cell.* 91:617-26.
- Jing, S.Q., T. Spencer, K. Miller, C. Hopkins, and I.S. Trowbridge. 1990. Role of the human transferrin receptor cytoplasmic domain in endocytosis: localization of a specific signal sequence for internalization. *J Cell Biol.* 110:283-94.
- Jordan, B.A., N. Trapaidze, I. Gomes, R. Nivarthi, and L.A. Devi. 2001. Oligomerization of opioid receptors with beta 2-adrenergic receptors: a role in trafficking and mitogen-activated protein kinase activation. *Proc Natl Acad Sci U S A.* 98:343-8.
- Jourdain, L., P. Curmi, A. Sobel, D. Pantaloni, and M.F. Carlier. 1997. Stathmin: a tubulin-sequestering protein which forms a ternary T2S complex with two tubulin molecules. *Biochemistry.* 36:10817-21.
- Juberg, E.N., K.P. Minneman, and P.W. Abel. 1985. beta1- and beta2-adrenoceptor binding and functional response in right atria and left atria of rat heart. *Naunyn-Schmiedeberg Arch. Pharmacol.* 330:199-202.
- Jung, H., R. Windhaber, D. Palm, and K.D. Schnackerz. 1996. Conformation of a beta-adrenoceptor-derived signal transducing peptide as inferred by circular dichroism and ¹H NMR spectroscopy. *Biochemistry.* 35:6399-405.

1. The first part of the document discusses the importance of maintaining accurate records of all transactions and activities. It emphasizes that this is crucial for ensuring transparency and accountability in the organization's operations.

2. The second part of the document outlines the various methods and tools used to collect and analyze data. It highlights the need for consistent and reliable data collection processes to support effective decision-making.

- Karoor, V., L. Wang, H.Y. Wang, and C.C. Malbon. 1998. Insulin stimulates sequestration of beta-adrenergic receptors and enhanced association of beta-adrenergic receptors with Grb2 via tyrosine 350. *J Biol Chem.* 273:33035-41.
- Keith, D.E., S.R. Murray, P.A. Zaki, P.C. Chu, D.V. Lissin, L. Kang, C.J. Evans, and M. von Zastrow. 1996. Morphine activates opioid receptors without causing their rapid internalization. *J Biol Chem.* 271:19021-4.
- Kim, O.J., B.R. Gardner, D.B. Williams, P.S. Marinec, D.M. Cabrera, J.D. Peters, C.C. Mak, K.M. Kim, and D.R. Sibley. 2004. The role of phosphorylation in D1 dopamine receptor desensitization: evidence for a novel mechanism of arrestin association. *J Biol Chem.* 279:7999-8010.
- Kim, Y.M., L.S. Barak, M.G. Caron, and J.L. Benovic. 2002. Regulation of arrestin-3 phosphorylation by casein kinase II. *J Biol Chem.* 277:16837-46.
- King, R.W. 1999. Chemistry or biology: which comes first after the genome is sequenced? *Chem Biol.* 6:R327-33.
- Klebes, A., B. Biehs, F. Cifuentes, and T.B. Kornberg. 2002. Expression profiling of *Drosophila* imaginal discs. *Genome Biol.* 3:RESEARCH0038.
- Klein, U., M.T. Ramirez, B.K. Kobilka, and M. von Zastrow. 1997. A novel interaction between adrenergic receptors and the alpha-subunit of eukaryotic initiation factor 2B. *J Biol Chem.* 272:19099-102.
- Klein-Seetharaman, J., J. Hwa, K. Cai, C. Altenbach, W.L. Hubbell, and H.G. Khorana. 2001. Probing the dark state tertiary structure in the cytoplasmic domain of rhodopsin: proximities between amino acids deduced from spontaneous disulfide

- bond formation between Cys316 and engineered cysteines in cytoplasmic loop 1. *Biochemistry*. 40:12472-8.
- Ko, D.C., M.D. Gordon, J.Y. Jin, and M.P. Scott. 2001. Dynamic movements of organelles containing Niemann-Pick C1 protein: NPC1 involvement in late endocytic events. *Mol Biol Cell*. 12:601-14.
- Kobilka, B. 1992. Adrenergic receptors as models for G protein-coupled receptors. *Annu Rev Neurosci*. 15:87-114.
- Koch, W.J., C.A. Milano, and R.J. Lefkowitz. 1996. Transgenic manipulation of myocardial G protein-coupled receptors and receptor kinases. *Circ Res*. 78:511-6.
- Koch, W.J., H.A. Rockman, P. Samama, R.A. Hamilton, R.A. Bond, C.A. Milano, and R.J. Lefkowitz. 1995. Cardiac function in mice overexpressing the beta-adrenergic receptor kinase or a beta ARK inhibitor. *Science*. 268:1350-3.
- Koenig, J.A., and J.M. Edwardson. 1996. Intracellular trafficking of the muscarinic acetylcholine receptor: importance of subtype and cell type. *Mol Pharmacol*. 49:351-9.
- Koenig, J.A., and J.M. Edwardson. 1997. Endocytosis and recycling of G protein-coupled receptors. *Trends Pharmacol Sci*. 18:276-87.
- Koenig, J.A., J.M. Edwardson, and P.P. Humphrey. 1997. Somatostatin receptors in Neuro2A neuroblastoma cells: ligand internalization. *Br J Pharmacol*. 120:52-9.
- Kohout, T.A., F.S. Lin, S.J. Perry, D.A. Conner, and R.J. Lefkowitz. 2001. beta-Arrestin 1 and 2 differentially regulate heptahelical receptor signaling and trafficking. *Proc Natl Acad Sci U S A*. 98:1601-6.

- Krueger, K.M., Y. Daaka, J.A. Pitcher, and R.J. Lefkowitz. 1997. The role of sequestration in G protein-coupled receptor resensitization. Regulation of beta2-adrenergic receptor dephosphorylation by vesicular acidification. *J Biol Chem.* 272:5-8.
- Krupnick, J.G., and J.L. Benovic. 1998. The role of receptor kinases and arrestins in G protein-coupled receptor regulation. *Annu Rev Pharmacol Toxicol.* 38:289-319.
- Krupnick, J.G., O.B. Goodman, Jr., J.H. Keen, and J.L. Benovic. 1997. Arrestin/clathrin interaction. Localization of the clathrin binding domain of nonvisual arrestins to the carboxy terminus. *J Biol Chem.* 272:15011-6.
- Kudo, K., Y. Kondo, K. Abe, Y. Igarashi, K. Tada, and K. Yoshinaga. 1991. Evidence for presence of functional beta-adrenoceptor in rabbit S2 proximal straight tubules. *Am J Physiol.* 261:F393-9.
- Kuntziger, T., O. Gavet, V. Manceau, A. Sobel, and M. Bornens. 2001. Stathmin/Op18 phosphorylation is regulated by microtubule assembly. *Mol Biol Cell.* 12:437-48.
- Lackie, J.M. 1986. *Cell Movement and Cell Behavior.* Allen & Unwin.
- LaJeunesse, D.R., B.M. McCartney, and R.G. Fehon. 1998. Structural analysis of *Drosophila* merlin reveals functional domains important for growth control and subcellular localization. *J Cell Biol.* 141:1589-99.
- Lamaze, C., L.M. Fujimoto, H.L. Yin, and S.L. Schmid. 1997. The actin cytoskeleton is required for receptor-mediated endocytosis in mammalian cells. *J Biol Chem.* 272:20332-5.

1. The first part of the document discusses the importance of maintaining accurate records of all transactions and activities. It emphasizes that this is crucial for ensuring transparency and accountability in the organization's operations.

2. The second part of the document outlines the various methods and tools used to collect and analyze data. It highlights the need for consistent and reliable data collection processes to support informed decision-making.

- Lampson, M.A., J. Schmoranzer, A. Zeigerer, S.M. Simon, and T.E. McGraw. 2001. Insulin-regulated release from the endosomal recycling compartment is regulated by budding of specialized vesicles. *Mol Biol Cell*. 12:3489-501.
- Lanthier, J., A. Bouthillier, M. Lapointe, M. Demeule, R. Beliveau, and R.R. Desrosiers. 2002. Down-regulation of protein L-isoaspartyl methyltransferase in human epileptic hippocampus contributes to generation of damaged tubulin. *J Neurochem*. 83:581-91.
- Laporte, S.A., W.E. Miller, K.M. Kim, and M.G. Caron. 2002. beta-Arrestin/AP-2 interaction in G protein-coupled receptor internalization: identification of a beta-arrestin binding site in beta 2-adaptin. *J Biol Chem*. 277:9247-54.
- Laporte, S.A., R.H. Oakley, J.A. Holt, L.S. Barak, and M.G. Caron. 2000. The interaction of beta-arrestin with the AP-2 adaptor is required for the clustering of beta 2-adrenergic receptor into clathrin-coated pits. *J Biol Chem*. 275:23120-6.
- Larsson, N., B. Segerman, B. Howell, K. Fridell, L. Cassimeris, and M. Gullberg. 1999. Op18/stathmin mediates multiple region-specific tubulin and microtubule-regulating activities. *J Cell Biol*. 146:1289-302.
- Lasek, R.J., J.A. Garner, and S.T. Brady. 1984. Axonal transport of the cytoplasmic matrix. *J Cell Biol*. 99:212s-221s.
- Lau, A.G., and R.A. Hall. 2001. Oligomerization of NHERF-1 and NHERF-2 PDZ domains: differential regulation by association with receptor carboxyl-termini and by phosphorylation. *Biochemistry*. 40:8572-80.

- Lebrand, C., M. Corti, H. Goodson, P. Cosson, V. Cavalli, N. Mayran, J. Faure, and J. Gruenberg. 2002. Late endosome motility depends on lipids via the small GTPase Rab7. *Embo J.* 21:1289-300.
- Lefkowitz, R.J. 1998. G protein-coupled receptors. III. New roles for receptor kinases and beta-arrestins in receptor signaling and desensitization. *J Biol Chem.* 273:18677-80.
- LeJemtel, T., E. Sonnenblick, and W. Frishman. 2001. Diagnosis and Management of Heart Failure. *In* Hurst's The Heart. Vol. 1. V. Furster, R. Alexander, and R. O'Rourke, editors. McGraw-Hill. 687-750.
- Li, M., J.C. Bermak, Z.W. Wang, and Q.Y. Zhou. 2000. Modulation of dopamine D(2) receptor signaling by actin-binding protein (ABP-280). *Mol Pharmacol.* 57:446-52.
- Liggett, S.B., M.G. Caron, R.J. Lefkowitz, and M. Hnatowich. 1991. Coupling of a mutated form of the human beta 2-adrenergic receptor to Gi and Gs. Requirement for multiple cytoplasmic domains in the coupling process. *J Biol Chem.* 266:4816-21.
- Lin, F., H. Wang, and C.C. Malbon. 2000. Gravin-mediated formation of signaling complexes in beta 2-adrenergic receptor desensitization and resensitization. *J Biol Chem.* 275:19025-34.
- Lin, F.T., K.M. Krueger, H.E. Kendall, Y. Daaka, Z.L. Fredericks, J.A. Pitcher, and R.J. Lefkowitz. 1997. Clathrin-mediated endocytosis of the beta-adrenergic receptor is regulated by phosphorylation/dephosphorylation of beta-arrestin1. *J Biol Chem.* 272:31051-7.

- Lin, F.T., W.E. Miller, L.M. Luttrell, and R.J. Lefkowitz. 1999. Feedback regulation of beta-arrestin1 function by extracellular signal-regulated kinases. *J Biol Chem.* 274:15971-4.
- Liu, F.Y., and M.G. Cogan. 1989. Angiotensin II stimulates early proximal bicarbonate absorption in the rat by decreasing cyclic adenosine monophosphate. *J Clin Invest.* 84:83-91.
- Lohse, M.J., S. Engelhardt, and T. Eschenhagen. 2003. What is the role of beta-adrenergic signaling in heart failure? *Circ Res.* 93:896-906.
- Luttrell, L.M., S.S. Ferguson, Y. Daaka, W.E. Miller, S. Maudsley, G.J. Della Rocca, F. Lin, H. Kawakatsu, K. Owada, D.K. Luttrell, M.G. Caron, and R.J. Lefkowitz. 1999. Beta-arrestin-dependent formation of beta2 adrenergic receptor-Src protein kinase complexes. *Science.* 283:655-61.
- Macia, E., F. Luton, M. Partisani, J. Cherfils, P. Chardin, and M. Franco. 2004. The GDP-bound form of Arf6 is located at the plasma membrane. *J Cell Sci.* 117:2389-98.
- Mallik, R., B.C. Carter, S.A. Lex, S.J. King, and S.P. Gross. 2004. Cytoplasmic dynein functions as a gear in response to load. *Nature.* 427:649-52.
- Marklund, U., O. Osterman, H. Melander, A. Bergh, and M. Gullberg. 1994. The phenotype of a "Cdc2 kinase target site-deficient" mutant of oncoprotein 18 reveals a role of this protein in cell cycle control. *J Biol Chem.* 269:30626-35.
- Marsh, E.W., P.L. Leopold, N.L. Jones, and F.R. Maxfield. 1995. Oligomerized transferrin receptors are selectively retained by a luminal sorting signal in a long-lived endocytic recycling compartment. *J Cell Biol.* 129:1509-22.

1. The first part of the document discusses the importance of maintaining accurate records of all transactions. It emphasizes that proper record-keeping is essential for the integrity of the financial system and for the ability to detect and prevent fraud.

2. The second part of the document outlines the specific requirements for record-keeping, including the need to maintain original documents and to ensure that all records are accessible and retrievable. It also discusses the importance of regular audits and the role of internal controls in ensuring the accuracy of the records.

- Marullo, S., V. Faundez, and R.B. Kelly. 1999. Beta 2-adrenergic receptor endocytic pathway is controlled by a saturable mechanism distinct from that of transferrin receptor. *Receptors Channels*. 6:255-69.
- Matteoni, R., and T.E. Kreis. 1987. Translocation and clustering of endosomes and lysosomes depends on microtubules. *J Cell Biol*. 105:1253-65.
- Maucuer, A., J. Moreau, M. Mechali, and A. Sobel. 1993. Stathmin gene family: phylogenetic conservation and developmental regulation in *Xenopus*. *J Biol Chem*. 268:16420-9.
- Maudsley, S., A.M. Zamah, N. Rahman, J.T. Blitzer, L.M. Luttrell, R.J. Lefkowitz, and R.A. Hall. 2000. Platelet-derived growth factor receptor association with Na(+)/H(+) exchanger regulatory factor potentiates receptor activity. *Mol Cell Biol*. 20:8352-63.
- Maxfield, F.R., and T.E. McGraw. 2004. Endocytic recycling. *Nat Rev Mol Cell Biol*. 5:121-32.
- Mayor, S., J.F. Presley, and F.R. Maxfield. 1993. Sorting of membrane components from endosomes and subsequent recycling to the cell surface occurs by a bulk flow process. *J Cell Biol*. 121:1257-69.
- McCabe, J.B., and L.G. Berthiaume. 2001. N-terminal protein acylation confers localization to cholesterol, sphingolipid-enriched membranes but not to lipid rafts/caveolae. *Mol Biol Cell*. 12:3601-17.
- McCaffrey, M.W., A. Bielli, G. Cantalupo, S. Mora, V. Roberti, M. Santillo, F. Drummond, and C. Bucci. 2001. Rab4 affects both recycling and degradative endosomal trafficking. *FEBS Lett*. 495:21-30.

1. The first part of the document discusses the importance of maintaining accurate records of all transactions and activities. It emphasizes that this is crucial for ensuring transparency and accountability in the organization's operations.

2. The second part of the document outlines the various methods and tools used to collect and analyze data. It highlights the need for consistent and reliable data collection processes to support effective decision-making and strategic planning.

- McDonald, P.H., N.L. Cote, F.T. Lin, R.T. Premont, J.A. Pitcher, and R.J. Lefkowitz. 1999. Identification of NSF as a beta-arrestin1-binding protein. Implications for beta2-adrenergic receptor regulation. *J Biol Chem.* 274:10677-80.
- Mehta, A.D., R.S. Rock, M. Rief, J.A. Spudich, M.S. Mooseker, and R.E. Cheney. 1999. Myosin-V is a processive actin-based motor. *Nature.* 400:590-3.
- Mellman, I. 1996. Endocytosis and molecular sorting. *Annu Rev Cell Dev Biol.* 12:575-625.
- Menard, L., S.S. Ferguson, J. Zhang, F.T. Lin, R.J. Lefkowitz, M.G. Caron, and L.S. Barak. 1997. Synergistic regulation of beta2-adrenergic receptor sequestration: intracellular complement of beta-adrenergic receptor kinase and beta-arrestin determine kinetics of internalization. *Mol Pharmacol.* 51:800-8.
- Meng, E.C., and H.R. Bourne. 2001. Receptor activation: what does the rhodopsin structure tell us? *Trends Pharmacol Sci.* 22:587-93.
- Meurer-Grob, P., J. Kasparian, and R.H. Wade. 2001. Microtubule structure at improved resolution. *Biochemistry.* 40:8000-8.
- Michaely, P.A., C. Mineo, Y.S. Ying, and R.G. Anderson. 1999. Polarized distribution of endogenous Rac1 and RhoA at the cell surface. *J Biol Chem.* 274:21430-6.
- Michel, J.J., and J.D. Scott. 2002. AKAP mediated signal transduction. *Annu Rev Pharmacol Toxicol.* 42:235-57.
- Moe, O.W. 1999. Acute regulation of proximal tubule apical membrane Na/H exchanger NHE-3: role of phosphorylation, protein trafficking, and regulatory factors. *J Am Soc Nephrol.* 10:2412-25.

- Moe, O.W., M. Amemiya, and Y. Yamaji. 1995. Activation of protein kinase A acutely inhibits and phosphorylates Na/H exchanger NHE-3. *J Clin Invest.* 96:2187-94.
- Mohler, P.J., S.M. Kreda, R.C. Boucher, M. Sudol, M.J. Stutts, and S.L. Milgram. 1999. Yes-associated protein 65 localizes p62(c-Yes) to the apical compartment of airway epithelia by association with EBP50. *J Cell Biol.* 147:879-90.
- Mohrmann, K., R. Leijendekker, L. Gerez, and P. van Der Sluijs. 2002. rab4 regulates transport to the apical plasma membrane in Madin-Darby canine kidney cells. *J Biol Chem.* 277:10474-81.
- Montixi, C., C. Langlet, A.M. Bernard, J. Thimonier, C. Dubois, M.A. Wurbel, J.P. Chauvin, M. Pierres, and H.T. He. 1998. Engagement of T cell receptor triggers its recruitment to low-density detergent-insoluble membrane domains. *Embo J.* 17:5334-48.
- Moore, R.H., H.S. Hall, J.L. Rosenfeld, W. Dai, and B.J. Knoll. 1999a. Specific changes in beta2-adrenoceptor trafficking kinetics and intracellular sorting during downregulation. *Eur J Pharmacol.* 369:113-23.
- Moore, R.H., E.E. Millman, E. Alpizar-Foster, W. Dai, and B.J. Knoll. 2004. Rab11 regulates the recycling and lysosome targeting of {beta}2-adrenergic receptors. *J Cell Sci.* 117:3107-3117.
- Moore, R.H., N. Sadovnikoff, S. Hoffenberg, S. Liu, P. Woodford, K. Angelides, J.A. Trial, N.D. Carsrud, B.F. Dickey, and B.J. Knoll. 1995. Ligand-stimulated beta 2-adrenergic receptor internalization via the constitutive endocytic pathway into rab5-containing endosomes. *J Cell Sci.* 108 (Pt 9):2983-91.

- Moore, R.H., A. Tuffaha, E.E. Millman, W. Dai, H.S. Hall, B.F. Dickey, and B.J. Knoll. 1999b. Agonist-induced sorting of human beta2-adrenergic receptors to lysosomes during downregulation. *J Cell Sci.* 112 (Pt 3):329-38.
- Moritz, M., Y. Zheng, B.M. Alberts, and K. Oegema. 1998. Recruitment of the gamma-tubulin ring complex to Drosophila salt-stripped centrosome scaffolds. *J Cell Biol.* 142:775-86.
- Moskowitz, H.S., J. Heuser, T.E. McGraw, and T.A. Ryan. 2003. Targeted chemical disruption of clathrin function in living cells. *Mol Biol Cell.* 14:4437-47.
- Mu, F.T., J.M. Callaghan, O. Steele-Mortimer, H. Stenmark, R.G. Parton, P.L. Campbell, J. McCluskey, J.P. Yeo, E.P. Tock, and B.H. Toh. 1995. EEA1, an early endosome-associated protein. EEA1 is a conserved alpha-helical peripheral membrane protein flanked by cysteine "fingers" and contains a calmodulin-binding IQ motif. *J Biol Chem.* 270:13503-11.
- Mukherjee, S., V.V. Gurevich, A. Preninger, H.E. Hamm, M.F. Bader, A.T. Fazleabas, L. Birnbaumer, and M. Hunzicker-Dunn. 2002. Aspartic acid 564 in the third cytoplasmic loop of the luteinizing hormone/choriogonadotropin receptor is crucial for phosphorylation-independent interaction with arrestin2. *J Biol Chem.* 277:17916-27.
- Muller, D.R., P. Schindler, H. Towbin, U. Wirth, H. Voshol, S. Hoving, and M.O. Steinmetz. 2001. Isotope-tagged cross-linking reagents. A new tool in mass spectrometric protein interaction analysis. *Anal Chem.* 73:1927-34.

- Mundell, S.J., R.P. Loudon, and J.L. Benovic. 1999. Characterization of G protein-coupled receptor regulation in antisense mRNA-expressing cells with reduced arrestin levels. *Biochemistry*. 38:8723-32.
- Murk, J.L., B.M. Humbel, U. Ziese, J.M. Griffith, G. Posthuma, J.W. Slot, A.J. Koster, A.J. Verkleij, H.J. Geuze, and M.J. Kleijmeer. 2003. Endosomal compartmentalization in three dimensions: implications for membrane fusion. *Proc Natl Acad Sci U S A*. 100:13332-7.
- Murray, A.W. 1991. Cell cycle extracts. *Methods Cell Biol*. 36:581-605.
- Murthy, A., C. Gonzalez-Agosti, E. Cordero, D. Pinney, C. Candia, F. Solomon, J. Gusella, and V. Ramesh. 1998. NHE-RF, a regulatory cofactor for Na(+)-H+ exchange, is a common interactor for merlin and ERM (MERM) proteins. *J Biol Chem*. 273:1273-6.
- Musch, A., D. Cohen, and E. Rodriguez-Boulan. 1997. Myosin II is involved in the production of constitutive transport vesicles from the TGN. *J Cell Biol*. 138:291-306.
- Naren, A.P., B. Cobb, C. Li, K. Roy, D. Nelson, G.D. Heda, J. Liao, K.L. Kirk, E.J. Sorscher, J. Hanrahan, and J.P. Clancy. 2003. A macromolecular complex of beta 2 adrenergic receptor, CFTR, and ezrin/radixin/moesin-binding phosphoprotein 50 is regulated by PKA. *Proc Natl Acad Sci U S A*. 100:342-6.
- Neer, E.J., and T.F. Smith. 1996. G protein heterodimers: new structures propel new questions. *Cell*. 84:175-8.
- Nguyen, R., D. Reczek, and A. Bretscher. 2001. Hierarchy of merlin and ezrin N- and C-terminal domain interactions in homo- and heterotypic associations and their

relationship to binding of scaffolding proteins EBP50 and E3KARP. *J Biol Chem.* 276:7621-9.

Nie, Z., D.S. Hirsch, and P.A. Randazzo. 2003. Arf and its many interactors. *Curr Opin Cell Biol.* 15:396-404.

O'Dowd, B.F., M. Hnatowich, M.G. Caron, R.J. Lefkowitz, and M. Bouvier. 1989.

Palmitoylation of the human beta 2-adrenergic receptor. Mutation of Cys341 in the carboxyl tail leads to an uncoupled nonpalmitoylated form of the receptor. *J Biol Chem.* 264:7564-9.

Oakley, R.H., S.A. Laporte, J.A. Holt, M.G. Caron, and L.S. Barak. 2000. Differential affinities of visual arrestin, beta arrestin1, and beta arrestin2 for G protein-coupled receptors delineate two major classes of receptors. *J Biol Chem.* 275:17201-10.

Obremski, V.J., A.M. Hall, and C. Fernandez-Valle. 1998. Merlin, the neurofibromatosis type 2 gene product, and beta1 integrin associate in isolated and differentiating Schwann cells. *J Neurobiol.* 37:487-501.

Odde, D.J., L. Ma, A.H. Briggs, A. DeMarco, and M.W. Kirschner. 1999. Microtubule bending and breaking in living fibroblast cells. *J Cell Sci.* 112 (Pt 19):3283-8.

Odley, A., H.S. Hahn, R.A. Lynch, Y. Marreez, H. Osinska, J. Robbins, and G.W. Dorn, 2nd. 2004. Regulation of cardiac contractility by Rab4-modulated beta2-adrenergic receptor recycling. *Proc Natl Acad Sci U S A.* 101:7082-7.

Odorizzi, G., and I.S. Trowbridge. 1997. Structural requirements for basolateral sorting of the human transferrin receptor in the biosynthetic and endocytic pathways of Madin-Darby canine kidney cells. *J Cell Biol.* 137:1255-64.

Orozco, J.T., K.P. Wedaman, D. Signor, H. Brown, L. Rose, and J.M. Scholey. 1999.

Movement of motor and cargo along cilia. *Nature*. 398:674.

Ostrom, R.S., C. Gregorian, R.M. Drenan, Y. Xiang, J.W. Regan, and P.A. Insel. 2001.

Receptor number and caveolar co-localization determine receptor coupling efficiency to adenylyl cyclase. *J Biol Chem*. 276:42063-9.

Ostrowski, J., M.A. Kjelsberg, M.G. Caron, and R.J. Lefkowitz. 1992. Mutagenesis of

the beta 2-adrenergic receptor: how structure elucidates function. *Annu Rev Pharmacol Toxicol*. 32:167-83.

Palczewski, K., T. Kumasaka, T. Hori, C.A. Behnke, H. Motoshima, B.A. Fox, I. Le

Trong, D.C. Teller, T. Okada, R.E. Stenkamp, M. Yamamoto, and M. Miyano.

2000. Crystal structure of rhodopsin: A G protein-coupled receptor. *Science*.

289:739-45.

Parsons, S.F., and E.D. Salmon. 1997. Microtubule assembly in clarified *Xenopus* egg

extracts. *Cell Motil Cytoskeleton*. 36:1-11.

Paschal, B.M., H.S. Shpetner, and R.B. Vallee. 1987. MAP 1C is a microtubule-activated

ATPase which translocates microtubules in vitro and has dynein-like properties. *J*

Cell Biol. 105:1273-82.

Peters, P.J., V.W. Hsu, C.E. Ooi, D. Finazzi, S.B. Teal, V. Oorschot, J.G. Donaldson, and

R.D. Klausner. 1995. Overexpression of wild-type and mutant ARF1 and ARF6:

distinct perturbations of nonoverlapping membrane compartments. *J Cell Biol*.

128:1003-17.

- Pippig, S., S. Andexinger, K. Daniel, M. Puzicha, M.G. Caron, R.J. Lefkowitz, and M.J. Lohse. 1993. Overexpression of beta-arrestin and beta-adrenergic receptor kinase augment desensitization of beta 2-adrenergic receptors. *J Biol Chem.* 268:3201-8.
- Pippig, S., S. Andexinger, and M.J. Lohse. 1995. Sequestration and recycling of beta 2-adrenergic receptors permit receptor resensitization. *Mol Pharmacol.* 47:666-76.
- Pitcher, J.A., N.J. Freedman, and R.J. Lefkowitz. 1998a. G protein-coupled receptor kinases. *Annu Rev Biochem.* 67:653-92.
- Pitcher, J.A., R.A. Hall, Y. Daaka, J. Zhang, S.S. Ferguson, S. Hester, S. Miller, M.G. Caron, R.J. Lefkowitz, and L.S. Barak. 1998b. The G protein-coupled receptor kinase 2 is a microtubule-associated protein kinase that phosphorylates tubulin. *J Biol Chem.* 273:12316-24.
- Pollock, N., E.L. de Hostos, C.W. Turck, and R.D. Vale. 1999. Reconstitution of membrane transport powered by a novel dimeric kinesin motor of the Unc104/KIF1A family purified from Dictyostelium. *J Cell Biol.* 147:493-506.
- Presley, J.F., S. Mayor, T.E. McGraw, K.W. Dunn, and F.R. Maxfield. 1997. Bafilomycin A1 treatment retards transferrin receptor recycling more than bulk membrane recycling. *J Biol Chem.* 272:13929-36.
- Qualmann, B., M.M. Kessels, and R.B. Kelly. 2000. Molecular links between endocytosis and the actin cytoskeleton. *J Cell Biol.* 150:F111-6.
- Radeke, H.S., C.A. Digits, R.L. Casaubon, and M.L. Snapper. 1999. Interactions of (-)-ilimaquinone with methylation enzymes: implications for vesicular-mediated secretion. *Chem Biol.* 6:639-47.

1. The first part of the document discusses the importance of maintaining accurate records of all transactions. It emphasizes that proper record-keeping is essential for the integrity of the financial system and for the ability to detect and prevent fraud.

2. The second part of the document outlines the specific procedures for recording transactions. It details the steps involved in the accounting cycle, from identifying the transaction to posting it to the appropriate ledger account.

- Radeke, H.S., and M.L. Snapper. 1998. Photoaffinity study of the cellular interactions of ilimaquinone. *Bioorg Med Chem.* 6:1227-32.
- Raiborg, C., K.G. Bache, D.J. Gillooly, I.H. Madshus, E. Stang, and H. Stenmark. 2002. Hrs sorts ubiquitinated proteins into clathrin-coated microdomains of early endosomes. *Nat Cell Biol.* 4:394-8.
- Raiborg, C., K.G. Bache, A. Mehlum, E. Stang, and H. Stenmark. 2001. Hrs recruits clathrin to early endosomes. *Embo J.* 20:5008-21.
- Raiborg, C., T.E. Rusten, and H. Stenmark. 2003. Protein sorting into multivesicular endosomes. *Curr Opin Cell Biol.* 15:446-55.
- Raposo, G., M.N. Cordonnier, D. Tenza, B. Menichi, A. Durrbach, D. Louvard, and E. Coudrier. 1999. Association of myosin I alpha with endosomes and lysosomes in mammalian cells. *Mol Biol Cell.* 10:1477-94.
- Ravelli, R.B., B. Gigant, P.A. Curmi, I. Jourdain, S. Lachkar, A. Sobel, and M. Knossow. 2004. Insight into tubulin regulation from a complex with colchicine and a stathmin-like domain. *Nature.* 428:198-202.
- Rebhun, L.I. 1972. Polarized intracellular particle transport: saltatory movements and cytoplasmic streaming. *Int Rev Cytol.* 32:93-137.
- Reczek, D., M. Berryman, and A. Bretscher. 1997. Identification of EBP50: A PDZ-containing phosphoprotein that associates with members of the ezrin-radixin-moesin family. *J Cell Biol.* 139:169-79.
- Reczek, D., and A. Bretscher. 2001. Identification of EPI64, a TBC/rabGAP domain-containing microvillar protein that binds to the first PDZ domain of EBP50 and E3KARP. *J Cell Biol.* 153:191-206.

- Ren, M., G. Xu, J. Zeng, C. De Lemos-Chiarandini, M. Adesnik, and D.D. Sabatini. 1998. Hydrolysis of GTP on rab11 is required for the direct delivery of transferrin from the pericentriolar recycling compartment to the cell surface but not from sorting endosomes. *Proc Natl Acad Sci U S A.* 95:6187-92.
- Rennick, B.R. 1981. Renal tubule transport of organic cations. *Am J Physiol.* 240:F83-9.
- Roth, N.S., P.T. Campbell, M.G. Caron, R.J. Lefkowitz, and M.J. Lohse. 1991. Comparative rates of desensitization of beta-adrenergic receptors by the beta-adrenergic receptor kinase and the cyclic AMP-dependent protein kinase. *Proc Natl Acad Sci U S A.* 88:6201-4.
- Rothenberger, S., B.J. Iacopetta, and L.C. Kuhn. 1987. Endocytosis of the transferrin receptor requires the cytoplasmic domain but not its phosphorylation site. *Cell.* 49:423-31.
- Rusan, N.M., C.J. Fagerstrom, A.M. Yvon, and P. Wadsworth. 2001. Cell cycle-dependent changes in microtubule dynamics in living cells expressing green fluorescent protein-alpha tubulin. *Mol Biol Cell.* 12:971-80.
- Russ, J.C. 1999. *The Image Processing Handbook.* CRC Press, Boca Raton.
- Rybin, V.O., X. Xu, M.P. Lisanti, and S.F. Steinberg. 2000. Differential targeting of beta-adrenergic receptor subtypes and adenylyl cyclase to cardiomyocyte caveolae. A mechanism to functionally regulate the cAMP signaling pathway. *J Biol Chem.* 275:41447-57.
- Sakamoto, T., I. Amitani, E. Yokota, and T. Ando. 2000. Direct observation of processive movement by individual myosin V molecules. *Biochem Biophys Res Commun.* 272:586-90.

- Sako, Y., and A. Kusumi. 1995. Barriers for lateral diffusion of transferrin receptor in the plasma membrane as characterized by receptor dragging by laser tweezers: fence versus tether. *J Cell Biol.* 129:1559-74.
- Salahpour, A., H. Bonin, S. Bhalla, U. Petaja-Repo, and M. Bouvier. 2003. Biochemical characterization of beta2-adrenergic receptor dimers and oligomers. *Biol Chem.* 384:117-23.
- Sanan, D.A., and R.G. Anderson. 1991. Simultaneous visualization of LDL receptor distribution and clathrin lattices on membranes torn from the upper surface of cultured cells. *J Histochem Cytochem.* 39:1017-24.
- Santini, F., I. Gaidarov, and J.H. Keen. 2002. G protein-coupled receptor/arrestin3 modulation of the endocytic machinery. *J Cell Biol.* 156:665-76.
- Saxton, M.J., and K. Jacobson. 1997. Single-particle tracking: applications to membrane dynamics. *Annu Rev Biophys Biomol Struct.* 26:373-99.
- Schubart, U.K., W. Alago, Jr., and A. Danoff. 1987. Properties of p19, a novel cAMP-dependent protein kinase substrate protein purified from bovine brain. *J Biol Chem.* 262:11871-7.
- Schulein, R., R. Hermosilla, A. Oksche, M. Dehe, B. Wiesner, G. Krause, and W. Rosenthal. 1998. A dileucine sequence and an upstream glutamate residue in the intracellular carboxyl terminus of the vasopressin V2 receptor are essential for cell surface transport in COS.M6 cells. *Mol Pharmacol.* 54:525-35.
- Scoles, D.R., D.P. Huynh, M.S. Chen, S.P. Burke, D.H. Gutmann, and S.M. Pulst. 2000. The neurofibromatosis 2 tumor suppressor protein interacts with hepatocyte growth factor-regulated tyrosine kinase substrate. *Hum Mol Genet.* 9:1567-74.

- Scott, M.G., A. Benmerah, O. Muntaner, and S. Marullo. 2002. Recruitment of activated G protein-coupled receptors to pre-existing clathrin-coated pits in living cells. *J Biol Chem.* 277:3552-9.
- Seachrist, J.L., P.H. Anborgh, and S.S. Ferguson. 2000. beta 2-adrenergic receptor internalization, endosomal sorting, and plasma membrane recycling are regulated by rab GTPases. *J Biol Chem.* 275:27221-8.
- Seibold, A., B.G. January, J. Friedman, R.W. Hipkin, and R.B. Clark. 1998. Desensitization of beta2-adrenergic receptors with mutations of the proposed G protein-coupled receptor kinase phosphorylation sites. *J Biol Chem.* 273:7637-42.
- Seibold, A., B. Williams, Z.F. Huang, J. Friedman, R.H. Moore, B.J. Knoll, and R.B. Clark. 2000. Localization of the sites mediating desensitization of the beta(2)-adrenergic receptor by the GRK pathway. *Mol Pharmacol.* 58:1162-73.
- Sheff, D.R., R. Kroschewski, and I. Mellman. 2002. Actin dependence of polarized receptor recycling in Madin-Darby canine kidney cell endosomes. *Mol Biol Cell.* 13:262-75.
- Shenolikar, S., C.M. Minkoff, D.A. Steplock, C. Evangelista, M. Liu, and E.J. Weinman. 2001. N-terminal PDZ domain is required for NHERF dimerization. *FEBS Lett.* 489:233-6.
- Shenolikar, S., and E.J. Weinman. 2001. NHERF: targeting and trafficking membrane proteins. *Am J Physiol Renal Physiol.* 280:F389-95.
- Shenoy, S.K., P.H. McDonald, T.A. Kohout, and R.J. Lefkowitz. 2001. Regulation of receptor fate by ubiquitination of activated beta 2-adrenergic receptor and beta-arrestin. *Science.* 294:1307-13.

- Shih, M., F. Lin, J.D. Scott, H.Y. Wang, and C.C. Malbon. 1999. Dynamic complexes of beta2-adrenergic receptors with protein kinases and phosphatases and the role of gravin. *J Biol Chem.* 274:1588-95.
- Shorr, R.G., R.J. Lefkowitz, and M.G. Caron. 1981. Purification of the beta-adrenergic receptor. Identification of the hormone binding subunit. *J Biol Chem.* 256:5820-6.
- Shorr, R.G., D.R. McCaslin, M.W. Strohsacker, G. Alianell, R. Rebar, J.M. Stadel, and S.T. Crooke. 1985. Molecular structure of the beta-adrenergic receptor. *Biochemistry.* 24:6869-75.
- Shorr, R.G., M.W. Strohsacker, T.N. Lavin, R.J. Lefkowitz, and M.G. Caron. 1982. The beta 1-adrenergic receptor of the turkey erythrocyte. Molecular heterogeneity revealed by purification and photoaffinity labeling. *J Biol Chem.* 257:12341-50.
- Shumay, E., X. Song, H.Y. Wang, and C.C. Malbon. 2002. pp60Src mediates insulin-stimulated sequestration of the beta(2)-adrenergic receptor: insulin stimulates pp60Src phosphorylation and activation. *Mol Biol Cell.* 13:3943-54.
- Sibley, D.R., R.H. Strasser, J.L. Benovic, K. Daniel, and R.J. Lefkowitz. 1986. Phosphorylation/dephosphorylation of the beta-adrenergic receptor regulates its functional coupling to adenylate cyclase and subcellular distribution. *Proc Natl Acad Sci U S A.* 83:9408-12.
- Siegel, L.M., and K.J. Monty. 1966. Determination of molecular weights and frictional ratios of proteins in impure systems by use of gel filtration and density gradient centrifugation. Application to crude preparations of sulfite and hydroxylamine reductases. *Biochim Biophys Acta.* 112:346-62.

1. The first part of the document discusses the importance of maintaining accurate records of all transactions and activities. It emphasizes that this is crucial for ensuring transparency and accountability in the organization's operations.

2. The second part of the document outlines the various methods and tools used to collect and analyze data. It highlights the need for consistent data collection procedures and the use of advanced analytical techniques to derive meaningful insights from the data.

3. The third part of the document focuses on the role of technology in data management and analysis. It discusses how modern software solutions can streamline data collection, storage, and analysis processes, thereby improving efficiency and accuracy.

4. The fourth part of the document addresses the challenges associated with data management, such as data quality, security, and privacy. It provides strategies to mitigate these risks and ensure that the data remains reliable and secure throughout its lifecycle.

5. The fifth part of the document concludes by summarizing the key findings and recommendations. It stresses the importance of a data-driven approach in decision-making and the need for continuous monitoring and improvement of data management practices.

- Simon, J.R., S.F. Parsons, and E.D. Salmon. 1992. Buffer conditions and non-tubulin factors critically affect the microtubule dynamic instability of sea urchin egg tubulin. *Cell Motil Cytoskeleton*. 21:1-14.
- Simonin, F., P. Karcher, J.J. Boeuf, A. Matifas, and B.L. Kieffer. 2004. Identification of a novel family of G protein-coupled receptor associated sorting proteins. *J Neurochem*. 89:766-75.
- Singh, H., and S. Linas. 1996. Beta 2-adrenergic function in cultured rat proximal tubule epithelial cells. *Am J Physiol Renal Physiol*. 271:F71-7.
- Smith, D.A., and R.M. Simmons. 2001. Models of motor-assisted transport of intracellular particles. *Biophys J*. 80:45-68.
- Sonnichsen, B., S. De Renzis, E. Nielsen, J. Rietdorf, and M. Zerial. 2000. Distinct membrane domains on endosomes in the recycling pathway visualized by multicolor imaging of Rab4, Rab5, and Rab11. *J Cell Biol*. 149:901-14.
- Speck, O., S.C. Hughes, N.K. Noren, R.M. Kulikauskas, and R.G. Fehon. 2003. Moesin functions antagonistically to the Rho pathway to maintain epithelial integrity. *Nature*. 421:83-7.
- Steyer, J.A., and W. Almers. 1999. Tracking single secretory granules in live chromaffin cells by evanescent-field fluorescence microscopy. *Biophys J*. 76:2262-71.
- Stoorvogel, W., V. Oorschot, and H.J. Geuze. 1996. A novel class of clathrin-coated vesicles budding from endosomes. *J Cell Biol*. 132:21-33.
- Stossel, T.P., J. Condeelis, L. Cooley, J.H. Hartwig, A. Noegel, M. Schleicher, and S.S. Shapiro. 2001. Filamins as integrators of cell mechanics and signalling. *Nat Rev Mol Cell Biol*. 2:138-45.

Stroheim. 1922. *Variety*.

Stryer, L. 2002. *Biochemistry*. W. H. Freeman, New York.

Sussman, J.L., D. Lin, J. Jiang, N.O. Manning, J. Prilusky, O. Ritter, and E.E. Abola.

1998. Protein Data Bank (PDB): database of three-dimensional structural information of biological macromolecules. *Acta Crystallogr D Biol Crystallogr*. 54:1078-84.

Tabb, J.S., B.J. Molyneaux, D.L. Cohen, S.A. Kuznetsov, and G.M. Langford. 1998.

Transport of ER vesicles on actin filaments in neurons by myosin V. *J Cell Sci*. 111 (Pt 21):3221-34.

Takizawa, P.A., J.K. Yucel, B. Veit, D.J. Faulkner, T. Deerinck, G. Soto, M. Ellisman, and V. Malhotra. 1993. Complete vesiculation of Golgi membranes and inhibition of protein transport by a novel sea sponge metabolite, ilimaquinone. *Cell*.

73:1079-90.

Tanowitz, M., and M. Von Zastrow. 2002. Ubiquitination-independent trafficking of G protein-coupled receptors to lysosomes. *J Biol Chem*. 277:50219-22.

Tanowitz, M., and M. von Zastrow. 2003. A novel endocytic recycling signal that distinguishes the membrane trafficking of naturally occurring opioid receptors. *J Biol Chem*. 278:45978-86.

Tao, J., H.Y. Wang, and C.C. Malbon. 2003. Protein kinase A regulates AKAP250 (gravin) scaffold binding to the beta2-adrenergic receptor. *Embo J*. 22:6419-29.

Taunton, J., B.A. Rowning, M.L. Coughlin, M. Wu, R.T. Moon, T.J. Mitchison, and C.A. Larabell. 2000. Actin-dependent propulsion of endosomes and lysosomes by recruitment of N-WASP. *J Cell Biol*. 148:519-30.

1. The first part of the document is a list of names and addresses of the members of the committee. The names are listed in alphabetical order, and the addresses are listed below each name. The list includes names such as Mr. J. H. Smith, Mr. W. B. Jones, and Mr. C. D. Brown, among others.

2. The second part of the document is a list of names and addresses of the members of the committee. The names are listed in alphabetical order, and the addresses are listed below each name. The list includes names such as Mr. J. H. Smith, Mr. W. B. Jones, and Mr. C. D. Brown, among others.

- Traub, L.M. 2003. Sorting it out: AP-2 and alternate clathrin adaptors in endocytic cargo selection. *J Cell Biol.* 163:203-8.
- Traub, L.M., and G. Apodaca. 2003. AP-1B: polarized sorting at the endosome. *Nat Cell Biol.* 5:1045-7.
- Tsao, P., T. Cao, and M. von Zastrow. 2001. Role of endocytosis in mediating downregulation of G-protein-coupled receptors. *Trends Pharmacol Sci.* 22:91-6.
- Tsao, P.I., and M. von Zastrow. 2000. Type-specific sorting of G protein-coupled receptors after endocytosis. *J Biol Chem.* 275:11130-40.
- Ullrich, O., S. Reinsch, S. Urbe, M. Zerial, and R.G. Parton. 1996. Rab11 regulates recycling through the pericentriolar recycling endosome. *J Cell Biol.* 135:913-24.
- Ungerer, M., M. Bohm, J.S. Elce, E. Erdmann, and M.J. Lohse. 1993. Altered expression of beta-adrenergic receptor kinase and beta 1-adrenergic receptors in the failing human heart. *Circulation.* 87:454-63.
- Vale, R.D. 1991. Severing of stable microtubules by a mitotically activated protein in *Xenopus* egg extracts. *Cell.* 64:827-39.
- Vale, R.D., and R.J. Fletterick. 1997. The design plan of kinesin motors. *Annu Rev Cell Dev Biol.* 13:745-77.
- van der Sluijs, P., M. Hull, P. Webster, P. Male, B. Goud, and I. Mellman. 1992. The small GTP-binding protein rab4 controls an early sorting event on the endocytic pathway. *Cell.* 70:729-40.
- van Der Sluijs, P., M. Hull, A. Zahraoui, A. Tavitian, B. Goud, and I. Mellman. 1991. The small GTP-binding protein rab4 is associated with early endosomes. *Proc Natl Acad Sci U S A.* 88:6313-7.

- Vander, A., J. Sherman, and D. Luciano. 1990. *Human Physiology: The Mechanisms of Body Function*. McGraw-Hill.
- Vargas, G.A., and M. Von Zastrow. 2004. Identification of a novel endocytic recycling signal in the D1 dopamine receptor. *J Biol Chem*. 279:37461-9.
- von Zastrow, M., and B.K. Kobilka. 1992. Ligand-regulated internalization and recycling of human beta 2-adrenergic receptors between the plasma membrane and endosomes containing transferrin receptors. *J Biol Chem*. 267:3530-8.
- von Zastrow, M., and B.K. Kobilka. 1994. Antagonist-dependent and -independent steps in the mechanism of adrenergic receptor internalization. *J Biol Chem*. 269:18448-52.
- Vorobjev, I.A., T.M. Svitkina, and G.G. Borisov. 1997. Cytoplasmic assembly of microtubules in cultured cells. *J Cell Sci*. 110 (Pt 21):2635-45.
- Wade, J.B., J. Liu, R.A. Coleman, R. Cunningham, D.A. Steplock, W. Lee-Kwon, T.L. Pallone, S. Shenolikar, and E.J. Weinman. 2003. Localization and interaction of NHERF isoforms in the renal proximal tubule of the mouse. *Am J Physiol Cell Physiol*. 285:C1494-503.
- Walczak, C.E., E.C. Gan, A. Desai, T.J. Mitchison, and S.L. Kline-Smith. 2002. The microtubule-destabilizing kinesin XKCM1 is required for chromosome positioning during spindle assembly. *Curr Biol*. 12:1885-9.
- Walczak, C.E., T.J. Mitchison, and A. Desai. 1996. XKCM1: a *Xenopus* kinesin-related protein that regulates microtubule dynamics during mitotic spindle assembly. *Cell*. 84:37-47.

- Walker, J.K., K. Peppel, R.J. Lefkowitz, M.G. Caron, and J.T. Fisher. 1999. Altered airway and cardiac responses in mice lacking G protein-coupled receptor kinase 3. *Am J Physiol.* 276:R1214-21.
- Wan, J., M.E. Taub, D. Shah, and W.C. Shen. 1992. Brefeldin A enhances receptor-mediated transcytosis of transferrin in filter-grown Madin-Darby canine kidney cells. *J Biol Chem.* 267:13446-50.
- Wedlich-Soldner, R., A. Straube, M.W. Friedrich, and G. Steinberg. 2002. A balance of KIF1A-like kinesin and dynein organizes early endosomes in the fungus *Ustilago maydis*. *Embo J.* 21:2946-57.
- Weigert, R., A. Colanzi, A. Mironov, R. Buccione, C. Cericola, M.G. Sciulli, G. Santini, S. Flati, A. Fusella, J.G. Donaldson, M. Di Girolamo, D. Corda, M.A. De Matteis, and A. Luini. 1997. Characterization of chemical inhibitors of brefeldin A-activated mono-ADP-ribosylation. *J Biol Chem.* 272:14200-7.
- Weinman, E.J., D. Steplock, K. Tate, R.A. Hall, R.F. Spurney, and S. Shenolikar. 1998. Structure-function of recombinant Na/H exchanger regulatory factor (NHE-RF). *J Clin Invest.* 101:2199-206.
- Weinman, E.J., D. Steplock, J.B. Wade, and S. Shenolikar. 2001. Ezrin binding domain-deficient NHERF attenuates cAMP-mediated inhibition of Na(+)/H(+) exchange in OK cells. *Am J Physiol Renal Physiol.* 281:F374-80.
- Whistler, J.L., J. Enquist, A. Marley, J. Fong, F. Gladher, P. Tsuruda, S.R. Murray, and M. Von Zastrow. 2002. Modulation of postendocytic sorting of G protein-coupled receptors. *Science.* 297:615-20.

- Whistler, J.L., P. Tsao, and M. von Zastrow. 2001. A phosphorylation-regulated brake mechanism controls the initial endocytosis of opioid receptors but is not required for post-endocytic sorting to lysosomes. *J Biol Chem.* 276:34331-8.
- Whiteheart, S.W., and E.A. Matveeva. 2004. Multiple binding proteins suggest diverse functions for the N-ethylmaleimide sensitive factor. *J Struct Biol.* 146:32-43.
- Wilson, J.M., M. de Hoop, N. Zorzi, B.H. Toh, C.G. Dotti, and R.G. Parton. 2000. EEA1, a tethering protein of the early sorting endosome, shows a polarized distribution in hippocampal neurons, epithelial cells, and fibroblasts. *Mol Biol Cell.* 11:2657-71.
- Wordeman, L. 2005. Microtubule-depolymerizing kinesins. *Curr Opin Cell Biol.* 17:82-8.
- Wright, S.H., and W.H. Dantzler. 2004. Molecular and cellular physiology of renal organic cation and anion transport. *Physiol Rev.* 84:987-1049.
- Wu, G., J.G. Krupnick, J.L. Benovic, and S.M. Lanier. 1997. Interaction of arrestins with intracellular domains of muscarinic and alpha2-adrenergic receptors. *J Biol Chem.* 272:17836-42.
- Wu, X., B. Bowers, K. Rao, Q. Wei, and J.A.r. Hammer. 1998. Visualization of melanosome dynamics within wild-type and dilute melanocytes suggests a paradigm for myosin V function In vivo. *J Cell Biol.* 143:1899-918.
- Xiang, Y., E. Devic, and B. Kobilka. 2002a. The PDZ binding motif of the beta 1 adrenergic receptor modulates receptor trafficking and signaling in cardiac myocytes. *J Biol Chem.* 277:33783-90.

1. The first part of the document discusses the importance of maintaining accurate records of all transactions and activities. It emphasizes that this is crucial for ensuring transparency and accountability in the organization's operations.

2. The second part of the document outlines the various methods and tools used to collect and analyze data. It highlights the need for consistent and reliable data collection processes to support informed decision-making.

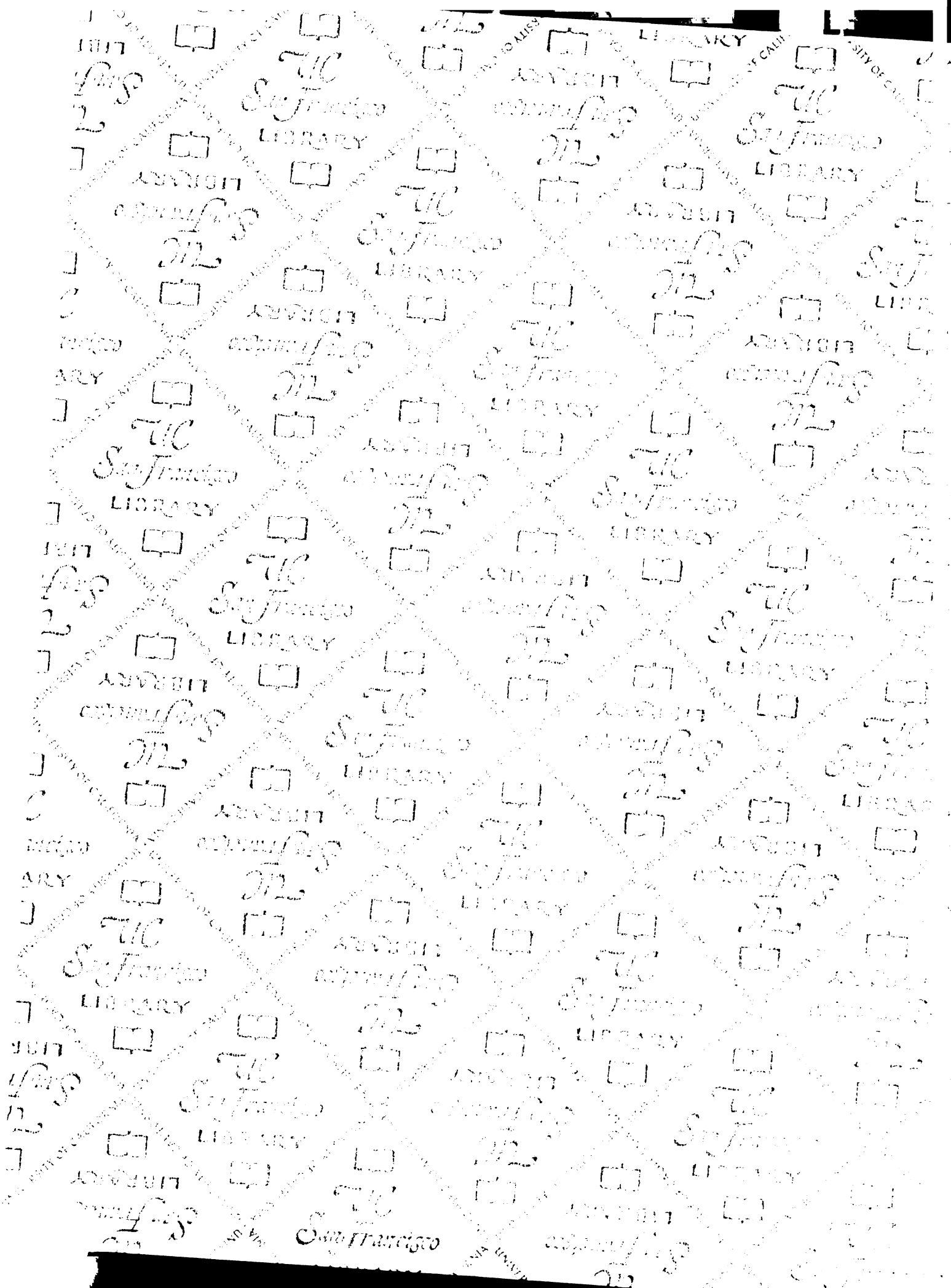
3. The third part of the document focuses on the role of technology in modern data management. It discusses how advanced software solutions can streamline data collection, storage, and analysis, leading to more efficient and accurate results.

4. The fourth part of the document addresses the challenges associated with data security and privacy. It stresses the importance of implementing robust security measures to protect sensitive information from unauthorized access and breaches.

5. The fifth part of the document concludes by summarizing the key findings and recommendations. It reiterates the importance of a data-driven approach and encourages the organization to continue investing in data management capabilities to stay competitive in the market.

- Xiang, Y., and B. Kobilka. 2003a. The PDZ-binding motif of the beta2-adrenoceptor is essential for physiologic signaling and trafficking in cardiac myocytes. *Proc Natl Acad Sci U S A*. 100:10776-81.
- Xiang, Y., and B.K. Kobilka. 2003b. Myocyte adrenoceptor signaling pathways. *Science*. 300:1530-2.
- Xiang, Y., V.O. Rybin, S.F. Steinberg, and B. Kobilka. 2002b. Caveolar localization dictates physiologic signaling of beta 2-adrenoceptors in neonatal cardiac myocytes. *J Biol Chem*. 277:34280-6.
- Xiao, R.P., P. Avdonin, Y.Y. Zhou, H. Cheng, S.A. Akhter, T. Eschenhagen, R.J. Lefkowitz, W.J. Koch, and E.G. Lakatta. 1999a. Coupling of beta2-adrenoceptor to Gi proteins and its physiological relevance in murine cardiac myocytes. *Circ Res*. 84:43-52.
- Xiao, R.P., H. Cheng, Y.Y. Zhou, M. Kuschel, and E.G. Lakatta. 1999b. Recent advances in cardiac beta(2)-adrenergic signal transduction. *Circ Res*. 85:1092-100.
- Xiao, R.P., X. Ji, and E.G. Lakatta. 1995. Functional coupling of the beta 2-adrenoceptor to a pertussis toxin-sensitive G protein in cardiac myocytes. *Mol Pharmacol*. 47:322-9.
- Xu, J., J. He, A.M. Castleberry, S. Balasubramanian, A.G. Lau, and R.A. Hall. 2003. Heterodimerization of alpha 2A- and beta 1-adrenergic receptors. *J Biol Chem*. 278:10770-7.
- Yamamoto, A., H. Takagi, D. Kitamura, H. Tatsuoka, H. Nakano, H. Kawano, H. Kuroyanagi, Y. Yahagi, S. Kobayashi, K. Koizumi, T. Sakai, K. Saito, T. Chiba, K. Kawamura, K. Suzuki, T. Watanabe, H. Mori, and T. Shirasawa. 1998.

- Deficiency in protein L-isoaspartyl methyltransferase results in a fatal progressive epilepsy. *J Neurosci.* 18:2063-74.
- Yu, S.S., R.J. Lefkowitz, and W.P. Hausdorff. 1993. Beta-adrenergic receptor sequestration. A potential mechanism of receptor resensitization. *J Biol Chem.* 268:337-41.
- Yun, C.H., G. Lamprecht, D.V. Forster, and A. Sidor. 1998. NHE3 kinase A regulatory protein E3KARP binds the epithelial brush border Na⁺/H⁺ exchanger NHE3 and the cytoskeletal protein ezrin. *J Biol Chem.* 273:25856-63.
- Zhang, J., S.S. Ferguson, L.S. Barak, L. Menard, and M.G. Caron. 1996. Dynamin and beta-arrestin reveal distinct mechanisms for G protein-coupled receptor internalization. *J Biol Chem.* 271:18302-5.
- Zhang, J., S.S. Ferguson, P.Y. Law, L.S. Barak, and M.G. Caron. 1999. Agonist-specific regulation of delta-opioid receptor trafficking by G protein-coupled receptor kinase and beta-arrestin. *J Recept Signal Transduct Res.* 19:301-13.
- Zhang, M., N.K. Dwyer, D.C. Love, A. Cooney, M. Comly, E. Neufeld, P.G. Pentchev, E.J. Blanchette-Mackie, and J.A. Hanover. 2001. Cessation of rapid late endosomal tubulovesicular trafficking in Niemann-Pick type C1 disease. *Proc Natl Acad Sci U S A.* 98:4466-71.
- Zhu, W.Z., M. Zheng, W.J. Koch, R.J. Lefkowitz, B.K. Kobilka, and R.P. Xiao. 2001. Dual modulation of cell survival and cell death by beta(2)-adrenergic signaling in adult mouse cardiac myocytes. *Proc Natl Acad Sci U S A.* 98:1607-12.
- Zizak, M., G. Lamprecht, D. Steplock, N. Tariq, S. Shenolikar, M. Donowitz, C.H. Yun, and E.J. Weinman. 1999. cAMP-induced phosphorylation and inhibition of



UNIVERSITY OF CALIFORNIA
SAN FRANCISCO
LIBRARY
ADVISIT
STAMPING
UC

Not to be taken
from the room.

For reference

7399499



3 1378 00739 9499

